Indian J Chem
MARCH 1991
CODEN:IJOCAP 30A(3) 203-300 (1991)
ISSN:0019-5103

1057
28/2/91
28/2/91
Lib

Indian Journal of CHEMISTRY

SECTION A

Inorganic, Bio-inorganic, Physical, Theoretical & Analytical Chemistry

Published by
PUBLICATIONS & INFORMATION DIRECTORATE, CSIR, NEW DELHI
in association with
THE INDIAN NATIONAL SCIENCE ACADEMY, NEW DELHI

Announcement

Shanti Swarup Bhatnagar Prizes in Science and Technology

Nominations are invited by the Council of Scientific & Industrial Research for the Shanti Swarup Bhatnagar Prizes in science, including engineering and technology, for 1991. The prizes are to be given for research contributions made primarily in India during the past five years. The upper age limit of nominees for the prize is 45 years.

The prizes, each of the value of Rs 50,000, may be awarded annually for notable and outstanding research, applied or fundamental, in the following disciplines: (1) biological sciences, (2) chemical sciences, (3) earth, atmospheric, oceanic and planetary sciences, (4) engineering sciences, (5) mathematical sciences, (6) medical sciences and (7) physical sciences.

Nominations should be sent in the prescribed proforma by 1 April 1991. Regulations governing the prize and the proforma for nomination may be obtained from the Head, Human Resource Development Group, Extramural Research, CSIR Complex, NPL Campus, New Delhi 110 012.

फार्म 4/FORM IV

[नियम 8 देखिए/(*See* Rule 8)]

1. प्रकाशन स्थान/Place of publication	New Delhi
2. प्रकाशन अवधि/Periodicity of its publication	Monthly
3. मुद्रक का नाम/Printer's Name	Dr G P Phondke
(क्या भारत का नागरिक है?)/(Whether citizen of India?)	Yes
(यदि विदेशी है तो मूल देश)/(If foreigner, state the country of origin)	
पता/Address	Publications & Information Directorate Hillside Road, New Delhi 110 012
4. प्रकाशक का नाम/Publisher's Name	Dr G P Phondke
(क्या भारत का नागरिक है?)/(Whether citizen of India?)	Yes
(यदि विदेशी है तो मूल देश)/(If foreigner, state the country of origin)	
पता/Address	As above in (3)
5. संपादक का नाम/Editor's Name	S. S. Saksena
(क्या भारत का नागरिक है?)/(Whether citizen of India?)	Yes
(यदि विदेशी है तो मूल देश)/(If foreigner, state the country of origin)	
पता/Address	As above in (3)
6. उन व्यक्तियों के नाम व पते जो समाचार–पत्र के स्वामी हों तथा जो समस्त पूंजी के एक प्रतिशत से अधिक के साझेदार या हिस्सेदार हों। Names and addresses of individuals who own the newspaper and partners or share holders holding more than one per cent of the total capital.	

मैं, ————————, एतद्द्वारा घोषित करता हूं कि मेरी अधिकतम जानकारी एवं विश्वास के अनुसार ऊपर दिए गए विवरण सत्य हैं।

I, Dr. G. P. Phondke hereby declare that the particulars given above are true to the best of my knowledge and belief.

Sd/- G. P. Phondke

ता०/Dated 1 March 1991

प्रकाशन के हस्ताक्षर/Signature of Publisher

INDIAN JOURNAL OF CHEMISTRY

Section A: Inorganic, Bio-inorganic, Physical, Theoretical & Analytical Chemistry

Editorial Board

Prof. C N R Rao
Director
Indian Institute of Science
Bangalore 560 012

Prof. D V S Jain
Chemistry Department
Panjab University
Chandigarh 160 014

Prof. S Mitra
Tata Institute of Fundamental Research
Homi Bhabha Road
Bombay 400 005

Prof. P Natarajan
Department of Inorganic Chemistry
University of Madras
Madras 600 025

Dr R M Iyer
Director, Chemical Group
Bhabha Atomic Research Centre
Trombay, Bombay 400 085

Prof. R C Mehrotra
Chemistry Department
Rajasthan University
Jaipur 302 004

Prof. U C Agarwala
Department of Chemistry
Indian Institute of Technology
Kanpur 208 016

Prof. J C Ahluwalia
Department of Chemistry
Indian Institute of Technology
Delhi 110 016

Prof. C L Khetrapal
National NMR Facility
Indian Institute of Science
Bangalore 560 012

Dr P Ratnasamy
National Chemical Laboratory
Pune 411 008

Dr N Venkatasubramanian
Director
Centre for Post-Graduate Studies
Government of Pondicherry
Pondicherry 605 008

Prof. N K Ray
Department of Chemistry
Delhi University
Delhi 110 007

Prof. S S Krishnamurthy
Department of Inorganic & Physical Chemistry
Indian Institute of Science
Bangalore 560 012

Prof. K K Kundu
Department of Chemistry
Jadavpur University
Calcutta 700 032

Prof. M V Kaulgud
Department of Chemistry
Nagpur University
Nagpur 440 010

Dr G P Phondke, Director, PID

Editors: S S Saksena, B C Sharma, S Sivakamasundari and S K Bhasin

Sr. Scientific Assistant: Geeta Mahadevan

Published by the Publications & Information Directorate (CSIR), Hillside Road, New Delhi 110 012

Director: Dr G P Phondke

Copyright, 1990, by the Council of Scientific & Industrial Research, New Delhi 110 012

The Indian Journal of Chemistry is issued monthly in two sections: A and B. Communications regarding contributions for publication in the journal should be addressed to the Editor, Indian Journal of Chemistry, Publications & Information Directorate, Hillside Road, New Delhi 110 012.

Correspondence regarding subscriptions and advertisements should be addressed to the Sales & Distribution Officer, Publications & Information Directorate, Hillside Road, New Delhi 110 012.

The Publications & Information Directorate (CSIR) assumes no responsibility for the statements and opinions advanced by contributors. The Editorial Board in its work of examining papers received for publication is assisted, in an honorary capacity by a large number of distinguished scientists, working in various parts of India.

Annual Subscription: Rs. 400.00 £ 100.00 $ 150.00; 50% discount admissible to research workers and students and 25% discount to non-research individuals on annual subscription.

Single Copy : Rs. 40.00 $ 15.00 £ 10.00

Payments in respect of subscriptions and advertisements may be sent by cheque, bank draft, money order or postal order marked payable to Publications & Information Directorate, Hillside Road, New Delhi 110 012.

Claims for missing numbers of the journal will be allowed only if received within 3 months of the date of issue of the journal plus the time normally required for postal delivery of the journals and the claim.

Aditya Napur 266
Aminabhavi T M 209
Anbukulandainathan M 230
Arifien A E 235
Awasthi Sanjay K 215

Bag S P 281
Banerjea D 269
Banerjee D 219
Banerjee T K 281
Basu Rama 266
Bhatnagar Deepa 296
Bhattacharya U 255
Bose J M 219
Brahma S K 281
Brahmaiah A 247

Easwaramoorthy D 275
El-Gamal O A 286
El-Reash G M Abu 286

Girgis M M 235
Guha D 219
Guha Supriya 269
Gupta R 261

Halli M B 290
Harogoppad S B 209
Hiremath A C 290

Kesavan B 299
Krishnamoorthy P V 230
Krishna Rao G S R 239
Krishnaprasad K P 299

Lekshmana Thanulingam T 272

Manikyamba P 247
Mehrotra R C 261
Mikhailov O V 252
Misra G P 203
Mohapatra B K 255
Murthy P S N 239
Murugesan R 272

Nepali Deepawati R 293

Osman A H 235

Parashar D C 296
Pujapanda P K 255

Qureshi Z S 290

Raju J R 243
Ramachandran M S 275
Ramakrishna K 239
Ramchandran R 296
Rane Arvind T 293
Rastogi R P 203
Reddy K M 290
Rout A K 255

Sahoo B 255
Sambrani M I 243
Sanecki Przemyslaw 225
Satyanarayan Reddy M 278
Shallaby A M 286
Shunmugasundaram A 272
Singh A 261
Singh Kiran 283
Srivastava A K 215
Subba Rao P V 239
Sundaram E V 247
Syal V 203

Taha Fim 286
Tandon J P 283
Taqui Khan M M 278

Venkatakrishna Iyer S 230
Vivekanandam T S 275

Indian Journal of Chemistry

Sect. A: Inorganic, Bioinorganic, Physical, Theoretical & Analytical

VOL. 30A NUMBER 3 MARCH 1991

SCIENTIFIC & RESEARCH
Accession No.
28 FEB 1991
P.I.R.I. REGIONAL CENTRE LUDHIANA

CONTENTS

Thermodynamic analysis of critical limits in Belousov-Zhabotinskii reaction system . 203
R P Rastogi*, V Syal & G P Misra

Dimensional response of engineering polymeric elastomers in the presence of halo-substituted benzenes 209
S B Harogoppad & T M Aminabhavi*

Template copolymerization of methyl methacrylate and styrene on poly(methyl methacrylate) 215
Sanjay K Awasthi & A K Srivastava*

Studies on NO_x conversion over transition metal ion (TMI) doped alumina-boria system . 219
J M Bose*, D Banerjee & D Guha

Variation of the electrochemical transfer coefficient in the electroreduction of aromatic two-ring disulfonyl difluorides 225
Przemyslaw Sanecki

Coadsorption of organic molecules on mercury electrode 230
P V Krishnamoorthy, M Anbukulandainathan & S Venkatakrishna Iyer*

Electron-transfer interactions of chloranil/bromanil with hexacyanometalate (4-), $K_4[M(CN)_6]$, where M = Fe, Ru and Os 235
M M Girgis*, A H Osman & A E Arifien

Kinetics of chromic acid-oxalic acid reaction catalysed by manganese(II)—Kinetic analysis of the consecutive pathway 239
P V Subba Rao*, G S R Krishna Rao, K Ramakrishna & P S N Murthy

Kinetics and mechanism of cooxidation of oxalic acid and arsenic(III) by chlorochromate in aqueous acetic acid 243
M I Sambrani & J R Raju*

Oxidation of diphenylamines by iodate—A kinetic study 247
A Brahmaiah, P Manikyamba* & E V Sundaram

Enzyme-assisted matrix isolation of novel dithiooxamide complexes of nickel(II) . . 252
O V Mikhailov

Macrocyclic metal complexes: Part XXI—Syntheses of binuclear sepulchral complexes by the interaction of formaldehyde with tris-(3,6-dimethyl-4,5-diazaocta-3,5-diene-2,7-dihydrazone)dimetal(II) ions 255
B K Mohapatra, U Bhattacharya, P K Pujapanda, A K Rout & B Sahoo*

Continued overleaf

Novel chloride isopropoxides and allied hetero-bimetallic complexes of iron(III) with aluminium(III) 261
(Miss) R Gupta, A Singh & R C Mehrotra*

Notes

Charge-transfer interaction of some aromatic hydrocarbons with chloranil . . . 266
Nupur Aditya & Rama Basu*

Kinetics and mechanism of dissociation of some *para*-substituted phenylbiguanide complexes of nickel(II) in aqueous hydrochloric acid 269
Supriya Guha & D Banerjea*

Kinetics of retroaldol reaction of *para*-substituted β-nitrostyrenes and β-methyl-β-nitrostyrenes 272
A Shunmugasundaram*, T Lekshmana Thanulingam & R Murugesan

Oxidation of methionine by N-chloroacetamide—Catalytic effect of formaldehyde . 275
M S Ramachandran*, D Easwaramoorthy & T S Vivekanandam

Synthesis and characterization of ruthenium(II) complexes with monotertiary phosphines and arsines 278
M M Taqui Khan & M Satyanarayan Reddy*

Synthesis and vibrational studies of molybdenum dinitrosyl complexes with hydroxamic acids as ligands 281
T K Banerjee, S K Brahma & S P Bag*

Synthesis and spectral studies of methylsilicon(IV) chloride complexes with biologically active heterocyclic benzothiazolines 283
(Mrs) Kiran Singh* & J P Tandon

Synthesis and characterization of metal complexes with a schiff base formed by condensation of S-benzyl dithiocarbazate with isatin (H_2IBD) 286
G M Abu El-Reash*, Fim Taha, A M Shallaby & O A El-Gamal

Synthesis and characterization of Co(II),Ni(II),Cu(II),Zn(II),Cd(II),Hg(II),dioxouranium(VI) and Th(IV) complexes with a schiff base 290
A C Hiremath*, Z S Qureshi, K M Reddy & M B Halli

Kinetics of extraction of cobalt(II) by quinolinol and its back extraction using ^{58}Co tracer . 293
(Late) Arvind T Rane & Deepawati R Nepali*

A spectrophotometric method for the determination of traces of silicon in copper and aluminium alloys 296
Deepa Bhatnagar, R Ramachandran & D C Parashar*

Extraction and spectrophotometric determination of microgram amounts of niobium(V) . 299
B Keshavan* & K P Krishnaprasad

Authors for correspondence are indicated by (*)

Indian Journal of Chemistry
Vol. 30A, March 1991, pp. 203-208

Thermodynamic analysis of critical limits in Belousov-Zhabotinskii reaction system

R P Rastogi*, V Syal & G P Misra

Department of Chemistry, Banaras Hindu University, Varanasi 221 005

Received 6 August 1990; accepted 27 August 1990

Stability of the Belousov-Zhabotinskii (B-Z) reaction system containing bromate, ceric ammonium sulphate, sulphuric acid and mixed organic substrates (oxalic acid + acetone) has been examined using the thermodynamic theory of Glansdorff and Prigogine at the two critical limits of [acetone] and also in the oscillatory domain. The sign of excess entropy production due to perturbation in [$HBrO_2$] has been estimated by taking into account the subset of reactions involving $HBrO_2$. Numerical estimates of sign of relative excess entropy production for different reactions have been made using the latest accepted values of the rate constants (Field and Försterling) as well as values of Field and Boyd. The thermodynamic analysis suggests that the reaction system is stabilized either when (i) the contribution to the excess entropy production due to destruction of $HBrO_2$ by Br^- exceeds the negative contribution due to autocatalytic reaction step or when (ii) the contribution of disproportionation of $HBrO_2$ to the excess entropy production exceeds or becomes comparable to the negative contribution due to autocatalytic reaction step. Situation (i) corresponds to lower limit of [acetone] while (ii) corresponds to upper limit of [acetone]. Instability can occur when the negative contribution due to the autocatalytic reaction exceeds the sum of contributions of disproportionation of $HBrO_2$ and its destruction by Br^-.

Non-equilibrium thermodynamics predicts that instability in a reacting system can occur when (i) the system is far away from equilibrium and (ii) the reaction subset contains an autocatalytic, cross-catalytic or auto-inhibitory step in the overall reaction mechanism. These predictions have been confirmed in a number of systems where multi-stability, temporal oscillations and spatio-temporal oscillations have been observed. According to the thermodynamic condition of stability[1-3] of non-equilibrium steady states, the excess entropy production $(\delta^2 S)_{E,V}$ is given by Eq. (1)

$$(\delta^2 S)_{E,V} = \frac{1}{T}\sum \delta J_i \cdot \delta A_i > 0 \qquad \ldots (1)$$

where δJ_i denotes the perturbation in chemical reaction rate J_i and δA_i denotes the perturbation in chemical affinity A_i of the ith step of reaction. Now since in non-biological reactions, all the reaction steps are independent[4], we must also have

$$\delta J_i \cdot \delta A_i > 0$$

for each ith step in order to ensure stability. Since only the autocatalytic, cross-catalytic or autoinhibitory reaction can yield negative contribution to excess entropy production, it is worthwhile to examine such reactions alone in depth in order to predict stability in such reacting systems.

In the context of Eq. (1), it should be noted that at constant internal energy E and volume V, entropy change $(dS)_{E,V} > 0$ is a necessary (but not sufficient) condition for a reaction or process to occur while $(dS)_{E,V} < 0$, is a necessary and sufficient condition for a process not to occur. In the same manner while $(\delta^2 S)_{E,V} > 0$, is the necessary and sufficient condition for stability, $(\delta^2 S)_{E,V} < 0$ is only a necessary condition for instability.

The question of validity of Eq. (1) for far-from-equilibrium conditions has been debated over a number of years[2,5]. For such situations, entropy S is given by Eq. (2)

$$S = S(\rho_i, \ldots \rho_n\{\nabla \rho_i\}; \{\nabla^2 \rho_i\} \ldots; \left\{\frac{\delta \rho_i}{\delta t}\right\}, \ldots; r, t). \qquad \ldots (2)$$

where ρ's are the thermodynamic variables, such as energy, volume and concentration and r denotes the position.

Microscopic meaning of such a function for far-from-equilibrium condition when the gradients $\{\nabla \rho_i\}$ and of the time-derivative $(\partial \rho_i / \partial t)$ are significant is not very explicit. For local equilibrium, however, $\nabla \rho_i$, $\nabla^2 \rho_i$ and $\partial \rho_i / \partial t$ are not significant. Hence, it has been pointed out that Eq. (1) is valid for local equilibrium for (a) complex systems of

chemical reactions with highly non-linear kinetics provided the rate of elastic collisions remains larger than the rate of reactive collisions, and (b) biological processes in dense media.

On the other hand, Eq. (1) is not valid for phenomena such as shock waves, flows in rarefied systems and plastic deformation of solids. The concept of local equilibrium in non-linear thermodynamics has been recently reexamined by Ross and Garcia-Colin[6] in the context of reactive systems in continuous-flow stirred tank reactor (CSTR) and batch reactor. According to them "for most reactions, especially in liquids, reaction times are long compared to other relaxation times (vibration etc.) which are of the order of 10^{-11} s or shorter. For such cases, the thermodynamic variables and progress variables are on the same time scale" and concept of local equilibrium would be valid.

In view of the controversy[1,2,5-8] regarding the validity of Eq. (1) or otherwise for far-from-equilibrium conditions, it would be instructive to compare the experimental results[9] for Belousov-Zhabotinskii (B-Z) reaction with oxalic acid + acetone system with thermodynamic analysis based on Eq. (1).

Thermodynamic analysis

In the B-Z reactions, the key subsets of reactions determining stability of B-Z oscillator are the following:

$$H^+ + Br^- + HBrO_2 \underset{k_{-2}}{\overset{k_2}{\rightleftharpoons}} 2HOBr \qquad (R2)$$

$$HBrO_2 + BrO_3^- + H^+ \underset{k_{-3}}{\overset{k_3}{\rightleftharpoons}} 2BrO_2 + H_2O \qquad (R3)$$

$$Ce^{3+} + BrO_2^{\cdot} + H^+ \underset{k_{-3'}}{\overset{k_{3'}}{\rightleftharpoons}} HBrO_2 + Ce^{4+} \qquad (R3')$$

$$2HBrO_2 \underset{k_{-4}}{\overset{k_4}{\rightleftharpoons}} HOBr + BrO_3 + H^+ \qquad (R4)$$

The equilibrium (R5)

$$HOBr + H^+ + Br^- \underset{k_{-7}}{\overset{k_7}{\rightleftharpoons}} Br_2 + H_2O \qquad (R5)$$

and the following reactions involved in bromine removal are also important since, these control the concentration of HOBr and in turn that of $HBrO_2$.

$$Br_2 + \text{acetone} \rightarrow \text{Bromoacetone} + H^+ + Br^-$$

$$2Ce^{4+} + HOOCCOOH \rightarrow 2Ce^{3+} + 2CO_2 + 2H^+$$

The intermediates produced in B-Z reaction are Br^-, $BrO_2^{\cdot}$, Br_2, HOBr and $HBrO_2$. For evaluating excess entropy production in the context of instability, we need only consider those intermediates which can yield negative contribution. Out of these $HBrO_2$ is autocatalytically produced about which there is a general agreement. Therefore, we shall consider the excess entropy production only with respect to perturbation in the concentration of $HBrO_2$. Accordingly, we would estimate the negative contributions of (R2) to (R4) which involve $HBrO_2$ to net excess entropy production. Now considering reactions (R3) and (R3′) we have

$$\frac{1}{2}\frac{d[BrO_2^{\cdot}]}{dt} = k_3[HBrO_2][BrO_3^-][H^+] - k_{-3}[BrO_2^{\cdot}]^2 \qquad \ldots (3)$$

and

$$-\frac{d[BrO_2^{\cdot}]}{dt} = k_{3'}[BrO_2^{\cdot}][H^+][Ce^{3+}] - k_{-3'}[Ce^{4+}][HBrO_2] \qquad \ldots (4)$$

In the stationary state, the rate of production of $BrO_2^{\cdot}$ is equal to the rate of consumption. Hence, we can write

$$2k_3[HBrO_2][BrO_3^-][H^+] - 2k_{-3}[BrO_2^{\cdot}]^2 = k_{3'}[BrO_2^{\cdot}][H^+][Ce^{3+}] - k_{-3'}[Ce^{4+}][HBrO_2] \ldots (5)$$

Further more taking into account reactions (R3) and (R3′) we can write

$$J_1 = \frac{d[HBrO_2]}{dt} = k_{3'}[H^+][BrO_2^{\cdot}][Ce^{3+}] - k_{-3'}[Ce^{4+}][HBrO_2] + k_{-3}[BrO_2^{\cdot}]^2 - k_3[HBrO_2] \times [BrO_3^-][H^+] \qquad \ldots (6)$$

Using Eq. (5) we can write,

$$J_1 = \frac{d}{dt}[HBrO_2] = k_3[HBrO_2][BrO_3^-][H^+] - k_3[BrO_2^{\cdot}]^2 \qquad \ldots (7)$$

For perturbation ($\delta[HBrO_2]$) in the concentration of $HBrO_2$, the corresponding perturbation in the reaction rate J_1 would be given by Eq. (8)

$$\delta J_1 = k_3[BrO_3^-][H^+]\,\delta[HBrO_2] \qquad \ldots (8)$$

For evaluating the corresponding changes in δA_1, we consider the equilibrium (R6)

$$HBrO_2 + BrO_3^- + 3H^+ + 2Ce^{3+} \underset{}{\overset{k_1}{\rightleftharpoons}} 2Ce^{4+} + 2HBrO_2 + H_2O \qquad (R6)$$

Now the affinity A_1 of the reaction (R6) can be written as expressed by Eq. (9)

$$A_1 = RT \ln K_1$$

$$- RT \ln \frac{[Ce^{4+}]^2[HBrO_2]^2[H_2O]}{[HBrO_2][BrO_3^-][H^+]^3[Ce^{3+}]^2} \quad \ldots (9)$$

where K_1 is the equilibrium constant of (R6).

Differentiating Eq. (9) with respect to $[HBrO_2]$, we get

$$\delta A_1 = - \frac{RT}{[HBrO_2]} \delta [HBrO_2] \quad \ldots (10)$$

Therefore from Eqs (8) and (10), we can write

$$\delta J_1 \cdot \delta A_1 = - \frac{RT k_3[BO_3^-][H^+]}{[HBrO_2]} (\delta [HBrO_2])^2 \quad \ldots (11)$$

Considering the reaction (R2), the rate J_2 and affinity A_2 can be written as Eqs (12) and (13)

$$J_2 = k_2[HBrO_2][H^+][Br^-] - k_{-2}[HOBr]^2 \quad \ldots (12)$$

$$A_2 = RT \ln k_2 - RT \ln \frac{[HOBr]^2}{[HBrO_2][H^+][Br^-]} \quad \ldots (13)$$

Differentiating Eqs (12) and (13) with respect to $[HBrO_2]$ we get,

$$\delta J_2 = k_2[H^+][Br^-] \delta [HBrO_2] \quad \ldots (14)$$

$$\delta A_2 = \frac{RT}{[HBrO_2]} \delta [HBrO_2] \quad \ldots (15)$$

Therefore,

$$\delta J_2 \cdot \delta A_2 = RT \frac{k_2[H^+][Br^-]}{[HBrO_2]} \quad \ldots (16)$$

Considering the reaction (R4), the rate J_3 and affinity A_3 can be expressed by Eqs (17) and (18) respectively

$$J_3 = 2k_4[HBrO_2]^2 - 2k_{-4}[HOBr][BrO_3^-][H^+] \quad \ldots (17)$$

$$A_3 = RT \ln k_3 - RT \ln \frac{[HOBr][BrO_3^-][H^+]}{[HBrO_2]^2} \quad \ldots (18)$$

Differenciating Eqs (17) and (18) with respect to $[HBrO_2]$, we get,

$$\delta J_3 = 4k_4[HBrO_2] \delta [HBrO_2] \quad \ldots (19)$$

$$\delta A_3 = \frac{2RT}{[HBrO_2]} \delta [HBrO_2] \quad \ldots (20)$$

Therefore,

$$\delta J_3 \cdot \delta A_3 = 8k_4 RT (\delta [HBrO_2])^2 \quad \ldots (21)$$

From Eqs (11), (16) and (21), we can express the total contribution of reactions (R2) to (R4) to the excess entropy production by Eq. (22):

$$\frac{1}{T} \sum_{i=1}^{i=3} \delta J_i \cdot \delta A_i = R[-A + B + C] \cdot (\delta [HBrO_2])^2 \quad \ldots (22)$$

where

$$A = k_3 \frac{[BrO_3^-][H^+]}{[HBrO_2]};$$

$$B = k_2 \frac{[H^+][Br^-]}{[HBrO_2]}; \; C = 8k_4$$

Now, the B-Z reaction system would be stable if

$\frac{1}{T} \sum_{i=1}^{i=3} \delta J_1 \cdot \delta A_i$ is positive, i.e., if

$$k_2 \frac{[H^+][Br^-]}{[HBrO_2]} + 8k_4 > k_3 \frac{[BrO_3^-][H^+]}{[HBrO_2]} \quad \ldots (23)$$

This would certainly be so if

$$k_2 \frac{[H^+][Br^-]}{[HBrO_2]} > k_3 \frac{[BrO_3^-][H^+]}{[HBrO_2]} \quad \ldots (24)$$

i.e.

$$r_2 > r_3 \quad \ldots (25)$$

or

$$\frac{[Br^-]}{[BrO_3^-]} > \frac{k_3}{k_2} \quad \ldots (26)$$

where $[Br^-]/[BrO_3^-]$ may be called FKN (Field-Körös-Noyes) ratio[10] following the terminology of Tyson[11]; and r_2 and r_3 are the reaction rates of steps (R2) and (R3) respectively. Equation (26) is also predicted by FKN mechanism[10,11]. Thus, the thermodynamic and kinetic analysis are in agreement.

Inequality (1) would also be satisfied if

$$8k_4 > k_3 \frac{[BrO_3^-][H^+]}{[HBrO_2]}$$

or

$$\frac{[HBrO_2]}{[BrO_3^-][H^+]} > \frac{k_3}{8k_4} \quad \ldots (27)$$

or

$$4r_4 > r_3 \quad \ldots (28)$$

where r_4 is the rate of step (R4).

Thus, stability would be assured when inequality (26) or (27) is satisfied. However, instability can occur when simultaneously

$$\frac{[Br^-]}{[BrO_3]} < \frac{k_3}{k_2} \quad \ldots (29)$$

and

$$\frac{[HBrO_2]}{[BrO_3^-][H^+]} < \frac{k_3}{8k_4} \quad \ldots (30)$$

is satisfied.

It should be noted that even if these inequalities are satisfied, it does not mean that instability would necessarily occur.

Results and Discussion

The relative contribution to excess entropy production can be numerically computed by evaluating the values of constants, *A*, *B*, and *C*. The sign of $\delta J_i \cdot \delta J_i$ will be governed by the relative magnitude of *B*, *C* and *A*. Now, *A*, *B* and *C* can be calculated provided the values of $[H^+]$, $[Br^-]$, $[BrO_3^-]$ and $[HBrO_2]$ for an open system are known, since the values k_2, k_3 and k_4 are available in the literature[12,13].

The values of $[Br^-]$ and $[HBrO_2]$ for the upper and lower limits of [acetone] were obtained from the numerical solution of bromine hydrolysis controlled model[13] which envisages the mechanism consisting of steps (S1 to S8)

$$A + Y \rightarrow X + P \quad (S1)$$
$$X + Y \rightarrow 2P \quad (S2)$$
$$A + X \rightarrow 2X + Z \quad (S3)$$
$$X + X \rightarrow P + A \quad (S4)$$
$$Z \rightarrow \text{inert product} \quad (S5)$$
$$P \rightarrow Y \quad (S6)$$
$$P + Y \rightleftharpoons W \quad (S7)$$
$$W \rightarrow Y \quad (S8)$$

(where $X = HBrO_2$, $Y = Br^-$, $Z = 2Ce^{4+}$, $P = HOBr$, $W = Br_2$ and $A = BrO_3^-$) and the differential equations (D1 to D5)

$$\frac{dX}{dt} = k_1AY - k_2XY + k_3AX(C' - Z)/C' - 2k_4X^2 \quad (D1)$$

$$\frac{dY}{dt} = -k_1AY - k_2XY + k_6P - k_7PY + k_{-7}W + k_8/(1 \times 10^{-7} + W) \quad (D2)$$

$$\frac{dZ}{dt} = k_3AX(C' - Z)/Z - k_5Z \quad (D3)$$

$$\frac{dP}{dt} = k_1AY + 2k_2XY + k_4X^2 - k_6P - k_7PY + k_{-7}W \quad (D4)$$

$$\frac{dW}{dt} = k_7PY - k_{-7}W - k_8W/(1 \times 10^{-7} + W) \quad (D5)$$

where C′ is total cerium and k_1, k_2, k_3, k_4, k_5, k_6, k_7 and k_8 are rate constants of first and subsequent steps respectively and k_{-7} is the rate constant of backward reaction of 7th step.

Calculations have been made for the reaction system having $[BrO_3^-] = 2.0 \times 10^{-2}$ *M*, $[H^+] = 1.5$ *M*, [oxalic acid] $= 2.99 \times 10^{-2}$ *M*; total cerium $= 5.0 \times 10^{-4}$ *M* at different values of [acetone].

We assume the $[BrO_3^-]$, $[H^+]$ and [acetone] to be equal to $[BrO_3^-]_0$, $[H^+]_0$ and $[acetone]_0$ as used in the numerical simulation. The subscript 0, denotes the initial concentration. Thus, the situation corresponds to pool chemical model. Using these values, we implicitly assume the system to remain open.

We have also made similar calculations for the batch reactor model. The calculations in both the cases have been made using the set of rate constants used by Field and Boyd[13] (set I) and also another set involving rate constants suggested by Field and Försterling[12] (set II). Both the sets of rate constants are given in Table 1.

We have computed the values of *A*, *B* and *C* of Eq. (22) at the limits of [acetone] as obtained from computer calculations and also for the intermediate concentrations of acetone. We note that *A* is related to autocatalytic reaction, *B* is related to the destruction of $HBrO_2$ by Br^- while *C* is related to disproportionation of $HBrO_2$. The computed values of *A*, *B* and *C*, recorded in Table 2, show that (i) at the upper limit of [acetone] as obtained from computer

Table 1—Values of rate constants

Rate constant	FB value[13] (set I)	FF value[12] (set II)
k_2	$2.0 \times 10^9\ M^{-2}\ s^{-1}$	$3.0 \times 10^6\ M^{-2}\ s^{-1}$
k_3	$1.0 \times 10^4\ M^{-2}\ s^{-1}$	$42.0\ M^{-2}\ s^{-1}$
k_4	$4.0 \times 10^7\ M^{-1}\ s^{-1}$	$3.0 \times 10^3\ M^{-1}\ s^{-1}$

calculations, $C > A$ while B < A and (ii) at the lower limit of [acetone], $B > A$ while $C < A$. In between the two limits A is greater than both B and C. Noting the inequalities (29) and (30) the results confirm that oscillation proceeds so long as autocatalytic reaction predominates over (R2) and (R4). However, the system becomes stable when (R2) predominates over the autocatalytic reaction. This happens at the lower limit. Again, the system becomes stable when (R4) predominates over autocatalytic reaction which happens at the upper limit of [acetone]. The results recorded in Table 2 show that the conclusions are unaffected by the choice of rate constants.

The results can be expressed more effectively graphically. In Figs 1-3, values of A, B and C have been expressed as a function of time. At the lower limit of [acetone], $B > A$ all along while at the upper limit of [acetone], $C > A$ all along. Results plotted in Fig. 3 show how in the oscillatory domain, A, B and C change with time. The values of A, B and C oscillate since $[Br^-]$ and $[HBrO_2]$ oscillate. In the range PQ, P′Q′ and P″Q″, the magnitude of A is higher than the corresponding values of B and C, hence oscillations are possible. In the time space QQ′ or Q′Q″, we find that the magnitude of B and C is higher than A and autocatalysis is not possible. This is what we observe actually in oscillatory reaction (see Fig. 4).

It should be noted that thermodynamic theory of stability[1] inspite of its limitations as pointed out earlier, only provides a guideline. It can only indicate when the system can get destabilized. Numerical solution of appropriate differential equations, relating to the chemical dynamics, is needed ultimately to predict when oscillations would occur. Even for computation of parameters required in the theory, concentrations obtained from computer results are needed. Thus, both kinetic and thermodynamic approaches together provide a better insight into the characteristics of the BZ oscillators containing mixed organic substrates.

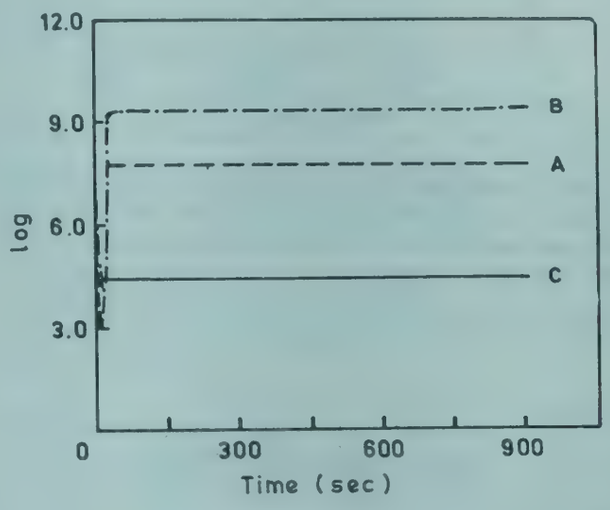

Fig. 1—Plot of computed values of A, B and C versus time at the lower limit of [acetone] based on Eq. (22) and the BHC model [System: oxalic acid (2.99×10^{-2} M) + acetone (1.0×10^{-2} M) + Ce^{4+} (5.0×10^{-4} M) + BrO_3^- (2.0×10^{-2} M) + H_2SO_4 (1.5 M)]

Table 2—Values of constnats A, B and C at two limits and for intermediate ranges of [acetone]

[Acetone]		Using rate constants of	Value of Parameter (M^{-1} s^{-1})		
			A	B	C
Upper limit	Pool chemical model	Set I	2.6×10^8	7.6×10^6	3.2×10^8
		Set II	1.0×10^4	4.0×10^2	2.4×10^4
Oscillatory domain (near upper limit)	do	Set II	7.6×10^5	7.5×10^5	2.4×10^4
Oscillatory domain (near lower limit)	do	Set II	1.1×10^6	7.5×10^5	2.4×10^4
Lower limit	do	Set I	4.5×10^{12}	1.3×10^{14}	3.2×10^8
		Set II	6.3×10^7	3.6×10^9	2.4×10^4
Upper limit	Batch reactor model	Set I	1.0×10^8	1.0×10^7	3.2×10^8
		Set II	7.5×10^3	3.5×10^2	2.4×10^4
Oscillatory domain (near upper limit)	do	Set II	1.2×10^6	1.4×10^6	2.4×10^4
Oscillatory domain (near lower limit)	do	Set II	7.1×10^5	7.9×10^5	2.4×10^4
Lower limit	do	Set I	3.8×10^{12}	1.4×10^{14}	3.2×10^8
		Set II	6.1×10^7	2.3×10^9	2.4×10^4

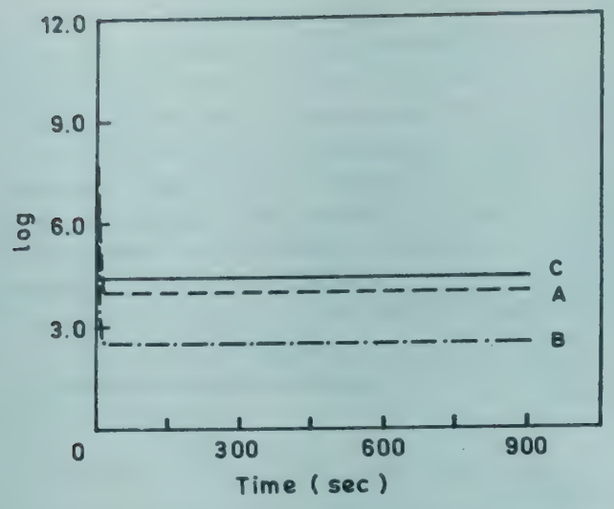

Fig. 2—Plot of computed values of A, B and C versus time at the upper limit of [acetone] based on Eq. (22) and the BHC model [System: oxalic acid (2.99×10^{-2} M) + acetone (1.4 M) + Ce^{4+} (5.0×10^{-4} M) + BrO_3^- (2.0×10^{-2} M) + H_2SO_4 (1.5 M)]

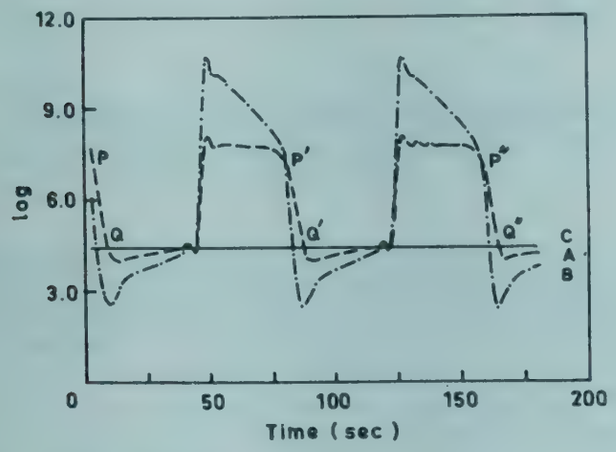

Fig. 3—Plot of computed values of A, B and C versus time for the oscillatory domain of [acetone] based on Eq. (22) and the BHC model [System: oxalic acid (2.99×10^{-2} M) + acetone (1.0 M) + Ce^{4+} (5.0×10^{-4} M) + BrO_3^- (2.0×10^{-2} M) + H_2SO_4 (1.5 M)]

The phenomena of critical limits can be understood as follows:

At high [Br^-], reaction (R2) removes $HBrO_2$ from the system sufficiently fast so that reaction (R3) is suppressed and the autocatalytic production of $HBrO_2$ by the sequence of reactions (R3) + (R4′) does not occur. A pseudo-steady state is reached in which $HBrO_2$ is produced in the reaction

$$Br^- + BrO_3^- + 2H^+ \rightleftarrows HOBr + HBrO_2$$

and consumed in the step (R2). The [Br^-] does decrease, though because of factor that removes Br_2 from the system. When [Br^-] falls sufficiently low, reaction (R2) can no longer remove $HBrO_2$ fast enough to suppress (R3) and auto-catalytic oxidation of Ce^{3+} to Ce^{4+} begins. The auto-catalytic production of $HBrO_2$ is limited by its disproportionation in

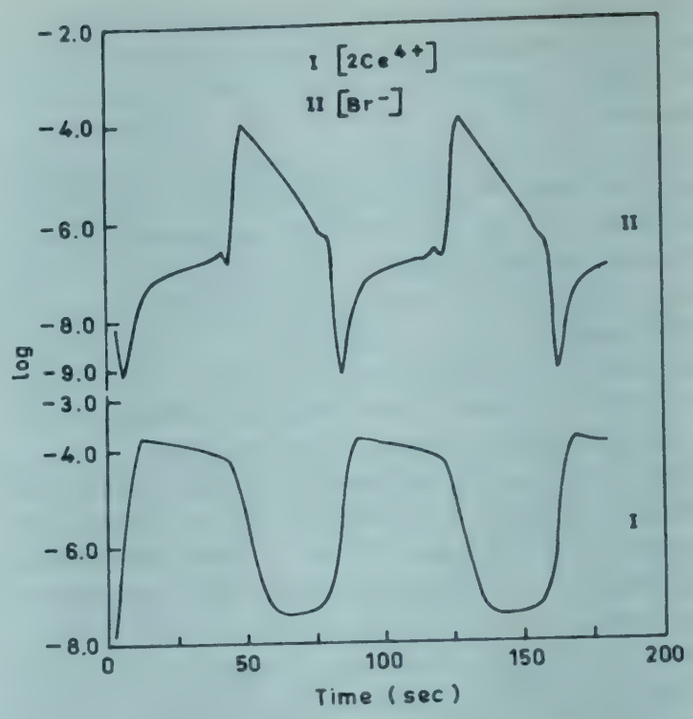

Fig. 4—Plot of computed values of (I) log [$2Ce^{4+}$] and (II) log [Br^-] versus time based on the BHC model [System: oxalic acid (2.99×10^{-2} M) + acetone (1.0 M) + Ce^{4+} (5.0×10^{-4} M) + BrO_3^- (2.0×10^{-2} M) + H_2SO_4 (1.5 M)]

reaction (R4) leading to a new pseudo-steady state in which $HBrO_2$ is produced in the reactions (R3) and (R3′) and consumed in the reaction (R4). HOBr produced by (R4) is reduced to Br_2.

Acknowledgement

The authors are thankful to the UGC, New Delhi for supporting the investigation.

References

1 Glansdorff P & Prigogine I, *Thermodynamic theory of structure, stability and fluctuations* (Wiley Interscience, New York) 1971.
2 Nicolis G & Prigogine I, *Self-organization in non-equilibrium systems* (Wiley Interscience, New York) 1977.
3 Rastogi R P & Ram Shabd, *J chem Edn*, 60 (1983) 540.
4 Rastogi R P & Ram Shabd, *J nonequilib Thermodyn*, 6 (1981) 201.
5 Keizer J, *Statistical thermodynamics of non-equilibrium processes* (Springer-Verlag, New York) 1987, pp 361.
6 Ross J & Garcia-Colin L S, *J phys Chem*, 93 (1989) 2091.
7 Garcia-Colin L S, De la Selva S M T & Pina E, *J phys Chem*, 90 (1987) 953.
8 Lebom G, Torrisi M & Valenti A, *J phys Chem*, 91 (1987) 5103.
9 Rastogi R P & Verma M K, *Indian J Chem*, 22A (1983) 830.
10 *Oscillations and travelling waves in chemical systems* edited by R J Field and M Burger (John Wiley, New York) 1985.
11 Tyson J J in ref 10, pp 100.
12 Field R J & Försterling H D, *J phys Chem*, 90 (1986) 5400.
13 Field R J & Boyd P M, *J phys Chem*, 89 (1985) 3707.

Indian Journal of Chemistry
Vol. 30A, March 1991, pp. 209-214

Dimensional response of engineering polymeric elastomers in the presence of halo-substituted benzenes

S B Harogoppad & T M Aminabhavi*

Department of Chemistry, Karnatak University, Dharwad, 580 003

Received 20 February 1990; revised 4 September 1990; accepted 22 October 1990

Dimensional response of several engineering polymers in the presence of halo-substituted benzenes has been studied by weight-gain and swelling measurements. The experimental data have been used to estimate the diffusion coefficients, kinetic rate constants, activation parameters and molar mass between crosslinks for all the polymer-solvent systems.

The swelling of a crosslinked network polymeric elastomer by a solvent is one of the possible structural changes which measure the dimensional stability of a polymer in the presence of a solvent. These structural changes require a rearrangement of chain segments which can dominate the sorption kinetic behaviour and solvent transport into the polymer matrix. The mechanism of liquid transport in rubbery polymers has been fairly well understood, yet the exact mathematical modelling of the phenomenon is still not available[1-3]

Styrene butadiene rubber (SBR), nitrile butadiene rubber (NBR), natural rubber (NR), polychloroprene (CR) and ethylene propylene diene terpolymer (EPDM) have been widely used as engineering polymers. In a variety of applications, these polymers may come into contact with organic solvents in addition to other foreign ingredients. On coming in contact with such liquids, many polymers have a tendency to swell thereby restricting their usage. In view of this, a study has been initiated in our laboratory to assess the transport behaviour of polymer membranes in the presence of organic solvents[4-7]. In continuation of this work, we now present results of experimental and theoretical studies on the transport characteristics of SBR, NBR, CR, NR and EPDM elastomeric polymer membranes with respect to chlorobenzene, bromobenzene and fluorobenzene.

Materials and Methods

Polymer sheets of SBR, NBR, CR, NR and EPDM in dimensions of $1/16'' \times 6'' \times 6''$ were supplied as gift samples by UTEX Industries, Texas (courtesy of Mr A. Kutac). Mixing and moulding of the polymer compounds was done in a 12″ laboratory mill and the polymer sheets were cured at 160°C for 20 min.

Reagent grade solvents, namely chlorobenzene, bromobenzene and fluorobenzene were doubly distilled before use.

Diffusion experiments

Circular samples of polymers were cut (diameter = 1.94 cm) by means of a sharp-edged steel die and their thicknesses were measured at several points on the membranes using a micrometer (accuracy ±0.001 cm). The diffusion experiments were performed for each polymer-solvent system by soaking the samples in the respective solvents (≃ 20 ml) taken in test bottles maintained at 25 ± 0.5°C in a thermostatic oven (Memmert, Germany). The mass-gain of the samples and changes in their thickness were measured at periodic intervals by removing the samples out of the test bottles. Details of the experimental procedures have been published earlier[4].

Results and Discussion

The output data from a diffusion experiment is the per cent weight gain, $Q(t)$ (expressed as mol per cent increase) and per cent increase in thickness, $L(t)$, of the sample versus square root of time, $t^{1/2}$. Such plots (Fig. 1), referred to as sorption curves, are independent of material thickness for a Fickian diffusion process[3]. Similarly, the curves for percentage increase in thickness are shown in Fig. 2. It is, however, clear that either $Q(t)$ or $L(t)$ increases linearly with $t^{1/2}$, during early stages of diffusion experiments; at longer time intervals, these curves level off. For all the solvents, either $Q(t)$ or $L(t)$ values are found to be higher in the case of SBR, whereas lower values are observed for EPDM membrane (see Fig. 2). This suggests that EPDM would be a better barrier membrane in view of its lower values of swelling. The sorption behaviour of EPDM and CR membranes is almost identical (see Fig. 1) and the

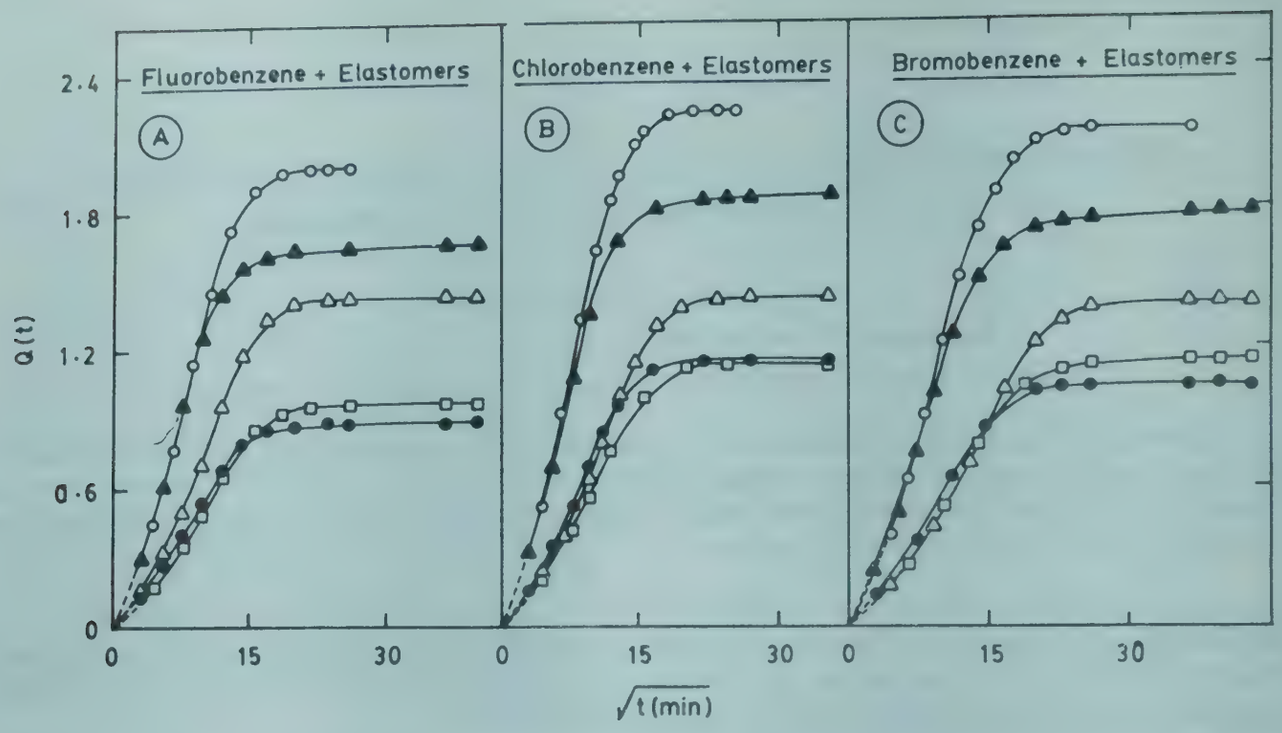

Fig. 1—Sorption curves, i.e., $Q(t)$ vs $t^{1/2}$ for (A) fluorobenzene with (○) SBR; (△) NBR, (□) CR, (●) EPDM and (▲) NR; (B) chlorobenzene with the same polymer membranes as in (A); and (C) bromobenzene with the same polymer membranes as in (A).

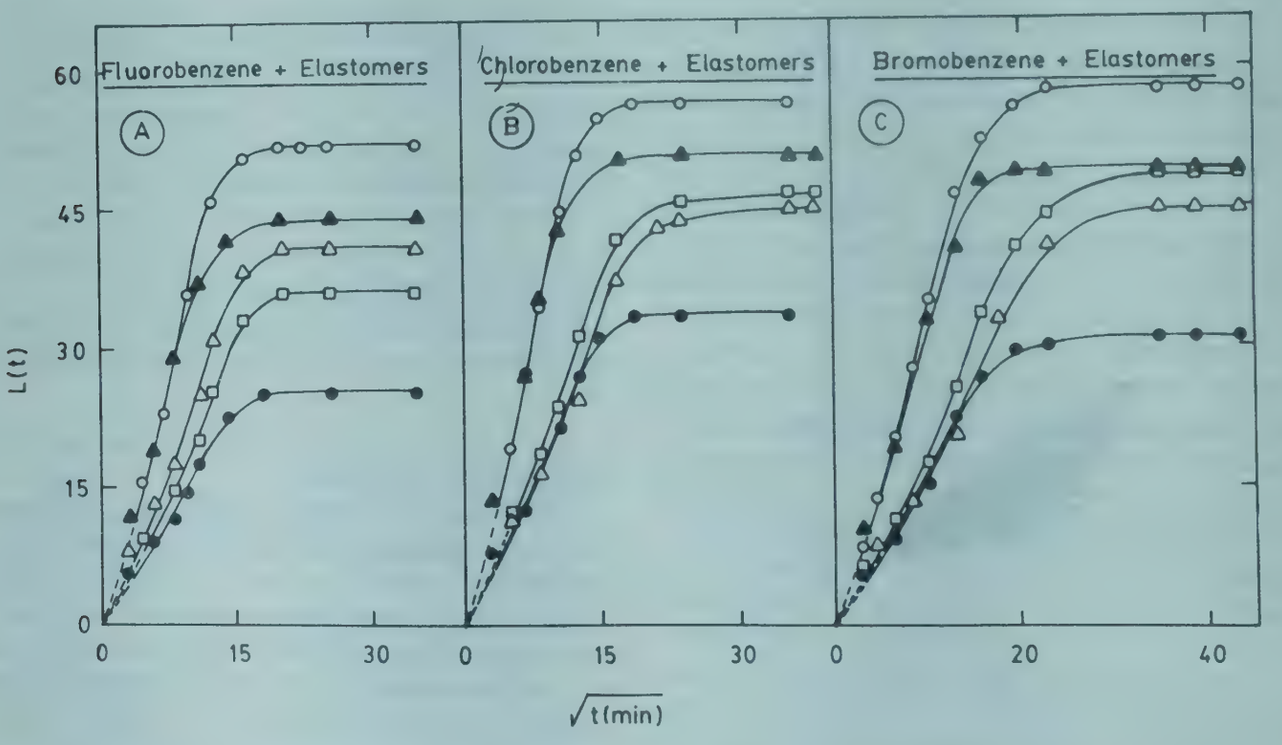

Fig. 2—Sorption curves, i.e., $L(t)$ vs $t^{1/2}$ for (A) fluorobenzene with (○) SBR, (△) NBR, (□) CR, (●) EPDM and (▲) NR; (B) chlorobenzene with the same polymer membranes as in (A); and (C) bromobenzene with the same polymer membranes as in (A).

sorption curves for such membranes may be rationalized in terms of chain segment motions relative to the concurrent solvent diffusion rates[3].

The sorption curves of Figs 1 and 2 suggest that the transport phenomenon follows the Fickian mechanism. It is, therefore, possible to estimate the concentration-independent diffusion coefficients[4] (D_Q) by using Eq. 1,

$$D_Q = \pi (h\,\theta/4Q_\infty)^2 \qquad \ldots (1)$$

where h is polymer thickness, θ is the slope of the initial linear portion of the sorption curves shown in

Fig. 1 and Q_∞ represents the maximum sorption values (saturation equilibrium values) of the polymer-solvent systems as obtained from the plateau regions.

In an analogous manner, diffusion coefficients can also be estimated from the maximum swelling data (L_∞) (see Fig. 2) as[4],

$$D_L = (h\,\theta/4L_\infty)^2 \qquad \ldots (2)$$

where θ is the slope of the intial linear portion of the sorption curves given in Fig. 2. Due to the significant swelling of the polymer samples in the presence of liquids considered, an attempt was made to apply correction to diffusion coefficients, D_L, to include 3-dimensional transport. This can be done by following the procedure suggested by Shen and Springer[8] for a rectangular geometry of the sample. For disc shaped polymer samples, the modified relation would be,

$$\bar{D}_L = D_L\left[1 + \frac{\bar{h}}{\bar{r}} + \frac{\bar{h}}{2\pi\bar{r}}\right]^2 \qquad \ldots (3)$$

where $\bar{D}_L$ is the average value of the diffusion coefficient, $\bar{h}$ and $\bar{r}$ represent, respectively, average thickness and radius of polymer samples. The maximum equilibrium data, i.e., Q_∞ and L_∞ along with D_Q and $\bar{D}_L$ values are summarized in Table 1. It is heartening to note that there is an excellent agreement between the D_Q and $\bar{D}_L$ values for the majority of polymer-solvent systems.

From the foregoing discussion, it is apparent that the sorption is a rate controlled kinetic process which can be studied by the first order kinetic rate equation[9]. Thus,

$$\frac{dc}{dt} = k\,(C_\infty - C_t) \qquad \ldots (4)$$

where k (min^{-1}) is the first order rate constant; C_t and C_∞ are the concentrations at time t and at infinite time t_∞ respectively. Upon integration, Eq. 1 yields,

$$kt = 2.303 \log\left(\frac{C_\infty}{C_\infty - C_t}\right) \qquad \ldots (5)$$

In order to investigate the temperature-dependent kinetic rate behaviour, sorption experiments were carried out at 44° and 60°C in addition to room temperature. The estimated rate constants at 25°, 44° and 60°C and the activation energies (E_a) as estimated from the Arrhenius relationship[10] are given in Table 2.

Some useful kinetic plots are given in Figs 3 and 4. From the results of rate constants and activation energies given in Table 2 and evaluated from Fig. 5, we could not conclude any quantitative correlationship, yet some general tendencies could be observed. For instance, lower E_a values as observed in the cases of SBR and NR compared to those for CR and EPDM are attributed to the easy transport of solvents through the membranes. This fact is also supported by the higher values of $\bar{D}_L$ or D_Q for SBR and NR than those for CR and EPDM membranes. For NBR, however, diffusion coefficients are small and the E_a values are somewhat high (see Table 2).

Table 1—Some transport data of polymer-solvent systems at 25°C

Solvent	Property	Polymer membranes				
		NBR	CR	EPDM	SBR	NR
Fluorobenzene	Q_∞ (mole %)	1.42	0.97	0.88	1.99	1.65
	L_∞ (%)	40.80	36.10	25.10	51.90	44.10
	$D_Q.10^7$ (cm^2/s)	5.30	6.47	6.94	8.32	10.67
	$\bar{D}_L.10^7$ (cm^2/s)	4.40	5.52	4.90	6.78	9.75
Bromobenzene	Q_∞ (mole %)	1.39	1.14	1.03	2.14	1.78
	L_∞ (%)	44.70	48.40	30.90	57.50	48.60
	$D_Q.10^7$ (cm^2/s)	2.76	4.47	4.91	5.09	5.98
	$\bar{D}_L.10^7$ (cm^2/s)	2.81	4.04	4.16	8.82	7.51
Chlorobenzene	Q_∞ (mole %)	1.42	1.14	1.15	2.22	1.87
	L_∞ (%)	44.90	46.50	33.30	56.10	50.50
	$D_Q.10^7$ (cm^2/s)	4.43	6.55	7.49	8.90	9.93
	$\bar{D}_L.10^7$ (cm^2/s)	4.20	6.58	3.91	8.01	9.61

Table 2—Sorption kinetic data for polymer-solvent systems, activation energies and molar mass between crosslinks

Polymer	Property[a]	Solvent								
		Fluorobenzene			Chlorobenzene			Bromobenzene		
		25°C	44°C	60°C	25°C	44°C	60°C	25°C	44°C	60°C
NBR	$k.10^3$	7.29	11.53	16.15	6.47	8.64	11.17	3.68	6.02	8.59
	E_a		18.82 ± 0.29[b]			12.87 ± 0.25			20.11 ± 0.30	
	M_c	175			589			639		
CR	$k.10^3$	7.37	9.52	13.22	7.03	9.68	12.88	5.28	7.59	9.45
	E_a		13.64 ± 0.27			14.24 ± 0.31			13.80 ± 0.36	
	M_c	458			820			933		
EPDM	$k.10^3$	9.59	14.07	19.02	9.66	14.07	17.19	6.95	9.71	13.00
	E_a		16.16 ± 0.26			13.72 ± 0.40			14.75 ± 0.25	
	M_c	819			823			1109		
SBR	$k.10^3$	11.20	16.01	18.04	11.92	14.35	17.02	7.59	10.46	12.72
	E_a		11.46 ± 0.24			8.39 ± 0.31			12.25 ± 0.22	
	M_c	619			968			1591		
NR	$k.10^3$	14.56	19.18	23.07	13.36	17.14	19.83	9.19	11.90	14.06
	E_a		10.91 ± 0.25			9.38 ± 0.33			10.09 ± 0.23	
	M_c	871			1333			1728		

[a] k in min^{-1}; E_a in kJ/mol.
[b] relative standard error at 95% confidence level.

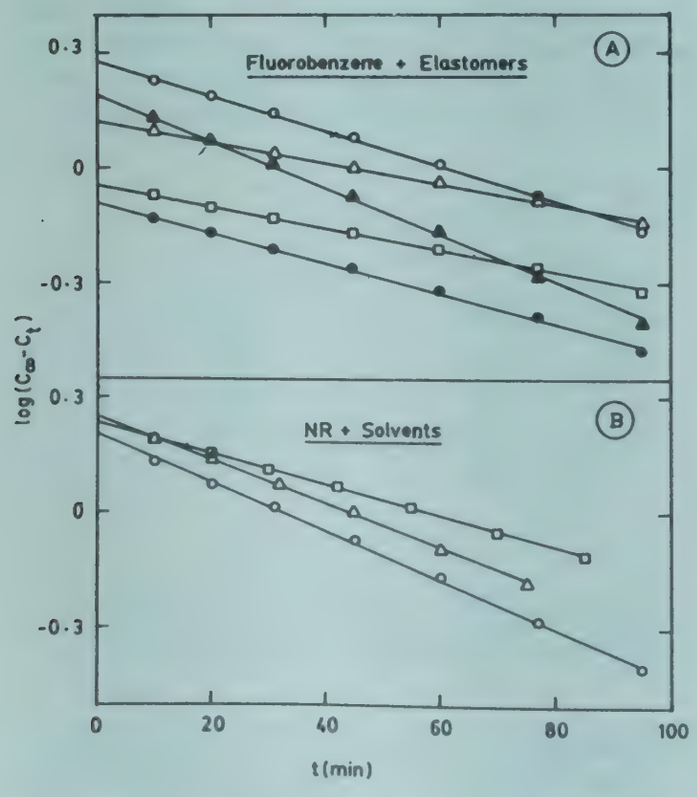

Fig. 3—Plots of log $(C_\infty - C_t)$ vs t for (A) fluorobenzene with elastomers: (○) SBR, (△) NBR, (□) CR, (●) EPDM, (▲) NR; (B) NR with solvents: (○) fluorobenzene, (△) chlorobenzene, (□) bromobenzene.

For a comprehensive understanding of the structure-property relationships of the elastomers in the presence of a solvent, it is necessary to know the magnitude of polymer-solvent interaction parameter (χ) and hence the molar mass between crosslinks (M_c). The criterion for swelling equilibrium was first recognized by Frenkel[11] and was later developed by Flory and Rehner[12] (FR). For a successful calculation of M_c by this theory, we need reliable values of χ for the solvent-polymer pair. A number of methods of determining χ have been suggested in the literature[13]. All these methods are empirical and require the use of solubility parameter of the solvent. Instead, we suggest calculation of χ based on the phenomenological approach. This method is based on expressing the FR equation into a derivative of volume fraction of the polymer (ϕ_p) in the completely swollen state with respect to temperature. Thus,

$$\left(\frac{d\phi_p}{dT}\right) = \frac{\chi\phi_p^2/T}{2\chi\phi_p - \frac{\phi_p}{1-\phi_p} - [\ln(1-\phi_p) + \phi_p + \chi\phi_p^2]N} \quad \ldots (6)$$

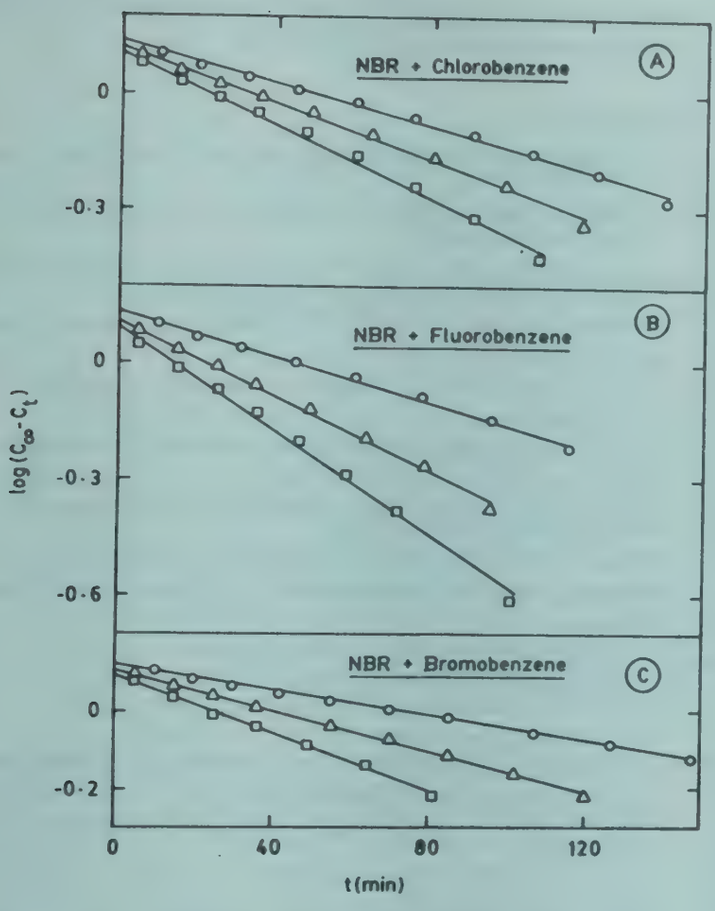

Fig. 4—Plots of $\log (C_\infty - C_t)$ vs t for (A) NBR with chlorobenzene at (○) 25°C, (△) 44°C, (□) 60°C; (B) NBR with fluorobenzene at (○) 25°C, (△) 44°C, (□) 60°C; (C) NBR with bromobenzene at (○) 25°C, (△) 44°C, (□) 60°C.

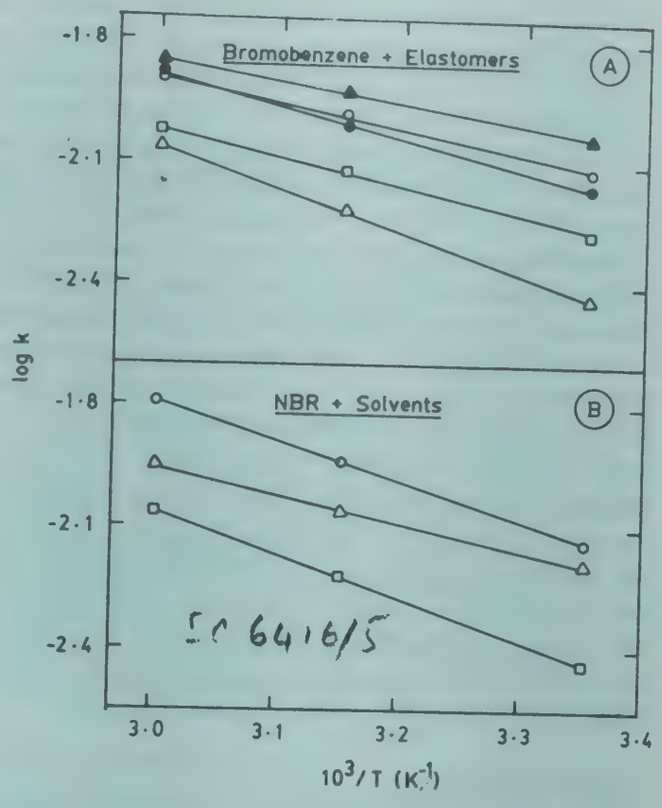

Fig. 5—Arrhenius plots of $\log k$ vs $1/T$ for (A) bromobenzene with elastomers: (○) SBR, (△) NBR, (□) CR, (●) EPDM, (▲) NR; (B) NBR with solvents: (○) fluorobenzene, (△) chlorobenzene, (□) bromobenzene.

where $N = \dfrac{\left(\dfrac{\phi_p^{2/3}}{3} - \dfrac{2}{3}\right)}{(\phi_p^{1/3} - 2\phi_p/3)}$ ... (7)

so that

$$\chi = \frac{(d\phi_p/dT)[\{\phi_p/(1-\phi_p)\} + N\ln(1-\phi_p) + N\phi_p]}{[2\phi_p(d\phi_p/dT) - \phi_p^2 N(d\phi_p/dT) - \phi_p^2/T]} \quad \ldots (8)$$

The volume fraction ϕ_p of the swollen polymer can be calculated as:

$$\phi_p = \left[1 + \frac{\rho_p}{\rho_s}\left(\frac{M_a}{M_b}\right) - \left(\frac{\rho_p}{\rho_s}\right)\right]^{-1} \quad \ldots (9)$$

Here, M_b and M_a are respectively the mass of polymer before and after swelling, ρ_s is solvent density and ρ_p is density of the polymer (ρ_p values are: SBR = 1.15; EPDM = 1.09; NBR = 1.21; CR = 1.42; and NR = 1.14). Computation of $(d\phi_p/dT)$ can be done from a least-squares fit of the ϕ_p data versus temperature (T).

The molar mass between crosslinks can then be obtained from the FR model as:

$$M_c = \frac{-\rho_p V_s[(\phi_p)^{1/3} - \phi_p/2]}{[\ln(1-\phi_p) + \phi_p + \chi\phi_p^2]} \quad \ldots (10)$$

where V_s is molar volume of solvent and the parameter χ used here has been estimated from Eq. 8. The estimated M_c values are also included in Table 2.

Wide variations in M_c values are observed, which depend on the nature of interacting solvents. For instance, in the case of NBR + fluorobenzene system, M_c is about 175 whereas higher values are observed for NBR with chloro- and bromobenzene, i.e., 589 and 639 respectively. In general, for fluorobenzene, M_c values are smaller than those observed for either chlorobenzene or bromobenzene. To some extent, this discrepancy may be attributed to the limitations of the FR theory.

It should be realized that if we can calculate the χ values directly from the classical relationship given by Hildebrand *et al.*[14] based on the solubility parameter concept, further calculations of M_c from Eq. 10 are somewhat identical to those based on our values of χ from Eq. 8. For instance, in the case of CR + bromobenzene a value of $M_c = 869$ agrees

somewhat with our calculated M_c (933). At any rate, our method of sorption and hence the computed M_c data given in Table 2 may be regarded as realistic.

The status of the FR theory is still unresolved. It appears that the interaction of the solvent with the crosslinks is different from that with mid chain segments. If this is the case, the elastic modulus may be solvent-dependent because inappropriate account had been taken of the crosslink-solvent mixing term. However, calculations made to estimate χ on swelling showed that this is an unlikely source of the limitation of the FR theory. A need for the modification of FR model has been recently suggested[15] in a study where it has been demonstrated that the assumption of separability of mixing and elastic free energies is incorrect. Our present data suggest that the elastic free energy of isotropically swollen elastomer cannot be evaluated without a viable theory. We hope to continue these measurements in the future with other systems to explore the thermodynamic variables which influence such results.

Acknowledgement

The authors appreciate the generous support from the UGC, New Delhi, India in the form of teacher fellowship to Mr. S.B. Harogoppad to study at Karnatak University, Dharwad.

References

1 Crank J & Park G S, *Diffusion in polymers* (Academic Press, New York) 1968.
2 Crank J, *The mathematics of diffusion*, 2nd ed (Clarendon Press, Oxford) 1975.
3 Aminabhavi T M, Aithal U S & Shukla S S, *J macromol Sci Rev Macromol Chem Phys*, C 28(3&4) (1988) 421.
4 Aithal U S, Aminabhavi T M & Cassidy P E, *Polymer Prepr*, 30(1) (1989) 17.
5 Aminabhavi T M & Cassidy P E, *Polym Commun*, 27 (1986) 254.
6 Cassidy P E, Aminabhavi T M, Manjeshwar L S & Balundgi R H, *J sci ind Res*, 45 (1986) 244.
7 Britton L N, Ashman R B, Aminabhavi T M & Cassidy P E, *J chem Educ*, 65 (1988) 368.
8 Shen C H & Springer G S, *J Comp Mat*, 10 (1976) 2.
9 Harogoppad S B & Aminabhavi T M, *J chem Educ*, (1990) in press.
10 Golden D M, *J chem Educ*, 48 (1971) 235.
11 Frenkel J, *Rubb Chem Technol*, 13 (1940) 264.
12 Flory P J & Rehner (Jr) J, *J chem Phys*, 11 (1943) 521.
13 Takahashi S, *J appl polym Sci*, 28 (1983) 2847.
14 Hildebrand J H & Scott R L, *Solubility of nonelectrolytes*, 3rd ed (Reinhold, New York), 1950.
15 Neuberger N A & Eichinger B E, *Macromolecules*, 21 (1988) 3060.

Indian Journal of Chemistry
Vol. 30A, March 1991, pp. 215-218

Template copolymerization of methyl methacrylate and styrene on poly(methyl methacrylate)

Sanjay K Awasthi & A K Srivastava*
Department of Chemistry, Harcourt Butler Technological Institute, Kanpur 208002

Received 23 July 1990; revised 14 September 1990; accepted 1 October 1990

The radical copolymerization of methyl methacrylate and styrene using syn-poly(methyl methacrylate) ($\bar{M}_v$ = 98,890) as template in dimethylformamide (DMF), at 60° for 150 minutes results in an alternate copolymer, as evidenced from NMR spectroscopy. Viscometric measurements have shown that complexation between template and oligomer of syn-PMMA is maximum at template/copolymer ratio of 1:1 and the time of complexation is about 9 min. The average molecular weight ($\bar{M}_v$) of daughter copolymer is not identical to that of template because of chain transfer reaction to template. The template effect and average molecular weight ($\bar{M}_v$) of daughter copolymer are direct functions of concentration as well as $\bar{M}_v$ of template. The energies of activation for template and blank polymerization are 46.0 and 64.0 kJ mol^{-1}, respectively. The system follows Mechanism II, as evidenced from effect of an analogue and dioxane.

Template polymerization helps to synthesise polymers or copolymers having precise structures and microstructures complementary to those of the template. A search of literature reveals that almost all reports on template polymerization have been published in connection with biosynthesis of proteins and self-replication of DNA and on homopolymerization[1-6] of vinyl monomer. Only a few systems have been studied in which two monomers are polymerized in the presence of template[7,8].

The present study has been undertaken to throw more light on the mechanism of template polymerization. Further it has been established that poly(methyl methacrylate) (PMMA) can be successfully used for the copolymerization of methyl methacrylate and styrene.

Materials and Methods

Reagent grade methyl methacrylate (MMA) and styrene (Sty) after purification were stored at 0°C. α, α′-Azobisisobutyronitrile (AIBN) was recrystallised twice from methanol (m.p. 102°C). Syn-PMMA used as a template, was obtained by polymerization of MMA in dry benzene ([MMA] = 6.92 mol dm^{-3}) under nitrogen at 30°C using [AIBN] = 2.03 × 10^{-2} mol dm^{-3} as an initiator. The average molecular weight of template was calculated from viscosity data, determined in benzene at 30°C, using the relationship[9],

$$[\eta] = 8.35 \times 10^{-5} \bar{M}_v^{0.73} \quad \ldots (1)$$

When benzene was replaced by a chain transfer promoting solvent, viz. toluene, syn-PMMA of low molecular weight was obtained.

Template polymerization

The sample, containing MMA, Sty, PMMA and AIBN in DMF was flushed with nitrogen and injected into a modified dilatometer, which was placed in a thermostat bath (60±0.1°C). The progress of reaction was monitored with the help of a cathetometer as meniscus movement per unit volume per unit time. The rate of copolymerization (R_p) was calculated from slope of the plots of per cent conversion versus time. The polymerization was terminated after 150 min. and the polymerization mixture was poured into a large amount of methanol containing hydroquinone to precipitate the polymer. The resulting polymer was purified by reprecipitation from methanol and dried in a vacuum oven. The polymer was refluxed with acetonitrile to remove template and PMMA (homopolymer) and then with cyclohexane to remove polystyrene. The yield of daughter copolymer was used to calculate per cent conversion.

The intrinsic viscosity [η] of daughter copolymer, determined in toluene at 30°C with a Ubbelohde viscometer, was used to calculate the average viscosity molecular weight ($\bar{M}_v$), using the following relationship[10].

$$[\eta] = 13.2 \times 10^{-5} \bar{M}_v^{0.71} \quad \ldots (2)$$

Results and Discussion

Viscometric measurements

In order to investigate complexation between syn-PMMA and copolymer, the polymers were dissolved in DMF and mixed and change in reduced viscosity $[\eta]_{red}$ ($=\eta_{sp}/C$) of the mixture of

syn-PMMA and copolymer in DMF as a function of composition was plotted (Fig. 1). The curve showed a minimum of PMMA/copolymer ratio of 1:1. The solvent treatment of copolymer reveals that weight loss with acetonitrile is more than that with cyclohexane. This indicates, that complexation between template and oligomer of PMMA takes place. Complexation is very fast and rapid drop of η_{red} within 9 min. (Fig. 2) shows that the complexation is virtually completed in 9 min. Early reports[11] regarding complete complex formation in template homopolymerization, also showed that the time required for complete complex formation was generally 10 to 20 min.

Effect of concentration of template

The influence of varying [template], expressed as V_R (where $V_R = R_P$ (template)/R_p (blank) is compiled in Table 1. There is a continuous increase in V_R with [template] and reaches a maximum at syn-PMMA/copolymer ratio of 1:1 and thereafter it becomes constant. This shows that the system follows Mechanism II. This also suggests that the growing oligomers, created in solution and which have attained a minimum critical chain length, can form complex with template. It is clear that as the concentration of template increases (Table 1), the $\bar{M}_v$ of daughter polymer increases, although it is not identical to that of template possibly because of the reasons mentioned above. Table 1, also shows the effect of $\bar{M}_v$ of template on the V_R and $\bar{M}_v$ of the daughter copolymer which increases with $\bar{M}_v$ of template, as expected for template polymerization.

Effect of varying [monomer]

The results on the effect of varying [monomer] are presented in Table 2. The plots of V_R against [MMA] and [Sty] are linear, indicating that there is preferential adsorption of oligomer into the template. This further confirms[4] that the system follows Mechanism II, because in case of Mechanism I, the shape of curve would have been concave[13]. The order of reaction with respect to monomers, calculated from the slope of plots of log R_p versus log [monomer], is unity, for both the monomers.

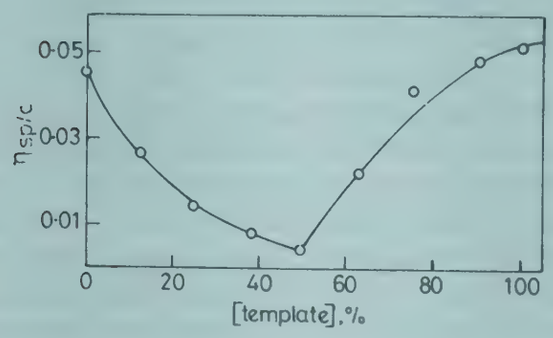

Fig. 1—Relationship between η_{sp}/C and per cent template concentration at 60 ± 0.1°C

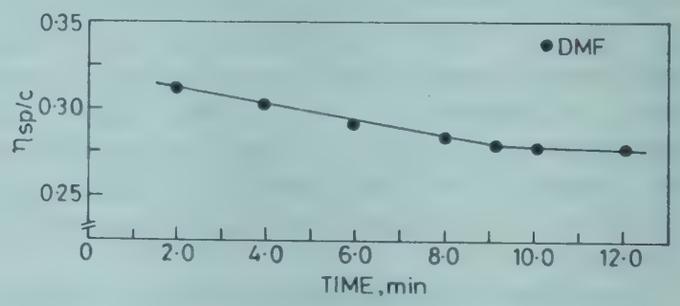

Fig. 2—Relationship between η_{sp}/C and time

Table 1—Effect of [template] and molecular weight of template on the polymerization of methyl methacrylate with styrene [MMA] = 0.45 mol dm^{-3}; [Sty.] = 0.45 mol dm^{-3}; [AIBN] = 2.03 × 10^{-2} mol dm^{-3}; time = 150 min; temp = 60 ± 0.1°C

[Template] base *M*	Mol wt of template	$R_p \times 10^5$ mol $dm^{-3}s^{-1}$	Per cent conversion	V_R	Mol wt of daughter polymer
0.00	—	2.00	18.98	0.00	20,110
0.12	98,890	3.75	36.99	1.87	36,000
0.24	98,890	4.04	42.02	2.02	40,160
0.48	98,890	5.00	44.06	2.50	53,390
0.72	98,890	5.42	44.53	2.71	69,020
0.90	98,890	6.00	46.00	3.00	71,740
0.93	98,890	6.02	46.12	3.01	—
0.96	98,980	6.01	46.02	3.00	—
1.00	98,890	6.00	46.00	3.00	—
0.90	65,360	2.10	18.95	1.05	40,160
0.90	75,820	2.83	21.98	1.41	57,390
0.90	84,016	3.00	23.65	1.50	66,340
0.90	92,640	3.60	32.05	1.80	70,070

Table 2—Effect of [monomer] and [initiator] on the template copolymerization of methyl methacrylate and styrene

[PMMA] = 0.90 base M; time = 150 min; temp = 60 ± 0.1°C

[Sty.] mol dm^{-3}	[MMA] mol dm^{-3}	[AIBN] × 10^2 mol dm^{-3}	Per cent conversion	$R_p \times 10^5$ mol $dm^{-3}s^{-1}$	V_R
0.45	0.45	2.03	46.00	6.00	3.00
0.86	0.45	2.03	54.26	10.50	5.25
1.29	0.45	2.03	55.62	15.23	7.61
0.45	0.45	2.03	46.00	6.00	3.00
0.45	0.90	2.03	53.69	10.30	5.15
0.45	1.35	2.03	55.01	14.40	7.20
0.45	0.45	1.52	39.99	5.02	2.51
0.45	0.45	2.54	43.99	6.65	3.32
0.45	0.45	3.04	52.10	7.61	3.80

Effect of varying [initiator]

The influence of [AIBN] on the copolymerization of MMA with styrene was studied by varying [AIBN] from 1.52 × 10^{-2} to 3.04 × 10^{-2} mol dm^{-3}. The R_p is direct function of [AIBN] and the order of reaction, calculated from the slope of log R_p versus log [AIBN], is 0.5 (Table 2).

Effect of solvent

In order to further confirm the applicability of Mechanism II the effect of polar solvent viz. dioxane, has been studied. As expected, for Mechanism II, the rate enhancement is more in weakly polar dioxane as compared to that in strongly polar solvent DMF. In case of Mechanism I, solvent would not have enhanced the rate[13].

Effect of temperature

The overall energy of activation in the presence and absence of syn-PMMA for template polymerization is 48.0 kJ mol^{-1}, which is less than the blank polymerization (64.0 kJ mol^{-1}), as expected[4] for template polymerization.

Effect of analogue of template

In order to be certain that the influence is due to the polymeric character of the template, the rate was also determined by adding a molecular analogue of PMMA viz. ethyl propionate. In the presence of 0.9 mol ethyl propionate, the polymerization rate at 60°C is found to be 6 × 10^{-5} mol $dm^{-3}s^{-1}$ which is identical to the rate of 6 × 10^{-5} mol $dm^{-3}s^{-1}$ found in the presence of PMMA. The result shows that the rate of copolymerization remains unaffected hence this system follows Mechanism II[3], because in the case of Mechanism I, the addition of an analogue of the template generally reduces the overall rate of polymerization.

Table 3—Copolymer composition

[PMMA] base M	Molar ratio in feed [MMA]/[Sty.]	Mole fraction in copolymer	
		MMA*	Sty†
0.90	3.00	0.79	0.21
0.90	2.00	0.65	0.35
0.90	1.00	0.60	0.40
0.00	1.00	0.56	0.44
0.90	0.52	0.47	0.53

*Estimated from methoxy protons.

†Estimated from phenyl protons.

Characterization of copolymer

In the ^1H NMR spectrum of copolymer, the methoxy protons appear as a triplet in the range of τ 6.4-7.8. The methyl protons also appear as triplet in the range of τ 9.0-9.4. The ratio of aromatic protons to aliphatic protons is 5:11. The composition (Table 3) of copolymer determined from the ^1H NMR spectrum, matches well with that given in literature[14-16] for alternating copolymer.

Acknowledgement

The authors are thankful to DST, New Delhi, for financial assistance and the Director of the Institute for facilities.

References

1 Bartels T, Tan Y Y & Challa G, *J polym Sci Polym Chem Ed*, 15 (1977) 341.

2 Gons J, Slagter W O & Challa G, *J polym Sci Polym Chem Ed*, 17 (1979) 771.

3 Srivastava A K, Nigam S K, Shukla A K, Saini S, Kumar P & Tewari N, *J makromol Sci Review in makromol chem Phys*, C27(2) (1987) 171.

4 Tewari N & Srivastava A K, *J polym Sci Polym Chem Ed*, 27 (1989) 1065.

5 Tewari N & Srivastava A K, *Acta polymerica*, 39 (1988) 679.

6 Awasthi S K, Srivastava A K, *J photochem photobiol*, 51 (1990) 443.

7 Shima Y, Kakui, Kinoshita M & Imoto M, *Makromol chem*, 154 (1972) 247.
8 Polowinski S, *Eur polym J*, 19 (1983) 679.
9 Brandrup J & Immergut E H I, *Polymer Handbook*, (1979), p IV 12.
10 Brandrup J & Immergut E H I, *Polymer Handbook*, (1979) p IV 12.
11 Smid J, Smid Y Y & Challa G, *Polymer Commun*, 27 (1987) 148.
12 Smid J, Smid Y Y & Challa G, *Eur polym J*, 20 (1984) 1095.
13 Tan Y Y & Challa G, *Makromol chem makromol Symp*, 10 (1987) 215.
14 Hirooka M, Yobuuchi H, Iseki J & Nakai Y, *J polym Sci, Part A*-1, 6 (1988) 1381.
15 Nigam S K & Srivastava A K, *Acta Polymerica*, 38 (1987) 244.
16 Srivastava A K & Mathur G N, *Polymer*, 23 (1982) 20.
17 Tewari N & Srivastava A K, *Indian J chem*, 29A (1990) 324.

Indian Journal of Chemistry
Vol. 30A, March 1991, pp. 219-224

Studies on NO_x conversion over transition metal ion (TMI) doped alumina-boria system

J M Bose*, D Banerjee† & D Guha‡
Central Mining Research Station, Dhanbad

Received 23 February 1990; revised 13 July 1990; accepted 5 November 1990

Catalytic decomposition of NO_x has been studied using a fixed bed tubular flow reactor in the temperature range 573-773K, over six aluminium-borate catalysts (containing $2Al_2O_3.B_2O_3$ as the major phase and $9Al_2O_3.2B_2O_3$ as the minor phase) doped with different transition metals. The catalyst phases have been characterised by XRD, IR, ESR and ESCA studies on fresh and used catalyst samples. The results indicate structural stability of the catalyst phase over the experimental temperature range and oxidation of Co^{2+} to Co^{3+} accompanied by surface migration of Co^{3+} species. No valence change in the other transition metal ions and surface oxygen enrichment in the used catalyst is observed. Kinetic studies show a first order dependence on NO_x partial pressure in the lower temperature region, except in the case of the mixed doped catalyst. Breaks in the Arrhenius plots at about 673K are noted for all the catalysts.

NO_x constitutes a serious health hazard[1] and stringent permissible limits for NO_x concentration in ambient and industrial atmosphere have been laid down[2,3]. A need, therefore, exists to develop viable means to convert NO_x to acceptable products; the catalytic decomposition of NO_x becomes attractive from this point of view[4].

Alumina-boria systems, with or without incorporated transition metal ions (TMI), have been widely used in catalytic reactions. The solid state reaction between alumina and boric oxide has been investigated by many workers[5-8]. Literature reports indicate that calcination of alumina-boria mixtures in the temperature range 1523-2873K produces definite crystalline phases of the compositions $9Al_2O_3.2B_2O_3$ and $2Al_2O_3.B_2O_3$. However, a lower calcination temperature favours an optimum combination of crystallinity, porosity, surface area, and other desirable properties, so that the maximum activity is achieved from active metals dispersed on such supports[4], such catalysts have also been reported to exhibit a very good thermal and mechanical stability at temperatures of about 2773 to 3273K depending upon the type of active metals present.

In view of the desirable catalytic properties of alumina-boria systems, with or without incorporation of TMI, coupled with the added advantage of structural stability and good mechanical strength[4] and in view of insufficient information available regarding the basic performance of the above catalyst, it was considered worthwhile to make a thorough investigation on the alumina-boria system, using NO_x conversion as a model reaction.

Materials and Methods

(A) *Catalyst preparation*: The catalysts were prepared by dry mixing of equimolar proportions of γ-alumina and orthoboric acid (BDH), with required quantity of cobaltous chloride, cupric sulphate or nickel nitrate (BDH). Different samples were prepared by mixing 1 mol% Co(II), Cu(II) or Ni(II); 3 mol% of Cu(II) and a combination of 1 mol% Co(II), Cu(II) and Ni(II) in an agate mortar, with the addition of benzene[9] to facilitate grinding. A portion of each of these mixtures was oven dried and then DTA studies were conducted to ascertain the calcination temperature. The mixtures were then pelletised under a pressure of 4.9×10^4 N m^{-4}, calcined at 773K for 5h, crushed again, ground in an agate mortar with benzene, oven dried and pelletised as before. Calcination was carried out again at 1023K for 5h to get the final catalysts. Chemical analysis of the final catalysts confirmed that nó loss of TMI occurred during the preparative stage.

(B) *NO_x concentration determination*: NO_x was prepared by the action of conc. HNO_3 on copper turnings and its concentration was determined by using a photo-electric colorimeter (Carl Zeiss, Model-ELKO-111), as per the standard method[10].

(C) *Conversion studies*: The conversion studies

†National Thermal Power Corporation, Delhi.
‡Department of Applied Chemistry, Indian School of Mines, Dhanbad.

were conducted in a static bed tubular flow reactor placed in a tube furnace whose temperature could be controlled with an accuracy of ±2°C. A chromel alumel thermojunction was placed near the centre of the catalyst bed through a thermocouple well, for measurement of catalyst temperature. The feed gas (NO_x + air) was passed through a preheater tube at flow rates of 3.3×10^{-6} m^3 s^{-1}, 6.0×10^{-6} m^3 s^{-1}, 7×10^{-6} m^3 s^{-1}, 9×10^{-6} m^3 s^{-1} and 11.6×10^{-6} m^3 s^{-1} by suction at the outlet over the broken pellets (about 10^{-3} m dia) through the sample (~2g) packed between glasswool plugs. For analysis, the inlet and outlet gases were withdrawn in 10 ml portions using a glass syringe.

(D) *Characterisation*: The XRD studies were conducted using a Philip's PM 9920/05 X-ray diffractometer with Cu/Fe target at a chart speed of 2 cm min^{-1}. The IR studies were conducted using a Perkin-Elmer IR spectrophotometer, in KBr in the range 200-4000 cm^{-1}. The ESR experiments for Co(II) were carried out on an X-band (Super heterodyne) spectrometer with scan range 4000G and field set at 2000G. The spectra were recorded at liquid nitrogen temperature. The ESR spectra were recorded for Cu(II) and Ni(II) on a Varian E_{109} X-band spectrometer with scan range 4000G and field set at 3000G. The spectra were recorded at room temperature. The ESCA studies were conducted using an ESCA spectrometer supplied by M/s V.G. Scientific Instruments Ltd., with the powdered catalyst spread over a silver paste under a vacuum of 10^{-9} torr, using carbon standard. No noble gas ions sputtering or gold decoration was used. The source used was AlK_α. The specific surface values of the powdered samples were measured by the BET technique by nitrogen adsorption at liquid nitrogen temperature.

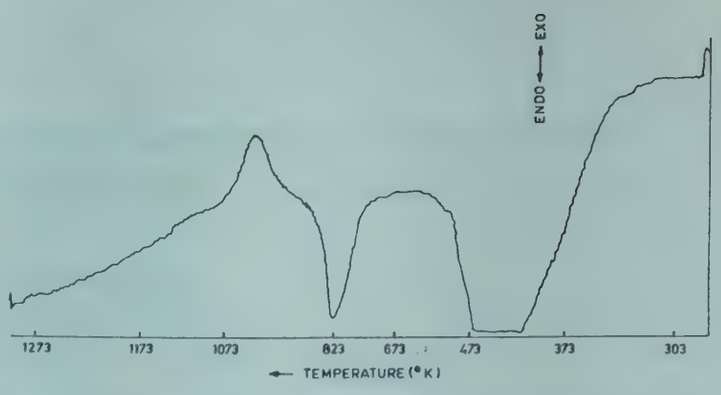

Fig.1—DTA diagram of the catalyst taken at the preparative stage

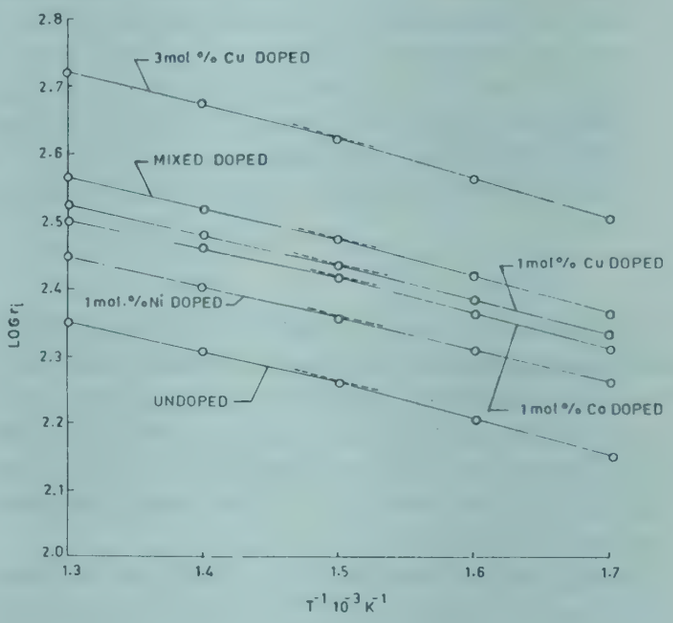

Fig.2—Arrhenius plots for (a) 3 mol% Cu-doped, (b) mixed doped, (c) 1 mol% Cu-doped, (d) 1 mol% Co-doped, (e) 1 mol% Ni-doped and (f) undoped catalysts

Results

The DTA diagram (Fig. 1) shows two endothermic peaks at 423K and 823K, and an exothermic peak at 1023K. The endothermic peaks may be assigned to moisture loss and evolution of gases, respectively, and the exothermic peak probably indicates a solid state reaction between the components leading to the formation of aluminium borate.

From Table 1 it can be seen that the maximum single pass conversion efficiency is that of the sample doped with 3 mol% Cu. The slope at origin of a typical conversion isotherm gives the initial conversion, plots of logarithms of the slope against the reciprocal of the corresponding temperature (K) give the Arrhenius plots. From the extrapolation of these plots to any desired temperature, the conversion at that temperature can be calculated. This method was used to obtain comparative figures for conversion by the different catalysts.

The Arrhenius plots (Fig. 2) indicate a common break temperature of 673K for all the catalyst samples, the slopes in the lower temperature regions being slightly greater than those in the higher temperature region.

Table 1 lists the apparent Arrhenius parameters for the six catalysts and it also includes the relative activities at two selected temperatures below and above the point of break, namely 623K and 723K respectively, calculated from the Arrhenius plots. While not much difference in the high temperature activation energies is noted for the different catalysts, the low temperature activation energy value shows a more pronounced variation from catalyst to catalyst. The lowest activation energies at the higher temperature are shown by 1 mol% Cu-doped and

Table 1—Apparent Arrhenius parameters, activity at selected temperatures and maximum per cent conversion per g catalyst for NO_x conversion over the catalysts studied

Catalyst		Apparent activation energy (kJ/mol)		Activity		Apparent pre-exp. factor $\times 10^3$		Maximum % conversion/g catalyst
Mol% doped	Dopant metal	723K	623K	723K	623K	723K	623K	Single pass
0	—	8.97	9.59	20	16	0.91	1.02	22
1	Ni	8.50	9.59	25	20	1.05	1.29	28
1	Cu	8.50	9.59	30	24	1.20	1.51	34
1	Co	9.59	9.97	29	23	1.45	1.59	32
3	Ni,Cu,Co (in equimolar proportions)	9.59	10.9	33	26	1.66	2.13	36
3	Cu	9.59	11.5	47	36	2.35	3.31	52

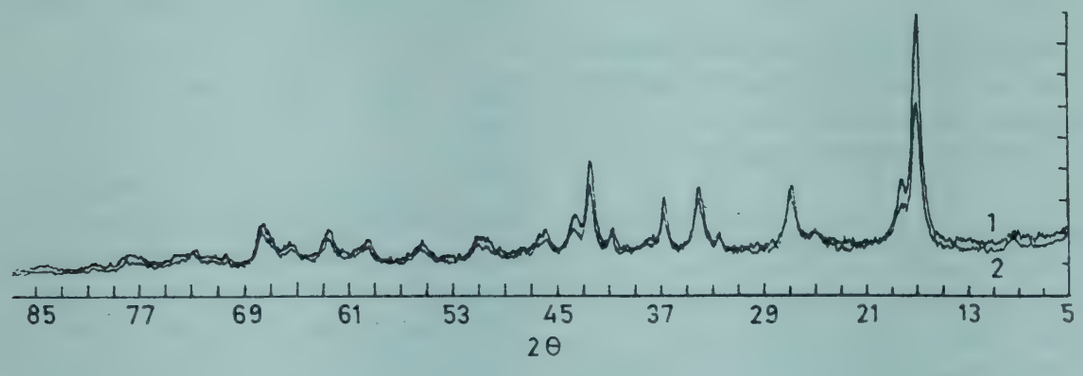

Fig.3—XRD of the catalyst (Co-doped) (1) before and (2) after use in the reaction

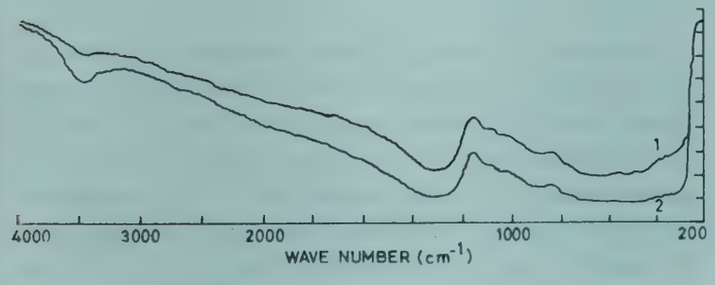

Fig. 4—IR spectra of the catalyst (Co-doped) (1) before and (2) after use in the reaction

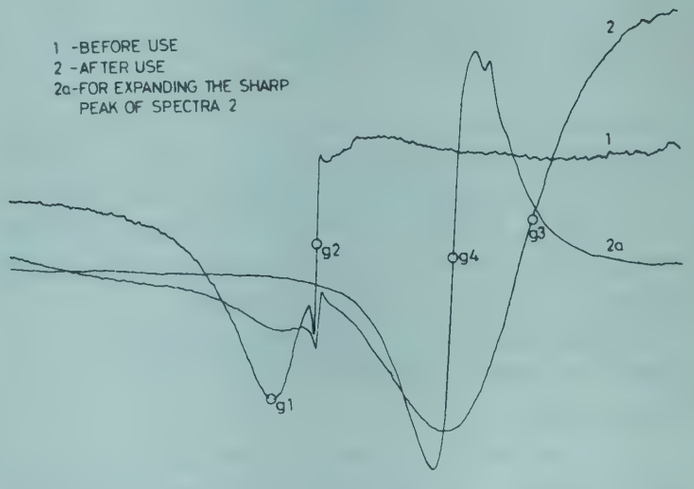

Fig.5—ESR patterns of the fresh and used catalysts (Co-doped)

1 mol% Ni doped samples, which, however, are not very active in view of their relatively lower pre-exponential factors. The undoped catalyst has somewhat higher activation energy and the lowest activity in the series. The most active catalyst among the present catalysts, namely 3 mol% Cu-doped sample, has a relatively higher activation energy which is offset by its highest pre-exponential factor. Similar considerations also apply to the low temperature region.

From Fig. 3, we note that the major phase formed by the solid state reaction between γ-alumina and orthoboric acid is $2Al_2O_3.B_2O_3$. The minor phase is $9Al_2O_3.2B_2O_3$. Traces of unreacted γ-alumina are indicated but no free boria. The doped TMI is in a too finely dispersed state to be detected by XRD. There appears to be no detectable structural change in the course of the catalytic reaction.

The IR patterns shown in Fig. 4 also corroborate that free boria is not present since its characteristic

Table 2—The calculated g-values obtained from ESR spectra

Description of the spectra	g-values
1. Spectra No. 1 taken before use as a catalyst in NO_x conversion.	g_1-4.91589 g_2-4.24116
2. Spectra No. 2 taken after use as a catalyst in NO_x conversion.	g_3-2.57499
3*. Spectra No. 2a taken after use as a catalyst in NO_x conversion.	g_4-2.00277

*Spectra 2a taken for expanding the sharp peak of spectra 2.

IR absorption at 530 cm^{-1} (medium strength) was not obtained. The structure of the catalyst is such that B – O bond is weakened due to the neighbouring Al atoms. Weak but multiple bands in the range 1150-850 cm^{-1} suggest that traces of a tetraborate type of species also exist. However, this could not be confirmed by XRD.

From the ESR patterns, it is seen that while no change in the oxidation state of Cu and Ni occurs as a result of the catalytic reaction, Co^{2+} changes to Co^{3+} after participating in NO_x conversion (Fig. 5, Table 2).

From Table 3, it is seen that oxygen dispersion increases in the used catalyst; also, Co appears as a surface dispersed species in the used catalyst. The binding energies of $B_{1s_{3/2}}$ and of $Al_{2p_{3/2}}$ and $Al_{2p_{1/2}}$, as well as their surface dispersion, are seen to decrease in the sample used in the catalytic conversion. This could be due to a surface restructuring for accommodating increased oxygen dispersion in the used catalyst. The dispersion trends were calculated from FWHM values[22].

A first order dependence on NO_x partial pressure was noted in the lower temperature region, except in the case of the mixed doped catalyst. This observation suggests that the available adsorption sites are far too numerous to affect the reaction order, leading to a pseudo-first order dependence.

The average value of BET surface area measured for all the catalysts was found to be 13.5 $m^2 g^{-1}$.

Discussion

The unusually low activation energies obtained in these studies could be an indication of external diffusion limitations. The catalysts were found to have low specific surface and consequently low porosity. Normally, it should not be associated with diffusion control processes; still, we took the added precautions of using different quantities of the catalysts in the tubular flow reactor and obtained the conversion per unit mass of the catalyst in each case. The values obtained are comparable, suggesting that there is little probability of diffusion control. Because of limitations in the analytical procedure used by us, we could not determine very low concentrations, to get conversion near the origin in conversion versus time plots, which is the usual practice to check external diffusion limitations. Hence, we employed the usual statistical method. Arrhenius plots were then constructed and the apparent Arrhenius parameters were calculated in the usual manner.

The decomposition of NO_x is assumed to be a two step process (Eqs. 1, 2), as proposed by Wikstrom and Nobe[11]

$$NO_2 \xrightarrow{k_1} NO + 1/2\, O_2 \quad \ldots (1)$$

$$NO \xrightarrow{k_2} 1/2\, N_2 + 1/2\, O_2 \quad \ldots (2)$$

The adsorption of NO has been proposed to be unimolecular followed by dissociative chemisorption of NO at oxygen vacancy sites[12] as shown below:

$$2e + V_0 + NO \rightarrow O^{2-} + N_{ads} \quad \ldots (i)$$

$$N_{ads} + NO_{ads} \rightarrow N_2O \quad \ldots (ii)$$

$$2N_{ads} \rightarrow N_2 \quad \ldots (iii)$$

Where V_0 is an oxygen vacancy. If the above mechanism proposed by Voorhoeve is applicable in the present case, there should be two types of oxygen in the used catalyst, one obtained from NO decomposition and the other from adsorbed oxygen.

Louis Raj *et al.*[13], working on the kinetics of N_2O decomposition on a perovskite surface, also proposed two different oxygen species, one obtained from N_2O decomposition and the other from the adsorbed oxygen.

Ross and Fairbridge[14], working on NO and oxygen reaction with 1-butene over Mn(III) oxide, postulated two O_{1s} binding energy values, 530 eV for chemisorbed oxygen on metal oxides and 533 eV for a molecular oxygen species[15]. Thus, oxygen is activated and adsorbed on the catalyst surface as O^- and O_2^- species[16]. Both the Louis Raj *et al.*[13] mechanism and that proposed by Ross and Fairbridge[14], predict two $O_{1s_{1/2}}$ binding energies. However, our ESCA studies gave only one $O_{1s_{1/2}}$ binding energy, both for the fresh and for the used catalyst, which corresponded to that of the molecular oxygen species proposed by Ross and Fairbridge[14].

We noted breaks in the Arrhenius plots at 673K for all the catalysts studied. In the case of very low activation energies, small differences are often taken to be due to experimental errors. However, we noted such breaks in a number of cases. Since we got nearly identical readings in repeated runs, we could not assign the breaks to experimental errors. In addition, we employed the usual statistical methods to ascertain that breaks in the Arrhenius plot do exist.

The Voorhoeve's[12] mechanism suggests that the

Table 3—The relative FWHM values alongwith binding energies and peak intensities of Co-doped catalyst for NO_x conversion

Elements with orbitals	B.E. (eV)		FWHM (eV)		Peak intensity (meter × 10^{-2})	
	Fresh	Used	Fresh	Used	Fresh	Used
$Al_{2p_{1/2}} \cdot Al_{2p_{3/2}}$	74	73	2.55	2.25	4.40	2.90
$O_{1s_{1/2}}$	532	532	2.80	3.00	9.80	11.00
$B_{1s_{1/2}}$	194	192	2.80	2.50	2.50	2.00
C_{1s}	286	286	3.20	3.35	1.10	1.90
Co_{2p}	—	793.5	—	—	—	—

initial step is the dissociative chemisorption of NO at the oxygen vacancy sites (step i). The NO may be present as such in NO_x or NO_x may consist entirely of NO_2, in view of the easy oxidation of NO to NO_2 in presence of air. If NO_2 is predominant, it must first dissociate to NO[11]. The NO thus formed could then undergo dissociative chemisorption. These chemisorption sites could be oxygen vacancies (V_0). The adsorbed nitrogen could then continue to form nitrogen molecules in a surface reaction, which subsequently desorbs. The (step i) above highlights the role of oxygen vacancies in the adsorption of NO. The incorporated TMI probably helps in the creation of oxygen vacancies leading to increased NO adsorption. This contention is corroborated by the fact that higher pre-exponential factors are observed in the TMI doped samples. The difference is more pronounced in the lower temperature regions. The pre-exponential factors are consistently higher in the low temperature zones. The lower value of the pre-exponential factor in the high temperature zones suggests that oxygen vacancy concentration is lowered at higher temperatures, probably because of surface migration of oxide ions. In terms of activation energies in the two temperature zones, the higher temperature activation energies are consistently lower, which also suggests higher mobility of surface oxygen and/or oxygen vacancies. The breaks in the Arrhenius plots noted in our studies probably reflect the mobility differences of these species in the two temperature zones.

The NO_2 molecule can attach to a lewis base site (such as an oxygen vacancy) through the electron deficient nitrogen atom, as nitro species ($-NO_2$) or through a π-bonded electron deficient oxygen atom, as nitrite species ($-NO$). The nitro species is more stable compared to the nitrite species[17]. NO can adsorb more strongly on reduced transition metal oxides[18], probably acting as a ligand for coordinately unsaturated surface atoms. It can adsorb as a chelate with oxygen end bound to the metal[19], accompanied with oxidation of the catalyst[18,20]. Our ESR, studies (Fig. 5) show that oxidation does occur in the used cobalt doped catalyst.

An increase in peak intensity of oxygen has been reported for NO conversion over a silica molybdena catalyst by Best *et al.*[21]. Similar increase in peak intensity along with increased value of FWHM of $O_{1s_{1/2}}$ (Table 3), probably indicates an increase in surface dispersion of oxygen in the used catalyst. We can assume (Table 3), a Co_{2p} peak at 793.5 eV (though it is small and difficult to identify due to background noise) in the used catalyst, whereas in the case of the fresh catalyst it could not be identified. This suggests a higher dispersion of Co_{2p} in the former in comparison to the latter. This result, considered along with the ESR result, suggests the oxidation of Co^{2+} to Co^{3+} in the course of the catalytic reaction and probable migration of the Co^{3+} species to the substrate. This should be favoured by the smaller size of Co^{3+} ions. Such an oxidation might appear to be unlikely because of the high stability of $CoAl_2O_4$, which may be formed during Co doping. However, the very low concentration of cobalt could result in a high dispersion of this spinel with consequent small particle size and high reactivity. Thus, a redox cycle Co^{2+}/Co^{3+} could be established, which would necessitate the preconditioning and regeneration step. However, the sustained activity of the catalyst system observed by us suggests that the regeneration is a dynamic process occurring simultaneously with the catalytic reaction.

It is noted that the activity enhancement is due to pre-exponential factor, suggesting the predominant role of oxygen vacancies in the catalytic reaction. Since the catalyst is structurally quite stable, with favourable mechanical properties, it can well be used for the removal of NO_x pollutants in the form of afterburners in automobile exhausts chimney emission etc.

Acknowledgement

The authors are grateful to the Director, Central Mining Research Station, Dhanbad for encouragement and kind interest in the work.

References

1 Shy C M, Creason J P, Pearlman M E, McClain K E & Benson F B, *J Air Pollut Control Assoc*, 20 (1970) 582; *Arch Env Health*, 37 (1982) 75.

2 F A Patty, *Industrial hygiene & toxicology*, 2nd Edn (John Wiley, New York) 1967, 923.
3 Aggarwal G D, *NIOH Bulletin*, 8 (1983) 1, No. 7.
4 McArthur D P, *U.S. Pat*, 4, 024, 171; *Chem Abstr*, 87 (1977) 438.
5 Mallard E, *C R Acad Sci Paris*, 105 (1887) 1260; *Nature*, 195 (1962) 69.
6 Baumann H N & Moore C M, *J Am Ceram Soc*, 26 (1942) 391; *Nature*, 195 (1962) 69.
7 Scholze H, *Z anorg allgem Chem*, 284 (1956) 272.
8 Gielisse P J M & Foster W R, *Nature*, 195 (1962) 69.
9 Guha D, *Studies on the electrical and catalytic properties of vanadium pentoxide and vanadium bronzes*, Ph D Thesis, IIT, Bombay, 1976.
10 Gage J C, Strafford N & Truhant R, *Methods for the determination of toxic substances in air, International Union of Pure and Applied Chemistry* (Butterworths Scientific Publications, London) (1959) 16.1.
11 Wikstrom L L & Nobe K, *Ind Engg Chem*, 4 (1965) 191.
12 Voorhoeve R J H, in *Advanced materials in catalysis*, edited by J J Burton & R L Garten (Academic, New York) 1977, 129.
13 Louis Raj S, Viswanathan B & Srinivasan V, *Indian J Chem*, 21A (1982) 689.
14 Ross R A & Fairbridge C, *Can J Chem*, 61 (1983) 2767.
15 Roberts M W, *Adv Catal*, 29 (1980) 55.
16 Haber J & Witko M, *Acc Chem Res*, 14 (1981) 1; *Can J Chem*, 61 (1983) 2767.
17 Durant P J & Durant B, *Introduction to advanced inorganic Chemistry*, (Longman Group Ltd., London) 1970, 693.
18 Yao H C & Shelef M, *J Catal*, 31 (1973) 377.
19 Kugler E L, Kadit A B & Cryeler J W, *J Catal*, 41 (1976) 72.
20 Voorhoeve R J H, Remaika J P & Trimble L E, *The catalytic chemistry of nitrogen oxides*, edited by R L Klimseh & J G Larsen (Plenum, New York) (1975) 215.
21 Best S A, Squires R G & Walton R A, *J Catal*, 60 (1979) 171.
22 Fleisch T H, Hicks R F & Bell A T, *J Catal*, 87 (1984) 398.

Indian Journal of Chemistry
Vol. 30A, March 1991, pp. 225-229

Variation of the electrochemical transfer coefficient in the electroreduction of aromatic two-ring disulfonyl difluorides

Przemyslaw Sanecki

Department of General Chemistry,
Faculty of Chemistry, I. Lukasiewicz Technical University, ul. W. Pola 2, 35-959 Rzeszów, Poland

Received 9 April 1990; re .sed and accepted 12 September 1990

An attempt has been made to describe quantitatively the variation of transfer coefficient with potential in the electroreduction of twelve aromatic two-ring disulfonyl fluorides of FO_2S-Ar-M-Ar-SO_2F type, where -M- is a bridging group. Each compound exhibits two two-electron steps of $-SO_2F$ reduction. Linear relationship exists between αn and the potential, E. The average value of $\partial\alpha/\partial E$ is 0.42 V^{-1}. The limiting values of potential corresponding to $\alpha = 1$ and $\alpha = 0$ are calculated and discussed. The series of compounds covers ca. 40% of the total range of α variability.

The variation of the electrochemical transfer coefficient with potential has been an important subject of electrochemical interest for over three decades. Recent reports suggest that the transfer coefficient, α, does change with potential (cf. reference 1 and references cited therein) in the way predicted by the modern theories of charge transfer[2-4].

This work deals with the investigation of variation in transfer coefficient not within the potential range of a single compound, but for a series of related compounds, with the aim of covering, possibly, the widest range of potentials. Hence, the variation of α from compound to compound is considered. Furthermore, the presence of two reactive groups in one molecule makes it possible to follow the changes in α while two successive groups in a single compound are being reduced. The problem of α variation within a single functional group has been investigated earlier[1] and it is not considered here.

Variation of transfer coefficient for a different series of substituted compounds with the same reactive group has already been discussed[5]. The significance and utility of the transfer coefficient values for some organic compounds was the subject of another paper[6].

Materials and Methods

The compounds listed in Table 1 were prepared specially for this work. No published data on any of them were found in literature. All were prepared by the known reaction between potassium fluoride and the respective sulfonyl chloride[7,8]. (The data on the latter can be found in ref. 9). Mass spectra of the compounds confirmed their calculated molecular weights.

The measurement system was a three-electrode one and was used in conjunction with an XY-4105 recorder and an EP20A potentiostat. The capillary yield in a circuit open to air was 1.090×10^{-3} g/s. It was siliconated using the procedure described in literature[10]. The measurements were made at 298 ± 0.05K. Solutions of sulfonyl fluorides (1.3×10^{-3} M) in 0.1 M methanolic $N(C_2H_5)_4I$ were used. The reference electrode was SCE containing LiCl solution in methanol. Platinum electrode served as the auxiliary electrode. The two electrodes were separated from the sample solution with a transition vessel with glass sinter.

All current-potential curves were recorded point by point in 0.005 V steps; the constant drop time was 2.00 s. The number of electron exchanged was determined in the standard way by using diaphragm electrolyser. The catholyte volume was 100 cm^3 and depolarizer mass: 3×10^{-4} mol.

Results

The reduction

Each of the twelve compounds studied in this work reacted in such a way that one could distinguish steps of reduction of individual SO_2F groups, although for most of them a detailed examination was required (Table 2). Compound 8, for example, yielded two well separated waves, each related to reduction of one SO_2F group. The second wave partially overlapped a third one.

Table 1—Aromatic disulfonyl difluorides used in the present study*

Number	Compound	Melting point, °C
1	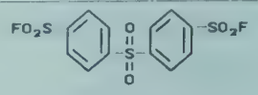	249-250
2	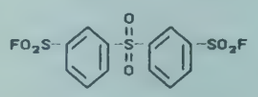	183-184.5
3	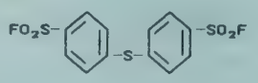	122-123
4	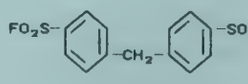	126.5-127.5
5	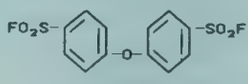	111-112
6	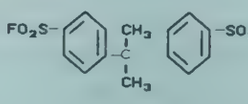	138.5-141.5
7	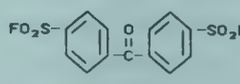	144-144.5
8	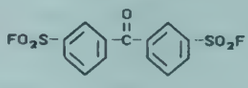	120-122
9	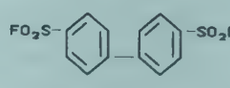	201.5-202.5
10	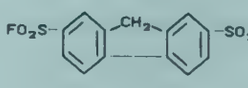	246.5-247.5
11	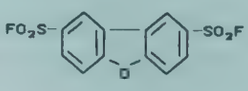	277-279
12	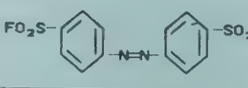	246-247

*All compounds were purified by repeated crystallization from chloroform. Compound 6 was additionally purified by sublimation

This third wave remained unchanged after full hydrolysis of the compound as revealed by a separate experiment and hence it was attributed to the reduction of carbonyl group. This wave was of no significance to the main results.

Compound 7 yielded two nearly fully separated reduction waves of SO_2F groups and a separate third wave at a more negative potential. Only this third wave remained after complete hydrolysis of the compound.

Compounds 1 and 2 each yielded one (unsplit) wave attributable to reduction of both $-SO_2F$ groups and another one at much more negative potentials. Only the last one remained after complete hydrolysis of the compounds.

Compounds 3-6 and 9-11 produced single waves due to SO_2F reduction; for compounds 9-11, however, the waves nearly split (inflexion could be seen on current vs. potential curves).

For compound 12, a single wave was observed in the potential range -0.4 to -0.6 V, which was ascribed to reduction of $-N=N-$ bridge. Another wave appeared in the range -1.55 to -1.85 V corresponding to reduction of both the SO_2F groups. After hydrolysis, only the first wave remained, with its potential range and limiting current being very similar to those in the original compound 12.

It was found coulometrically that each wave corresponding to the reduction of SO_2F group was a two-electron wave, or in the case of overlapping waves, a four-electron one. Respective sulfinic acids were the products of reduction.

The separated two-electron waves were dealt with in the standard way; the values $(E_{1/2})_1$, $(\alpha n)_{obs,1}$ and $(E_{1/2})_2$, $(\alpha n)_{obs,2}$ were determined for each SO_2F group. The values of k_h were calculated from Tafelian segments[11,12] of polarographic waves using the typical relationship,

$$i = nFAk_h c_{ox} \qquad \ldots (1)$$

where c_{ox} is the reagent concentration (mol/cm^3), A is the electrode surface (cm^2), i is the current (A), and

$$k_h = k_{h,o} \exp[\alpha nF(E - E_0)/RT] \qquad \ldots (2)$$

with $k_{h,o}$ being k_h at the potential assumed to be zero.

Evaluation of the individual values of $(E_{1/2})_1$, $(\alpha n)_1$, $(E_{1/2})_2$, $(\alpha n)_2$ from the complex four-electron waves required selection of several representative points on the curve in the whole range of the complex wave, calculation of the currents (i_{calcd}) at respective potentials, and their comparison with the experimental values of currents, i_{exp}. The analysis was carried out until all calculated currents fell onto the experimental i vs. E curve with the lowest error. The least squares method was used for this. The results are presented in Table 2.

Table 2 contains the products $(\alpha n)_{obs,T}$ for four compounds from the series of sulfonyl fluorides evaluated in Tafelian regions of i vs. E curves. $\bar{E}$ denotes the potential in the middle of Tafelian region. The values were determined only for the compounds with separated waves or for those at least exhibiting well pronounced limiting current inflexion in i vs. E curve.

Table 2 – Electroreduction of disulfonyl difluorides in 0.1 *M* methanolic $N(C_2H_5)_4I$. Values of halfwave potentials, $E_{1/2}$, and the products $(\alpha n)_{obs}$, and $(\alpha n)_{obs,T}$ determined from Tefelian relations; $\bar{E}$ denotes the middle of Tafelian segment

No.	$(E_{1/2})_1$, $(E_{1/2})_2$, [V]	$(\alpha n)_{obs,1}$ $(\alpha n)_{obs,2}$	Standard devn, [%]	$\bar{E}$, [V]	$(\alpha n)_{obs,T,1}$ $(\alpha n)_{obs,T,2}$
1	−0.949	1.05	1.9		
	−1.011	0.96			
2	−1.048	1.14	2.0		
	−1.110	1.13			
3	−1.183	0.91	2.0	−1.099	0.95
	−1.318	0.76		—	—
4	−1.443	0.84	3.5		
	−1.495	0.64			
5	−1.496	0.76	2.6		
	−1.615	0.58			
6	−1.515	0.76	3.5	−0.788	1.25
	−1.589	0.64		—	—
7	−0.828	1.37	1.2	−0.788	1.25
	−0.966	1.35		—	—
8	−1.025	1.16	—	−0.960	1.08
	−1.362	0.84		−1.275	0.79
9	−1.134	1.01	1.8	−1.059	0.96
	−1.280	0.92		—	—
10	−1.126	0.95	1.5	−1.058	0.91
	−1.307	0.82		—	—
11	−1.416	0.87	2.3	−1.360	0.74
	−1.558	0.76		—	—
12	−1.645	0.78	2.2		
	−1.730	0.62			

The parameters that characterize reduction processes (for each wave under consideration) are: (i) electrochemical order with respect to substrate: 1 ± 0.1; (ii) reaction order with respect to $N(C_2H_5)_4^+$: 0.85 ± 0.1; and (iii) reaction constant $\rho_\pi(\rho) > 0$ (slope of the relation $E_{1/2}$ vs. σ or log k_h vs. σ).

Discussion

The plots of $(\alpha n)_{obs}$ vs. $E_{1/2}$ and of $(\alpha n)_{obs,T}$ vs. $\bar{E}$ drawn by using data from Table 2 were both found to be linear. The relevant equations are:

$$(\alpha n)_{obs} = (1.892 \pm 0.208) + (0.7637 \pm 0.1572)\, E_{1/2} \quad \ldots (3)$$

($n = 24$ points; $r = 0.9066$)

and

$$(\alpha n)_{obs,T} = (1.918 \pm 0.230) + (0.8874 \pm 0.2091)\bar{E} \quad \ldots (4)$$

($n = 7$ points, $r = 0.9796$).

The second equation describes reduction of SO_2F groups in the compounds with separated waves or with at least clear inflexion in the limit-

ing current line on the first wave. Hence, it is related to the reduction of one SO_2F group. The Tafelian relationships refer to the initial region of wave formation. Therefore, for the parameters to have physical significance for the first reduced group, the reduction current for the second wave has to be negligibly small. Calculations confirmed it to be true in each case. This is why Eq. (4) covers the compounds with sufficiently different $(E_{1/2})_1$ and $(E_{1/2})_2$ values.

An interpretation of the relationships presented in Figs 1 and 2 becomes possible after discussing the mechanism of reduction in detail. The results suggest the following stepwise mechanism of electroreduction of SO_2F groups.

$$FO_2S-Ar-SO_2F+2e \rightarrow FO_2S-Ar-SO_2^- + F^- \quad \ldots (5)$$

$$FO_2S-Ar-SO_2^- + 2e \rightarrow {}^-O_2S-Ar-SO_2^- + F^- \quad \ldots (6)$$

The values of $(\alpha n)_{obs}$ presented in Table 2 are related to a two-electron electroreduction of SO_2F group and hence they must be complex quantities. It is known that electroreduction of SO_2X group (where X is a halogen) is an irreversible process that does not split into two one-electron steps in both protic and aprotic media[13,14]. Disproportionation of the anion-radical resulting from addition of the first electron can probably be excluded; otherwise, a part of the substrate would have formed inactive Ar-SO_3^- anion and the measured number of electron exchanged would have fallen below 2F/mol of SO_2F. The actual experimental value is 2 ± 0.05, or 4 ± 0.1 for the two overlapping waves. Furthermore, the radicals containing sulfur are rather inactive[15]. Further electroreduction of anion radical seems, therefore, justified.

All this reasoning together with experimental findings discussed above including the high (αn) values suggest the following mechanism of reduction:

$$Ar-SO_2F+e \underset{k_{h,-1}}{\overset{k_{h,1}}{\rightleftarrows}} [Ar-SO_2F] \quad \ldots (7)$$

$$[Ar-SO_2F]+e \xrightarrow{k_{h,2}} Ar-SO_2^- + F^- \quad \ldots (8)$$

The mechanism represented by Eqs 7-8 is of IIB type according to Albery's classification of multistep processes[16] with the observed rate constant,

$$k_{h,obs} = \frac{k_{h,1}\, k_{h,2}}{k_{h,-1}} \quad \ldots (9)$$

This IIB case (with $k_{h,-1} > k_{h,2}$) is more sensitive to potential (two electrons in transition state) than IIA where $k_{h,1}$ value controls the total rate of the process. Hence, using Eq. (9) and the definition of transition coefficient, we can write

$$\alpha_{obs} = \alpha_1 + \alpha_2 - \alpha_{-1} \quad \ldots (10)$$

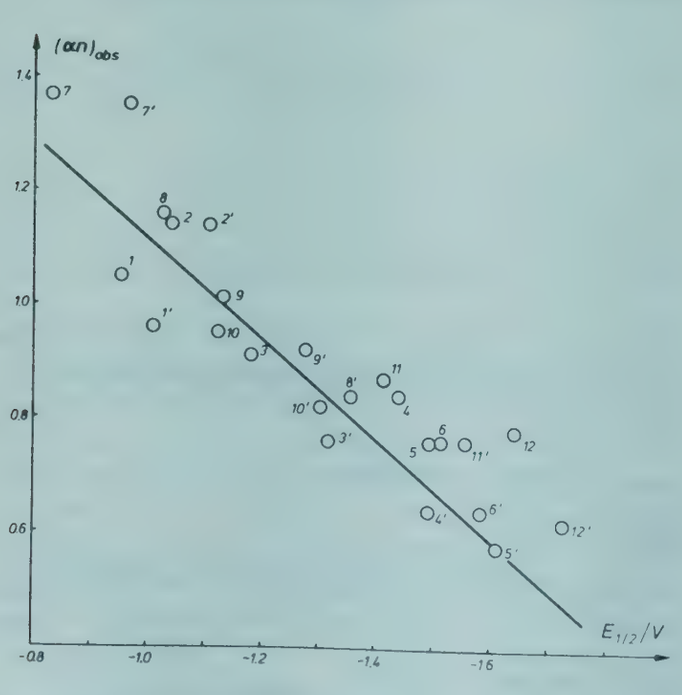

Fig. 1 – Electroreduction of a series of disulfonyl difluorides in 0.1 *M* methanolic $N(C_2H_5)_4I$. The plot shows relationship between $(\alpha n)_{obs}$ and half wave potentials determined using the equation describing irreversible waves.

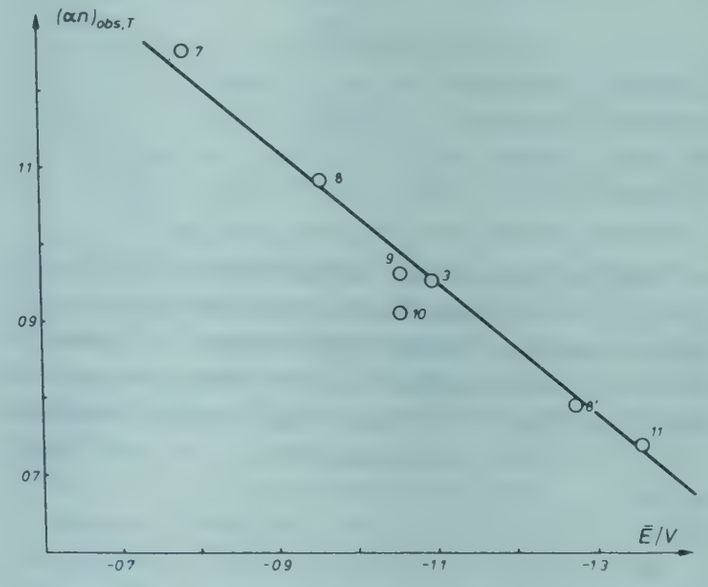

Fig. 2 – Electroreduction of a series of disulfonyl difluorides in 0.1 *M* methanolic $N(C_2H_5)_4I$. The plot of $(\alpha n)_{obs,T}$, determined from Tafelian relations, vs. $\bar{E}$, the potential in the middle of Tafelian segments.

A relation similar to (10) can be deduced by using Eq. (1) for the currents: $i = i_1 + i_2$, where i_1 and i_2 are the currents for one-electron steps. Thus,

$$(\alpha n)_{obs} = \alpha_1 + \alpha_2 \quad \ldots (11)$$

Equations (10) and (11) reveal the origin of the complex (αn) values and make it possible to discuss their variations.

Of particular interest are the limiting values of potential obtained by extrapolation of $(\alpha n)_{obs}$ and $(\alpha n)_{obs,T}$ [Eqs (1) and (2)] to the limits 0 and 2. The limiting value of 2 should be replaced by the value of $\alpha_i = 1$ if one considers Eq. (10) with $\alpha_{-1} = 0$ (oxidation process) or $\alpha_i = 1$ directly by Eq. (11). The average limiting values are $E = -2.35 \mp 0.15$ V $\{(\alpha n)_{obs} = \alpha_{obs} = 2\alpha_i = 0\}$ and $E = 0.12 \mp 0.02$ V $\{(\alpha n)_{obs} = \alpha_{obs} = 2\alpha_i = 2\}$ respectively.

The significance of $E = -2.35$ is that starting from that value potential does not affect the electroreduction process any more and the rate is controlled by addition of electron to the substrate in the so called activationless process[17]. According to the polarization theory of metal-electrolyte interface[18], desorption of the so called surface hydrated electron takes place with the formation of free hydrated electron. The limiting potential is also close to the potential of decomposition of supporting electrolyte ($\approx 2.2 \pm 0.1$ V for 0.1 M $N(C_2H_5)_4I$ in methanol). According to Antropov[19], such a decomposition is accompanied by emission of hydrated electron to solution.

The other limiting value of 0.12 V, close to zero in hydrogen scale, determines the range of the maximum effect of the potential upon electroreduction process where the rate is controlled solely by subtraction of electron from electrode. From the theoretical point of view, this corresponds to the so called barrierless process[17].

The limiting values of α and corresponding potentials resulting from Eqs (3) and (4) are consistent with those predicted by the theory.

A similar discussion of the limiting values of transfer coefficients might be carried out referring to the close analogy between the equations of electrochemical kinetics and Brønsted equation. Here, it seems important that the experimental lowest and highest αn values: 0.58 and 1.37, respectively (Table 2), or $\alpha_i = 0.29$ and 0.69, correspond to the intermediate region of Brønsted linear relation and cover ca. 40% of the total range of variability of the elementary transfer, or Brønsted coefficient.

The average slope of the plot of $(\alpha n)_{obs}$ vs. potential, $d(\alpha n)_{obs}/dE$, is 0.42 V^{-1} and this magnitude is consistent with values both predicted theoretically and measured experimentally (cf. refs. 20 & 21). Quite unexpectedly, values very close to the same figure can be found among literature data. For example, Saveant and Tessier[1a] arrived at the mean value of $\partial\alpha/\partial E = 0.45$ for electroreduction of benzaldehyde in ethanol.

It seems that the reciprocal value, $\partial E/\partial\alpha$, may also be considered to have a physical meaning. It is the range of potential necessary to sweep up in order to observe the whole range of transfer coefficient variability, from 0 to 1. In this work, the value of $\partial E/\partial\alpha = 2.38$ V was obtained, whereas for the data taken from literature[1a] the value was 2.22 V.

Acknowledgement

This work was supported by the Project CPBP 01.15.

References

1 Saveant J M & Tessier D, *Faraday Disc Chem Soc*, 74, 57 (1982), 1a, p. 71.
2 Hush N S, *J chem Phys*, 28 (1958) 962.
3 Dogonadze R R, in *Reactions of molecules at electrodes*, edited by N S Hush (Wiley-Intersci., London), 1971.
4 Marcus R A, *J chem Phys*, 43 (1965) 679.
5 Sanecki P, *Electrochim Acta*, 31 (1986) 1187.
6 Reddy S J & Krishnan V R, *Indian J Chem*, 16A (1978) 805.
7 Davies W & Dick J H, *J chem Soc*, (1932) 483.
8 Houben-Weyl, *Methoden der organischen Chemie, B. IX*, (Georg Thieme Verlag, Stuttgart), 1955.
9 Sanecki P & Rokaszewski E, *Can J Chem*, 66 (1988) 3056.
10 Matysik J, Persona A & Klimek M, *J electroanal Chem*, 240 (1988) 317.
11 Conway B E, in *Techniques of electroorganic synthesis*, edited by N L Weinberg, (Wiley, N.Y.) 1974, Part I, p. 173.
12 Avila J L, Blázquez M & Ruiz J J, *Electrochim Acta*, 27 (1982) 1369.
13 Jeminet G, Simonet J & Gourcy J G, *Bull chim Soc Fr.*, 5-6 (1974) 1102.
14 Fleszar B & Sanecki P, *Electrochim Acta*, 25 (1980) 551.
15 Kice J L in *Free radicals*, edited by J K Kochi (Wiley, N.Y.) 1973, Vol. II, p. 736.
16 Albery J, *Electrode kinetics* (Clarendon Press, Oxford), 1975.
17 Krishtalik J L, *Elektrodyne reaktsii* (Nauka, Moscow), 1979.
18 Fleszar B in *Electrocatalysis*, Mat. IXth Symp. Electrochem. Sect. Polish. Chem. Soc. (Karniowice n/Cracow) 1988, p. 115.
19 Antropov L I in *Itogi Nauki. Electrokhimiya*, Vol. 6 (Viniti, Moscow) 1971, p. 5.
20 Saveant J M & Tessier D, *J electroanal Chem*, 65 (1975) 57.
21 Corrigan D A & Evans D H, *J electroanal Chem*, 111 (1980) 195.

Indian Journal of Chemistry
Vol. 30A, March 1991, pp. 230-234

Coadsorption of organic molecules on mercury electrode

P V Krishnamoorthy
Alagappa Government Arts College, Karaikudi 623 003, Tamilnadu, India
and
M Anbukulandainathan & S Venkatakrishna Iyer*
Central Electrochemical Research Institute, Karaikudi 623 006, Tamilnadu, India

Received 6 March 1990; revised 16 July 1990; accepted 3 September 1990

Coadsorption of *o*-hydroxybenzoic acid with *o*-methoxybenzoic acid and/or *o*-aminobenzoic acid at the mercury/0.1 *M* Na_2SO_4 solution interface has been studied using a capillary electrometer. Thermodynamic parameters, such as surface charge density (q^M), surface excess of the organic molecule adsorbed (Γ_{org}) and coverage (θ) have been evaluated. It is observed from the adsorption data that coadsorption takes place by the partial replacement of already adsorbed organic compound on the metal surface and the adsorption of both the compounds is found to take place over a wide range of potentials.

It is well known that the formation of strong adsorbed layers on metals plays an important role in electroplating and in corrosion inhibition. One way of producing adsorbed surface films, which are stable over a wide range of potentials, is by the coadsorption of organic molecule at the electrode/solution interface. Most of the studies at the electrode/solution interface have involved single organic molecules. Some studies have been carried out on the coadsorption of two organic molecules. It is observed that in the case of coadsorption, the coverage is less than the sum of coverages in individual adsorptions. The effect of concentration of adsorbate as well as the mechanism of adsorption has been studied for different organic adsorbents[1-11]. The present study aims at the investigation of the adsorption of *o*-hydroxybenzoic acid (OHB), *o*-aminobenzoic acid (OAB) and *o*-methylbenzoic acid (OMB) singly on a mercury electrode and also the coadsorption of OAB or OMB with OHB using a capillary electrometer.

Materials and Methods

Reagents

Mercury used was of AR grade and it was further purified electrolytically and distilled twice in all-glass pyrex Hullet still under reduced pressure[12]. AR(BDH) grade sodium sulphonate was twice recrystallised from deionised water and dried to the anhydrous state. OHB (pure) was a May and Baker product, while OMB was a Koch-Light (England) product. OAB was obtained from Riedel, Germany. As all the above-mentioned organic compounds were of extrapure quality, they were used without further purification. Throughout this study, it was assumed that the solute activity can be replaced by its molar concentration since fairly dilute solutions are involved.

Procedure

The evaluation of thermodynamic quantities for the adsorption at the mercury electrode necessitated the measurement of interfacial tension, using a capillary electrometer as described elsewhere[13]. Purified hydrogen was used for deaeration of experimental solutions. The capillary electrometer was calibrated with 1 *M* KCl, for which the interfacial tension was 424.2 mN/m[14], and rechecked with 1 *M* KI taking the electrocapillary maximum as 401.4 mN/m at 25°C. For each concentration at least two runs were made and results were found to be reproducible to ± 0.2 mN/m at the electrocapillary maximum and ± 1 mN/m at the extreme of the curve. All the measurements were made in an air thermostat controlled at a temperature of 25 ± 0.2°C.

To understand the mixed adsorption of organic molecules, first a study of adsorption of individual organic compounds is essential. So, interfacial tension measurements were carried out separately, using 0.1 *M* sodium sulphate as the base electrolyte. The mercury in the capillary electrometer was polarised at various values of potentials ranging from -0.1V to -1.6V applied with reference to Hg/Hg_2SO_4/0.1 *M* Na_2SO_4 electrode using a precision potentiometer. Two types of observations were made for the mixed adsorption of substances in the same base electrolyte. In one, the concentration of

adsorbate 1 was kept constant and the concentration of the adsorbate 2 was varied. In the second case, the concentration of adsorbate 1 was varied. One of the concentrations taken for the study of the adsorption of the individual organic compound was chosen as the common concentration for mixed adsorption studies.

Results and Discussion

The single adsorption of all the three organic compounds reported in this study has already been studied thoroughly[15] and only salient features are reported here.

The adsorption of OHB, OMB and OAB alone was studied at the mercury/0.1 *M* Na_2SO_4 solution interface. The adsorption of OHB was found to be more pronounced on the positive side of electrocapillary maximum and desorption occurred on the negative side of the electrocapillary maximum. A similar behaviour was observed in the case of OMB also, but the extent of adsorption was comparatively less. But OAB was found to adsorb on both the sides of electrocapillary maximum, though the adsorption was more on the positive side and less on the negative side. Maximum adsorption (maximum surface excess) for all the three compounds occurred at surface charges in the range of +2 to 3.5 $\mu C \cdot cm^{-2}$.

Based on the above observations, adsorption studies were carried out using OHB as one of the two adsorbates, keeping its concentration constant in one case and varying its concentrations in the other cases. The present study aims at examining the effect of addition of a second adsorbate (OMB or OAB) on the extent of adsorption of OHB. The order of adsorption in the single adsorbate system is OMB > OHB > OAB. This observed order is in accordance with the polarisabilities of these adsorbates. The electrode/solution system under study can be represented as Hg/Na_2SO_4 (0.1 *M*)x,y/ Hg_2SO_4(S)/Hg where x,y represent the two organic compounds.

Simultaneous adsorption of OHB with OMB and OAB

(i) *Electrocapillary curves*

Electrocapillary curves obtained in the presence of fixed concentrations of OHB and varying concentrations of OMB, or vice versa are shown in Figs 1 and 2. It is seen from these figures that curves are more separated for the systems with fixed concentration of OMB and variable concentrations of OHB than those for the system containing fixed concentration of OHB and varying concentrations of OMB. Moreover, the separation of the curve is greater near the electrocapillary maximum, than

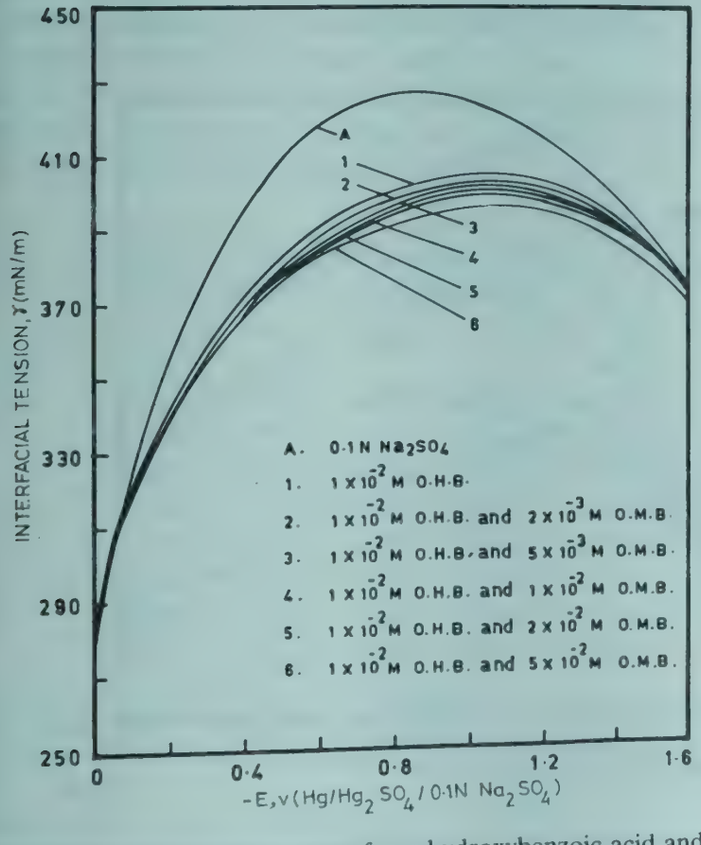

Fig. 1 – Electrocapillary curves for *o*-hydroxybenzoic acid and *o*-methylbenzoic acid

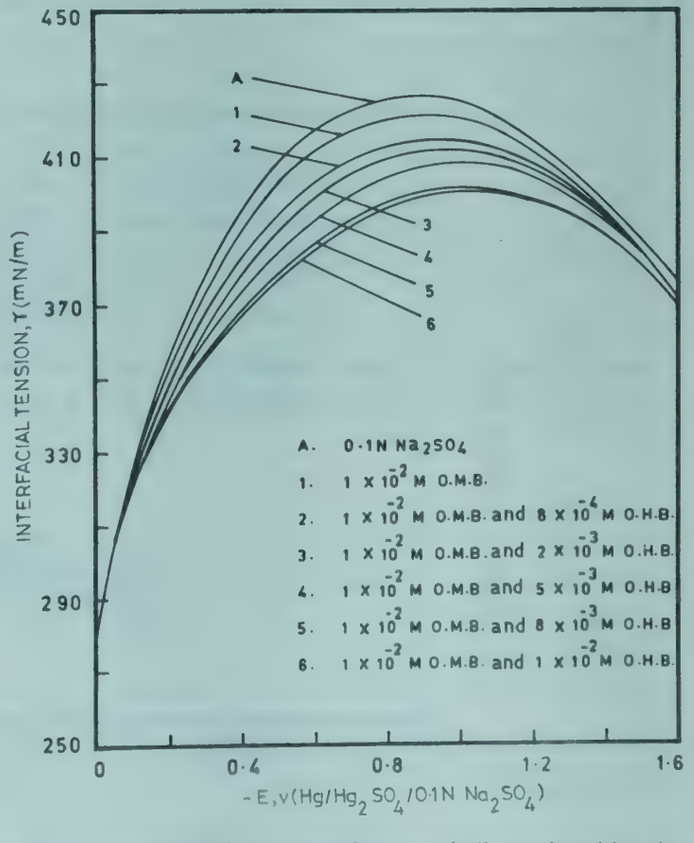

Fig. 2 – Electrocapillary curves for *o*-methylbenzoic acid and *o*-hydroxybenzoic acid

that at the extremes. It is also observed that both the compounds get desorbed at the extremes of potentials and that there is a shift in the electrocapillary maximum to more negative potentials on the addition of second adsorbate. These observations may be explained in terms of the adsorption of second compound occurring at the expense of the first, the substitution not being in the 1:1 ratio (which may be due to different polarisabilities of the two organic compounds). These observations further indicate that there is simultaneous adsorption of both the adsorbates. A similar behaviour was observed for the simultaneous adsorption of OHB and OAB. In both the systems it was observed that the lowering of interfacial tension was greater for the system where the varying concentration constituent was OAB or OMB and the fixed concentration constituent was OHB.

The electrocapillary equation for the above systems can be written as

$$-d\gamma = q^M dE^- + 1/2\,\Gamma_{Na^+} d\mu_{Na_2SO_4} + \Gamma_{OHB} d\mu_{OHB} + \Gamma_{OMB} d\mu_{OMB} \quad \ldots (1)$$

The above equation enables the evaluation of the charge density (q^M) and surface excess (Γ_{org}) for the individual organic compounds in the mixture at different potentials. This equation can be reduced to

$$\left(\frac{\partial\gamma}{\partial E^-}\right)_{\mu_{Na_2SO_4},\mu_{OHB},\mu_{OMB}} = -q^M \quad \ldots (2)$$

$$\left(\frac{\partial\gamma}{\partial\mu_{OHB}}\right)_{E^-,\mu_{Na_2SO_4},\mu_{OMB}} = \Gamma_{OHB} \quad \ldots (3)$$

$$\left(\frac{\partial\gamma}{\partial\mu_{OMB}}\right)_{E^-,\mu_{Na_2SO_4},\mu_{OHB}} = \Gamma_{OMB} \quad \ldots (4)$$

Similar equations can be obtained for the simultaneous adsorption of OHB and OAB on the mercury electrode.

(ii) *Surface excess versus charge density curves*

For a better understanding of the preferential adsorption of one adsorbate out of the chosen two, a study of the variation of relative surface excess with charge on the metal surface is essential. The surface excess of the adsorbate with varying concentration was obtained by the graphical differentiation of the γ vs RT ln C curve using Eqs (3) and (4) where C is the concentration of the altered adsorbate. As the ionic strength is not altered significantly, the activity of the varying adsorbate is equated to its concentration. Surface charge density values were obtained (using Eq. 2) for different potentials by the graphical differentiation of electrocapillary curves. Surface excess versus charge density curves obtained for the OHB-OMB system are shown inFigs 3 and 4. Similar curves were obtained for the OHB-OAB system. It is observed from these figures that surface excess obtained for the mixed system is always greater (for all concentrations) than that for systems with single

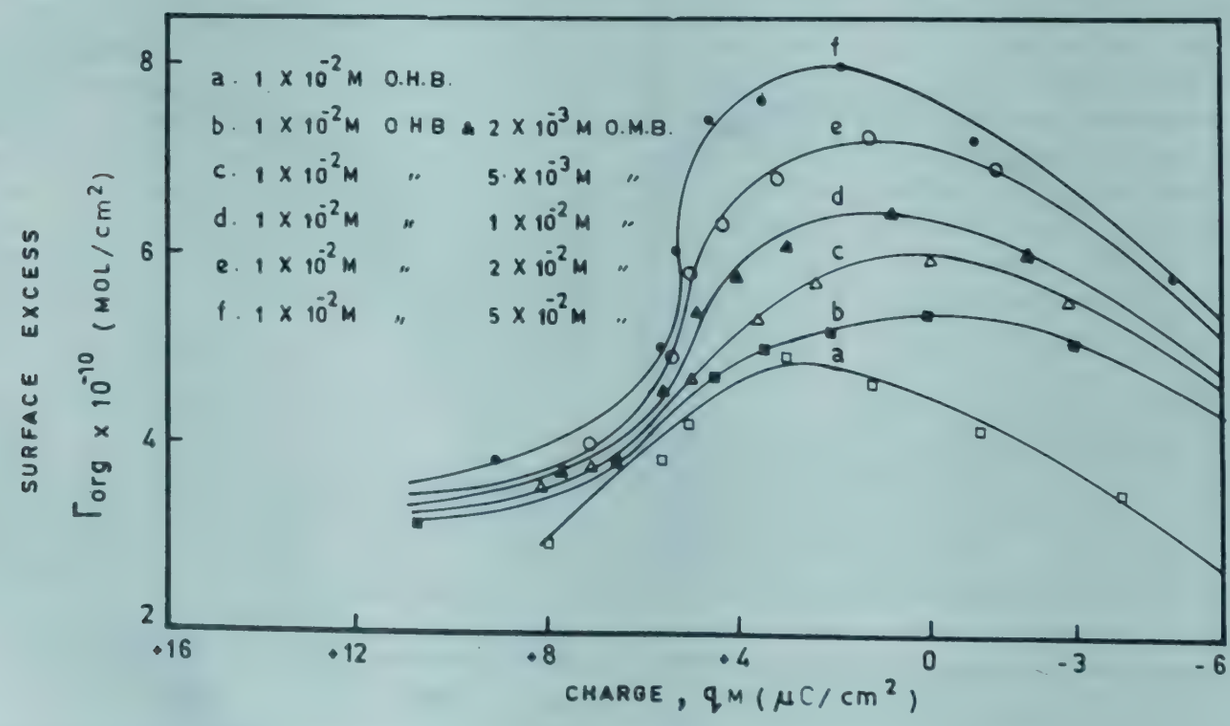
a. 1 X 10⁻² M O.H.B.
b. 1 X 10⁻² M O H B & 2 X 10⁻³ M O.M.B.
c. 1 X 10⁻² M " 5 X 10⁻³ M "
d. 1 X 10⁻² M " 1 X 10⁻² M "
e. 1 X 10⁻² M " 2 X 10⁻² M "
f. 1 X 10⁻² M " 5 X 10⁻² M "
SURFACE EXCESS
Γorg x 10⁻¹⁰ (MOL/cm²)
8
6
4
2
+16
+12
+8
+4
0
-3
-6
CHARGE, qM (μC/cm²)

Fig. 3 – Variation of Γ_{org} with q^M for the adsorption of fixed concentration of *o*-hydroxybenzoic acid with variable concentrations of *o*-methylbenzoic acid on mercury

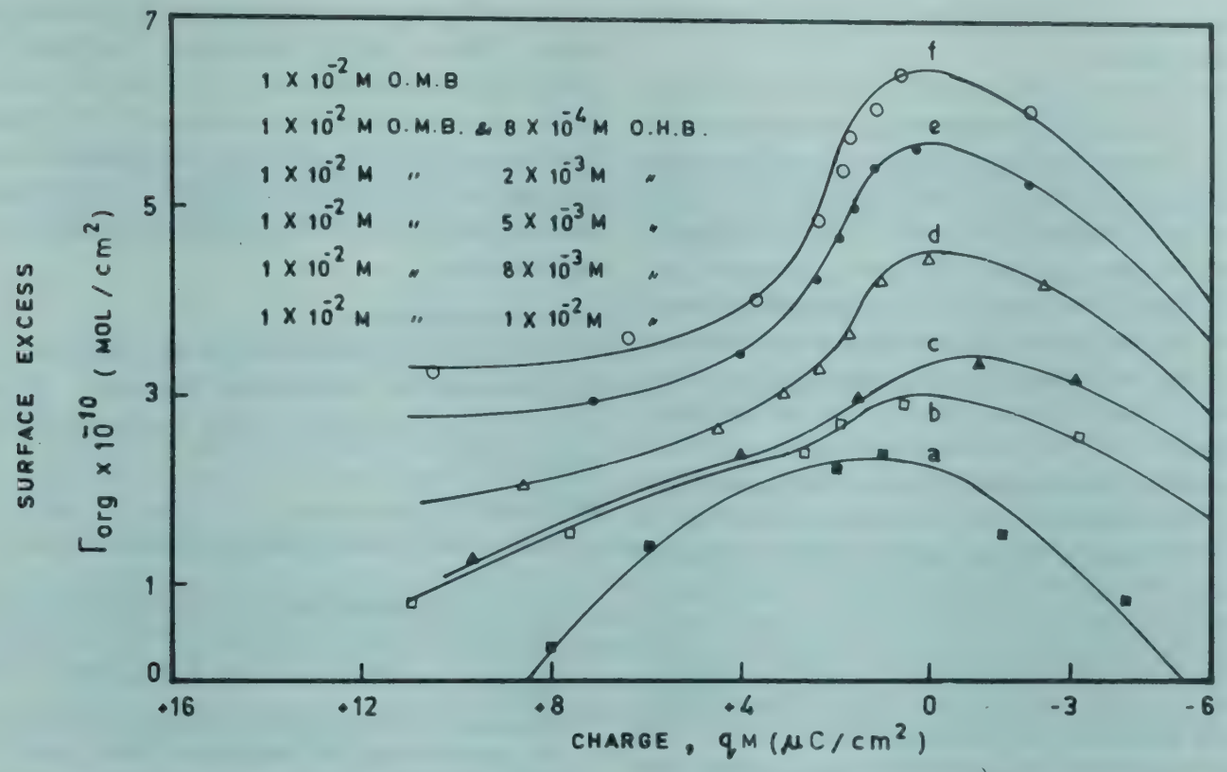

Fig. 4 – Variation of Γ_{org} with q^M for the adsorption of fixed concentration of *o*-methylbenzoic acid with variable concentrations of *o*-hydroxybenzoic acid on mercury

organic adsorbate. Another notable feature seen from these curves is that for all concentrations the surface excess of the mixed system is always less than the sum of surface excesses of individual components. It is also found that for both the mixed systems maximum surface excess is noticed at charge value ranging from $+3$ to $+4$ $\mu C \cdot cm^{-2}$. But for individual systems, maximum surface excess is obtained at less positive charges. This difference may probably be due to the simultaneous adsorption of two adsorbates on the mercury surface.

Table 1 – Variation of surface coverage for different surface charges at the mercury/solution interface

q^M ($\mu C \cdot cm^{-2}$)	θ_1	θ_2	θ_3	θ_4	$\theta_3+\theta_4$
8	0.5011	0.0568	0.3655	0.1742	0.5397
7	0.5919	0.1640	0.3765	0.2023	0.5730
6	0.6709	0.2494	0.4073	0.2308	0.6381
5	0.7340	0.3019	0.4460	0.2550	0.7010
4	0.7735	0.3194	0.4857	0.2620	0.7477
3	0.8089	0.3718	0.5057	0.2925	0.7982
2	0.8129	0.3938	0.5164	0.3068	0.8232
1	0.7893	0.4068	0.5206	0.3502	0.8708

θ_1: θ due to 1×10^{-2} *M* OHB + 0.1 *M* Na_2SO_4
θ_2: θ due to 1×10^{-2} *M* OMB + 0.1 *M* Na_2SO_4
θ_3: θ due to 1×10^{-2} *M* OHB + 2×10^{-3} *M* OMB + 0.1 *M* Na_2SO_4
θ_4: θ due to 1×10^{-2} *M* OMB + 2×10^{-3} *M* OHB + 0.1 *M* Na_2SO_4

(iii) *Coverage (θ) of the metal surface by adsorbed organic compounds*

Coverage (θ) was obtained using the relation $\theta = \Gamma/\Gamma_m$, where Γ_m is the maximum value of the surface excess. Values of Γ_m were evaluated from the slopes of C/Γ vs C curves for $q^M = 0$. It was found to be 8.0×10^{-10} mol·cm^{-2} for OMB, 12.75×10^{-10} mol·cm^{-2} for OHB and 14.64×10^{-10} mol·cm^{-2} for OAB. Values of coverage have been obtained for both the systems for different charge densities and are shown in Tables 1 and 2. From these data for coverage at different charge densities, the following general observations can be made:

Table 2 – Variation of surface coverage for different surface charges at the mercury/solution interface

q^M ($\mu C \cdot cm^{-2}$)	θ_1	θ_2	θ_3	θ_4	$\theta_3+\theta_4$
+8	0.5011	0.4193	0.2288	0.2189	0.4477
+6	0.6709	0.4574	0.2902	0.2653	0.5555
+4	0.7735	0.5869	0.3483	0.3493	0.6978
+2	0.8129	0.6937	0.3381	0.4684	0.8063
0	0.7577	0.6403	0.3278	0.4211	0.7489
−2	0.6551	0.5412	0.2902	0.2947	0.5849

θ_1: θ due to 1×10^{-2} *M* OHB + 0.1 *M* Na_2SO_4
θ_2: θ due to 1×10^{-2} *M* OAB + 0.1 *M* Na_2SO_4
θ_3: θ due to 1×10^{-2} *M* OHB + 8×10^{-4} *M* OAB + 0.1 *M* Na_2SO_4
θ_4: θ due to 1×10^{-2} *M* OAB + 8×10^{-4} *M* OHB + 0.1 *M* Na_2SO_4

(a) Simultaneous adsorption of both the components takes place.

(b) At very low concentrations, the extent of adsorption of the fixed concentration constituent from the mixed solution is found to be less than that of the same constituent studied individually. This fact clearly shows that the adsorption of one constituent of a mixture takes place by bringing down the adsorption of the other. So the adsorption of one constituent is found to take place by partial replacement of the already adsorbed organic compound and the adsorption of both is observed over the whole range of potential.

(c) At lower concentrations of the adsorbate with varying concentration, an important behaviour is noticed. The sum of the surface coverages of mixed adsorbates (θ_3 and θ_4) is almost equal to the coverage of the component which is adsorbed more as an individual adsorbate. It is seen from Table 1 that at a charge of $+4\ \mu C \cdot cm^{-2}$ the coverage values of the individual adsorbate (of concentration $1 \times 10^{-2}\ M$) are found to be 0.7733 and 0.3194 respectively. But coverages from mixed solutions, θ_3 and θ_4, are 0.4857 and 0.2620 respectively and the sum total is 0.7477. This is equal to the coverage (θ_1) of the adsorbate with more adsorption. A similar behaviour is observed from Table 2 also. This behaviour is shown almost at all electrode charges, especially at low concentrations of the varying constituent. These observations are in keeping with observations by previous workers[1-4].

(d) Though there is a general agreement and correlation among the chosen systems at very low concentrations, there is a considerable disagreement for more concentrated solutions. This may be due to an error in the value of θ obtained by graphical differentiation. Moreover, the calculation of coverage is based on assumptions that adsorbates are adsorbed in one orientation. But this may not be so in reality because π-electron interaction may involve a flat or mixed orientation. Calculation of θ, ignoring lateral interactions between like and unlike molecules, will introduce an error in the value of θ. The true value will vary depending on whether the interaction is attractive or repulsive and this depends on the orientation of the molecule at the metal/solution interface.

Acknowledgement

The authors are thankful to the Director, Central Electrochemical Research Institute, Karaikudi 623 006 for his interest in the work and for providing facilities.

References

1 Joshi K M & Rajagopalan S, *Electrochim Acta*, 17 (1972) 479.
2 Joshi K M & Rajagopalan S, *Indian J Chem*, 12 (1974) 1294.
3 Joshi K M & Urmila D J, *Indian J Chem*, 14A (1976) 749.
4 Urmila D J, Raut B S & Joshi K M, *Trans SAEST*, 15(3) (1980) 237.
5 Damaskin B B, Dobrokhotova Sterlina M E & Nekrasov L N, *Elektrokhimiya*, 25 (1989) 254.
6 Fishtik I F, Krylov V S, Kiryanov V A & Vatman I I, *Elektrokhimiya*, 21 (1985) 8.
7 Fastovets V V, Murashevich E V, Afanaseva L F & Nesterenko A F, *Elektrokhimiya*, 20 (1984) 1465.
8 Murashevich E V, Afanaseva L F, Bhakhtiarov N G, Nesterenko A F & Lashkarev M A, *Electrokhimiya*, 22 (1986) 1308.
9 Nesterenko A F, Bhakhtiarov N G, Tkachenko G V, Afanaseva L F, Khinov E I & Loshkarev M A, *Elektrokhimiya*, 24 (1988) 231.
10 Motheo A J, Gonzalez E R & Avaca L A, *Proceedings Chem Soc*, 171st Spring Meeting, Extended Abstract, Philadelphia, (1986).
11 Dutkiewicz E & Skoluda P, *J Electroanal Chem*, 213 (1986) 327.
12 Hullet G H & Minahein H P, *Phys Rev*, 25 (1905) 388.
13 Parsons R & Devanathan M A V, *Trans Faraday Soc*, 49 (1953) 404.
14 Peries P, *M.Sc. Thesis*, University of Ceylon, 1954.
15 Krishnamoorthy P V, *Ph.D. Thesis*, Madurai Kamaraj University, 1986.

Indian Journal of Chemistry
Vol. 30A, March 1991, pp. 235-238

Electron-transfer interactions of chloranil/bromanil with hexacyanometalate (4-), $K_4[M(CN)_6]$, where M = Fe, Ru and Os

M M Girgis*†, A H Osman & A E Arifien††
Chemistry Department, Faculty of Science, Assiut University, Assiut, Egypt

Received 7 June 1990; revised 24 September 1990; accepted 9 November 1990

UV-visible spectrophotometric studies on the interactions of chloranil/bromanil with the hexacyanometalate(4-), $[M(CN)_6]^{4-}$ ions, where M = Fe, Ru and Os, in 20-70% (vol./vol.) aqueous dimethyl sulphoxide media at 27°C demonstrate the formation of the negative semiquinone ion (I) derived from the halonil. New absorption spectral bands are immediately formed after mixing. The positions of the new bands are neither affected by the medium polarity nor by the nature of the metal in the hexacyanometalate (4-) ions. The reaction equilibrium constants and the molar absorptivities of (I) have been calculated. Experimental results indicate that (i) chloranil is the more powerful electron acceptor halonil, (ii) the abilities of the $[M(CN)_6]^{4-}$ ions to interact with the halonils depend on their redox potentials and follow the order Fe(II) > Os(II) > Ru(II), and (iii) the reaction equilibrium constants increase greatly with the increasing water content of the medium.

As a part of our research programme on the study of charge-transfer interactions[1-6] and in continuation of our earlier work[4] on the charge-transfer interactions of chloranil with nicotine, we report here the results of our investigations on the interaction of chloranil/bromanil with the hexacyanometalates (4-), $K_4[M(CN)_6]$, where M = Fe, Ru and Os in 20-70% (vol./vol.) aqueous dimethyl sulphoxide. The aim of the present study is to investigate the effect of the variation of (i) the halo atoms of the halonil molecules, (ii) the redox potentials of the hexacyanometalate(4-) ions, and (iii) the medium composition, on the reaction process. Chloranil, as a well known organic acceptor[7a], was chosen as a model for the quinones encountered in biological systems[8-12]. Electron-transfer interactions between chloranil/bromanil and the above mentioned hexacyanometalate(4-) ions have not been reported earlier.

Materials and Methods

Chloranil (Aldrich) was recrystallized repeatedly from benzene to get yellow platelets; m.p. 289°C. Bromanil was prepared by the method described earlier[13] and was recrystallized from glacial acetic acid to get golden yellow flakes, m.p. 299°C. Potassium hexacyanoferrate(II) (Aldrich reagent) and potassium hexacyanoruthenate(II) (Heraeus) were obtained as commercial samples and used as such. Potassium hexacyanoosmate(II) was prepared according to published procedure[14]. Spectrophotometric grade dimethyl sulphoxide (Aldrich) was used as such. Doubly distilled conductivity water was used in the preparation of water-DMSO mixed solvents.

Calculated amounts of chloranil or bromanil (1.5×10^{-3} mol dm^{-3}) in dimethyl sulphoxide and the hexacyanometalate(4-) ion (1.0×10^{-3} mol dm^{-3}) in water were transferred to a 10 ml dark coloured flask and the volume was made up to the mark by adding the desired amount of water and dimethyl sulphoxide. The initial concentration of chloranil/bromanil was varied in the range of $(0.10\text{-}10.91) \times 10^{-5}$ mol dm^{-3} while that of the hexacyanometalate(4-) ion was varied in the range $(0.98\text{-}11.82) \times 10^{-5}$ mol dm^{-3}. All solutions were freshly prepared each day, and their absorbances as well as those of their mixtures were measured within 5 hr. All the operations were performed in an air-conditioned room (~22°C) in subdued light. At the beginning of the measurements of a set of solutions, the spectra of pure compounds were recorded to detect any change.

Spectrophotometric measurements were made on a Shimadzu UV-200 S double beam spectrophotometer, using a rectangular cell of 1 cm pathlength and solvent as the blank. The absorption spectral bands of the semiquinone anion obtained due to the interaction between chloranil/bromanil and the hexacyanometalate(4-) ions were observed at wavelengths longer than those of λ_{max} of individual pure components at concentrations identical to those used in the mixture[4,15]. The absorbances were measured after ~5 min of placing the cell in a thermostated cell holder for allowing the equilibrium to be

†Address for correspondence: P.O. Box 161, (Assiut), Egypt.
††Chemistry Department, Faculty of Science, Assiut University, Aswan, Egypt.

attained. The accuracy of the measurements was ±0.01 absorbance unit.

Results and Discussion

Interaction of potassium hexacyanoosmate(II) with chloranil and bromanil

For hexacyanoosmate(II)-halonil mixtures in 20-70% (vol./vol.) aqueous dimethyl sulphoxide media, new strong electronic absorption spectral bands are immediately formed after mixing the constituents (Fig. 1 and Table 1). The positions of the new bands are not affected by the solvent polarity, but the absorbance diminishes with increasing the water content of the medium.

Several studies[4,9,10,16] have shown that in solvents of high ionizing power the major absorption band of chloranil (288 nm) is red-shifted on complex formation, a phenomenon particularly marked with strong donors[9]. The shift of the absorption is due to the formation of the negative semiquinone ion[4]. The resultant spectrum is, therefore, due to contributions from both neutral and ionized forms (Fig. 1).

In aqueous dimethyl sulphoxide, the solvation of the hexacyanoosmate(II) ion and halonil molecule immediately causes almost complete electron-transfer in the ground electronic state, i.e., the result is the formation of the negative semiquinone ion. In hexacyanoosmate(II)-chloranil system, for example, the absorption bands at 424 and 451 nm, which have been assigned to the negative semiquinone ion (I) derived from chloranil, are observed (Fig. 1).

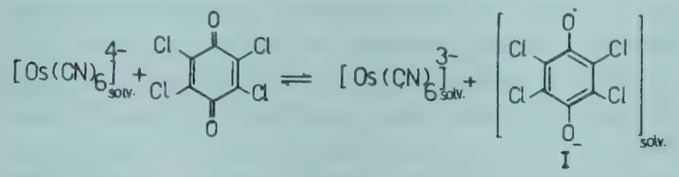

I

This assignment is supported by the facts that absorption positions are not affected by changes in the medium polarity or the nature of the metal in the $[M(CN)_6]^{4-}$ ions (Table 1), and the absorption spectra are similar to that of the product obtained by the reaction of chloranil with sodium iodide[17].

The electronic absorption spectrum of $[Os(CN)_6]^{3-}$ ions shows two bands at 261 and 283 nm[18] and has no absorption in the range 400 to 460 nm.

The stoichiometry of the electron-transfer interaction (2) between the donor hexacyanometalate(4-)

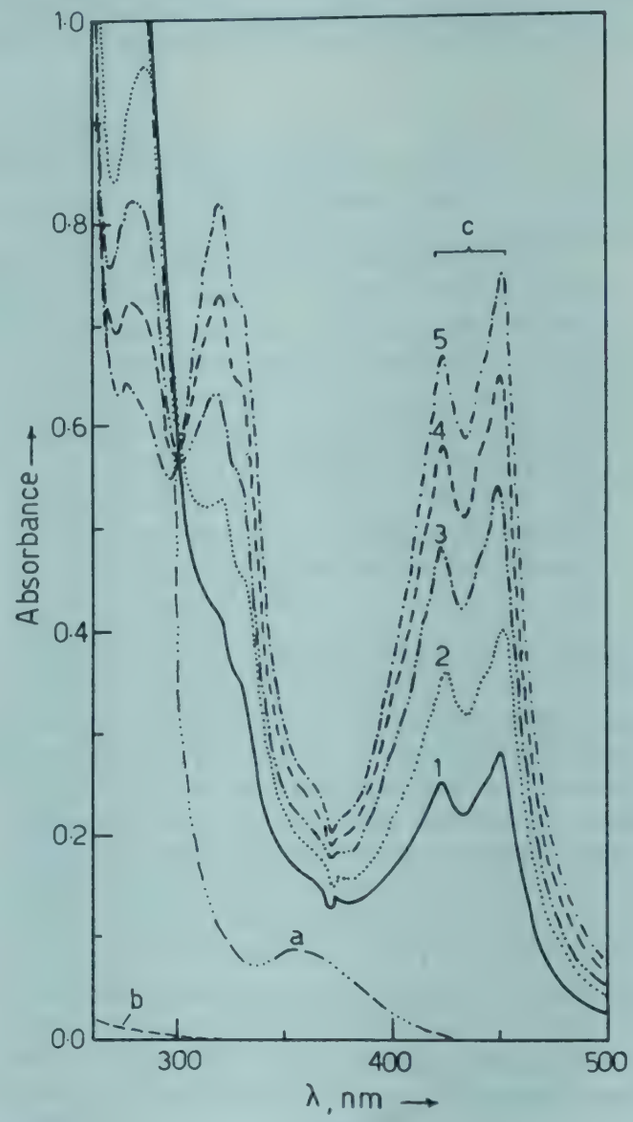

Fig. 1—The electronic absorption spectra in 20% (vol./vol.) aqueous dimethyl sulphoxide at 27°C of (a), chloranil (9.5×10^{-5} mol dm^{-3}); (b), $K_4[Os(CN)_6]$ (7.84×10^{-5} mol dm^{-3}); and (c), chloranil (9.5×10^{-5} mol dm^{-3}) to which the following amounts of $K_4[Os(CN)_6]$ (mol dm$^{-3} \times 10^{-5}$) were added: (1), 2.47; (2), 3.71; (3), 5.21; (4), 6.49; (5), 7.84×10^{-5} mol dm^{-3}.

Table 1—Absorption maxima ($\lambda_{max}^{A^-}$), molar extinction coefficients ($\varepsilon_{max}^{A^-}$) and equilibrium constants (K_c) obtained for the interactions between chloranil/bromanil and the hexacyanometalate (4-) ions in aqueous dimethyl sulphoxide media at 27°C

Medium (%, vol./vol.)	Acceptor (A)	Donor $[D]^{4-}$	λ_1 (nm)	λ_2 (nm)	λ_3 (nm)	λ_4 (nm)	λ_5 (nm)	$K_c \times 10^{-3}$ (dm^3 mol^{-1})	$\varepsilon_{max}^{A^-} \times 10^{-3}$ (cm^2 mol^{-1})
20% aqueous DMSO	Bromanil	$[Os(CN)_6]^{4-}$	408*sh*	—	424	—	454	4.51	57.1
	Chloranil	$[Os(CN)_6]^{4-}$	404*sh*	418*sh*	424	444*sh*	451	6.24	33.3
	Chloranil	$[Ru(CN)_6]^{4-}$	404*sh*	418*sh*	426	445*sh*	451	4.83	33.3
	Chloranil	$[Fe(CN)_6]^{4-}$	404*sh*	418*sh*	425	445*sh*	451	7.26	33.3
50% aqueous DMSO	Chloranil	$[Fe(CN)_6]^{4-}$	405*sh*	420*sh*	426	447*sh*	451	22.65	22.5
70% aqueous DMSO	Chloranil	$[Fe(CN)_6]^{4-}$	407*sh*	422*sh*	427	449*sh*	451	32.90	15.4

ion (D^{4-}) and the acceptor halonil molecule (A),

$$dD^{4-} + aA \rightleftharpoons D_d^{3-} + A_a^- \quad \ldots (2)$$

was determined applying Eq. (3)[7b]:

$$A_\lambda^{A^-} = K_c\, \varepsilon_\lambda^{A^-} [D^{4-}]^d [A]^a \quad \ldots (3)$$

where $A_\lambda^{A^-}$ and $\varepsilon_\lambda^{A^-}$ are the absorbance and the molar absorptivities, respectively, of the negative semiquinone ion (I) at wavelength λ, and K_c is the equilibrium constant. A log-log plot of $A_\lambda^{A^-}$ versus concentration of one component, keeping that of the other constant, proved that under the present experimental conditions the reaction stoichiometric ratio was one.

Since the absorption spectra slowly change with time due to air oxidation[19], the reaction equilibrium constants were determined from the spectra immediately recorded after mixing the reactants.

To study the reaction equilibrium constants (K_c), we have the following equations:

$$D^{4-} \rightleftharpoons D^{3-} + e \quad \ldots (4)$$

$$\begin{array}{ccccc} A & + & e & = & A^- \\ (a-x) & & (b-x) & & x \end{array} \quad \ldots (5)$$

$$K_c = \frac{x}{(a-x)(b-x)} \quad \ldots (6)$$

Equation (6) may be rearranged to obtain Eq. (7),

$$\frac{a}{x} = \frac{1}{K_c} \cdot \frac{1}{b} + \frac{a}{b} + 1 - \frac{x}{b} \quad \ldots (7)$$

Since the absorbance in the region of the new λ_{max} is due to the semiquinone anion (A^-) (Fig. 1), and the solution is of 1 cm path-length, according to Eq. (5), the molar absorptivity of the anion A^- at wavelength λ is given by Eq. (8),

$$\varepsilon_\lambda^{A^-} = \frac{A_\lambda^{A^-}}{x} \quad \ldots (8)$$

Combining Eqs (7) and (8), we get

$$\frac{a}{A_\lambda^{A^-}} = \frac{1}{K_c\, \varepsilon_\lambda^{A^-}} \cdot \frac{1}{b} + \frac{a}{b\, \varepsilon_\lambda^{A^-}} + \frac{1}{\varepsilon_\lambda^{A^-}} - \frac{x}{b\, \varepsilon_\lambda^{A^-}} \quad \ldots (9)$$

Since $b \gg x$, using the concentration of the electrons (b) as that of the hexacyanometalate(4-) ion as an approximation, it is positible to neglect the last term in the right hand side of Eq. (9)[20], so that

$$\frac{a}{A_\lambda^{A^-}} = \frac{1}{b}\left(\frac{1}{K_c \cdot \varepsilon_\lambda^{A^-}} + \frac{a}{\varepsilon_\lambda^{A^-}}\right) + \frac{1}{\varepsilon_\lambda^{A^-}} \quad \ldots (10)$$

For a series of solutions of constant a and varying b, a plot of $(a/A_\lambda^{A^-})$ against $(1/b)$ should be linear. The intercept of the line on the ordinate gives $(\varepsilon_\lambda^{A^-})^{-1}$ of the semiquinone anion A^- and the slope is equal to $[(K_c \cdot \varepsilon_\lambda^{A^-})^{-1} + a(\varepsilon_\lambda^{A^-})^{-1}]$, so that K_c and $\varepsilon_\lambda^{A^-}$ can be evaluated. Plots of Eq. (10) for chloranil-/bromanil-hexacyanoosmate(II) mixtures are represented in Fig. 2 while the K_c and $\varepsilon_\lambda^{A^-}$ values are given in Table 1.

From Table 1, it is clear that chloranil interacts more strongly with the hexacyanometalate(4-) ions. This can be attributed to the higher electron withdrawing character of the chlorine atoms which increases to some extent the acceptor ability of the chloranil molecule relative to the bromanil, due to a flow of more electronic charge from the 1,4-benzoquinone nucleus to the chlorine atoms.

Interaction of chloranil with the hexacyanometalate(4-), $K_4[M(CN)_6]$, where M = Fe, Ru and Os

Plots of Eq. (10) gave linear slopes which could be taken as an evidence for the validity of Eqs 5 and 10 (Fig. 2). The K_c and $\varepsilon_\lambda^{A^-}$ values are given in Table 1.

In 20% (vol./vol.) aqueous dimethyl sulphoxide it is evident that the ability of chloranil molecule to accept an electron from the hexacyanometalate(4-) ion depends on the redox potentials[21] of the $[M(CN)_6]^{4-/3-}$ ions and follows the order: Fe(II) > Os(II) > Ru(II) (Table 1). It is interesting to

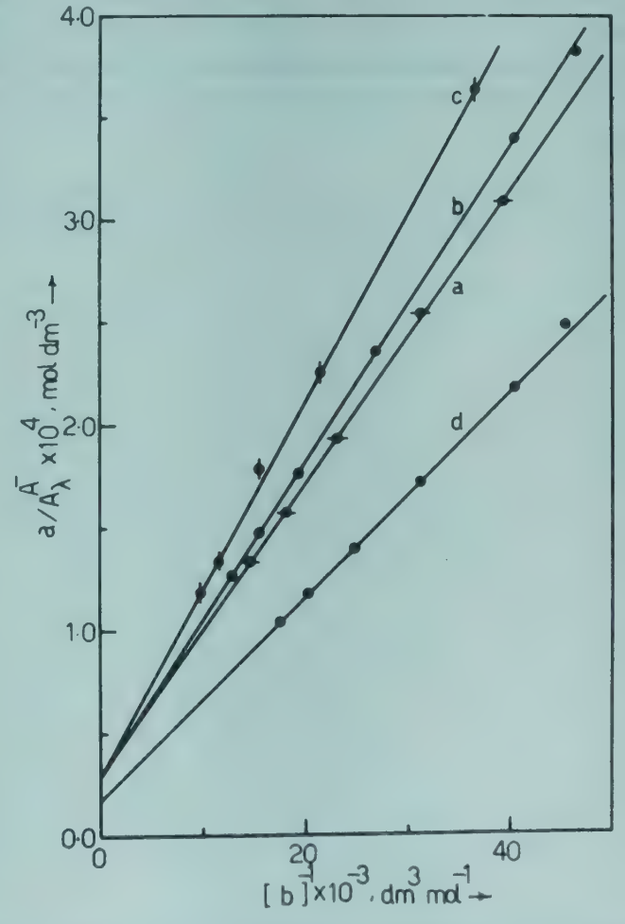

Fig. 2—Plots of $a/A_\lambda^{A^-}$ versus $[b]^{-1}$ for 20% (vol./vol.) aqueous dimethyl sulphoxide solution containing fixed [halonil] and different concentrations of $[M(CN)_6]^{4-}$ ions at 27°C. The systems are: (a), $K_4[Fe(CN)_6]$-chloranil; (b) $K_4[Os(CN)_6]$-chloranil; (c), $K_4[Ru(CN)_6]$-chloranil; and (d), $K_4[Fe(CN)]$-bromanil system.

find that the values of the equilibrium constants, K_c, are directly proportional to the redox potentials[21] of the hexacyanometalate(4-) ions. The increase in the negative $E_{1/2}$ value of the $[M(CN)_6]^{4-/3-}$ ion will decrease its electron donor ability and consequently lead to a smaller K_c value.

Table 1 also shows that the molar absorbance of the negative semiquinone ion (I), $\varepsilon_\lambda^{A^-}$, has a definite value ($33.3 \times 10^{-3}$ cm^2 mol^{-1}) in 20% aqueous dimethyl sulphoxide which is independent of the hexacyanometalate(4-) ion.

Solvent effects

The interaction of chloranil with hexacyanoferrate(II) ion, $[Fe(CN)_6]^{4-}$, was investigated in aqueous sulphoxide media with varying amounts of water content (from 20 to 70%, vol./vol.) with a view to investigate the influence of the medium composition on the electron-transfer process.

In the solvent mixtures used, it is evident that the ability of chloranil molecules to accept an electron from the hexacyanoferrate(II) ion strongly depends on the medium composition. The value of the equilibrium constants (K_c) increases greatly with increasing water content of the medium. The increase in the dielectric constant of the medium with increasing water content facilitates to a great extent the donor and acceptor abilities of the interacting species and consequently higher K_c values are obtained.

References

1 Girgis M M & Khalil Z H, *Croat Chem Acta*, 60 (1987) 225.
2 Girgis M M & Khalil Z H, *Indian J Chem*, 27A (1988) 474.
3 Girgis M M, Yanni A S & Khalil Z H, *Indian J Chem*, 29A (1990) 138.
4 Girgis M M, *Croat Chem Acta*, 63 (1990) 53.
5 Girgis M M, *Indian J Technol*, (1990) (in press).
6 Vogler A, Osman A H & Kumkely H, *Coord Chem Rev*, 64 (1985) 159.
7 Slifkin M A, *Charge-transfer interactions of biomolecules* (Academic Press, London) 1971, (a) p 55, 83, 97 & 119, (b) p 17.
8 Mourad A F, Nour-el Din A M, Hassan A A & Doepp D, *Bull Soc Chim Belg*, 95 (1986) 1045.
9 Slifkin M A, *Nature*, 198 (1963) 1301.
10 Slifkin M A, *spectrochim Acta*, 20 (1964) 1543.
11 Singh V & Sahai R, *Monatsh Chem*, 117 (1986) 345.
12 Koshkin L V, Rzhevskaya N N, Nazarova I A & Rodionova N M, *Izv Vyssh Uchebn Zaved, Khim Khim Tekhnol*, 25 (1982) 686.
13 Kempf M, *Ber dt chem Ges*, 47 (1914) 2615.
14 Martinus C A, *Justus Liebigs Ann Chem*, 117 (1861) 362.
15 Sharp A G, *The chemistry of cyano complexes of the transition metals* (Academic Press, London) 1976, p 106, 143 & 146.
16 Slifkin M A, *Biochim biophys Acta*, 103 (1965) 365.
17 Torrey H A & Hunter W H, *J Am chem Soc*, 34 (1912) 702.
18 Alexander J J & Gray H B, *J Am chem Soc*, 90 (1968) 4260.
19 Barton S D & Ollis w D, *Comprehensive organic chemistry*, edited by J F Stoddart (Pergamon Press, Oxford) 1979, 1213.
20 Foster R, *Organic charge-transfer complexes* (Academic Press, London) 1969, 135.
21 Curtis J C & Meyer T J, *Inorg Chem*, 21 (1982) 1562.

Indian Journal of Chemistry
Vol. 30A, March 1991, pp. 239-242

Kinetics of chromic acid-oxalic acid reaction catalysed by manganese(II)—Kinetic analysis of the consecutive pathway

P V Subba Rao*, G S R Krishna Rao, K Ramakrishna & P S N Murthy
School of Chemistry, Andhra University, Visakhapatnam 530 003

Received 21 February 1990; revised 7 August 1990; accepted 18 September 1990

Manganese(II) catalyses the chromic acid-oxalic acid reaction. The absorbance of the mixture of Cr(VI), oxalate and Mn(II) (at 480 nm) increases with time, reaches a maximum and thereafter decreases with time and this has been shown to be due to the consecutive path-way, $A \xrightarrow{k_a} I \xrightarrow{k_b} C$. D_{max} is directly proportional to $[Cr(VI)]_0$. k_a varies with variation in $[Mn(II)]_0$ and $[OX]_0$ whereas k_b is unaffected by variation in $[Mn(II)]_0$. Mechanism of the consecutive pathway has been proposed.

Unlike in many chromium(VI) oxidations, manganese(II) catalyses the chromic acid-oxalic acid reaction[1-5]. Ayyar[4] and Chakravarty and Ghosh[5] obtained evidence for Mn(III)-oxalate complex as an intermediate which undergoes intramolecular electron-transfer. It has also been shown[6] that Mn(II) is oxidised to Mn(III)-oxalate quantitatively by chromium(VI) in the presence of excess of oxalate. However, no kinetic analysis of this consecutive pathway has been so far made and we present that in this paper.

Materials and Methods

All the solutions were prepared in doubly distilled water. Stock solutions (10^{-1} mol dm^{-3}) of chromium(VI), oxalic acid and manganese(II) were standardised using standard methods. Ionic strength was maintained using sodium perchlorate solution (2 mol dm^{-3}).

The intermediate Mn(III)-oxalate complex has been found to have strong absorbance at 480 nm and hence the consecutive pathway was monitored by measuring the absorbance at this wavelength at different time intervals using a Hilger-UVispek spectrophotometer with thermostatic attachment. The absorption spectra were scanned using Milton-Roy spectronic-1201 spectrophotometer with microprocessor arrangement. The kinetic runs were carried out in the presence of sodium oxalate/oxalic acid buffer (*p*H 2.2-2.5).

Results and Discussion

The absorbance of the reaction mixture increases with increase in reaction time, reaches a maximum value and thereafter decreases (Fig. 1). Further, D_{max} is directly proportional to $[Cr(VI)]_0$. These results point to the consecutive pathway $A \xrightarrow{k_a} I \xrightarrow{k_b} C$, where A represents Cr(VI), I, the Mn(III)-oxalate complex and C the product(s). The [I] is given by Eq. (1)

$$[I] = \frac{k_a[Cr(VI)]_0}{(k_b - k_a)} (e^{-k_a t} - e^{-k_b t}) \quad \ldots (1)$$

Two rigorous methods are available[7,8] in support of the consecutive pathway. In the first method the plot of log P (where $P = D_t - D_\infty$) versus time is generally curved at early t but becomes linear at later t (Fig. 1). Thus the plot can be described by Eq. (2),

$$\log P = -k_{slow}\, t + \text{constant} \quad \ldots (2)$$

from which k_{slow} can be determined. Now the linear plot is extended to early t and the value of P′ is cal-

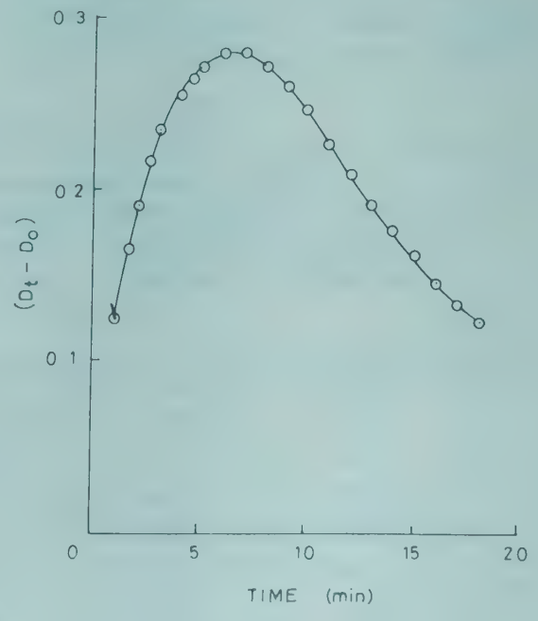

Fig. 1—Plot of absorbance versus time ($[Cr(VI)]_0 = 5.00 \times 10^{-4}$ mol dm^{-3}, $[Mn(II)]_0 = 2.50 \times 10^{-3}$ mol dm^{-3}, [oxalic acid]$_0 = 2.5 \times 10^{-2}$ mol dm^{-3}, $\mu = 0.50$ mol dm^{-3}; *p*H = 2.45, temp. = 30.0 ± 0.1°C)

culated at various times. P and P′ differ due to contribution from the faster of the consecutive steps (k_{fast}). The value of k_{fast} is given by the slope of the log (P′ − P) versus time plot which should be linear if the above consecutive mechanism holds. Such linear plots were obtained with the experimental data. A typical plot is presented in Fig. 2. The values of k_{slow} and k_{fast} were also determi ned using the alternative procedure[8] and the rate constants calculated by both the methods agree within ± 5%. The rate constant of the decomposition of I, k_b, can be considered to be k_{slow} whose value $(1.2\text{-}1.4)\times 10^{-3}$ s^{-1} at 30°C is in agreement with the rate of decomposition of manganese(III)-oxalate complex reported in the literature[9,10]. Thus k_a corresponds to k_{fast}.

The values of k_a and k_b have been determined at different initial $[Mn(II)]_0$, $[oxalate]_0$ and $[H^+]$ and are presented in Table 1. In all the cases, k_a increases with increase in $[Mn(II)]_0$, $[Ox]_0$ and $[H^+]$ where Ox represents total oxalate; k_b is independent of $[Mn(II)]_0$ under the experimental conditions employed. These kinetic features can be explained by assuming that fast equilibria are associated with the consecutive pathway. Mn^{2+} and Mn^{3+} are capable of forming 1:1, 1:2 and 1:3 complexes with oxalate ion(Ox) and the fraction of these complexes present in the system can be represented by Eq. (3).

$$[MOx]=\frac{K_1[C_2O_4^{2-}]}{N},\ [MOx_2]=\frac{K_1K_2[C_2O_4^{2-}]^2}{N}\ \text{and}$$

$$[MOx_3]=\frac{K_1K_2K_3[C_2O_4^{2-}]^3}{N} \qquad \ldots (3)$$

Under the conditions $[M]_0 \ll [Ox]_0$, (where M represents Mn^{2+} or Mn^{3+}) and $N = 1 + K_1[C_2O_4^{2-}] + K_1K_2[C_2O_4^{2-}]^2 + K_1K_2K_3[C_2O_4^{2-}]^3$.

$$[C_2O_4^{2-}]=\frac{K'_a K''_a[Ox]_0}{[H^+]^2+K'_a[H^+]+K'_aK''_a} \qquad \ldots (4)$$

$$\simeq \frac{K''_a[Ox]_0}{[H^+]} \qquad \ldots (5)$$

in the *p*H range employed.

In Eqs (3-5) K_1K_2 and K_3 are the stepwise stabil-

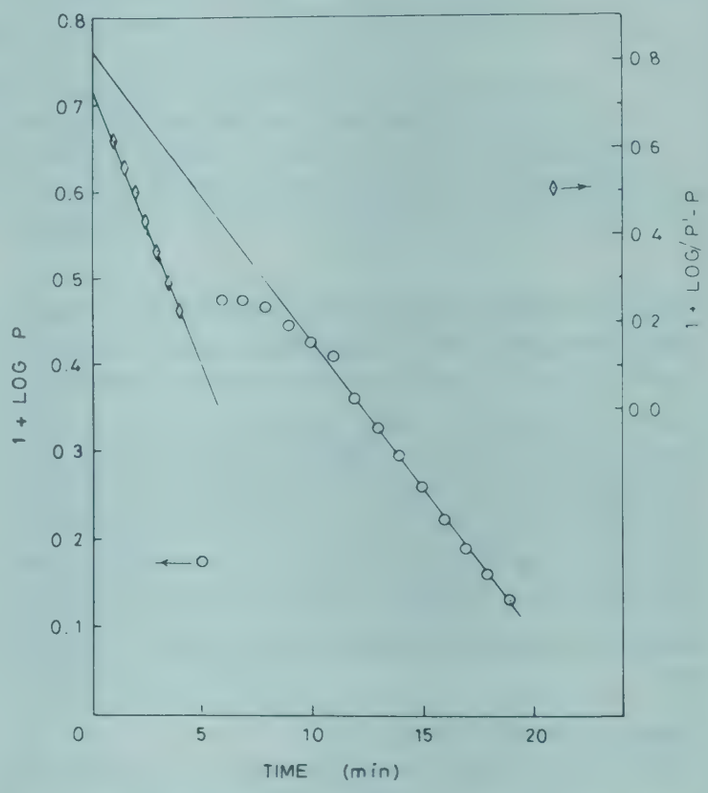

Fig. 2—Plot of log P versus time and plot of log |P′-P| versus time ($[Cr(VI)]_0 = 5.00\times10^{-4}$ mol dm^{-3}, $[Mn(II)]_0 = 2.5\times10^{-3}$ mol dm^{-3}, $[oxalic\ acid]_0 = 2.5\times10^{-2}$ mol dm^{-3}, $\mu = 0.50$ mol dm^{-3}; *p*H = 2.45, temp. = 30.0 ± 0.1°C)

Table 1—Consecutive rate constants under the conditions, $[Ox]_0 \gg [Mn(II)]_0$ {$[Cr(VI)]_0 = 5.0\times10^{-4}$ mol dm^{-3}, $\mu = 0.5$ mol dm^{-3}, temp. = 30.0 ± 0.1°C}

10^3 [Mn(II)] (mol dm^{-3})	10^2 $[Ox]_0$ (mol dm^{-3})	10^3 $[H^+]$ (mol dm^{-3})	10^3 k_a (s^{-1})	10^3 k_b (s^{-1})	10^3 k_b (s^{-1}) Calculated from Eq. 11b)
2.50	3.50	3.16	3.40	1.25	1.27
2.50	5.00	3.53	5.10	1.33	1.29
2.50	7.00	4.56	7.00	1.30	—
2.50	10.00	5.50	8.35	1.32	—
2.50	13.00	6.58	10.50	1.22	1.32
2.50	5.00	4.56	5.08	1.33	1.27
3.50	5.00	4.56	6.91	1.40	1.27
4.25	5.00	4.56	7.90	1.40	1.27
5.00	5.00	4.56	10.00	1.40	1.27
6.00	5.00	4.56	11.23	1.33	1.27

ity constants and K'_a and K'_a are the first and second ionisation constants of oxalic acid ($K'_a = 5.6 \times 10^{-2}$, $K''_a = 5.4 \times 10^{-5}$)[6]. In the case of Mn(II) (log $K_1 = 3.9$, log $K_2 = 1.43$ and log $K_3 < 0.1$)[6] only 1:1 complex, Mn C_2O_4, is predominant at *p*H 2.0-2.5. Considering the stability constants of manganese(III)-oxalate complexes, it can be shown that in the *p*H range employed, only 1:2 and 1:3 complexes predominate (log $K_1 = 9.88$, log $K_2 = 6.59$ and log $K_3 = 2.85$)[6] and hence contribution to the rate by the pathway involving 1:1 complex, $Mn(C_2O_4)^+$, can be neglected.

To study the nature of the coloured intermediate formed in the reaction, the absorption spectra of the reaction mixture after 1 min and 10 min were scanned setting the scanning time at 6 sec during which time the change in absorbance due to reaction has been found to be negligibly small. The spectra at both the times show broad peak at 465 and shoulder at 510 nm (Fig. 2a). Dingle[11] has reported that bis-oxalato-diaquomanganese(III) has absorption maximum at 460 nm ($\varepsilon = 130$) while the tris-oxalato manganese(III) exhibits peaks at 487 and 515 nm ($\varepsilon = 230$). Chromium(III) obtained as a reaction product as well as Cr(VI) under these conditions have been found to have negligible absorbances at these wavelengths. The peak at 465 nm indicates the presence of bis-oxalato manganese(III) and the shoulder due to the tris complex whose concentration is less than that of the bis complex under the experimental conditions employed. The peak due to the tris complex at 487 nm appears to be submerged in the peak at 465 nm.

The kinetic analysis can be carried out by analysing the k_a and k_b-paths separately[12]. These paths

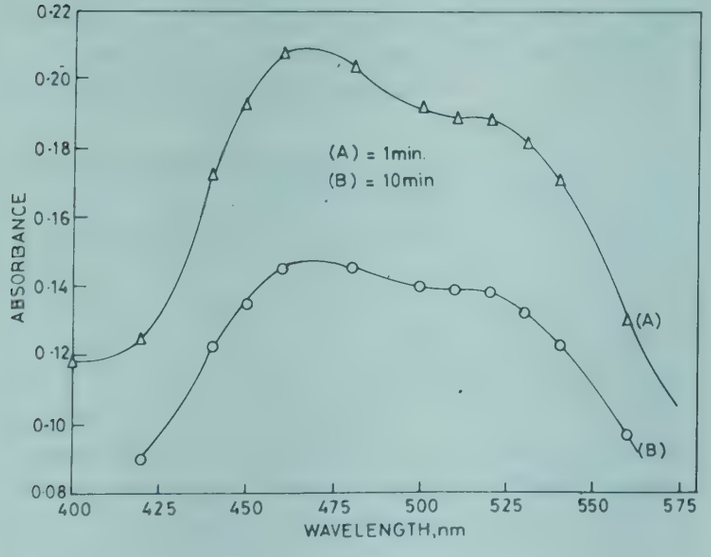

Fig. 2a—Visual absorption spectra of intermediate Mn(III)-oxalate complexes ($[Cr(VI)]_0 = 5.0 \times 10^{-4}$ mol dm^{-3}, $[Ox]_0 = 2.5 \times 10^{-2}$ mol dm^{-3}, $[Mn(II)]_0 = 5.0 \times 10^{-3}$ mol dm^{-3}, *p*H = 2.1; $\mu = 0.5$ mol dm^{-3}; temp. = 25.0 ± 0.1°C)

can be represented by Schemes (1) and (2) which explain all the results.

k_a-path

$$HCrO_4^- + H^+ \overset{K}{\rightleftharpoons} H_2CrO_4$$

$$Mn^{2+} + C_2O_4^{2-} \overset{K_1}{\rightleftharpoons} MnC_2O_4$$

$$MnC_2O_4 + H_2CrO_4 \overset{k_a}{\rightarrow} Mn(C_2O_4)^+ + Cr(V)$$

Scheme 1

k_b-path

$$Mn(C_2O_4)^+ + C_2O_4^{2-} \overset{K_2}{\rightleftharpoons} Mn(C_2O_4)_2^-$$

$$Mn(C_2O_4)_2^- + C_2O_4^{2-} \overset{K_3}{\rightleftharpoons} Mn(C_2O_4)_3^{3-}$$

$$Mn(C_2O_4)_2^- \overset{k'_2}{\rightarrow} \text{Products}$$

$$Mn(C_2O_4)_3^{3-} \overset{k''_2}{\rightarrow} \text{Products}$$

Scheme 2

If $[Mn(III)]_t$ is the total Mn(III) concentration and I_1, I_2 and I_3 be the concentrations of 1:1, 1:2 and 1:3 complexes, then

$$[Mn(III)]_t = I_1 + I_2 + I_3 \quad \ldots (6)$$

Since I_1 is negligible under these conditions, Eq. (6) may be approximated to

$$[Mn(III)]_t = I_2 + I_3 \quad \ldots (6a)$$

From Eq. (6a) it can be derived that

$$I_2 = \frac{\overline{Mn(III)_t}}{1 + K_3[C_2O_4^{2-}]} \text{ and } I_3 = \frac{K_3[Mn(III)]_t[C_2O_4^{2-}]}{1 + K_3[C_2O_4^{2-}]} \ldots (7)$$

Therefore, $\dfrac{d[Mn(III)]_t}{dt}$

$$= \frac{k_1 K K_1 K''_a [Mn(II)]_0 [Ox]_0 [H^+][HCrO_4^-]_0}{[H^+] + K_1 K''_a [Ox]_0}$$

$$-(k'_2[I_2] + k''_2[I_3]) \quad \ldots (8)$$

Using Eqs (5) and (7), Eq. (8) may be written as

$$\frac{d[Mn(III)]_t}{dt}$$

$$= \left\{ \frac{k_1 K K_1 K''_a [Mn(II)]_0 [Ox]_0 [H^+][HCrO_4^-]_0}{[H^+] + K_1 K''_a [Ox]_0} \right.$$

$$- \left(\frac{k'_2 [Mn(III)]_t}{1 + K_3 K''_a [Ox]_0 / [H^+]} \right.$$

$$\left. \left. + \frac{k''_2 K_3 K''_a [Mn(III)]_t [Ox]_0 / [H^+]}{1 + K_3 K''_a [Ox]_0 / [H^+]} \right) \right\} \quad \ldots (9)$$

which on integration leads to Eq. (10)

$$[Mn(III)]_t = \frac{k[HCrO_4^-]_0}{(k_b - k_a)}(e^{-k_a t} - e^{-k_b t}) \quad \ldots (10)$$

Equation (10) is the same as the equation for consecutive pathway (Eq. (1)), where

$$k_a = \frac{k_1 K K_1 K''_a [Mn(II)]_0 [Ox]_0 [H^+]}{[H^+] + K_1 K''_a [Ox]_0} \quad \ldots (11a)$$

and

$$k_b = \frac{k'_2}{1 + K_3 K''_a [Ox]_0/[H^+]} + \frac{k''_2 K_3 K''_a [Ox]_0/[H^+]}{1 + K_3 K''_a [Ox]_0/[H^+]} \quad \ldots (11b)$$

In agreement with this rate-law, the results obtained under these conditions (Table 1) show that k_a is directly proportional to $[Mn(II)]_0$. Further the values of $[Ox]_0[H^+]/([H^+] + K_1 K''_a [Ox]_0)$ were calculated taking the literature values of K''_a and K_1. A plot of k_a versus $[Ox]_0[H^+]/([H^+] + K_1 K''_a [Ox]_0)$ is linear passing through the origin establishing the validity of the rate-law.

Choosing any two values from Table 1, k'_2 and k''_2 can be calculated from Eq. (11b) using the values of K_3 and K''_a available in the literature; k'_2 and k''_2 have been found to be 1.17×10^{-3} s^{-1} and 1.52×10^{-3} s^{-1} respectively at 30°C. Using these data the values of k_b have been calculated for other runs mentioned in Table 1. k_b thus calculated is in good agreement with that obtained from the experimental results, showing the validity of the rate-law under the experimental conditions employed. The values of k'_2 and k''_2 are also in reasonable agreement with those reported in literature[9,10] ($k'_2 = 8 \times 10^{-4}$ s^{-1} at 20°C and $k''_2 = 0.49 \times 10^{-3}$ s^{-1} at 25°C).

References

1 Rocek J & Fariza H, *J Am chem Soc*, 94 (1972) 9073.
2 Bakore G V & Jain C L, *J inorg nucl Chem*, 31 (1969) 805.
3 Durham D A, *J inorg nucl Chem*, 31 (1969) 3549.
4 Ayyar R V V, Ph D Thesis, Andhra University, Waltair (1966).
5 Chakravarty D N & Ghosh S, *Proc Natl Acad Sci, India, Sect A*, 29 Pt. 2 (1960) 199.
6 Haight G P (Jr) & Huber C F, *J Am chem Soc*, 68 (1976) 14.
7 Jackson W G, Harrofield M & Vowles P D, *Int J chem Kinet IX* (1977) 535.
8 Espenson J H in *Chemistry: kinetics and reaction mechanisms* (McGraw-Hill, New York) 1981.
9 Duke F R, *J Am chem Soc*, 69 (1947) 2885.
10 Adler S J & Noyes R M, *J Am chem Soc*, 77 (1955) 2036.
11 Dingle R, *Acta Chem Scand*, 20 (1966) 35-36.
12 Buckingham D A, Francis D J & Sargeson A M, *Inorg Chem*, 13 (1974) 2630.

Indian Journal of Chemistry
Vol. 30A, March 1991, pp. 243-246

Kinetics and mechanism of cooxidation of oxalic acid and arsenic(III) by chlorochromate in aqueous acetic acid

M I Sambrani & J R Raju*
Department of Chemistry, Karnatak University, Dharwad 580 003

Received 23 April 1990; revised 20 July 1990; accepted 3 September 1990

The influence of oxalic acid on chromium(VI) oxidation of arsenic(III) is studied in the presence of chloride ion in 60% aqueous acetic acid and $I = 0.80$ mol dm^{-3} ($NaClO_4$). It is found that both arsenic(III) and oxalic acid are oxidised concertedly in a three equivalent step. It has been found that one mole of Cr(VI) oxidises one equivalent of oxalic acid and two equivalents of arsenic(III). The details of such a process are discussed.

Chromium(VI) oxidation of a mixture of 2-propanol and oxalic acid in aqueous solution leads to the oxidation of both the substrates in a concerted step[1]. A few other such cases of cooxidations by chromium(VI) have also been reported[2]. Mechanistically, a concerted process whereby a single step three equivalent change from Cr(VI) to Cr(III) is expected to facilitate the reaction as the intervention of the energetically unfavourable Cr(IV) is avoided. Chlorochromate, $ClCrO_3^-$, is a less potent oxidant than acid chromate, $HCrO_4^-$, and the latter is almost fully converted into chlorochromate in 60% acetic acid in the presence of 0.60 mol dm^{-3} chloride[3,4]. The chlorochromate oxidation of As(III) is slow enough to permit a study of the effect of oxalic acid on the reaction. The influence of oxalic acid on Cr(VI) oxidation of Tl(I) seems to be the only other known example besides the present study of cooxidation involving an inorganic reductant[5].

Materials and Methods

Oxalic acid, arsenic(III) oxide, sodium chloride and potassium dichromate (all BDH, AR samples) were used as such. Other chemicals were of reagent grade. Doubly distilled water was used for preparing the solutions. Purified acetic acid was used. A stock solution of As(III) was made by dissolving arsenic(III) oxide in 1.0 mol dm^{-3} sodium hydroxide and the solution was standardised with potassium iodate[6(a)], while stock solutions of potassium dichromate and sodium chloride were prepared by dissolution of the required quantities in water.

Kinetic runs

Kinetics were followed in 60% acetic acid (v/v) in the presence of 0.60 mol dm^{-3} chloride at 27°C unless otherwise stated. The ionic strength was maintained at 0.80 mol dm^{-3} with sodium perchlorate. The reaction rates were determined spectrophotometrically by following the decrease in absorbance of Cr(VI) at regular intervals at 360 nm ($\varepsilon = 1200 \pm 1\%$) using 1 cm cells in a Bausch and Lomb Spectronic 2000 spectrophotometer. Initial rates were obtained by plane mirror method[7] and pseudo-first order rate constants (k) from the slopes of plots of log[Cr(VI)] versus time. The reaction obeyed good first order kinetics when [substrate] $>>$ [oxidant]. The rate constants were averages of multiple determinations and were reproducible within $\pm 5\%$.

Results

Stoichiometry

Reaction mixtures containing different amounts of reactants, As(III), Cr(VI) and oxalic acid, in the presence of 0.60 mol dm^{-3} chloride at $I = 0.80$ mol dm^{-3} in 60% acetic acid were kept at 27°C for 24 hrs and analysed for As(III), oxalic acid and Cr(VI). The unreacted As(III) was analysed by (i) titration with standard iodate solution and (ii) titration with iodine solution[6(b)], while Cr(VI) was estimated spectrophotometrically at 360 nm. The total reductant of unreacted As(III) and oxalic acid (hot) was found by back titration of added excess Ce(IV) with Fe(II) solution[6(c)]. This procedure for oxalic acid, obtained by difference of total reductant and unreacted As(III), was satisfactory as it was ensured that Cr(VI) had completely reacted under the reaction conditions and the Ce(IV)-Cr(III) reaction was too slow to interfere in the Fe(II) titration of excess Ce(IV). Runs were

also monitored to find the yield of carbon dioxide using a Warburg apparatus[8]. The results are indicative of a 2:3 reaction when As(III) or oxalic acid alone is present. However, Cr(VI) oxidation of a mixture of oxalic acid and As(III) consumes two equivalents of As(III) and one equivalent of oxalic acid. The marginal excess yield of As(V) is presumably due to the direct Cr(VI)-As(III) reaction which may also be occurring to a small extent.

Effect of chloride and acetic acid—It was found that in the media of 60% acetic acid and 0.60 mol dm^{-3} chloride, virtually all the Cr(VI) employed (~98.5% or higher) was in the form of chlorochromate[3,4].

Order of reaction—Under the conditions 60% acetic acid, 0.60 mol dm^{-3} chloride, $I=0.80$ mol dm^{-3}, in the range of [As(III)] of 8.0×10^{-5} to 2.0×10^{-3} mol dm^{-3} and fixed [oxalic acid] of 5.0×10^{-4} mol dm^{-3}, the order in As(III) was approximately unity. At a constant [As(III)] of 4.0×10^{-4} mol dm^{-3}, in the range of [oxalic acid] 5.0×10^{-4} to 3.0×10^{-3}, the order in oxalic acid was 0.95. Between 2.0×10^{-5} and 4.0×10^{-4} mol dm^{-3} [Cr(VI)], the order in Cr(VI) was 0.96 at fixed [oxalic acid] (2.0×10^{-3} mol dm^{-3}) and [As(III)] (4.0×10^{-4} mol dm^{-3}).

Effect of acidity—Measurement of *p*H (employing a digital *p*H-meter, Elico model LI-120) and acidity function (H_0) by spectrophotometry[9] showed that no significant varition in acidity occurred in the reaction mixture containing varying amounts of oxalic acid. However, in the presence of small quantities of perchloric acid, the acidity function (H_0) falls and the increase in the first order rate constant corresponds to an order of approximately 0.4 in acidity.

Free radical intervention—In the presence of added acrylamide, the reaction mixture containing 1.6×10^{-2}, 3.0×10^{-2} and 8.0×10^{-3} mol dm^{-3} of As(III), oxalic acid and Cr(VI), respectively, shows polymer formation on dilution with methanol. This indicates the free radical intervention in the reaction. Furthermore, in the presence of acrylamide, the yield of carbon dioxide is marginally decreased whereas that of As(V) increased.

Effect of added products—Initially added products, As(V) and Cr(III) did not change the pseudo-first order rate constants to any appreciable extent; the pseudo-first order rate constants of the Cr(VI)-As(III) reaction were measured in presence of oxalic acid and As(V)/Cr(III).

Effect of aluminium chloride—When aluminium chloride was present in the reaction medium, the pseudo-first order rate constant decreased substantially. For example at [As(III)] $=4.0\times10^{-4}$, [oxalic acid] $=2.0\times10^{-3}$, [Cl^-] $=0.60$, $I=0.80$ mol dm^{-3}, temp. $=300$ K, 10^3k decreased from 0.72 to 0.58 s^{-1} when added [$AlCl_3$] $\times10^2$ was changed from 1.0 to 5.0 mol dm^{-3}.

Discussion

The chlorochromate oxidation of arsenic(III) and oxalic acid is approximately third order, first order in oxidant, arsenic(III) and oxalic acid. The effect of arsenic(III) on the chromium(VI) oxidation of oxalic acid is shown in Fig. 1 while the influence of oxalic acid on the chromium(VI)-arsenic(III) reaction is shown in Fig. 2. The latter reaction is rather fast as compared to the chromium(VI)-oxalic acid case but the data are clearly indicative of the combined effect of both oxalic acid and arsenic(III) in the reaction. When the two reductants are present together, the reaction is faster as compared to the case when only one of them is present. Thus, for example, the plots of log k versus log[As(III)] in respect of first order rate constants of the chromium(VI)-oxalic acid reaction, at several [oxalic acid], are linear and lie well above zero [oxalic acid] (Fig. 1). Likewise, the rate constants of the Cr(VI)-As(III) reaction at constant acidity and [As(III)] are influenced positively by the presence of even small amounts of oxalic acid of around 1% of As(III). These results together with the stoichiometry of two and one equivalents of As(III) and oxalic acid respectively being oxidised by a mole of oxidant indicate the likelihood of cooxidation.

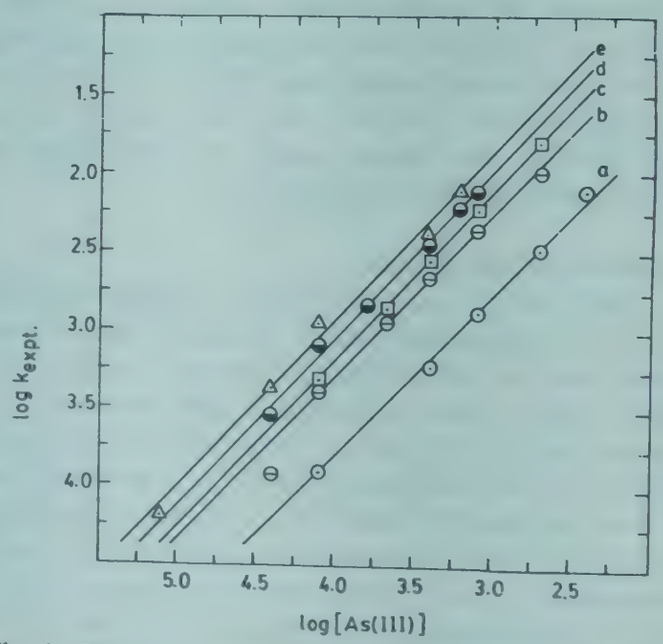

Fig. 1—Effect of arsenic(III) on the experimental rate constants at several constant oxalic acid concentrations (a) Zero, (b) 5.0×10^{-4}, (c) 10.0×10^{-4}, (d) 15.0×10^{-4} and (e) 30.0×10^{-4} mol dm^{-3} respectively and constant acidity. ([Cr(VI)] $=4.0\times10^{-5}$ mol dm^{-3}, [Cl^-] $=0.60$ mol dm^{-3}, $I=0.80$ mol dm^{-3}, 60% HOAc (v/v) and temp. $=300$ K).

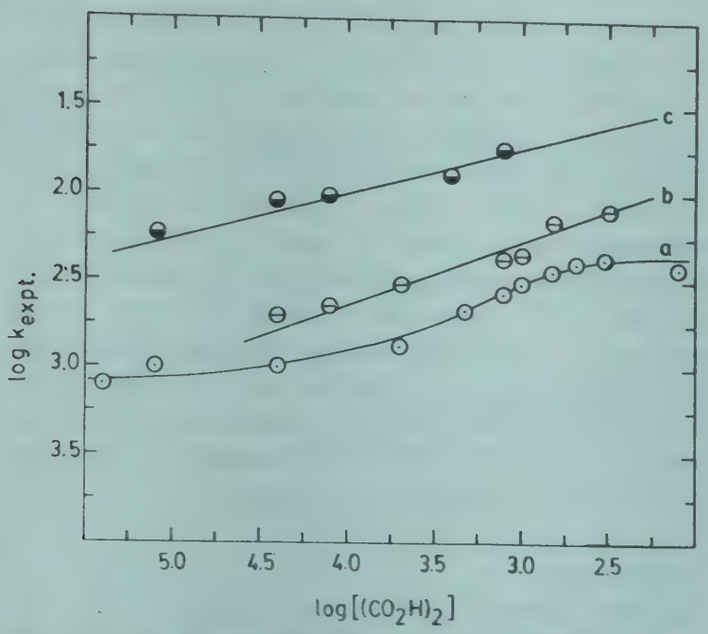

Fig. 2 – Effect of oxalic acid on the experimental rate constants at several constant arsenic(III) concentrations (a) 4.0×10^{-4}, (b) 8.0×10^{-4} and (c) 2.0×10^{-3} mol dm^{-3} respectively and constant acidity (other conditions as in Fig. 1).

In the case of As(III), increase in [oxalic acid] increases the rate constant initially and then reaches a plateau at higher [oxalic acid] and the order in [oxalic acid] tends to become zero. This behaviour is similar to that of Cr(VI) oxidation of 2-propanol in the presence of oxalic acid and is characteristic of the formation of an intermediate complex[1]. The formation of a 1:1 Cr(VI)-oxalic acid complex may be shown as in steps (1) and (2) in Scheme 1 and the concentration of the complex, C_1, is given by Eq. (3) where the total [Cr(VI)] is the sum of the free and complexed [oxidant]. The rate of reaction is given by Eqs (5) and (6). Since the reaction in the absence of oxalic acid may not be neglected, the total rate at constant acidity may be taken to be the sum of the rates of the two reactions, one due to the direct Cr(VI)-As(III) reaction and the other due to the faster Cr(VI) oxidation of As(III) and oxalic acid present together as shown in Eq. (6).

$$(CO_2H)_2 + Cr(VI) \overset{K_1}{\rightleftharpoons} \text{Complex, } C_1 \qquad \ldots (1)$$

$$C_1 + As(III) \overset{k_2}{\rightarrow} \text{Products} \qquad \ldots (2)$$

Scheme 1

$$[C_1] = \frac{K_1[(CO_2H)_2][Cr(VI)]_{total}}{(1+K_1[(CO_2H)_2])} \qquad \ldots (3)$$

$$\text{Rate} = k_2[C_1][As(III)] \qquad \ldots (4)$$

$$= \frac{k_2K_1[(CO_2H)_2][Cr(VI)]_{total}[As(III)]}{(1+K_1[(CO_2H)_2])} \qquad \ldots (5)$$

$$\text{Rate}_{total} = k_1[Cr(VI)]_{total}[As(III)] + \frac{k_2K_1[(CO_2H)_2][Cr(VI)]_{total}[As(III)]}{(1+K_1[(CO_2H)_2])} \qquad \ldots (6)$$

From Eq. (6), a plot of

$$\frac{[Cr(VI)]_{total}[As(III)]}{(\text{Rate}_{total} - k_1[Cr(VI)]_{total}[As(III)])} \text{ versus } \frac{1}{[(CO_2H)_2]}$$

should be linear (k_1, 1.41 dm^3 mol^{-1} s^{-1}, being taken from runs in the absence of oxalic acid, (Fig. 3). Values of K_1 and k_2 result from Fig. 3 as 42.9 ± 2.0 dm^6 mol^{-2} and 100 ± 10 dm^3 mol^{-1} s^{-1} respectively. Rates obtained from the calculated values of K_1 and k_2 show satisfactory agreement with the experimentally measured initial rates under different conditions.

The data of stoichiometry, that is, the products (As(V) and carbon dioxide) formed in approximately 1:1 ratio support a concerted three-electron reaction. In the Cr(VI) oxidation of As(III) and oxalic acid, the product ratio was around one mole of As(V) to 1.1-1.2 mole carbon dioxide which becomes almost a 1:1 ratio in the presence of free radical scavengers. In the presence of free radical scavengers, as argued by Rocek and Hasan[1], the free radicals are removed by nonoxidative bimolecular destruction so that the 1:1 reaction only is facilitated. As a matter of fact, there is

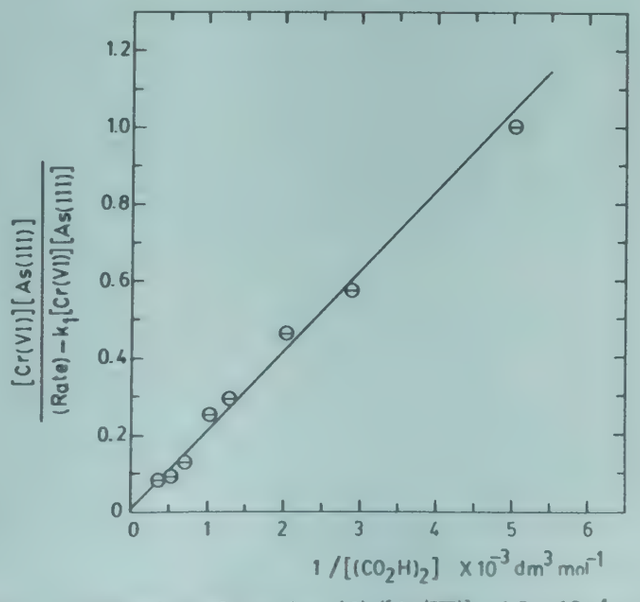

Fig. 3 – Verification of rate law (6) ([As(III)] = 4.0×10^{-4} mol dm^{-3}; other conditions as in Fig. 1)

decrease in the yield of carbon dioxide with increase in [acrylamide] and increase in the yield of As(V). Only one mole of carbon dioxide would be expected from the cooxidation; however, the free radical resulting from the concerted process can also generate a mole of carbon dioxide and hence more than a mole of carbon dioxide may result in the absence of free radical scavengers.

Added support to the single step three-electron mechanism in this case, comes from the results of the use of aluminium chloride in the reaction[10]. Oxalic acid can preferentially complex with Al(III) and thus prevent Cr(VI)-oxalic acid complex intermediate formation in the reaction. Thus, the first order rate constant should decrease in presence of added aluminium chloride and this is borne out by experiment. The reaction mechanism is shown in Scheme 2.

A cyclic intermediate similar to that shown in Eq. (7) was postulated in the Cr(VI)-oxalic acid reaction mechanism[11] and other studies[12,13]; it had an equilibrium constant of 9.5 dm^6 mol^{-2} in aqueous solution at 25°C and $I=0.63$ as against the value of 42.9 dm^6 mol^{-2} in the present case. A neutral complex is possible only if it is cyclic and such a neutral complex would be favoured in a less polar media to a greater extent as, in fact, indicated by the higher equilibrium constant of formation in the present case. The complex, C_1, formed by the elimination of the elements of water and HCl, reacts with arsenic(III) in step (8) to undergo a rate-determining decomposition into products in step (9). The products, Cr(III), As(V) and carbon dioxide are all quantitatively fixed (results) and the free radical formation also verified by free radical trapping experiments.

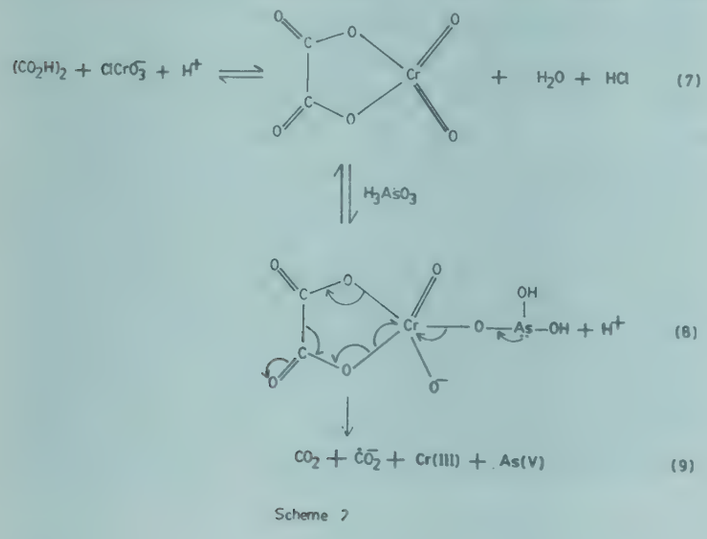

Scheme 2

References

1 Hasan F & Rocek J, *J Am chem Soc*, 94 (1972) 3181.

2 Granzow A, Wilson A & Ramirez F, *J Am chem Soc*, 96 (1974) 2454.

3 Cohen M & Westheimer F H, *J Am chem Soc*, 74 (1952) 4387.

4 Chimatadar S A, Nandibewoor S T & Raju J R, *J Indian chem Soc*, LXIV (1987) 187.

5 Gokavi G S, *Kinetics and mechanism of some oxidation reactions* Ph.D. Thesis, Karnatak University, Dharwad (1987) p. 101.

6 Vogel I, *Text book of quantitative inorganic analysis* (ELBS-Longman, New York) 1978 (a) p. 387, (b) p. 378, (c) p. 366.

7 Latshaw M, *J Am chem Soc*, 47 (1925) 793.

8 Umbreit W W, *Manometric techniques* (Burgess, Minneapolis, Minn) (1964).

9 Paul M A & Long F A, *Chem Rev*, 57 (1957) 1.

10 Chandra S, Shukla S N & Chatterji A C, *Z phys Chem (Leipzig)*, 237 (1968) 137.

11 Hasan F & Rocek J, *J Am chem Soc*, 94 (1972) 9073.

12 Vandegrift G F & Rocek J, *J Am chem Soc*, 98 (1976) 1371.

13 Hintze R E & Rocek J, *J Am chem Soc*, 99 (1977) 132.

Indian Journal of Chemistry
Vol. 30A, March 1991, pp. 247-251

Oxidation of diphenylamines by iodate —A kinetic study

A Brahmaiah, P Manikyamba*
Department of Chemistry, University Arts and Science College, Warangal 506 009
and
E V Sundaram
Department of Chemistry, Kakatiya University, Warangal 506 009

Received 24 May 1990; revised 4 October 1990; accepted 25 October 1990

Oxidation of diphenylamines (DPA) by iodate in aqueous methanol (70%, v/v) at 303 K is first order in [oxidant] and fractional order in [DPA] and is acid-catalysed. There is a dipole-dipole interaction between the oxidant and DPA. The substituent effect on the rate of reaction shows that electron-releasing groups on the benzene ring enhance the rate and electron-withdrawing groups retard the rate compared to the unsubstituted DPA. The product identified is the corresponding carbazole. Thermodynamic parameters are calculated and a suitable mechanism is proposed.

Secondary aromatic amines on oxidation give a variety of products depending upon the conditions employed and oxidant used. With diphenylamine, tetraphenylhydrazine[1], carbazole[2], diphenyl nitroxide[3], diphenylbenzidine[4] or N-phenyl-*p*-benzoquinoneimine[5] are reported to be the oxidation products using different oxidizing agents. However, the detailed kinetic and mechanistic studies on the oxidation of diphenylamines are scanty[5-8]. Hence, it was felt worthwhile to carry-out the title investigation.

Materials and Methods

Diphenylamine and diphenylamine-4-sulphonic acid were of AR grade (BDH). 3-Cl-, 3-CH_3- and 3-OCH_3-diphenylamines were procured from Aldrich Chemicals Co., USA. These diphenylamines were used as such, after verifying their melting or boiling point. Potassium iodate (AR, BDH), methanol (Qualigens ExcelaR) and D_2O (Sigma) were also used as such. The kinetic studies were made in aqueous methanol (70%, v/v) at 303 K. The reaction mixture consisted of iodate (0.002 mol dm^{-3}), diphenylamine (0.02 mol dm^{-3}) and sulphuric acid (0.4 mol dm^{-3}) and the kinetics were followed by estimating [unreacted iodate] iodometrically at regular time intervals. From the slopes of the plots of log$[IO_3^-]_t$ versus time, the pseudo-first order rate constants (k_{obs}) were obtained, which were reproducible within 5%.

Temperature was maintained constant with an accuracy of ±0.2°C. The UV spectra were recorded on a Shimadzu MPS-5000 spectrophotometer.

Solvent methanol did not undergo oxidation by iodate under the experimental conditions. The added acrylonitrile did not get polymerised indicating the absence of radical reactions.

The oxidation products of diphenylamines were the corresponding carbazoles as revealed by spot tests and UV spectral studies (compared with the authentic samples).

Results and Discussion

The stoichiometric study indicates that each mole of iodate reacts with three moles of diphenylamine in accordance with the following stoichiometric equation (1).

$$IO_3^- + 3C_{12}H_{11}N \rightarrow 3C_{12}H_9N + 3H_2O + I^- \quad \ldots (1)$$

Under the conditions of [DPA9 > $[IO_3^-]$, the pseudo-first order plots of log $[IO_3^-]_t$ versus time at different initial $[IO_3^-]_t$ (0.001 to 0.008 mol dm^{-3}) are linear suggesting first order dependence of rate on $[IO_3^-]$. However, k_{obs} (Table 1) decreased with increase in $[IO_3^-]_{initial}$. This decrease in k_{obs} can be explained by considering the following equilibrium[9] (2) in acid medium.

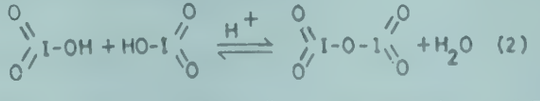

(2)

With increase in $[IO_3^-]$, the formation of I_2O_5 is more favourable resulting in the decrease of k_{obs}, since the product I_2O_5 is known to be weaker oxidizing agent compared to HIO_3. Hence the rate data are collected at a fixed [iodate].

The double logarithmic plots of log k_{obs} versus log[DPA] are linear with slopes of less than unity

Table 1 – Effect of $[IO_3^-]$ on k_{obs}:DPA – iodate system

$[DPA] = 0.02\ mol\ dm^{-3}$; $[H_2SO_4] = 0.4\ mol\ dm^{-3}$; aq. MeOH = 70% (v/v); temp. = 303 K

DPA	$k_{obs} \times 10^4\ s^{-1}$ at $[IO_3^-]$ (mol dm^{-3})			
	0.001	0.002	0.004	0.008
DPA	17.27	12.09	11.03	7.68
3-CH_3-DPA†	9.59	8.37	6.53	4.38
3-Cl-DPA††	0.31	0.12	0.14	0.10
4-SO_3H-DPA	6.40	4.47	3.60	2.40

†$[H_2SO_4] = 0.1\ mol\ dm^{-3}$; temp. = 293 K

††$[H_2SO_4] = 0.1\ mol\ dm^{-3}$.

Table 2 – Effect of $[H_2SO_4]$ on k_{obs}:DPA-iodate system

$[IO_3^-] = 0.002\ mol\ dm^{-3}$; [Substrate] = 0.02 mol dm^{-3}; aq. MeOH = 70% (v/v); temp. = 303 K

Substrate	$k_{obs} \times 10^4$ at $[H_2SO_4]$/mol dm^{-3}					
	0.1	0.2	0.4	0.6	0.8	1.0
DPA	1.79	2.51	12.09	21.52	—	40.31
3-CH_3-DPA†	8.39	16.31	31.47	—	60.68	86.52
3-Cl-DPA††	0.12	0.35	0.75	—	2.87	4.64
4-SO_3H-DPA	1.65	2.84	4.47	—	10.23	12.79

†Temp. = 293 K

suggesting that the order in [DPA] is fractional. The double reciprocal plots of k_{obs}^{-1} versus $[DPA]^{-1}$ are also linear with positive intercepts suggesting Michaelis-Menton type of kinetics, i.e. DPA forms a complex with iodate, which decomposes in a slow step.

k_{obs} values are either nearly constant or change marginally with change in the composition of the reaction medium. For example, under the conditions $[IO_3^-] = 0.002$ mol dm^{-3}, [substrate] = 0.02 mol dm^{-3}, $[H_2SO_4] = 0.4$ mol dm^{-3} and temp. = 303 K, $k_{obs} \times 10^4$ values remained constant at 1.23 ± 0.06 and 0.76 ± 0.07 for DPA and 3-Cl DPA when % MeOH in water-methanol medium was changed from 50 to 90. Further, when the reaction is studied at different added $[MnSO_4]$, no effect of added salt on rate is indicated. These two observations suggest that the neutral species of iodate and DPA participate in the oxidation process.

The reaction is acid catalysed (Table 2). Under identical conditions $k_{D_2O}/k_{H_2O} = 1.8$ ($k_{D_2O} = 11.26 \times 10^{-4}\ s^{-1}$ and $k_{H_2O} = 6.21 \times 10^{-4}\ s^{-1}$ when $[DPA] = 0.02$ mol dm^{-3}, $[IO_3^-] = 0.002$ mol dm^{-3}, $[H_2SO_4] = 0.2$ mol dm^{-3} in 70% (v/v) aqueous methanol at 303 K). This suggests a fast equilibrium protonation, preceding the rate-determining step. Since, D_2O is a weaker base than H_2O, the concentration of protonated species is usually larger in D_2O than in H_2O.

The protonation of iodate ion, giving HIO_3, $H^+ + IO_3^- \rightleftharpoons HIO_3$ is known to be facile with a dissociation constant K of 0.17 (ref. 10, 11). Since the solvent and salt effects suggest a dipole-dipole interaction between the reactants, in the subsequent step, it is proposed that HIO_3 and DPA interact giving a complex. This complex formation is confirmed from the Michaelis-Menton plots. The formation and decomposition constants of the complexes calculated from the slope and intercept of the Michaelis-Menton plots are 0.93 and $250 \times 10^{-4}\ s^{-1}$ for DPA, 0.72 and $33 \times 10^{-4}\ s^{-1}$ for 3-CH_3 DPA, 0.84 and $0.43 \times 10^{-4}\ s^{-1}$ for 3-Cl DPA and 0.85 and $2.5 \times 10^{-4}\ s^{-1}$ for 4-SO_3H DPA respectively. The possible mechanism is shown in Scheme 1.

$$H^+ + IO_3^- \overset{K_1}{\rightleftharpoons} HIO_3$$

$$DPA + HIO_3 \overset{K_2}{\rightleftharpoons} Complex$$

$$Complex \xrightarrow{k_3} Products$$

Scheme 1

Scheme 1 leads to rate expression (3)

$$\frac{-d[IO_3^-]}{dt} = k_3\,[Complex] \quad \ldots (3)$$

$$[Complex] = K_2[DPA][HIO_3]$$

$$= K_1K_2[DPA][H^+][IO_3^-] \quad \ldots (4)$$

$$[IO_3^-]_{Total} = [IO_3^-]_{Free} + [HIO_3]_{Free} + [HIO_3]_{Complex}$$

$$= [IO_3^-] + K_1[H^+][IO_3^-] + K_1K_2[DPA][H^+][IO_3^-]$$

$$= [IO_3^-](1 + K_1[H^+] + K_1K_2[DPA][H^+])$$

$$\text{Hence } [IO_3^-] = \frac{[IO_3^-]_{Total}}{1 + K_1[H^+] + K_1K_2[H^+][DPA]} \quad \ldots (5)$$

Substituting Eqs (4) and (5) in Eq. (3)

$$\frac{-d[IO_3^-]}{dt} = \frac{K_1K_2k_3[DPA][H^+][IO_3^-]_{Total}}{1+K_1[H^+]+K_1K_2[H^+][DPA]} \quad \ldots (6)$$

This rate expression explains the observed kinetics

$$k_{obs} = \frac{-d[IO_3^-]}{dt} \Big/ [IO_3^-]$$

$$= \frac{K_1K_2k_3[DPA][H^+]}{1+K_1[H^+]+K_1K_2[H^+][DPA]} \quad \ldots (7)$$

At a given $[H^+]$

$$k_{obs} = \frac{A[DPA]}{B+C[DPA]}$$

where $A = K_1K_2k_3[H^+]$, $B = 1+K_1[H^+]$ and $C = K_1K_2[H^+]$ which explains the fractional order dependence of rate on [DPA]. And also from Eq. (7)

$$\frac{1}{k_{obs}} = \frac{1}{K_1K_2k_3[DPA][H^+]} + \frac{1}{K_2k_3[DPA]} + \frac{1}{k_3} \text{ (or)}$$

$$k_{obs}^{-1} = \frac{1}{k_3} + \left(\frac{1}{K_2k_3} + \frac{1}{K_1K_2k_3[H^+]}\right)\frac{1}{[DPA]} \quad \ldots (8)$$

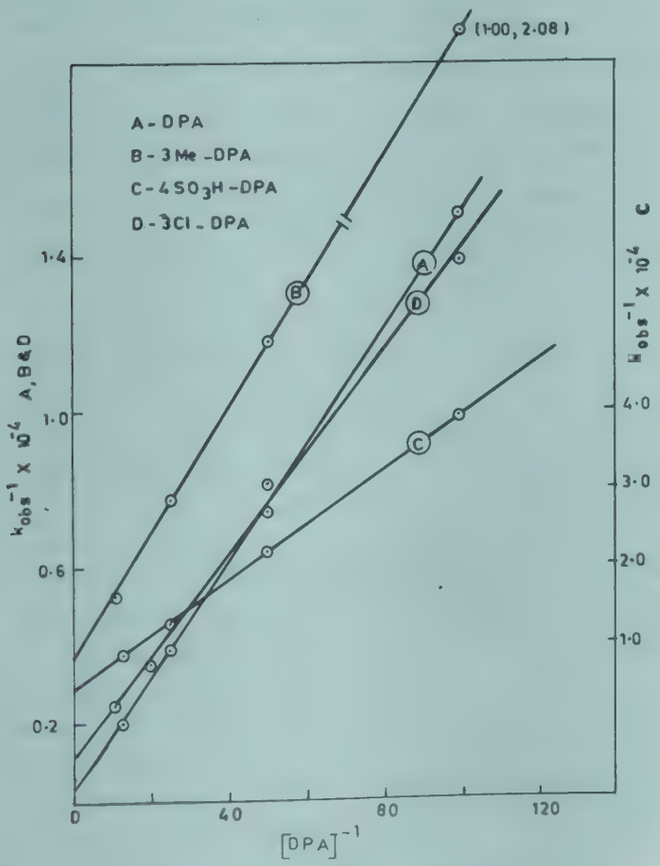

Fig. 1 – Plot of k_{obs}^{-1} versus DPA^{-1}

Equation (8) shows that the plot of k_{obs}^{-1} against $[DPA]^{-1}$ should be linear with a positive intercept and positive slope. This is confirmed by Fig. 1.

Equation (7) suggests a fractional order dependence of rate on $[H^+]$. The plots of log k_{obs} against $[H^+]$ are nearly linear but the slopes of these plots do not explain the above relation. However, when log k_{obs} is correlated with the Hammett's acidity function[12] H_0, a better correlation appears to exist with slopes of nearly −1.

The detailed mechanism is shown in Scheme 2. To know the effect of substituent on the rate of oxidation, the reactions are studied using 3-OCH_3, 3-CH_3, 3-Cl and 4-SO_3H diphenylamines in addition to the unsubstituted DPA. It has been found that $-OCH_3$ and $-CH_3$ groups enhance the rate and $-SO_3H$ and $-Cl$ groups retard it in comparison to that of the parent DPA. From Scheme 2 it is evident that when the electron density on the carbon atom adjacent to amino group increases, the ease of complex formation increases which is the case with the electron-releasing groups like $-CH_3$ and $-OCH_3$. The groups like $-SO_3H$ and $-Cl$ which are electron-withdrawing, should retard the rate. Attempt was made to correlate the log k_{obs} values with Hammett's σ values[13] of the substituents studied. A perusal of Scheme 2 indicates that the attack of oxidant is at the carbon atom *ortho* to the amino

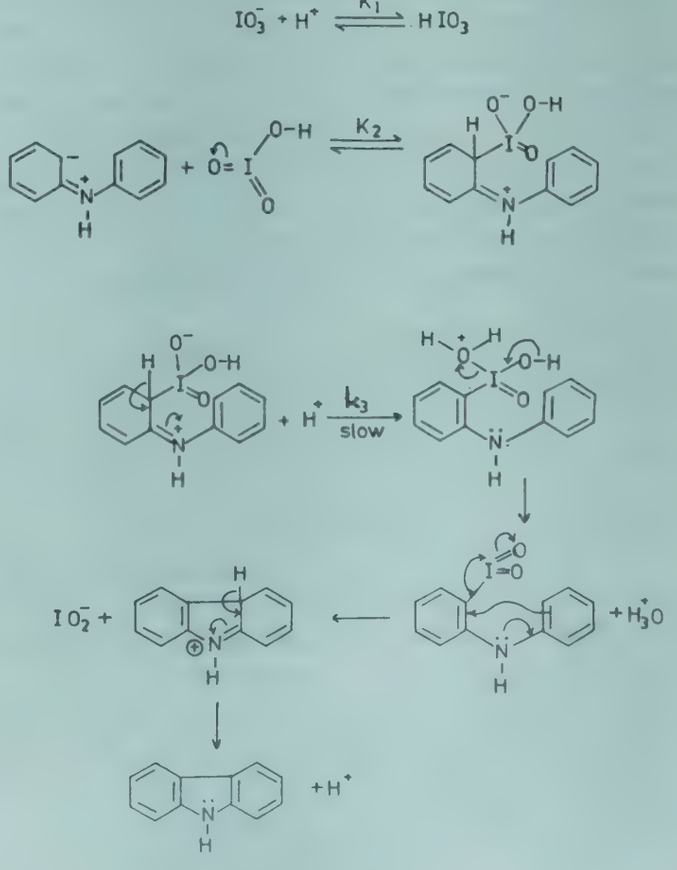

SCHEME 2

group. Hence, a *para* substituent will become *meta* and a *meta* substituent will become *para* to the reaction centre. Therefore, log k_{obs} is correlated with σ_{para} values for *meta* substituents and with σ_{meta} value for the *para* substituent. Such views have been extended in the oxidation of phenols by iodate[14], where the oxidant was shown to attack carbon atom *ortho* to the phenolic $-OH$ group but not the oxygen atom. Under these conditions linear Hammett's plots are obtained with a good correlation coefficient of 0.98. Figure 2 shows such plots at three temperatures 293, 298 and 303 K. These linear plots confirm the *ortho* attack by the oxidant. The ρ values obtained from the slopes of the above plots are -6.25, -6.07 and -5.96 at the above temperatures respectively. These high negative ρ-values confirm an electrophilic attack at the electron-rich carbon atom forming a polar transition state. When electron-releasing groups like $-CH_3$ or $-OCH_3$ are present on the benzene ring, the carbon atom at *ortho* position to the amine group will be at *para* position to the substituent and will become more electron-rich compared to parent DPA. Hence the attack by the oxidant would be more feasible as evidenced by k_{obs} values of these compounds. However, when an electron-withdrawing group like $-Cl$ is present on one of the phenyl rings, the other phenyl ring is expected to be attacked by the oxidant. But this attack cannot be kinetically confirmed, since the ultimate product is the same whether the phenyl ring having the substituent, or the other phenyl ring is attacked by the oxidant. The k_{obs} for ClDPA are slightly higher than the expected values. This indicates that the oxidant initially may attack the other benzene ring which does not have the substituent if the substituent is a strong electron-withdrawing group like $-Cl$ group.

The final products are carbazole and IO_2^- (Scheme 2). This iodite, being a potential oxidant[15] attacks another molecule of DPA and leaves as IO_3^-, which ultimately gets reduced to I^-, which has been identified. Thus it leads to a stoichiometry of 1:3 between IO_3^- and DPA.

The activation energies E_a, determined from the slopes of the Arrhenius plots of log k_{obs} versus T^{-1} and the other thermodynamic parameters $\Delta H^{\neq}$, $\Delta S^{\neq}$ and $\Delta G^{\neq}$ computed are given in Table 3. These values indicate that the present reaction is controlled by both $\Delta H^{\neq}$ and $\Delta S^{\neq}$ i.e., enthalpy and entropy controlled. The entropies of activation, $\Delta S^{\neq}$, are all negative suggesting the rigid nature of the transition state. Neither $\Delta H^{\neq}$ can be correlated with $\Delta S^{\neq}$, nor $\Delta G^{\neq}$ values remain constant. However, a glance at Table 3 shows that $\Delta G^{\neq}$ values for the diphenylamines studied vary linearly with the Hammett's substituent constant σ in accordance with the equation[16], $\Delta G^{\neq} = -2.303\ RT\ \rho\sigma$. This has been verified by plotting $\Delta G^{\neq}$ against σ. A linear plot is obtained with a good correlation coefficient ($r = 0.98$). The ρ-value obtained from the slope of this plot is 6.01 (at 303 K) which is in close agreement with that obtained from the plot of log k_{obs} versus σ. This linear relationship between $\Delta G^{\neq}$ and σ suggests that an identical mechanism is operative for all the diphenylamines studied. The non-linearity between $\Delta H^{\neq}$ and $\Delta S^{\neq}$ indicates the absence of enthalpy-entropy compensation effect[17] in this process. Further, the Eyring plots[18] of log (k_{obs}/T)

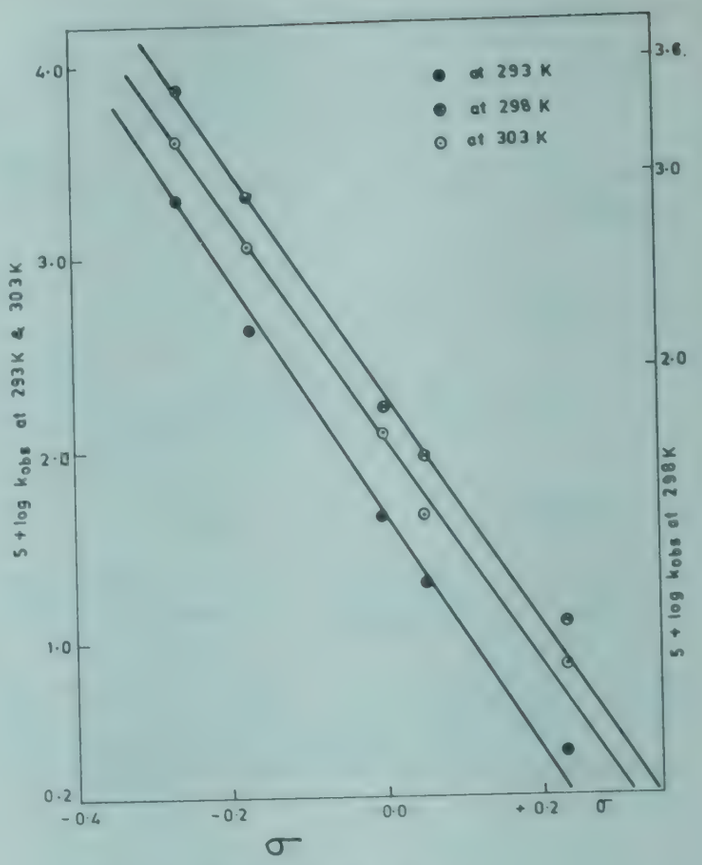

Fig. 2 – Plot of log k_{obs} versus σ

Table 3 – Thermodynamic Parameters:DPA-iodate system

Temp. = 303 K

Substrate	*Ea* (kJ mol^{-1})	$\Delta H^{\neq}$ (kJ mol^{-1})	$-\Delta S^{\neq}$ (JK^{-1} mol^{-1})	$\Delta G^{\neq}$ (kJ mol^{-1})
DPA	60.23	57.72	110	91.08
3-CH_3-DPA	66.13	63.61	72	85.38
3-Cl-DPA	72.69	70.17	92	98.11
4-SO_3HDPA	48.78	46.26	156	93.59
3-CH_3O-DPA	47.82	45.30	122	82.17

versus (1/T) for the compounds studied intersect at more than one point. These two observations suggest that there is no isokinetic relationship between the substrates used for the oxidation process.

References

1 Bansal W R, Ram Nathu & Sidhu K S, *Indian J Chem*, 13 (1975) 987.

2 Grellman K H, Sherman G M & Linschitz, *J Am chem Soc*, 85 (1963) 881.

3 Thomas J R, *J Am chem Soc*, 82 (1960) 5955.

4 Vogel A I, *Text book of quantitative inorganic analysis*, (Longmann, London) (1978) 294.

5 Sidhu K S, Bansal W R & Sukhjeet Kaur, *Indian J Chem*, 26A (1987) 740.

6 Gopa Das Gupta & Mahendra K Mahanti, *Indian J Chem*, 25A (1986) 958.

7 Nathuram & Sidhu K S, *Indian J Chem*, 16A (1978) 195.

8 Panigrahi G P & Nayak R N, *Indian J Chem*, 21A (1982) 361.

9 Emeleus H J & Sharp A G, *Advances in inorganic chemistry and radio-chemistry*, Vol. 5 (Academic Press, New York), 1964, 80.

10 Fuoss R A & Parker H C, *J Am chem Soc*, 44 (1922) 2429.

11 Fuoss R A & Krauss L A, *J Am chem Soc*, 55 (1933) 476.

12 Paul M P & Long F A, *Chem Rev*, 57 (1957) 1.

13 Wells P R, *Linear free energy relationships* (Academic Press, New York) (1968) 16.

14 Manikyamba P, Raghunath Rao P & Sundaram E V, *Indian J Chem*, 20A (1981) 1186.

15 Chapin R M, *J Am chem Soc*, 56 (1934) 2211.

16 Kenneth A Connors, *Reaction mechanism in organic analytical chemistry*, (Wiley Inter Science, New York) (1973) 130.

17 Alder M G & Leffler J E, *J Am chem Soc*, 76 (1954) 1425.

18 Glasstone S, Laidler K J & Eyring H, *The theory of rate processes*, (McGraw-Hill, London) (1941) 153.

Indian Journal of Chemistry
Vol. 30A, March 1991, pp. 252-254

Enzyme-assisted matrix isolation of novel dithiooxamide complexes of nickel(II)

O V Mikhailov
Department of Inorganic Chemistry, Kazan Institute of Chemical Technology,
K. Marx Street 68, 420 015 Kazan, U.S.S.R.

Received 4 June 1990; revised and accepted 30 October 1990

The complexation reaction proceeding on the Ni(II) hexacyanoferrate(II) matrix immobilized in the gelatin layer in contact with an alkaline solution of dithiooxamide has been studied. It has been shown that five different complexes can be obtained, four of which, i.e. $(Ni_2L)_2[Fe(CN)_6]$ (I), $NiL(H_2O)_2$ (II), $[NiL(H_2O)_2]_n$ (III) and $[Ni(HL)_2]_n$ (IV) are insoluble, and one of them, $[NiL_2]^{2-}$ (V) is soluble in water (HL^- is a partially deprotonated ligand form, L^{2-} is a fully deprotonated form). When ligand concentration in the solution is smaller than 1.0×10^{-3} mol.dm^{-3}, surface $Ni_2[Fe(CN)_6]$ concentration in the matrix more than 2.0×10^{-2} mol.m^{-2} and a (0.5-1.0) min time of complexing process, chelate I ($\lambda_{max.} = 590$-610 nm) is formed; when ligand concentration $\simeq 2.0 \times 10^{-3} - 2.0 \times 10^{-2}$ mol dm^{-3} and $Ni_2[Fe(CN)_6]$ concentration is smaller than 4.0×10^{-2} mol.m^{-2}, chelate II ($\lambda_{max.} = 580$ nm) is formed; when ligand concentration $\simeq 2.0 \times 10^{-2} - 5.0.10^{-2}$ mol.dm^{-3} and $Ni_2[Fe(CN)_6]$ concentration is more than 2.0×10^{-2} mol.m^{-2}, chelate III ($\lambda_{max.} = 570$ nm) is realized. It has been pointed out that chelate II is capable of an irreversible transformation into chelate IV upon processing in acid solution. When ligand concentration is more than 10^{-1} mol.dm^{-3} and $Ni_2[Fe(CN)_6$ concentration is smaller than 2.0×10^{-2}, complex V is formed. The structures of compounds I-V have been proposed and it has been indicated that chelate III and IV are coordination polymers. It has also been pointed out that complexation reaction on the immobilized $Ni_2[Fe(CN)_6]$ matrix in the Ni(II)-dithiooxamide system enables one to obtain more complex forms than with complexing in the same system in aqueous solution.

The complexes of dithiooxamide with nickel (II) have been investigated in a number of works[1-4] and it is generally agreed that in aqueous solution an insoluble 1:2 chelate complex [Ni(II): dithiooxamide] is formed. This coordination compound has two partially deprotonated ligand molecules in the inner coordination sphere[1,2]. It is noteworthy, however, that in the Ni(II)-dithiooxamide system, upon both homogeneous and heterogeneous complexation reactions, the formation of at least one more complex form has not yet been observed. The distinctive feature of the present investigation as compared to that of the earlier work is that four new chelate complexes of Ni(II) with dithiooxamide are obtained under specific conditions which have not been used in coordination chemistry before. The synthesis and study of these new chelates is the subject of the present paper.

Materials and Methods

Nickel(II) hexacyanoferrate(II) $Ni_2[Fe(CN)_6]$ matrix immobilized in a thin gelatin layer was used as a medium for spending complexation reaction for the Ni(II)-dithiooxamide system. The procedure and compositions employed to obtain $Ni_2[Fe(CN)_6]$-matrix are described in ref. 5. The resulting immobilized matrix was processed in an alkaline solution of dithiooxamide in the concentration range of 10^{-3} to 10^{-1} mol.dm^{-3} and *p*H 12.0 ± 0.1. The temperature of the gelatin layer with a matrix was maintained at 20 ± 0.5°C. The reaction time of a ligand solution with an immobilized matrix varied from 1 to 10 min. Then the gelatin layer containing the complex compounds formed therein was washed with large amounts of water and dried for 2-3 hr at room temperature. Nickel(II) chelate complexes containing dithiooxamide formed in the gelatin layer were released by processing the layer in special enzyme *Bazillus mesenterious* solutions capable of destroying the gelatin binding agent, but incapable of reacting with Ni(II) complexes. As a result, the gelatin decomposed to low molecular fragments and passed into solution; the chelate Ni(II) contained in the layer precipitated out and could be easily removed from the solution and analysed by various chemical and physical methods. The experiments performed specially on immobilized matrices with various types of gelatin showed that

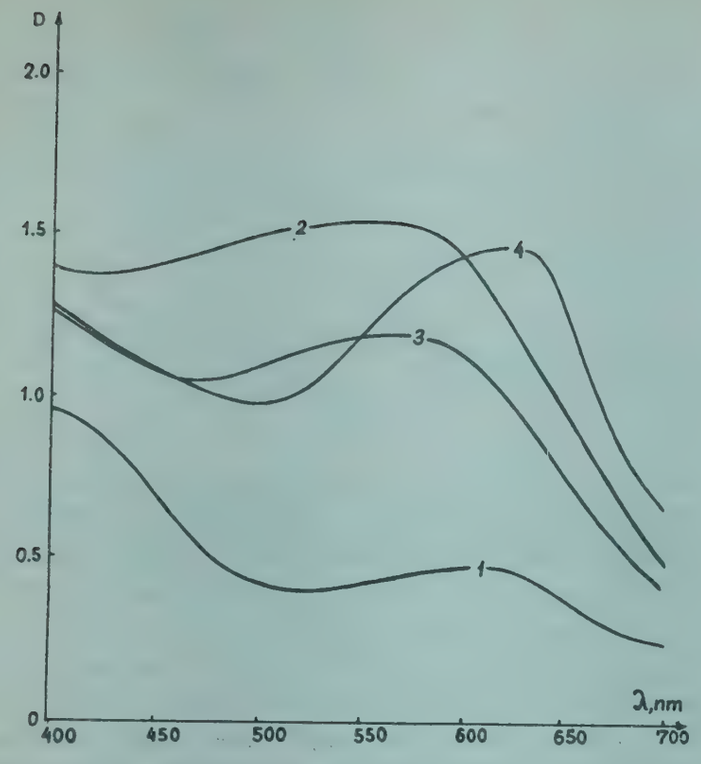

Fig. 1—Spectral characteristics of thin gelatin layers (1) chelate I ($C_F = 4.0.10^{-2}$ mol m^{-2}; $C_L = 1.0.10^{-3}$ mol dm^{-3}, t = 1 min at 20°C); (2) chelate II ($C_F = 1, 5.10^{-2}$ mol m^{-2}; $C_L = 8.0.10^{-3}$ mol dm^{-3}; t = 6 min at 20°C), (3) chelate III ($C_F = 4.0.10^{-2}$ mol m^{-2}; $C_L = 3.5.10^{-2}$ mol.dm^{-3}; t = 10 min at 20°C, (4) chelate IV ($C_F = 4.0.10^{-2}$ mol m^{-2}; $C_L = 4.0.10^{-3}$ mol dm^{-3}; t = 2 min at 20°C). The thickness of layers is 20 μm]

gelatin did not participate in complexing, since the character of complexing processes proceeding on the matrix did not depend on the type of gelatin.

Absorption spectra and absorbances of thin gelatin layers with Ni(II)-dithiooxamide chelates (see Fig. 1) were measured on a Specord spectrophotometer and photometer Macbeth TD-504 (Kodak Co., USA).

Results and Discussion

At $C_L < 1.0 \times 10^{-3}$ mol dm^{-3}, $C_F > 2.0 \times 10^{-2}$ mol.m^{-2} (where C_L represents the ligand concentration in solution, C_F denotes the concentration of $Ni_2[Fe(CN)_6]$ in the immobilized matrix) and a short contact time (0.5 to 1.0 min) of an immobilized matrix with a ligand solution, chelate I having greenish-blue colour with a grey shade ($\lambda_{max.}$ = 590-610 nm) is formed. At $C_L \simeq (2.0 \times 10^{-3}$ to $2.0 \times 10^{-2})$ mol.dm^{-3} and $C_F < 4, 0.10^{-2}$ mol.m^{-2} in whole range studied (0.5-10 min), chelate II having pink-violet colour ($\lambda_{max.}$ = 580 nm) is formed. At $C_L \simeq (2.0 \times 10^{-2}$ to $5.0 \times 10^{-2})$ mol.dm^{-3} $C_F > 2.0 \times 10^{-2}$ mol m^{-2}, chelate III having the violet colour ($\lambda_{max.}$ = 570 nm) is obtained in the gelatin layer. In this connection, it is noteworthy that upon processing the gelatin layer containing chelate II in acid solution (*p*H < 5), the pink-violet colour of the

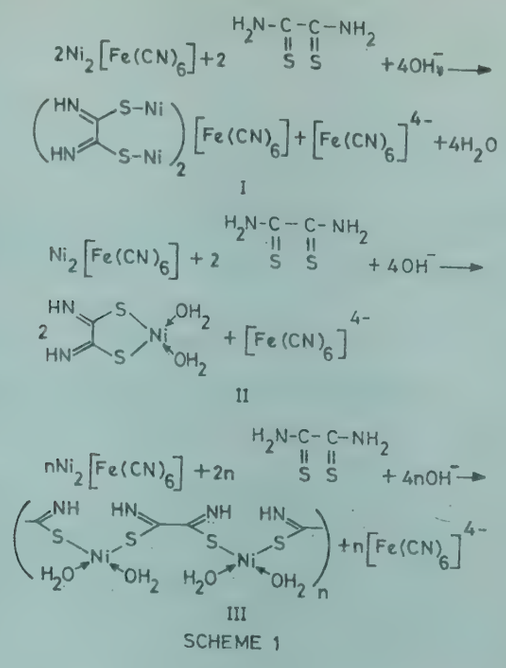

SCHEME 1

former is almost immediately changed to blue. This is suggestive of the transformation of chelate II into a new chelate IV ($\lambda_{max.}$ = 630-640 nm). Chelates I and II do not undergo such a colour change upon interaction with acid solutions. Finally, at $C_F < 2.0 \times 10^{-2}$ mol m^{-2} and $C_L > 10^{-1}$ mol dm^{-3} and more, a distinct disappearance of initially formed chelate II and III is observed, accompanied by a considerable decrease (almost down to a zero value) in the absorbance of the gelatin layer.

The compounds having grey-green (I), violet (II) and dark-violet (III) colours may be released from gelatin layers. The grey-green compound, based on analytical data (C, 17.85%;N, 20.24%; H, 0.66%; Ni, 34.18%; Fe, 8.26%) has been formulated as $Ni_4FeC_{10}N_{10}H_4S_4$, corresponding to a metal/ligand ratio of 2:1 with a fully deprotonated ligand form in the inner sphere (Calculated for the given formula: C, 17.54%; N, 20.47%; H_2O, 58%; Ni, 34.50%; Fe, 8.19%), while the violet and dark-violet compounds have been assigned empirical formulae $NiC_2S_2N_2H_6O_2$ corresponding to metal/ligand ratio of 1:1 and also with a completely deprotonated ligand form (Calc. for the given formula: C, 11. 26%; N, 13.14%; H, 2. 82%; Ni, 27. 69%; Found (for the violet compound): C, 11.42%; N, 12. 94%; H, 3.06% Ni, 27.96%; for the dark-violet chelates: C, 11.37%; N, 12.82%; H, 3.20%; Ni, 28.02%). No doubt the violet and dark-violet compounds appear as isomers. The differences in the two could be a result of extent of polymerisation when chelates II and III come in contact with acid solution. Chelate II, which changes its colour under the influence of acid solution, is a monomer, while chelate III is a coordination polymer, the "rigid" structure of which does not

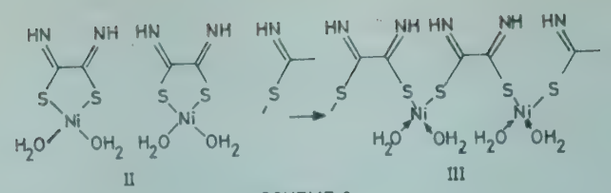

II III

SCHEME 2

provide for proton addition without the destruction of its chain. In view of all the above mentioned facts, the formation of chelates I, II and III, can be rationalised as shown in Scheme 1.

It should be noted that the formation of polymeric III is the result of "lacing" of monomer II molecules, as shown in Scheme 2.

The probability of such a "lacing" must increase with the concentration of monomer II in the gelatin layer and, consequently, with increase in C_L and C_F. Experimental data obtained are in full agreement with this conclusion.

From the gelatin layers containing chelate IV, a dark-blue compound could be obtained, which based on analytical data (C, 16.05; N, 19.14; H, 2.16; Ni, 19.52%) could be formulated as $NiC_4S_4N_4H_6$ corresponding to the metal ion/ligand ratio of 1:2, with a partially deprotonated ligand form in the inner sphere (Calculated for the given formula: C, 16.17%; N, 18.85; H, 2.04; Ni, 19.76%). Spectral characteristics of this compounds are substantially consistent with those available[1-3] for the aqueous colloid solution of Ni(II) chelate with dithiooxamide, with a nickel(II) ion/ligand ratio of 1:2. Moreover, upon processing of the gelatin layer containing chelate II in an acid solution, Ni(II) could be detected in the solution. Taking into account the fact that according to the blue chelate complex is a coordination polymer[1], the transition of compound II into IV can be suggested as given Scheme 3.

The transformation of chelate II into chelate IV is an irreversible process, i.e. upon rendering the gelatin layer containing chelate IV alkaline, the changeover of the dark-blue colour to pink-violet is not observed. This is an additional evidence that chelate

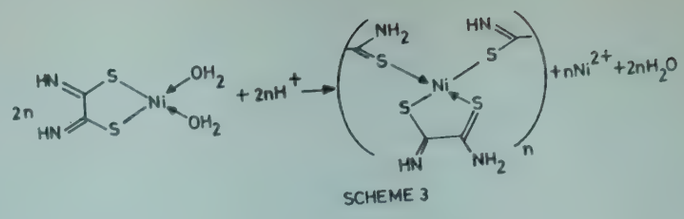

SCHEME 3

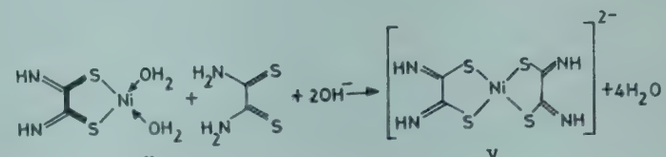

II V

SCHEME 4

IV, like chelate II, is a coordination polymer the structure of which does not provide for proton splitting without the destruction of its chain. Further, in this particular case, this is not supported on thermodynamic consideration.

In the range of $C_L \simeq 10^{-1}$ mol dm^{-3} probably the addition of the second ligand molecule to chelate II takes place. The reaction results in the formation of a soluble complex diffusing from the gelatin layer to the solution as shown in Scheme 4.

The support for Scheme 4 is provided by the fact that under these conditions nickel (II) is detected in the ligand solution in contact with the matrix. The formation of soluble complex V naturally decreases the amount of insoluble chelate II (or III) in the gelatin layer, and its absorbance decreases as compared to the case when the reaction outlined in Scheme 4 is substantially absent in the system.

On the basis of results presented in this investigation it can be seen that the complexation reaction proceeding on immobilised enzyme matrix offeres greater synthetic opportunities than that in solutions.

References

1 Jensen K A, *Z anorg allg Chem*, 252 (1944) 227.
2 Xavier J & Ray P, *J Indian Chem Soc*, 35 (1958) 432.
3 Yokota S & Shimada J, *Nippon Kagaku Zassi*, 79 (1958) 1144.
4 Faraday L & Janosi A, *Magyar Kem Folyoirat*, 63 (1957) 19.
5 Mihajlov O V & Polovnak V K, *Bild und Ton*, 41 (1988), 250.

Indian Journal of Chemistry
Vol. 30A, March 1991, pp. 255-260

Macrocyclic metal complexes: Part XXI – Syntheses of binuclear sepulchral complexes by the interaction of formaldehyde with tris-(3,6-dimethyl-4,5-diazaocta-3,5-diene-2,7-dihydrazone)dimetal(II) ions

B K Mohapatra, U Bhattacharya, P K Pujapanda, A K Rout & B Sahoo*
Department of Chemistry, Indian Institute of Technology, Kharagpur, West Bengal 721 302

Received 1 June 1990; revised 11 September 1990; accepted 24 October 1990

The tris-ligated binuclear metal complexes of biacetylazine dihydrazone (BAADH) react with formaldehyde in presence of acid to give tetracyclo binuclear clathrochelates of the type, $[M_2(Clathro)]X_4$[M = Ni(II), X = Cl^-, Br^-, I^-, NO_3^-, ClO_4^-, BF_4^-; M = Fe(II), X = Br^-, BF_4^-, ClO_4^-; and M = Co(II), X = ClO_4^-; clathro = $C_{30}N_{18}H_{48}$]. The nickel(II) and iron(II) tetracycloclathrochelates have spin triplet and spin quintet ground terms respectively and the cobalt(II) complex has a spin doublet ground term. Their spectra show some departure from the usual pattern observed for the respective metal ions in octahedral complexes and have been interpreted in terms of trigonal prismatic or pseudotrigonal prismatic approximations. Electrochemical studies of the binuclear clathrochelates reveal that they undergo two-step one-electron redox processes and their electrochemical behaviour is also consistent with the proposed structures.

Encapsulation of metal ions in three-dimensional cage ligands has become the subject of intensive research activity[1-8]. Entombing metal ions by capping of the oxime oxygen atoms of formally intermediate tris-oxime complexes gives an interesting group of such sepulchres. Thus, the reaction of $FeCl_2$ with dimethyl glyoxime/1,2-diphenylethane dioxime/2,4-pentanedione dioxime/1,2-cyclohexanedione dioxime and boric acid in various refluxing alcohols or boron trifluoride in acetonitrile yields red coloured low-spin Fe(II) complexes. These complexes approach trigonal prismatic structures like their cobalt(III) analogues[9] or like the regiment of clathrochelates derived by the action of boron trifluoride on the trigonal symmetric molecules, [tris-(2-carboxaldoxime-6-pyridyl)phosphine-cobalt(II)]$^+$ (refs 10,11).

Sargeson *et al.*[12,13] have reported a sepulchre of cobalt(III) formed by the action of formaldehyde and ammonia on tris-(ethylenediamine)cobalt(III) under comparatively mild conditions in presence of lithium carbonate. The mononuclear tris-(2,3-butanedionedihydrazone)cobalt(III)/iron(II)/nickel(II) complexes form clathrochelates through ring closure reactions with formaldehyde, structures of which resemble the phosphorus-bridgehead complexes[14].

A recent advance in the macrocyclic chemistry is the isolation of a variety of complexes enclosing a pair of metal ions within a large or supermacrocyclic ring[15,16]. However, enclosing a pair of metal ions within a molecular sepulchre has not been reported so far. Such binuclear sepulchres are likely to be more resistant to degradation and are expected to exhibit novel features in metal ion transport, catalysis and reaction mechanisms involving outer sphere electron transfer.

The terminal NH_2 groups in the binuclear tris-ligand metal complexes of 3,6-dimethyl-4,5-diazaocta-3,5-diene-2,7-dihydrazone, $[M_2(BAADH)_3]^{4+}$, [I][17,18], have the appropriate chemical and architectural environment to be fenced with methylene groups by the action of formaldehyde. The resultant products will constitute a new family of clathrochelates enclosing two metal centres. The desired clathrochelates with the three-dimensional cage ligand, 5, 6, 9, 10, 18, 19, 22, 23, 28, 29, 32, 33-dodecamethyl-1, 3, 4, 7, 8, 11, 12, 14,

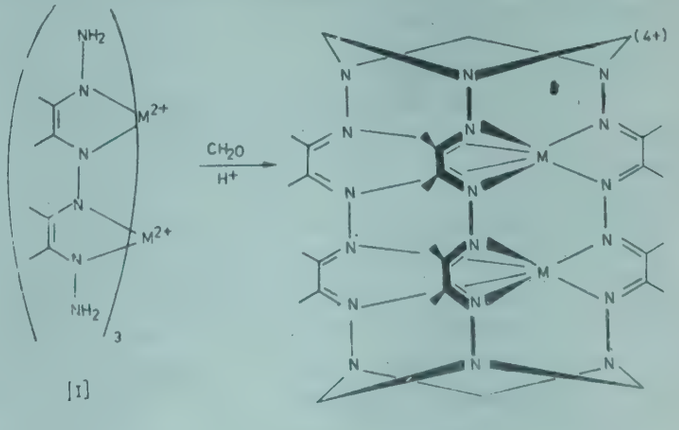

[I] [II]

M = Ni(II), Co(II), Fe(II)

Table 1 – Colour and analytical data of the clathrochelates

Clathrochelates (Clathro = $C_{30}N_{18}H_{48}$)	Colour	Found (Calc.), %				
		C	H	N	Metal	Anion
$[Ni_2(C_{30}N_{18}H_{48})]Cl_4.H_2O$	Dark brown	37.90 (38.38)	5.10 (5.11)	27.20 (26.86)	11.96 (12.58)	15.10 (15.14)
$[Ni_2(C_{30}N_{18}H_{48})]Br_4.H_2O$	Light pink	32.30 (32.25)	4.10 (4.48)	22.30 (22.58)	10.54 (10.52)	28.70 (28.67)
$[Ni_2(C_{30}N_{18}H_{48})]I_4.H_2O$	Light brown	27.1 (27.6)	3.70 (3.83)	19.50 (19.32)	8.56 (9.05)	37.80 (38.95)
$[Ni_2(C_{30}N_{18}H_{48})](NO_3)_4.H_2O$	Pink red	34.80 (34.48)	4.50 (4.79)	29.70 (29.50)	10.80 (11.30)	—
$[Ni_2(C_{30}N_{18}H_{48})](ClO_4)_4.H_2O$	Chocolate brown	29.80 (30.15)	4.10 (4.18)	21.2 (21.1)	9.60 (9.88)	—
$[Ni_2(C_{30}N_{18}H_{48})](BF_4)_4.H_2O$	Dark brown	31.20 (31.46)	4.20 (4.37)	22.00 (22.02)	9.77 (10.31)	—
$[Fe_2(C_{30}N_{18}H_{48})]Br_4.H_2O$	Violet	32.20 (32.43)	4.3 (4.5)	22.9 (22.7)	10.10 (10.09)	28.70 (28.82)
$[Fe_2(C_{30}N_{18}H_{48})](BF_4)_4.H_2O$	Dark violet	31.50 (31.63)	4.10 (4.39)	22.30 (22.14)	9.91 (9.84)	—
$[Fe_2(C_{30}N_{18}H_{48})](ClO_4)_4.H_2O$	Light violet	30.10 (30.30)	3.80 (4.21)	21.10 (21.21)	9.38 (9.42)	—
$[Co_2(C_{30}N_{18}H_{48})](ClO_4)_4.H_2O$	Brown	29.80 (30.15)	3.90 (4.18)	21.2 (21.1)	9.50 (9.88)	—

16, 17, 20, 21, 24, 25, 27, 30, 31, 34-octadecaazatetracyclo[12.12.8.1^{3,25}.1^{12,16}]hexatriaconta-4, 6, 8, 10, 17, 19, 21, 23, 27, 29, 31, 33-dodecaene-N^4, N^7, N^8, N^{11}, N^{17}, N^{20}, N^{21}, N^{24}, N^{27}, N^{30}, N^{31}, N^{34}[II] have been realised in the present work and we report here their syntheses, spectral and electrochemical properties.

Materials and Methods

The parent tris-complexes of nickel(II), iron(II) and cobalt(II) with BAADH were prepared as reported earlier[17,18].

$[Ni_2(C_{30}N_{18}H_{48})](BF_4)_4.H_2O$

The complex $[Ni_2(BAADH)_3](BF_4)_4$ (5.6 g, 0.005 mol) was dissolved in 150-200 ml of a mixture of acetonitrile:water (90:10) at about 40°C. 5.0 g of aqueous formaldehyde (37%) was added dropwise with continuous stirring over a period of one hour at 40°C and 0.05 ml of fluoroboric acid was added to catalyze the reaction when the colour of the solution changed from light brown to dark brown. The solution was concentrated and was allowed to stand when a dark brown solid precipitated within a day. It was filtered, washed with acetonitrile, ether and dried *in vacuo*.

A second crop of the crystals was obtained by treating the filtrate with a chilled solution of butanol-ether mixture (50:50).

The chloride, bromide, iodide and nitrate clathrochelates of nickel(II), and bromide and fluoroborate clathrochelates of iron(II) were readily prepared from their respective parent compounds by adopting similar procedures.

$[Fe_2(C_{30}N_{18}H_{48})](ClO_4)_4.H_2O$

5.8 g (0.005 mol) of the compound $[Fe_2(BAADH)_3](ClO_4)_4$ was dissolved in 150 ml of acetonitrile followed by dropwise addition of 5 g of aqueous formaldehyde (37%) with continuous

Table 2 – Magnetic moment and electronic spectral data of clathrochelates of nickel(II), iron(II) and cobalt(II)

Clathrochelate (Clathro = $C_{30}N_{18}H_{48}$)	μ_{eff}/metal ion (in B.M.)	λ_{max} (cm^{-1})
$[Ni_2(clathro)]Cl_4.H_2O$	2.92	8,160, 11,100, 19,200, 31,250
$[Ni_2(clathro)]Br_4.H_2O$	2.91	8,330, 16,000, 20,000, 32,250
$[Ni_2(clathro)]I_4.H_2O$	3.10	8,330, 13,800, 20,000
$[Ni_2(clathro)](NO_3)_4.H_2O$	3.07	8,400, 13,800, 19,600, 27,000
$[Ni_2(clathro)](ClO_4)_4.H_2O$	2.85	8,300 16,000, 20,000, 29,400
$[Ni_2(clathro)](BF_4)_4.H_2O$	2.97	8,300, 16,600, 20,000, 27,000
$[Fe_2(clathro)]Br_4.H_2O$	4.79	17,850 sh 25,650
$[Fe_2(clathro)](BF_4)_4.H_2O$	5.25	17,850 sh 25,000
$[Fe_2(clathro)](ClO_4)_4.H_2O$	4.80	17,850 sh 25,000
$[Co_2(clathro)](ClO_4)_4.H_2O$	1.90	16,000 sh 31,250

stirring at 35°-40°C. About 0.1 ml of perchloric acid was added to catalyze the reaction. The red colour of the parent compound changed to deep violet. The stirring was continued for 2 hr and the solution was concentrated and was allowed to stand for a few hours. It was then added slowly to a chilled mixture of butanol-ether (50:50) when a deep violet compound separated. It was filtered, washed with ether and dried *in vacuo*.

The perchlorate clathrochelates of nickel(II) and cobalt(II) were synthesized following similar procedures, maintaining a nitrogen atmosphere in the latter case.

Analytical data and colours of the clathrochelates are recorded in Table 1.

Results and Discussion

The tris-ligand binuclear nickel(II), iron(II) and cobalt(II) complexes, $[M_2(BAADH)_3]^{4+}$, readily undergo condensation with formaldehyde in the mole ratio 1:6 to yield the tetracyclo binuclear clathrochelates $[M_2(clathro)]^{4+}$. The addition of formaldehyde to the tris-chelates is accompanied by a rapid change in colour. The reaction is acid catalysed and is best carried out under dilute conditions and at a temperature of 40°-50°C. At low temperatures the reaction is sluggish, while at elevated temperatures the product often turns gummy. The clathrochelates are obtained in fine crystalline state, and are stable except the perchlorate complexes which are hygroscopic and explosive. They are sparingly soluble in water but are soluble in some organic solvents like DMF.

Infrared spectra

The IR spectra of the clathrochelates resemble one another except for the vibrations due to associated anions, but conspicuously differ from the spectra of precursor compounds. The spectra of the clathrochelates do not contain the characteristic asymmetric and symmetric stretching, deformation and rocking mode vibrations of the $-NH_2$ groups usually observed at ~3300, ~1650 and ~1250 cm^{-1} respectively.

The tris-BAADH parent complexes show a strong band near 1580 cm^{-1} due to C⋯⋯N stretch which is perturbed on encapsulation and shifts to the region 1600-1620 cm^{-1}. In most of the cases it appears as a doublet – the split seems to arise on account of distortions due to formation of the six-membered heterocyclic rings at the two extreme ends.

The spectra have new bands near 1160 and 800-750 cm^{-1} due to deformation vibrations of newly introduced $-CH_2-$ groups. Besides, the conventional CH_3 and CH_2 deformation bands appear in the range 1450-1200 cm^{-1}.

In the low frequency region, $\nu(M-N)$ bands are observed near 600 cm^{-1}.

These spectral observations suggest that the terminal nitrogen atoms are enlaced with methylene groups to yield the clathrochelates [II]; the resultant organic cage houses two metal ions with chromophors $[MN_6]$ in two compartments separated through the azine $(-N-N-)$ linkages and the most probable geometry of the molecule is trigonal prismatic. Further evidence for this comes from electronic spectral and polarographic data discussed hereinafter.

Electronic spectra and magnetic properties

The nickel(II) clathrochelates show magnetic moments of ~3.0 B.M. per gram ion of the metal. Known trigonal prismatic complexes of nickel(II) show moments around 3.0 B.M. and the values are slightly below those expected for octahedral complexes due to departure from octahedral symmetry or due to spin-spin coupling via a super exchange process involving the conjugated network of the ligand frame-work as observed in structurally similar binuclear (biacetylazinedioximato) nickel(II) complexes[19,20]. The electronic spectra are characterised by three to four ligand field bands (Table 2). The positions of spectral bands and their relative energies preclude the possibility of their being interpreted in terms of octahedral approximation. The ligating atoms are distorted from octrahedral arrangements and seem to adopt an arrangement intermediate between trigonal prismatic and trigonal antiprismatic structures.

Holm *et al.*[9,10], Wentworth[21] and Robbins and coworkers[8] have reported the spectra of some compounds believed to possess trigonal prismatic and trigonal antiprismatic structures such as $[Ni(Py)_3tach](ClO_4)_2$ and 1, 1′, 1″-tris-(pyridine-2-carboxaldimino)ethanenickel(II) diperchlorate, $[Ni(Py)_3tame](ClO_4)_2$. They compared the spectral data with those of some well established octahedral complexes but were unable to reach any definite conclusion in regard to specific assignments of ligand field bands under D_{3h} symmetry. However, certain empirical experimental observations associated with spectral changes indicated trigonal prismatic geometry. A comparison of the spectra of the present complexes with the spectra of established trigonal prismatic complexes indicates that the structure of the former approach a trigonal prismatic or distorted trigonal prismatic geometry. Under D_{3h} symmetry approximations, the band near 13,000 cm^{-1} (Δ_1) can be assigned to the transition $^3E' \leftarrow {}^3A'_2$ and the band near 20,000 cm^{-1} (Δ_2) to the transition $^3E'' \leftarrow {}^3A'_2$. The relative ratio $\Delta_1/\Delta_2 = 0.6$ is in good agreement with literature data[10].

The iron(II) clathrochelates are all high-spin type and show magnetic moments in the range 4.8 to 5.2 B.M. per gram ion of the metal. These values are close to spin-only value but somewhat lower than the expected moments for iron(II) octahedral complexes indicating deviation from regular octahedral geometry. The electronic spectra of the iron(II) clathrochelates are dominated by two relatively intense bands near 18,000 and 25,000 cm^{-1} which seem to be due to charge transfer transitions. The parent complexes show only one charge transfer band near 20,000 cm^{-1}; the splitting in the present molecules indicates cross-over from octahedral to trigonal prismatic or trigonal antiprismatic structure.

The binuclear cobalt(II) perchlorate clathrochelate is of low-spin type, having magnetic moment of 1.9 B.M. per gram ion of the metal in sharp difference to the behaviour of the parent precursor tris-complex whose magnetic moment is 4.4 B.M. at ambient temperatures. Trigonal prismatic clathrochelates are known to exist in both high-spin and low-spin states[10,14]. The mononuclear clathrochelates of cobalt(II) derived from 2,3-butanedion dihydrazone and formaldehyde are of low-spin type with the magnetic moment of 2.1 B.M., but the parent precursor complex is of high-spin type whose moment is 4.2 B.M.[22]. The spin cross-over is a clear manifestation of change in symmetry of the complex ion, i.e., transformation from approximately octahedral symmetry, O_h to trigonal prismatic (D_{3h}) symmetry. Most of the low-spin octahedral or square planar cobalt(II) complexes show ligand field bands near 16,000 and 19,000-23,000 cm^{-1}. The present complex shows a band near 16,000 cm^{-1} and a charge transfer band beyond 30,000 cm^{-1}.

Electrochemical studies

The polarographic data are recorded in Table 3. The binuclear clathrochelates of Co(II), Fe(II) and Ni(II) show two well-defined waves, excepting the fluoroborate complex of iron(II) which shows an additional well-defined third wave. The redox processes are diffusion controlled. The i_d values and slope^{-1} for the plot of $\log i_d - i/i$ vs. E show that each of the redox processes is reversible and is accompanied by one-electron transfer.

The redox processes of the tetracycloclathrochelates quite expectedly follow the pattern observed for the binuclear macrocyclic complexes derived from $M_2(BAADH)_2X_4$ and formaldehyde[23]. The overall electrochemical behaviour suggests that the encapsulated metal ions undergo stepwise reversible reduction. In the first step of reduction the product is stabilized as an ambivalent intermediate and in the following step each metal ion is reduced to univalent state (Scheme 1),

$$[M^{2+}M^{2+}\ \text{clathro}]^{4+} + e \rightleftharpoons [M^{2+}M^{1+}\ \text{clathro}]^{3+} + e$$
$$\text{(a)} \qquad\qquad \text{(b)}$$

$$\rightleftharpoons [M^{1+}M^{1+}\ \text{clathro}]^{2+}$$
$$\text{(c)}$$

Scheme 1

Table 3 – Electrochemical data of clathrochelates of nickel(II), iron(II) and cobalt(II) in aqueous DMF

Clathrochelates (Clathro = $C_{30}N_{18}H_{48}$)	1st wave			2nd wave		
	$-E_{1/2}$ (V, vs SCE)	Slope^{-1} (mV)	i_d	$-E_{1/2}$ (V, vs SCE)	Slope^{-1} (mV)	i_d
$[Ni_2(clathro)]Cl_4.H_2O$	0.887	65	2.36	1.38	76	2.22
$[Ni_2(clathro)]Br_4.H_2O$	0.960	73	2.70	1.52	53	2.16
$[Ni_2(clathro)]I_4.H_2O$	0.995	65	2.72	1.44	63	2.13
$[Ni_2(clathro)](NO_3)_4.H_2O$	0.950	61	2.76	1.51	72	2.08
$[Ni_2(clathro)](BF_4)_4.H_2O$	0.810	72	2.16	1.46	74	2.36
$[Ni_2(clathro)](ClO_4)_4.H_2O$	0.825	64	2.36	1.41	69	2.54
$[Fe_2(clathro)]Br_4.H_2O$	0.530	67	2.54	1.18	78	2.44
$[Fe_2(clathro)](BF_4)_4.H_2O$	0.51	76	2.62	1.010 [1.44]	69 [82]	2.20 [2.44]
$[Fe_2(clathro)](ClO_4)_4.H_2O$	0.35	62	2.96	1.100	66	2.36
$[Co_2(clathro)](ClO_4)_4.H_2O$	0.39	63	2.16	0.938	72	2.58
[Ni(BDHclathro)]$(ClO_4)_2$	0.52	68	2.1	—	—	—
[Co(BDHclathro)]$(ClO_4)_2$	0.38	64	2.6	—	—	—
[Fe(BDHclathro)]$(BF_4)_2$	1.05	68	2.2	—	—	—

Values in [ ] for 3rd wave.
(BDHclathro) = Clathrochelate derived from 2,3-butanedione dihydrazone[14].

The electrochemical behaviour of the parent complexes shows a two-electron one-step irreversible redox wave[18]. Cyclization with formaldehyde separates the two-electron waves into two one-electron waves, one anodic and the other cathodic with respect to the precursor complex molecules.

It has been observed earlier for Co(II) and Cr(II) complexes that two-electron transfer takes place in one-step for weaker ligands[24]. With increasing ligand field strength and increasing π-acceptor properties of the ligands[25-28], the two-electron wave separates into two one-electron waves, stabilizing the intermediate species with M^{1+} formal oxidation state. In the case of the present series of clathrochelates and the macrocyclic complexes described earlier, the macro-ring and the cage ligand contain a large number of α-diimine groups in the ligand backbone. They consequently exert a stronger ligand field about the metal centres as well as greatly enhance the π-acceptor properties and appear to be the primary cause of separation of the two-electron wave into two one-electron components.

The $E_{1/2}$ values for the first redox process show that the clathrochelates have the greatest electron affinities amongst the three series of complexes, i.e., the clathrochelates, the macrocyclic complexes and the parent precursors. This appears to be contrary to expectation if viewed in the light of coordination number alone, since each metal ion is (N_6)-hexa-coordinated. The results indicate sensitivity of redox potential to the geometry of the complex species. The complexes might adopt structures between the two extremes, trigonal antiprismatic (TAP) and trigonal prismatic (TP). With as many as six α-diimine groups around each metal ion, a progressive change of structures from TAP to TP will enhance the π-acceptor properties of the ligand and would shift the $E_{1/2}$ values in anodic direction.

In order to gain further insight into the redox behaviour of the present series of complexes, we have studied the redox pattern of a series of structurally similar mononuclear clathrochelates[14], $[M(clathro)]X_2$, {M = Ni(II), Co(II), $X = ClO_4^-$; M = Fe(II), $X = BF_4^-$; clathro = 5, 6, 14, 15, 20, 21-

hexamethyl-1, 3, 4, 7, 8, 10, 12, 13, 16, 17, 19, 22-dodecaazatetracyclo[8.8.4.$1^{3,17}$.$1^{8,12}$]tetracosa-4, 6, 13, 15, 19, 21-hexaene-N^4, N^7, N^{13}, N^{16}, N^{19}, N^{22}} derived from 2,3-butanedione dihydrazone and formaldehyde along with their parent tris-complexes under identical conditions[III]. It has

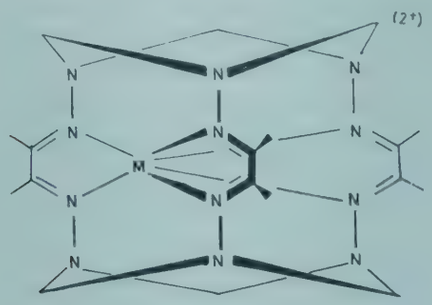

[III]

M = Ni(II), Co(II), Fe(II)

been stated by Goedken *et al.*[14], that these mononuclear complexes undergo reversible reductions which are either metal-based or ligand-based, though detailed results have not been published. Our results show that each of the mononuclear clathrochelates exhibits (Table 3) a single reversible one-electron redox wave and appears to be stabilized in formal +1 oxidation state. These waves occur at a more anodic potential in comparison with those for the parent tris-complexes. The stabilization of formal +1 oxidation states of metal ions as well as anodic shift of $E_{1/2}$ values on encapsulation are in agreement with the results for the series of binuclear clathrochelates. The $E_{1/2}$ values for the nickel(II) and cobalt(II) mononuclear clathrochelates are observed to be anodic with respect to the related family of macrocyclic complexes, [M(Me_4[14]tetraeneN_8)](X_2). The parallelism in the bahaviour of the mononuclear and the binuclear clathrochelates suggests that the overall geometry is similar and most probably it is nearer to a trigonal prismatic structure (TP).

A series of three-dimensional encapsulation complexes of Fe(II), Co(II) and Ni(II) ranging in structures from octahedral, distorted octahedral and trigonal prismatic to trigonal antiprismatic have been studied polarographically by Holm *et al.*[10]. The electrochemical behaviour of these complexes is similar to that of the complexes in the present series.

Acknowledgement

The authors gratefully acknowledge the award of a research associateship by CSIR, New Delhi, to A K Rout and FIP fellowships by the UGC, New Delhi, to U Bhattacharya and P K Pujapanda.

References

1 Jackels S C & Rose N J, *Inorg Chem*, 12 (1973) 1232.
2 Jackels S C, Dierdorf D S, Rose N J & Zektzer J, *J chem Soc Chem Commun*, (1972) 1291.
3 Rai H C, Jena A K & Sahoo B, *Inorg chim Acta*, 35 (1979) 29.
4 Shankar R, Rout A K & Sahoo B, *Indian J Chem*, 26A (1987) 156.
5 Boston D R & Rose N J, *J Am chem Soc*, 90 (1968) 6859.
6 Zakrzewski G A, Ghillardi C A & Lingafelter, *J Am chem Soc*, 93 (1971) 4411.
7 Nazarenko A Y & Voloshin Y Z, *Zh neorg Khim*, 29 (1984) 1776.
8 Robbins M K, Naser D W, Heiland J L & Grzybowski J J, *Inorg Chem*, 24 (1985) 3381.
9 Parks J E, Wagner B E & Holm R H, *J Am chem Soc*, 92 (1970) 3500; *Inorg Chem*, 10 (1971) 2472.
10 Larsen E, Lamar G N, Wagner B E, Parks J E & Holm R H, *Inorg Chem*, 11 (1972) 2652.
11 *Comprehensive coordination chemistry*, edited by Geoffrey Wilkinson (Pergamon Press, New York) Vol. 5 (1987) 1232.
12 Creaser I I, Harrowfield J M, Herlt A J, Sargeson A M, Springborg J, Geue R J & Snow M R, *J Am chem Soc*, 99 (1977) 3181.
13 Harrowfield J M, Herlt A J & Sargeson A M, *Inorg Synth*, XX (1980) 85.
14 Goedken V L, *Inorg Synth*, XX (1980) 87.
15 Patra N C, Rout A K & Sahoo B, *Indian J Chem*, 28A (1989) 973 and references therein.
16 Melson G A, *Coordination chemistry of macrocyclic compounds* (Plenum Press, New York and London), 1979, 124.
17 Stratton W J & Busch D H, *J Am chem Soc*, 82 (1960) 4834.
18 Mohapatra B K & Sahoo B, *Indian J Chem*, 21A (1982) 376.
19 Satpathy S & Sahoo B, *J inorg nucl Chem*, 33 (1971) 1313.
20 Singh C B, Rai H C & Sahoo B, *Indian J Chem*, 14A (1976) 504.
21 Wentworth R A D, *Inorg Chem*, 10 (1971) 2615.
22 Stoufer R C, Smith D W, Clevenger E A & Norris T E, *Inorg Chem*, 5 (1966) 1167.
23 Mohapatra B K & Sahoo B, *Indian J Chem*, 22A (1983) 494.
24 Vlček A A, *Progr inorg Chem*, 5 (1967) 211.
25 Saji T & Aoyagui S, *J electroanalyt Chem*, 58 (1975) 401.
26 Saji T, Yamada T & Aoyagui S, *J electroanalyt Chem*, 53 (1975) 325.
27 Vlček A A, *Nature*, 189 (1961) 393.
28 Lichum H, Rock M, Murakami N, Jordar J & Rabockai T, *J electroanalyt Chem*, 76 (1977) 277.

Indian Journal of Chemistry
Vol. 30A, March 1991, pp. 261-265

Novel chloride isopropoxides and allied heterobimetallic complexes of iron(III) with aluminium(III)

(Miss) R Gupta, A Singh & R C Mehrotra*
Department of Chemistry, University of Rajasthan, Jaipur 302 004

Received 21 August 1990; accepted 10 October 1990

Reactions of freshly sublimed anhydrous $FeCl_3$ with potassium tetraisopropoxoaluminate (**1**) in 1:1 and 1:2 molar ratios yield novel heterobimetallic chloride isopropoxides **2a** and **2b** respectively of iron(III) with aluminium(III) of the formula $FeCl_{3-x}\{Al(OPr^i)_4\}_x$ (**2a**, x = 1; **2b**, x = 2). The replacement of chloride in **2a** and **2b** with $\{Al(OEt)_4\}^-$, $acac^-$ and $-OC_6H_4CMe{=}NPr\text{-}o$ ligands results in the formation of new mixed ligand heterobimetallic derivatives. Alcoholysis of **2a** and **2b** with methyl and *t*-butyl alcohols have also been studied. The new complexes have been characterized by elemental analyses, spectroscopic and magnetic studies as well as by molecular weight measurements.

The only previously reported examples of heterobimetallic alkoxides of iron(III) are $Na\{Fe(OEt)_4\}$ (ref. 1), $K_3Fe(OMe)_6$ (ref. 2), $[Li\{Fe(OCHBu^t_2)_4\}.Bu^t_2CHOH]$ (ref. 3) and $Fe\{Zr_2(OPr^i)_9\}_3$ (ref. 4). More recently[5] we have used heterobimetallic chloride isopropoxides of iron(III) for the synthesis of some novel heteroter- and tetra-metallic isopropoxides of iron(III), but the chemistry of simpler precursor complexes has not been explored so far. We report herein synthesis and chemistry of heterobimetallic chloride isopropoxides of iron(III) with aluminium(III).

Materials and Methods

Anhydrous ferric chloride (Fluka) was sublimed under dry Cl_2 atmosphere before use. All solvents were rendered anhydrous and distilled before use. Acetylacetone (BDH) was dried over anhydrous $MgSO_4$, filtered and fractionated over $Al(OPr^i)_3$. All reactions were conducted under strictly moisture-free atmosphere.

Infrared (4000-200 cm^{-1}) and reflectance spectra in nujol were recorded on a Perkin-Elmer 557 and Beckman DK-2 spectrophotometers respectively. Magnetic susceptibilities were measured on a Bruker magnetic balance by the Gouy method. Molecular weights were determined ebullioscopically (Gallenkamp apparatus) in benzene.

Iron and aluminium were estimated either as mixed oxide or as Fe_2O_3 and aluminium as oxinate after separation. Alkoxy groups were estimated by oxidation with 1*N* $K_2Cr_2O_7$ in 12.5% sulphuric acid[6] and chloride by Vohlard's method[7].

Synthesis of heterobimetallic alkoxide complexes

These were generally prepared by the metathetic reaction (involving exchange of chloride by an appropriate anionic ligand), but in some cases alcoholysis tecnique was also employed.

(a) *Preparation of $FeCl\{Al(OPr^i)_4\}_2$* (**2b**) *by metathetical reaction: General procedure*

To a suspension of freshly sublimed ferric chloride (0.64 g; 3.9 mmole) in benzene (~30 ml), potassium tetraisopropoxoaluminate [prepared from equimolar interaction of potassium (0.31 g; 7.9 mmole) and aluminium isopropoxide (1.61 g; 7.9 mmole) in isopropanol and benzene] in benzene (~20 ml) and isopropanol (~5 ml) mixture, was gradually added with constant stirring. The reaction mixture was refluxed for ~12 hr. The precipitated KCl (0.58 g; 7.7 mmole) was filtered off and the solvent removed from the filtrate under reduced pressure to yield a brown-red viscous mass (2.34 g, 3.8 mmole) of **2b**.

(b) *Preparation of $Fe\{Al(OEt)_4\}\{Al(OPr^i)_4\}_2$* (**2c**)

To a benzene (~20 ml) solution of **2b** (1.94 g; 3.1 mmole) was added $KAl(OEt)_4$ [prepared by refluxing potassium (0.12 g; 3.1 mmole) and aluminium ethoxide (0.50 g; 3.1 mmole) in ethanol (~10 ml) and benzene (~30 ml) and solvent removed] suspension in benzene (~30 ml). The resulting reaction mixture was refluxed (~8 hr) with constant stirring, cooled to room temperature, and filtered to remove the precipitated KCl (0.23 g; 3.1 mmole). After removing volatiles from the filtrate under reduced pressure, brown red highly viscous liquid product was obtained in

~100% yield. The product was purified by distillation at 175°C/0.5 mm in ~60% yield.

By carrying out equimolar interactions of **2b** with potassium reagents of appropriate anionic ligands, such as $acac^-$, $OC_6H_4.C(Me)=NPr\text{-}o$, complexes of the types $Fe(acac)\{Al(OPr^i)_4\}_2$ **(2d)** and $Fe(OC_6H_4.C(Me)=Pr\text{-}o)\{Al(OPr^i)_4\}_2$ (**2e**) were obtained in quantitative yields respectively.

(c) *Reaction of $FeCl_2\{Al(OPr^i)_4\}$ (**2a**) with excess methanol: General procedure*

Addition of excess methanol (~30 ml) with constant stirring to a solution of **2a** (2.93; 7.5 mmole) in dry benzene (30 ml) at room temperature resulted in the immediate precipitation of a brown-red solid. The reaction mixture was refluxed for 2 hr, cooled and filtered. The insoluble product was washed several times with anhydrous methanol and dried under reduced pressure to yield $FeCl_2\{Al(OMe)_4\}$ (**2i**) as a brown-red solid, yield 95%.

(d) *Reaction of $FeCl_2\{Al(OPr^i)_4\}$ (**2a**) with excess of t-butyl alcohol under refluxing conditions*

A solution consisting of **2a** (2.11 g; 5.4 mmole) in dry benzene (~50 ml) and *t*-butyl alcohol (35 ml) was refluxed and the liberated isopropyl alcohol (0.96; 16.2 mmole) collected azeotropically until the azeotrope gave a negative test for isopropyl alcohol (8 hr). The solvent was removed under reduced pressure to afford $FeCl_2\{Al(OPr^i)(Obu^t)\}$ (**2k**) as yellow-bronw sticky mass; yield 97%.

Results and Discussion

Refluxing of freshly sublimed anhydrous $FeCl_3$ with potassium tetraisopropoxoaluminate (**1**) in appropriate stoichiometry (1:1 and 1:2) in benzene produce $FeCl_2\{Al(OPr^i)_4\}$ (**2a**) or $FeCl\{Al(OPr^i)_4\}_2$ (**2b**) in quantitative yields (Table 1).

$$FeCl_3 + XK\{Al(OPr^i)_4\} \rightarrow \underset{\mathbf{1}}{} FeCl_{(3-x)}\{Al(OPr^i)_4\}_x + XKCl$$

2*a*, x = 1; 2*b*, x = 2

The chloride group of **2a** and **2b** can easily be replaced by a variety of anionic bidentate ligands by refluxing in benzene to obtain mixed ligand heterobimetallic alkoxides (Table 1).

$$\mathbf{2b} + KX \rightarrow XFe\{Al(OPr^i)_4\}_2 + KCl$$

2c, X = $Al(OEt)_4^-$; **2d**, X = $acac^-$;
2e, X = $OC_6H_4\cdot C(Me)=NPr\text{-}o$

$$\mathbf{2a} + 2KX \rightarrow X_2Fe\{Al(OPr^i)_4\} + 2KCl$$

2f, X = $\{Al(OEt)_4\}^-$; **2q**, X = $acac^-$;
2h, X = $OC_6H_4\cdot C(Me)=NPr\text{-}o$

The reactions of **2a** and **2b** in benzene with excess methyl alcohol at room temperature were facile and resulted in the precipitation of an insoluble methoxide derivative (Table 1)

$$\mathbf{2a} + 4MeOH \rightarrow FeCl_2\{Al(OMe)_4\} + 4Pr^iOH$$
(excess) **2i**

$$\mathbf{2b} + 8MeOH \rightarrow FeCl\{Al(OMe)_4\}_2 + 8Pr^iOH$$
(excess) **2j**

By contrast, reactions of **2a** and **2b** with *t*-butyl alcohol were less facile and even under refluxing conditions with continuous removal of the liberated isopropyl alcohol azeotropically resulted in only the formation of partial substituted *t*-butoxide derivatives (Table 1).

$$\mathbf{2a} + 3Bu^tOH \rightarrow FeCl_2\{Al(OPr^i)(OBu^t)_3\} + 3Pr^iOH$$
2k

$$\mathbf{2b} + 6Bu^tOH \rightarrow FeCl\{Al(OPr^i)(OBu^t)_3\}_2 + 6Pr^iOH$$
2l

The partial replacement observed in the alcoholysis reaction with *t*-butyl alcohol can be explained on the basis of steric factors as the monoisopropoxo tris-*t*-butoxoaluminate $\{(Opr^i)(OBu^t)_3Al\}$ moiety appears to be too crowded[6,8] to be coordinated to another *t*-butyl alcohol molecule, as a precursor for the substitution of the fourth isopropoxy group.

All these new heterobimetallic complexes are coloured (yellow, reddish brown, brown-red or dark-brown) solids or highly viscous materials. These are soluble in benzene except the methoxy derivatives **2i** and **2j**, which are insoluble even in parent alcohol. Most of these derivatives (**2c-2h, 2k** and **2l**) appear to be monomeric in refluxing benzene, whereas, **2a** and **2b** are probably partially associated.

The tentative assignments of the IR peaks in the regions, 360 ± 20 (νFe-Cl), 420-460 (νFe-O),

Table 1 – Analytical data and physical properties of bimetallic alkoxide derivatives of iron(III)

Sl. No.	Reactants (g; mmol)		Product {yield (g, %)} and nature	Found (calc.) %			μ_{eff} (B.M.)
				Mixed oxide Fe/Al	Cl	OPr^i	
1.	$FeCl_3$ (1.41; 8.7)	+ $K\{Al(OPr^i)_4\}$ {K(0.34;8.7) + $Al(OPr^i)_3$(1.76;8.6)}	$FeCl_2\{Al(OPr^i)_4\}$ (**2a**) (3.26;96) Dark-brown viscous semi solid	33.00 (33.50)	18.10 (18.20)	59.70 (60.50)	5.22
2.	$FeCl_3$ (0.64;3.9)	+ $2K\{Al(OPr^i)_4\}$ {K(0.31;7.9) + $Al(OPr^i)_3$ (1.61;7.9)	$FeCl\{Al(OPr^i)_4\}_2$ (**2b**) {2.34; ~ 98} Brown-red highly viscous liquid	29.00 (29.20)	5.78 (5.70)	75.20 (75.90)	5.42
3.	$FeCl\{Al(OPr^i)_4\}_2$ (1.94;3.1)	+ $K\{Al(OEt)_4\}$ {K(0.12;3.1) + $Al(OEt)_3$(0.50;3.1)}	$Fe\{Al(OEt)_4\}\{Al(OPr^i)_4\}_2$ (**2c**) {2.40; ~ 100} Dark-red highly viscous liquid	Fe 7.30 (7.10) Al 10.10 (10.30)	—	—	6.16
4.	$FeCl\{Al(OPr^i)_4\}_2$ (3.22;5.2)	+ K(acac) {K(0.20;5.1) + acacH(0.52;5.1)}	$Fe(acac)\{Al(OPr^i)_4\}_2$ (**2d**) {3.51; ~ 99} Brown-red highly viscous liquid	Fe 8.80 (8.11) Al 7.10 (7.80)	—	—	5.94
5.	$FeCl\{Al(OPr^i)_4\}_2$ (2.53;4.1)	+ K(Schiff base) {K(0.16;4.1) + Schiff base (0.72;4.1)}	$Fe\{Al(OPr^i)_4\}_2$(Schiff base) (**2e**) {3.00; ~ 99} Reddish brown highly viscous liquid	Fe 7.70 (7.46) Al 7.09 (7.21)	N 1.20 (1.87)	—	5.94
6.	$FeCl_2\{Al(OPr^i)_4\}$ (3.61;9.3)	+ $2K\{Al(OEt)_4\}$ {K(0.73;18.6) + $Al(OEt)_3$(6.00;18.6)}	$Fe\{Al(OEt)_4\}_2\{Al(OPr^i)_4\}$(**2f**) {6.70; ~ 100} Highly viscous reddish brown liquid	Fe 7.70 (7.60) Al 11.00 (11.03)	—	—	6.21
7.	$FeCl_2\{Al(OPr^i)_4\}$ (2.11;5.4)	+ 2K(acac) {K(0.42;10.7) + acacH(1.09;10.8)}	$Fe(acac)_2\{Al(OPr^i)_4\}$(**2g**) {2.57; ~ 93} Reddish-brown solid	Fe 11.00 (10.80) Al 5.06 (5.20)	—	—	5.76
8.	$FeCl_2\{Al(OPr^i)_4\}$ (2.33;6.0)	+ 2K (Schiff base) {K(0.47;12.0) + Schiff base (2.10;12.0)	$Fe(Schiff\ base)_2\{Al(OPr^i)_4\}$ (**2h**) {3.79; ~ 99} Reddish-brown solid	Fe 8.73 (8.91) Al 4.07 (4.22)	N 4.28 (4.37)	—	5.60
9.	$FeCl_2\{Al(OPr^i)_4\}$ (2.93;7.5)	+ MeOH (~ 30 ml)	$FeCl_2\{Al(OMe)_4\}$ (**2i**) {1.99; ~ 95} Brown-red solid	45.90 (45.90)	25.30 (25.40)	—	4.66
10.	$FeCl\{Al(OPr^i)_4\}_2$ (2.86; 4.6)	+ MeOH (~ 30 ml)	$FeCl\{Al(OMe)_4\}_2$ (**2j**) {1.82; ~ 100} Brown-red solid	45.80 (46.13)	8.82 (9.01)	—	4.82
11.	$FeCl_2\{Al(OPr^i)_4\}$ (2.11;5.4)	+ Bu^tOH (~ 35 ml)	$FeCl_2\{Al(OPr^i)(OBu^t)_3\}$ (**2k**) {2.30; ~ 97} Yellow-brown semi-solid	29.06 (29.17)	17.10 (16.80)	13.70 (13.60)	5.34
12.	$FeCl\{Al(OPr^i)_4\}_2$ (2.56;4.2)	+ Bu^tOH (~ 30 ml)	$FeCl\{Al(OPr^i)(OBu^t)_3\}_2$ (**2l**) {2.92; ~ 98} Yellow-brown semi-solid	25.90 (25.50)	4.97 (5.00)	17.10 (17.20)	5.90

500-680 (νAl-O), 950-1080 (νC-O-M), 1530 ± 10 (νC=C), 1590 (νC=O) and 1600 cm^{-1} (νC=N) have been made on the basis of published data on iron(III) chloride complexes[9], metal [e.g., aluminium(III) and iron(III)] alkoxides[10a,b], acetylacetonates[11] and schiff base complexes[12].

The ν(M-halide) modes are known to give good information on the stereochemistry of the molecule[13]. The appearance of ν(Fe-Cl) in the region of 360 ± 20 cm^{-1} in bimetallic chloride alkoxides (**2a, 2b, 2i-2l**) is close to ν(Fe-Cl) in $FeCl_3$, dioxane[14,15] (380 cm^{-1}) and $FeCl_3$ (4-cyanopyridine)$_2$ (ref. 16) (372 cm^{-1}), for which trigonal bipyramidal geometry has been suggested. Such a geometry get further support in X-ray crystallography in the latter case. However, on the basis of ν(Fe-Cl) alone it is difficult to decide the correct environment about iron(III), because the tetrahedral anion[17a,b] $\{FeCl_4\}^-$ shows ν(Fe-Cl) at ~380 cm^{-1}, while in the case of neutral tetrahedral complexes[18] of the type $FeCl_3(PR_3)$(R = Cyclohexyl or Bu^t) the ν(Fe-Cl) mode is observed at 395 and 350 cm^{-1}. In the $\{FeCl_5\}^{-2}$ species, ν(Fe-Cl) mode[19] appears at 336 cm^{-1}. Certainly the ν(Fe-Cl) mode is expected to shift progressively to lower wave numbers as the coordination number of the metal increases from four to six, although anomaly in the trend may occur due to effects of steric interaction, double bonding and differences in *d* subshell populations[20].

The diffuse reflectance spectra of the new heterobimetallic alkoxides of iron(III) do not generally show transitions in the visible region. This may be due to the fact that *d-d* transitions are both spin and Laporte forbidden[21] for transition metal ions with d^5 electronic configuration. However, the visible spectra of some of these complexes (**2b, 2c, 2e, 2g, 2k** and **2l**) do exhibit absorptions at ~22.9 × 10^3 cm^{-1}, which is more likely due to charge-transfer[22]. This is due to the fact that, for iron(III) ion, the optical electronegativity is much higher so that the weak *d-d* transitions are infact masked by the spread into the visible spectrum of strong CT bands belonging to the near UV ligand-metal CT bands which lie at lower energies and their tails often hide the weak spin-forbidden ligand field bands.

The room temperature magnetic moments (Table 1) for the complexes **2e-2h** and **2l** are in the range 5.6-6.2 B.M., indicating high spin nature of the derivatives[23]. However, some complexes such as **2a, 2b** and **2i-2k** exhibit magnetic moments in the range of 4.6-5.4 B.M., which could be due to the weak intermolecular antiferromagnetic interactions[24] through the bridging groups in these complexes. In this connection, a noteworthy feature is that molecular weights of freshly prepared **2a, 2b** and **2k** indicate these to be monomeric in benzene; however, samples kept for 1-2 days show molecular complexity of generally two. Such ageing phenomenon[6,10,25] is well known in metal alkoxide chemistry.

On the basis of the molecular weights and magnetic data and generally observed bidentate nature of $\{Al(OPr^i)_4\}^-$ (ref. 26, 27), acetylacetonate[28], and schiff base ligands[29], six-coordinate (octahedral) and five-coordinate (trigonal bipyramidal or tetragonal pyramidal) appear to be the most plausible geometries for the complexes **2e-2h, 2j** and **2a, 2b, 2i, 2k, 2l** respectively.

Acknowledgement

One of us (RG) gratefully acknowledges the University of Rajasthan, Jaipur for the award of a junior research fellowship.

References

1 Meerwein H & Bersin T, *Ann*, 476 (1929) 113.
2 Ludman C J & Waddington T C, *J chem Soc (A)*, (1966) 1816.
3 Bochmann M, Wilkinson G, Young G B, Hursthouse M B & Malik K M A, *J chem Soc Dalton Trans*, (1980) 1863.
4 Shah A, Singh A & Mehrotra R C, *Indian J Chem*, 26A (1987) 485.
5 Dubey R K, Shah A, Singh A & Mehrotra R C, *Rev Trav Chim Pays-Bas*, 107 (1988) 237.
6 Mehrotra R C, *J Indian chem Soc*, 30 (1953) 585.
7 Vogel A I, *A text book of quantitative inorganic analysis* (Longmans, London) 1978.
8 Mehrotra R C & Mehrotra A, *Inorg chim Acta Rev*, 5 (1971) 127.
9 Cotton S A, *Coord chem Rev*, 8 (1972) 185 and references therein.
10 (a) Barraclough C G, Bradley D C, Lewis J & Thomas I M, *J chem Soc*, (1961) 2601; (b) Bradley D C, Mehrotra R C & Gaur D P, *Metal alkoxides* (Academic Press, New York), 1978.
11 Mehrotra R C, Bohra R & Gaur D P, *Metal β-diketonates and allied derivatives* (Academic Press, London), 1978.
12 Percy G C & Thornton D A, *J inorg nucl Chem*, 34 (1972) 3369.
13 Ferraro J R, *Low-frequency vibrations of inorganic and coordination compounds*, (Plenum Press, New York), 1971, Chapter 6.
14 Fowles G W A, Rice D A & Walton R A, *J chem Soc(A)*, (1968) 1842.
15 Maeda Y & Takashima Y, *Inorg nucl Chem Lett*, 12 (1976) 313.
16 Daran J C, Jeannin & Martin L M, *Inorg Chem*, 19 (1980) 2935.
17 (a) Woodward L A & Taylor M J, *J chem Soc*, (1960) 4473; (b) Bancroft G M, Maddock A G, Ong W K & Prince R H, *J chem Soc (A)*, (1966) 723.

18 Walker J D & Poli R, *Inorg Chem*, 29 (1990) 756.
19 Creaser C S & Creighton J A, *J inorg nucl Chem*, 41 (1979) 469.
20 Clark R J H, *Spectrochim Acta*, 21 (1965) 955.
21 Sutton D, *Electronic spectra of transition metal complexes* (McGraw-Hill, London), 1968.
22 Lever A B P, *Inorganic electronic spectroscopy*, 2nd Edn (Elsevier, Oxford) 1982.
23 (a) Figgis B N & Lewis J, *Progr inorg Chem*, 6 (1964) 37; (b) Earnshaw A, *Introduction to magnetochemistry* (Academic Press, London) 1968.
24 Murray K S, *Coord chem Rev*, 12 (1974) 1.
25 Mehrotra R C & Aggrawal M, *Polyhedron*, 4 (1985) 1141.
26 Mehrotra R C, *J Indian chem Soc*, LIX (1982) 715.
27 Mehrotra R C & Singh J V, *Inorg Chem*, 23 (1984) 1046.
28 Mehrotra R C, Bohra R & Gaur D P, *Metal β-diketonates and allied derivatives* (Academic Press, London), 1978.
29 (a) Van der Bergen A, Murray K S, O'Connor M J, Rehak N & West B O, *Aust J Chem*, 21 (1968) 1505; (b) Davies J E & Gate house B M, *Chem Commun*, (1970) 1166.

Indian Journal of Chemistry
Vol. 30A, March 1991, pp. 266-268

Charge-transfer interaction of some aromatic hydrocarbons with chloranil

Nupur Aditya & Rama Basu*

Department of Pure Chemistry, University College of Science, 92, Acharya Prafulla Chandra Road, Calcutta 700 009

Received 21 December 1989; revised 2 April 1990; rerevised and accepted 31 August 1990

The interaction of different substituted naphthalenes with chloranil has been studied spectrophotometrically in chloroform. Symmetrically substituted naphthalenes give one new absorption band while the unsymmetrically substituted naphthalenes show two new absorption bands. The formation constants for the charge-transfer complexes have been determined using Benesi-Hildebrand's method. Linear plots for $h\nu$ against ionization potential of the donors have been obtained.

Observation of two charge-transfer absorption bands in π-π^* complexes having substituted benzenes as the donor component was explained by Orgel[1] in terms of the possibility of the transferred electron coming from either of the two levels arising when the degeneracy of the E_1 level of benzene is removed by substitution. Orgel used a simple first order perturbation calculation to evaluate both the shift in position of the CT absorption from that found in the complex of benzene with a given acceptor and the splitting resulting from substitution of the benzenoid donor in various possible ways. Later, many other workers[2-4] studied the charge-transfer spectra of systems containing substituted benzenes. Recently, Dwivedi and Agarwal[5] studied the charge-transfer spectra of a number of hydrocarbons with chloranil and DDQ and have located multiple charge-transfer band only in the case of pyrene. In order to see whether these types of multiple charge-transfer bands appear in other higher hydrocarbons, e.g., naphthalene, we have carried out studies on a number of substituted naphthalenes.

Considering also that for stable π-π^* complexes the most stable configurations have been shown to be those where donors and acceptors lie above each other with their molecular planes more or less parallel, we have chosen chloranil as acceptor which is known to form a good π-π^* complex with its molecular plane being parallel to that of the donors.

Experimental

The hydrocarbons used were 1, 2, 4, 5-tetramethylbenzene (BDH), 2-methylnaphthalene, 2, 3-dimethylnaphthalene, 2, 6-dimethylnaphthalene, 1, 3-dimethylnaphthalene (Koch Light Laboratories), 1, 2, 3-trimethylbenzene, and 1-methylnaphthalene (Fluka). These were used as such. The solvent chloroform was procured from S.D. Chemicals (Bombay). The solvent was thoroughly dried and distilled just before use. Chloranil was an E. Merck reagent and used after several recrystallizations. Finally, its purity was checked on the basis of its melting point.

The spectral data were taken on a Cary 2390 spectrophotometer at 25 ± 1°C using 1 cm matched silica cells.

In locating the position of a characteristic absorption maximum, a solution of the donor and the acceptor (chloranil) in chloroform was balanced against a solution of chloranil of the same strength, as the hydrocarbons do not absorb in the region being studied. The concentration ratio of the donor to acceptor was nearly 100:1. The donors were used at a

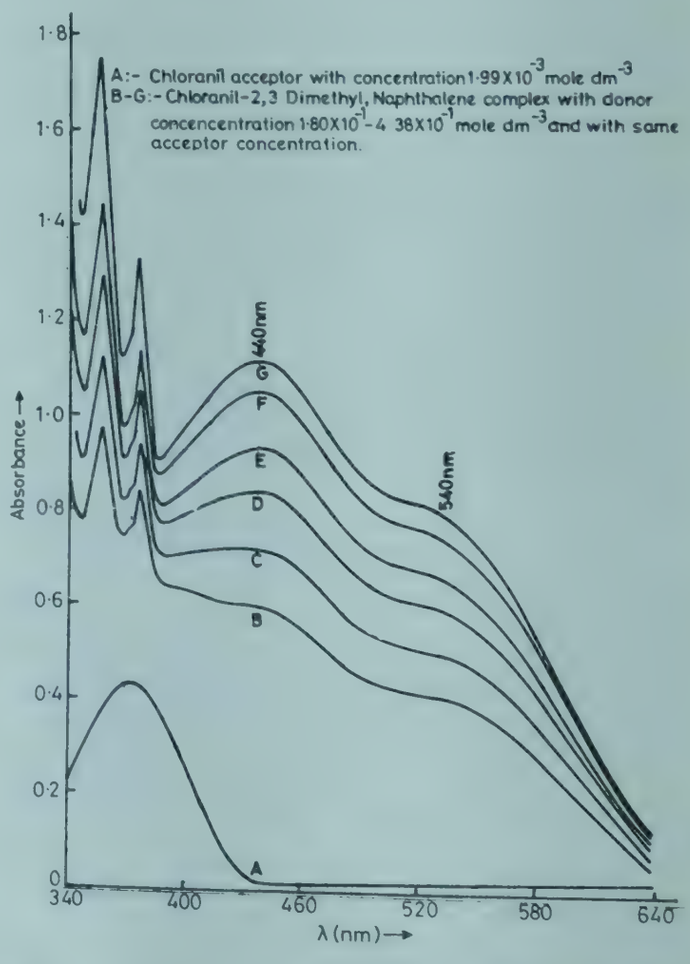

Fig. 1—Spectra of chloranil and chloranil-2, 3-dimethyl-naphthalene complex

concentration of 10^{-1} mol dm^{-3} and chloranil (acceptor) at a concentration of 10^{-3} mol dm^{-3}.

The formation constants (K) and molar extinction coefficients (ε) of complexes of different donors with chloranil were calculated by the Benesi-Hildebrand[6], Scott[7] and Rose-Drago[8] methods. The Benesi-Hildebrand plots for methylbenzene-chloranil mixture and of the other donor-chloranil mixtures in chloroform were linear indicating the formation of 1:1 molecular complexes. Moreover, the absorbance

Table 1—The formation constant and molar extinction coefficient data for charge-transfer complexes

Donor	ν– (cm^{-1}) $\times 10^{-4}$	$h\nu$ (eV)	[Acceptor] (mol dm^{-3}) $\times 10^3$	K (dm^3 mol^{-1}) $\times 10$‡			I.P. (eV)
				[6]B.H. method	[7]Scott method	[8]Rose & Drago method	
1,2,3-Trimethylbenzene	2.38	2.95	2.85	3.95	5.26	11.8±0.3	8.49[a]
			1.42	(1.81)	(1.53)	(1.13)	
				3.96	4.20		
				(3.03)	(2.93)		
1,2,4,5-Tetramethylbenzene	2.08	2.58	0.46	8.66	6.22	7.4±0.2	8.53[b]
			0.93	(3.33)	(4.19)	(3.2)	
			1.39	8.81	7.40		
				(2.85)	(3.13)		
				7.25	6.70		
				(3.33)	(3.52)		
1-Methylnaphthalene	1.92	2.38	2.30	3.94	4.97	5±0.1	8.41[a]
				(1.19)	(1.06)	(1.02)	
			0.87	4.0	4.12		
				(1.66)	(1.62)		
2-Methylnaphthalene	1.98	2.46	0.94	8.16	9.6	8.7±0.3	8.48[a]
			1.41	(1.0)	(0.87)	(0.95)	
			2.08	10.66	—		
				(0.8)	—		
				6.66	5.66		
				(1.33)	(1.40)		
2,3-Dimethylnaphthalene	1.85	2.29	1.33	13.5	10.89	10.7±0.7	8.11[c]
	2.27	2.81	1.99	(1.53)	(1.70)	(1.65)	
				11.12	7.89		
				(1.66)	(1.53)	6.60±0.05	
				11.65	11.30	(2.02)	
				(1.17)	(1.73)		
				9.29	10.95		
				(1.33)	(1.22)		
2,6-Dimethylnaphthalene	1.86	2.31	1.65	18.39	16.65	—	—
				(0.85)	(0.94)		
1,3-Dimethylnaphthalene	1.81	2.25	3.31	46.7	35.65	—	—
	2.32	2.88	2.25	(0.39)	(0.48)		
				32.30	32.30		
				(0.42)	(0.46)		
				35.7	28.61		
				(0.47)	(0.53)		
				39.7	21.64		
				(0.35)	(0.59)		

[a] Streitwieser Andrew, *J Am chem Soc*, 82 (1960) 4123.

[b] Franklin J L, *J chem Phys*, 22 (1954) 1304.

[c] *Slifkin M A & Allison A C, Nature*, 215 (1967) 949.

‡ Values in parentheses are ε values in $dm^3mol^{-1}cm^{-1} \times 10^{-3}$

versus mole fraction plot for the systems gave a further proof of the 1:1 nature of the molecular complex.

Fig. 1 shows the absorption spectra of chloranil and chloranil plus 2,3-dimethylnaphthalene in chloroform. While chloranil has the absorption maximum at 375 nm, the chloranil-hydrocarbon mixture shows two peaks at 540 and 440 nm. As the hydrocarbon concentration is increased at a fixed chloranil concentration, the absorbance at both the bands increases. Evidently, the red shifted bands at 540 and 440 nm arise from a molecular complex formed between chloranil and the hydrocarbon. Table 1 shows the wave number of charge-transfer band (ν, cm^{-1}), the formation constant (K, dm^3mol^{-1}) and the molar extinction coefficients (ε, $dm^3\ mol^{-1}cm^{-1}$) of the complexes of the different donors with chloranil in chloroform as obtained by the three methods. Linear regression was carried out in the final stage of the computation. The points ([A]/absorbance) which were off by $\pm 0.1 \times 10^{-4}$ from the perfect linear curve were omitted in the linear regression calculations.

As is evident from Table 1, all the substituted benzenes and naphthalenes show a red-shifted band with respect to the donors and acceptors which is present neither in the donors nor in the acceptors. The $h\nu$ values of the red shifted bands when plotted against the ionization potentials of the respective donors gave a straight line. Accordingly, we may conclude that the complexes produced are of charge-transfer type. Moreover, among the donors, 2,3-dimethylnaphthalene and 1,3-dimethylnaphthalene show two charge-transfer bands. Orgel's idea of all substituted benzenes showing two charge-transfer bands is not corroborated in the case of naphthalene. According to Orgel, visible bands of chloranil complexes with alkylbenzenes are generally composite consisting of two overlapping charge-transfer bands. We, however, could not distinguish two overlapping bands (Table 1) with the resolution available with Cary 2390 instrument. The appearance of two charge-transfer bands in the cases of 2,3-dimethyl- and 1,3-dimethylnaphthalenes may be due to the loss of symmetry of the π-electronic structure of the naphthalene molecule by unsymmetrical substitution. The formation constants, and extinction coefficients calculated by three different methods as shown in Table 1 are more or less same. The high values of the extinction coefficients indicate that the complexes formed are quite stable in nature.

Acknowledgement

Our sincere thanks are due to Dr A S Ghosh for recording the spectrophotometric data on Cary 2390 spectrophotometer. One of us (N.A.) acknowledges her sincere thanks to the UGC, New Delhi for the award of a JRF.

References

1 Orgel L E, *J chem Phys*, 23 (1955) 1352.
2 Voigt E M, *J Am chem Soc*, 86 (1964) 3611.
3 Kuboyama A, *J chem Soc Japan*, 81 (1960) 558.
4 Schenk G H & Fryer P A, *Analyt Chem*, 42 (1970) 1694.
5 Dwivedi P C & Agarwal R, *Indian J Chem*, 24A (1985) 1015.
6 Benesi H A & Hildebrand J H, *J Am chem Soc*, 71 (1949) 2703.
7 Scott R L, *Proc Int Conf on co-ordination compounds*, Amsterdam (1955), p 265; *Recl Trav chim Pays-Bas Belg*, 75 (1956) 787; Foster R, *Organic charge transfer complexes* (Academic Press, London & New York) 1969, 129.
8 Rose N J & Drago R S, *J Am chem Soc*, 81 (1959) 6138, 6141; Foster R, *Organic charge transfer complexes* (Academic Press, London & New York) 1969, 135.

Indian Journal of Chemistry
Vol. 30A, March 1991, pp. 269-271

Kinetics and mechanism of dissociation of some *para*-substituted phenylbiguanide complexes of nickel (II) in aqueous hydrochloric acid

Supriya Guha & D Banerjea*

Department of Chemistry, University College of Science, 92, Acharya Prafulla Chandra Road, Calcutta 700 009

Received 8 August 1990; revised and accepted 6 November 1990

The rates of dissociation in aqueous hydrochloric acid medium of the bis complexes of nickel (II) with N^1-(4-methoxyphenyl)biguanide and N^1-(4-sulphophenyl)biguanide have been investigated by stopped-flow spectrophotometry and the results compared with those of the biguanide and N^1-phenylbiguanide complexes reported earlier. The complete dissociation of the complex to the $Ni(H_2O)_6^{2+}$ and free ligand (protonated) occurs in two consecutive steps, the first being relatively faster than the second; each step leading to loss of one ligand. For each step the rate is first order in acid concentration. The results are consistent with a solvent-assisted dissociative process involving the protonated complex; the rate varies due to the electronic effect of the substituent in the phenyl ring. For each of the steps isokinetic trend has been observed, and the biguanide complex also fits into the trend. The relative rates are more or less enthalpy controlled.

Recently the rates of dissociation of bis(biguanide)[1] and some bis(N^1-substituted biguanide)[2] complexes of nickel (II) including that of N^1-phenylbiguanide in aqueous acid have been investigated. Similar dissociation of bis{N^1-(4-methoxyphenyl)biguanide} and bis{N^1-(4-sulphophenyl)biguanide} complexes of Ni(II) into the corresponding free ligands and $Ni(H_2O)_6^{2+}$ has not been reported and hence the present investigation. The main objective is to study the effect of substituents in the phenyl ring on the rates of disociation of the complexes.

Experimental

Sodium bis{N^1-(4-sulphophenyl)biguanide}nickelate (II) trihydrate, $Na_2Ni(B)_2.3H_2O$ (where B = (4)-$O_3SC_6H_4C_2H_5N_5$) was prepared by known method[3] and its purity checked by elemental analyses. In solution in the presence of acid this forms $Ni(BH)_2$ complex. The bis-complex of Ni^{2+} with N^1-(4-methoxyphenyl)biguanide was prepared in solution by adding the requisite amount of alkali to a 1:2 mixture of $NiCl_2$ and the pure ligand. All other chemicals used were either of reagent grade or else purified by known methods. Solutions were prepared using double distilled water, second distillation from alkaline permanganate, and were stored in resistant glass vessels.

Apparatus and procedure

The kinetics of dissociation of the complexes (0.002 mol dm^{-3}) in aqueous solution containing varying amounts of HCl (0.02 to 0.05 mol dm^{-3} for N^1-(4-sulphophenyl)biguanide complex (I), and 0.01 to 0.035 mol dm^{-3} for N^1-(4-methoxyphenyl)biguanide complex (II) and KCl (to adjust the ionic strength to 0.1 mol dm^{-3}) were studied spectrophotometrically at the λ_{max} of the complexes (430 nm for complex I and 460 nm for the complex II), where the reaction products are virtually non-absorbing at the concentrations used. Canterbury-model stopped-flow spectrophotometer (SF-3A, Hi-Tech, England) coupled with an oscilloscope (OS-1000A, Advance Instruments, England) and a transient recorder (DL-905, Data Lab, England) was used for the purpose. The solutions and the cell were thermostatted at the desired temperature ($\pm 0.05°$).

Results and discussion

Detailed analysis by known procedure[4] of the absorbance versus time profile for the reactions revealed that these complexes undergo dissociation in two consecutive steps; an initial faster reaction (k_f) is followed by a relatively slower one (k_s); both being first order in [acid]. This can be interpreted by a mechanism similar to that proposed earlier[1] in which initial (faster) step involves protonation of the metal bound ligand in a fast equilibrium followed by bond rupture in the rate-determining step leading to the formation of the monobiguanide complex and releasing one biguanide ligand. The second step (slower) is a repetition of the process in the first step, involving loss of the remaining biguanide ligand, and forming the aqua-metal ion as the final product. Indeed the existence of such monobiguanide complexes, believed to be formed in the first step, has been established earlier in a few cases[5,6]. Protonation of the bound biguanide ligand can be explained on the basis of the known structure of biguanide complexes and this process would facilitate dissociation of the metal-ligand bond as discussed earlier[1,2,7-10].

Based on the proposed mechanism, the observed pseudo-first order rate constant for each step, i.e. k_f and k_s, will show acid dependence as follows:

$$k_x = k'_x[H^+] \quad (1)$$

Table 1—Kinetic parameters for acid catalysed dissociation of the biguanide complexes of nickel (II) in aqueous acid media ([Complex] = 0.002 mol dm^{-3}; I = 0.1 mol dm^{-3} (HCl+KCl))

Complex	Temp., °C	$10^{-3}k'_f$, $M^{-1}s^{-1}$	$10^{-3}k'_s$, $M^{-1}s^{-1}$
(A) $Ni(O_3S\text{-}PhbigH)_2$	20	2.79±0.08	1.20±0.03
	25	3.40±0.09	1.40±0.04
	30	4.14±0.10	1.63±0.06
$\Delta H‡$, kJ mol^{-1}		28.0±0.5	22.8±0.8
$\Delta S‡$, JK^{-1} mol^{-1}		−84.3±1.5	−101.9±2.1
(B) $Ni(MeO\text{-}PhbigH)_2^{2+}$	20	10.01±0.56	8.20±0.23
	25	11.10±0.48	9.0±0.31
	30	12.30±0.64	9.87±0.39
$\Delta H‡$, kJ mol^{-1}		14.0±0.2	10.5±0.2
$\Delta S‡$, JK^{-1} mol^{-1}		−121.4±1.8	−134.9±2.8
(C) $Ni(PhbigH)_2^{2+}$[a]	25	10.80±0.64	7.91±0.16
$\Delta H‡$, kJ mol^{-1}		15.1	13.9
$\Delta S‡$, JK^{-1} mol^{-1}		−119.7	−125.6
$Ni(BigH)_2^{2+}$[b]	25	3.63±0.05	2.32±0.03
$\Delta H‡$, kJ mol^{-1}		32.6	25.1
$\Delta S‡$, JK^{-1} mol^{-1}		−69.9	−98.3

(a) Values from ref. 2; (b) values from ref. 1.

where x refers to "f" (fast) or "s" (slow), as the case may be.

From the specific rate constant values k'_f and k'_s evaluated by least-square procedure from k_f and k_s values at different acid concentration at three temperatures (20, 25 and 30°) the corresponding activation parameters $\Delta H‡$ and $\Delta S‡$ have been evaluated making use of Eyring equation as usual and the values are given in Table 1 with the corresponding values for the biguanide[1] and phenylbiguanide[2] complexes for comparison.

The results show that at 25°C, for each step, the rates of dissociation of the different complexes follow the sequence $Ni(MeO\text{-}PhbigH)_2^{2+} > Ni(PhbigH)_2^{2+} > Ni(BigH)_2^{2+} > Ni(O_3S\text{-}PhbigH)_2$, while both $\Delta H‡$ and $\Delta S‡$ values for each step are in the sequence $Ni(BigH)_2^{2+} > Ni(O_3S\text{-}PhbigH)_2 > Ni(PhbigH)_2^{2+} > Ni(MeO\text{-}PhbigH)_2^{2+}$ so that the relative rates are more or less enthalpy-controlled. For each of the steps, k'_f and k'_s, the plot of $\Delta H‡$ versus $\Delta S‡$ is linear (see Fig. 1) and this isokinetic trend suggests similar mechanism for the dissociation of all these complexes; the highly negative $\Delta S‡$ values imply considerable solvent participation in the rate-determining step, presumably due to a solvent assisted dissociative process. The observed sequence of rates for the phenyl- and substituted phenyl-biguanide complexes may be explained on the basis of electronic effect exerted by the substituent in the

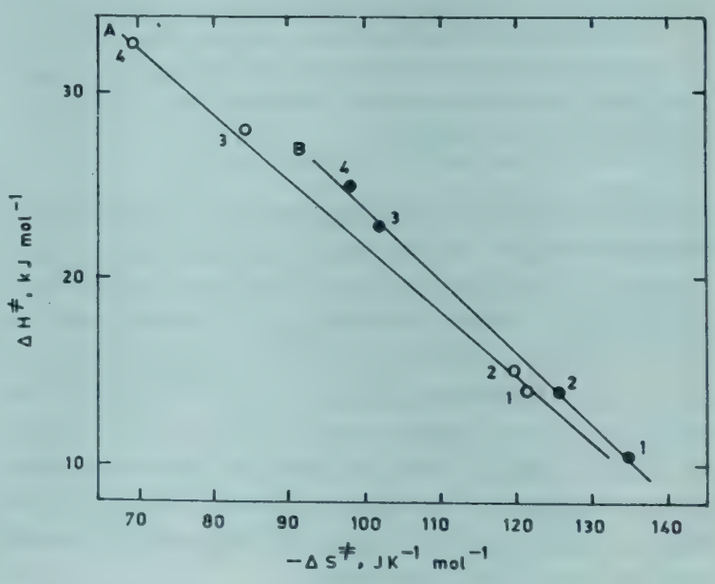

Fig. 1—Isokinetic plots for k'_f (A) and k'_s (B): (1) $Ni(MeO\text{-}PhbigH)_2^{2+}$; (2) $Ni(PhbigH)_2^{2+}$; (3) $Ni(O_3S\text{-}PhbigH)_2$; (4) $Ni(BigH)_2^{2+}$

para position of the phenyl ring. In contrast to the unsubstituted phenyl group the electron releasing methoxy will significantly increase electron density on N^1 and N^5 which will facilitate protonation at any of these sites and thus weakening the Ni-N bond leading to a higher rate of dissociation. On the other hand, the electron withdrawing sulphonate group will considerably reduce electron density on both N^1 and N^5 making protonation less favoured and hence reduce

the rate of acid catalysed dissociation. Consideration of pK_a values[2] of diprotonated biguanides indicate that the phenyl group in the phenyl biguanide reduces basicity of N^1 and N^5 to a comparable extent. Protonation however presumably occurs at N^5 (NH_2 group) which is more basic than the N^1 (NHPh group).

References

1 Banerjea D, *Trans Met Chem*, 7 (1982) 22.

2 Banerjee R N, Gangopadhyay S, Banerjee A K & Banerjea D, *J coord Chem*, 12 (1983) 287.

3 Ray P & Dutt R K, *J Indian chem Soc*, 25 (1948) 563.

4 Banerjee R N & Banerjea D, *Indian J Chem*, 17A (1979) 246.

5 Ray P, *Chem Rev*, 61 (1961) 313.

6 Banerjea D & Banerjee P, *Z anorg allgem Chem*, 393 (1972) 295.

7 Banerjee R N & Banerjea D, *J Indian chem Soc*, 55 (1978) 969.

8 Banerjea D & Chakravarty B, *J inorg nucl Chem*, 26 (1964) 1233.

9 Banerjea D & Sengupta S, *Z anorg allgem Chem*, 397 (1973) 215.

10 Banerjea D & Chattopadhyay B, *J inorg nucl Chem*, 36 (1974) 2351.

Indian Journal of Chemistry
Vol. 30A, March 1991, pp. 272-274

Kinetics of retroaldol reaction of *para*-substituted β-nitrostyrenes and β-methyl-β-nitrostyrenes

A Shunmugasundaram*, T Lekshmana Thanulingam & R Murugesan

Department of Chemistry, VHNSN College, Virudhunagar 626 001

Received 5 July 1990; revised 4 October 1990; accepted 30 October 1990

The kinetics of retroaldol reaction of β-nitrostyrene and β-methyl-β-nitrostyrene and their *para*-substituted derivatives have been studied spectrophotometrically in 1:1 methanol-water (v/v) in the presence of sodium hydroxide. The order is unity in [β-nitrostyrene] and fractional in [OH^-]. In the reaction of β-methyl-β-nitrostyrene the order in [substrate] and [OH^-] is unity each. On the basis of the kinetic data, a stepwise reaction mechanism has been proposed which involves nucleophilic attack of OH^- on the α-carbon and subsequent cleavage of $C_\alpha - C_\beta$ bond. The rate of β-methyl-β-nitrostyrene is less than that of β-nitrostyrene. Electron-withdrawing substituents accelerate the reaction and electron-releasing substituents retard it. Satisfactory Hammett correlations have been observed in both reaction series.

Kinetics of retroaldol cleavage of various unsaturated carbonyl compounds such as 3-methyl-2-butenal[1], 3-penten-2-one[2], crotonaldehyde[3] and chalcone[4] in aqueous sodium hydroxide have been studied. But no kinetic analysis for the retroaldol reactions of nitrostyrenes has been reported so far. We have now investigated the retroaldol reaction of various *para*-substituted β-nitrostyrenes (I) and β-methyl-β-nitrostyrenes (II).

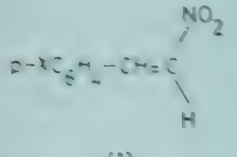

(I)

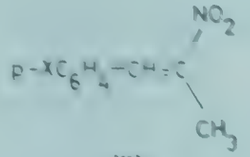

(II)

Experimental

The compounds I and II were prepared by literature method[5] and their purity checked by elemental analyses and physical measurements. Sodium hydroxide (AR, BDH) and distilled methanol were used. The kinetic measurements were carried out under pseudo-first order condition ([OH^-] ≫ [substrate]) in 1:1 methanol-water (v/v) by monitoring the absorption maxima at 459, 359, 333, 318, 320, 321, 320, 299, 303 and 309 nm for *p*-NMe_2, *p*-OMe, *p*-Me, H, *p*-F, *p*-Cl, *p*-Br, *p*-CF_3, *p*-CN and *p*-NO_2-β-nitrostyrene and 444, 348, 324, 316, 311, 314, 315, 296, 291 and 300 nm for *p*-NMe_2, *p*-OMe, *p*-Me, H, *p*-F, *p*-Cl, *p*-Br, *p*-CF_3, *p*-CN and *p*-NO_2-β-methyl-β-nitrostyrenes respectively. The pseudo-first order rate constants were given by the slopes of the linear plots of log (OD) versus time.

In the stoichiometric runs solutions of β-nitrostyrene and β-methyl-β-nitrostyrene in separate flasks containing an excessof hydroxide ion were kept for 24 hr at room temperature. Estimation of the unreacted [OH^-] showed that both β-nitrostyrene and β-methyl-β-nitrostyrene reacted with OH^- in 1:1 ratio.

Equal amounts of β-nitrostyrene and OH^- were mixed under kinetic conditions and after three half-lives the solvent was removed under reduced pressure, the residue was shaken with water (25 ml) and extracted with ether. The ether layer was washed with water several times, dried (anhydrous Na_2SO_4) and the solvent was removed. The residue was dissolved in ethanol and 2,4-dinitrophenylhydrazine was added and the reaction mixture was gently warmed for 5 min on a water bath. Solid formed was recrystallised from ethanol (yield 95%, m.p. 235°C). There was no depression in melting point on admixture with an authentic sample of 2,4-DNP derivative of benzaldehyde. The formation of benzaldehyde and nitromethane in the case of β-nitrostyrene and benzaldehyde and nitroethane in the case of β-methyl-β-nitrostyrene was also confirmed by comparing the UV spectra of reaction mixtures with those of authentic mixtures.

Results and discussion

From the stoichiometry and product analysis of the retroaldol reaction of compounds I and II, the overall reaction could be represented by Eq. (1).

Where R = H or $-CH_3$ group

The reaction of β-nitrostyrene is first order in [β-nitrostyrene] under pseudo-first order conditions and at different initial [β-nitrostyrene] and fixed [OH^-]. The plot of log k_1 versus log [OH^-] is linear ($r = 0.992$) with a slope of 1.67 indicating that the or-

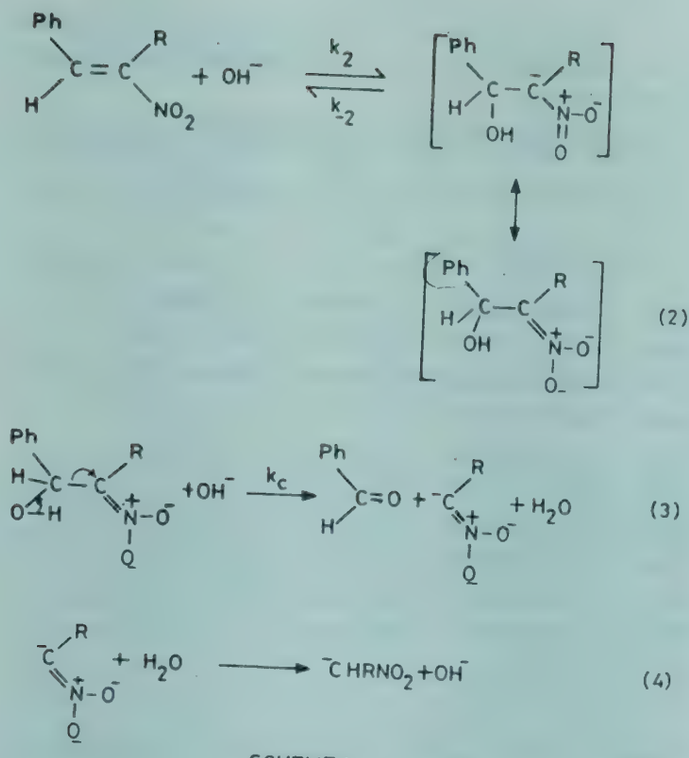

(2)

(3)

(4)

SCHEME 1

der with respect to $[OH^-]$ is 1.67. The rates remain unaffected by adding sodium perchlorate and acrylonitrile indicating that the reaction is not an ion-ion type and that there is no free radical formation in the reaction.

The retroaldol reaction of β-methyl-β-nitrostyrene follows total second order, first order each in [substrate] and $[OH^-]$. The rate of the reaction is almost constant with increase in methanol content in the reaction medium as found in the retroaldol reaction of β-nitrostyrene. Added sodium perchlorate and acrylonitrile have no effect on the reaction rate.

On the basis of the foregoing kinetic observations a plausible common mechanism in Scheme 1 may be proposed.

The second step in this mechanism is rate-determining for the reaction of β-nitrostyrene with OH^- ion. The dependence of k_1 on $[OH^-]$ is given by Eq. (5)

$$k_1 = \frac{Kk_c[OH^-]^2}{1 + K[OH^-]} \qquad \ldots (5)$$

where $K = k_2/k_{-2}$

Equations (2) and (3) constitute a chemical model compatible with the dependence of rate on $[OH^-]$. This reaction is thus shown to be very similar to the other hydrolytic cleavage reactions[6-8]. The values of k_c and K were evaluated from the intercept and slope of the plot of $[OH^-]/k_1$ versus $1/[OH^-]$ and the values of k_c and K obtained for various substituted β-nitrostyrenes are presented in Table 1.

The values of K obtained for β-nitrostyrene (Table 1) suggest substantial conversion of the reactant into $Ph-CH(OH)-\bar{C}HNO_2$. For β-nitrostyrene the values of k_c and K were evaluated to be $k_c = 19.35$, 31.96 and 47.54 $dm^3\ mol^{-1}\ s^{-1}$ and $K = 632$, 445 and 234 $dm^3\ mol^{-1}$ at 25°, 30° and 35°C respectively. The value of K decreases with temperature which shows a pre-equilibrium before rate-determining step. The activation parameters, $\Delta H^{\ddagger}$ and $\Delta S^{\ddagger}$ calculated based on k_c are 66.1 kJ mol^{-1} and 1.64 J K^{-1} mol^{-1} respectively. The values of rate constant k_c clearly indicate that electron withdrawing substituents increase the rate while electron-donating substituents retard it. Hammett correlation has been carried out by plotting log

Table 1 – Effect of structural variation on the rate of retroaldol reaction of β-nitrostyrene and *para*-substituted β-nitrostyrenes
[Substrate] = 5×10^{-5} mol dm^{-3}; $[OH^-] = 5 \times 10^{-4}$ mol dm^{-3}; Solvent: 50% methanol-water (v/v)

Substituent	$k_1 \times 10^3$				$k_c^{\ddagger}$	$K^{\ddagger}$	$\Delta H^{\ddagger *}$	$-\Delta S^{\ddagger *}$
	25°	30°	35°	40°C	($dm^3 mol^{-1} s^{-1}$)	($dm^3 mol^{-1}$)	(kJ mol^{-1})	(J K^{-1} mol^{-1})
NMe_2	0.590 ± 0.006	0.732 ± 0.005	0.899 ± 0.020	1.10 ± 0.020	1.661	1881	29.7 ± 1.1	209 ± 4
OMe	1.52 ± 0.12	2.10 ± 0.13	2.53 ± 0.33	3.38 ± 0.32	7.174	1427	37.7 ± 9.4	172 ± 32
Me	1.85 ± 0.07	2.77 ± 0.09	3.42 ± 0.18	4.54 ± 0.24	8.193	1599	42.7 ± 4.5	154 ± 15
H	2.47 ± 0.06	2.91 ± 0.04	3.75 ± 0.06	4.61 ± 0.12	19.35	632	30.3 ± 2.1	193 ± 7
F	3.60 ± 0.05	4.41 ± 0.04	5.66 ± 0.07	6.35 ± 0.07	19.30	1187	27.9 ± 1.2	198 ± 4
Cl	5.23 ± 0.14	6.38 ± 0.09	9.75 ± 0.26	12.7 ± 0.4	26.65	1295	45.2 ± 2.4	137 ± 8
Br	5.32 ± 0.17	6.94 ± 0.12	9.57 ± 0.28	13.4 ± 0.4	30.82	1039	45.4 ± 2.7	136 ± 9
CF_3	9.81 ± 0.09	12.1 ± 0.7	14.9 ± 0.6	18.1 ± 0.9	62.40	1017	29.2 ± 4.0	187 ± 14
CN	13.9 ± 0.6	18.2 ± 0.7	24.8 ± 0.6	25.0 ± 0.4	85.01	977	29.7 ± 4.1	181 ± 14
NO_2	16.7 ± 1.1	23.0 ± 0.5	30.6 ± 0.4	39.0 ± 0.8	114.7	822	41.3 ± 3.2	140 ± 11

†Evaluated from the plot of $[OH^-]/k_1$ versus $1/[OH^-]$ for each substrate at 25°C
*$\Delta H^{\ddagger}$ and $\Delta S^{\ddagger}$ values at 25°C

Table 2 – Second order rate constants and activation parameters for the retroaldol reaction of β-methyl-β-nitrostyrene and *para*-substituted β-methyl-β-nitrostyrenes

[Substrate] = 7×10^{-5} mol dm^{-3}; [OH^-] = 7.0-5.0 × 10^{-3} mol dm^{-3}; Solvent = 50% methanol-water (v/v)

Substituent	k_2 (dm^3 mol^{-1} s^{-1})				$\Delta H^{\ddagger}$ (kJ mol^{-1}) (at 30°C)	$-\Delta S^{\ddagger}$ (J K^{-1} mol^{-1}) (at 30°C)
	25°	30°	35°	40°C		
NMe_2	0.060 ± 0.001	0.078 ± 0.001	0.107 ± 0.007	0.135 ± 0.003	40.5 ± 1.6	132 ± 5
OMe	0.104 ± 0.001	0.239 ± 0.009	0.340 ± 0.010	0.481 ± 0.016	52.8 ± 2.8	82.8 ± 9.6
Me	0.115 ± 0.001	0.248 ± 0.005	0.365 ± 0.009	0.502 ± 0.016	72.3 ± 2.2	18.0 ± 7.6
H	0.176 ± 0.001	0.273 ± 0.006	0.382 ± 0.010	0.529 ± 0.012	53.9 ± 2.0	77.8 ± 6.8
F	0.197 ± 0.001	0.446 ± 0.007	0.621 ± 0.014	0.787 ± 0.026	67.4 ± 2.0	29.3 ± 6.8
Cl	0.223 ± 0.001	0.464 ± 0.008	0.684 ± 0.019	0.974 ± 0.034	72.3 ± 2.2	12.9 ± 7.5
Br	0.230 ± 0.001	0.481 ± 0.009	0.700 ± 0.020	0.959 ± 0.036	69.9 ± 2.9	20.2 ± 9.9
CF_3	0.628 ± 0.005	0.941 ± 0.006	1.38 ± 0.01	2.00 ± 0.03	57.3 ± 2.1	56.6 ± 7.6
CN	0.737 ± 0.005	1.32 ± 0.06	1.91 ± 0.11	2.49 ± 0.01	59.9 ± 2.9	44.9 ± 9.9
NO_2	0.954 ± 0.034	1.54 ± 0.05	2.14 ± 0.06	2.76 ± 0.06	52.2 ± 3.0	69.2 ± 10.4

k_c at 25°C versus σ. The value of ρ is calculated to be 1.15 + 0.09 (r = 0.996; s = 0.051; ψ = 0.099; n = 10). The positive ρ value suggests that the reaction centre is electron-rich in the transition state and is thus consistent with the proposed mechanism. The log k_1 values at 25°C also correlate well with the Hammett σ constants (ρ = 0.945 ± 0.087; r = 0.994; s = 0.051; ψ = 0.122; n = 10). $\Delta H^{\ddagger}$ and $\Delta S^{\ddagger}$ values were calculated from the overall pseudo-first order rate constants. $\Delta S^{\ddagger}$ values are all negative. Exner plot of log k_1 at 40°C versus log k_1 at 25°C is also linear (r = 0.991) showing that in this reaction series all the *para*-substituted β-nitrostyrenes follow the same mechanism.

In the case of β-methyl-β-nitrostyrene the observed second order rate constant k_2 is given by Eq. (6).

$$\text{rate} = k_2[\text{substrate}][OH^-] \quad \ldots(6)$$

Under the given conditions the value of $K[OH^-]$ is considerably greater than 1 in Eq. (5) and hence the reaction of β-methyl-β-nitrostyrene shows the first order dependence in [OH^-]. In this reaction the rate limiting step is the nucleophilic attack of OH^- on the α-carbon (Scheme 1, Eq. 2) and rapid subsequent cleavage of $C_\alpha - C_\beta$ bond. The change in the rate-limiting step from second to the first may be due to the partial deactivation of C = C by the β-methyl group making the α-carbon less electrophilic.

Second order rate constants for various *para*-substituted β-methyl-β-nitrostyrenes have been measured at 25°, 30°, 35° and 40°C and are given in Table 2. The results indicate that electron-withdrawing substituents enhance the reaction rate and electron-releasing substituents retard it. The plot of log k_2 at 30°C versus σ value is linear with ρ = 0.805 ± 0.097 (r = 0.990; s = 0.057; ψ = 0.158; n = 10). The positive ρ-value is in consonance with a mechanism involving the formation of an electron-rich transition state.

The $\Delta S^{\ddagger}$ values are all negative as expected for bimolecular reaction. The plot of $\Delta H^{\ddagger}$ against $\Delta S^{\ddagger}$ is linear (r = 0.981). Exner plot of log k_2 at 40°C versus log k_2 at 25°C is also linear (r = 0.968). Existence of good correlation in both the plots shows that all the *para*-substituted β-methyl-β-nitrostyrenes follow identical mechanism.

Acknowledgement

One of the authors (T L) thanks the CSIR, New Delhi for the award of a fellowship.

References

1 Guthrie J P & Dawson B A, *Can J Chem*, 61 (1983) 171.
2 Guthrie J P, *Can J Chem*, 59 (1981) 45.
3 Guthrie J P, *Can J Chem*, 52 (1974) 2037.
4 Guthrie J P, Cossar J, Cullimore P A, Kamkar N M & Tayler K F, *Can J Chem*, 61 (1983) 261.
5 Newman H & Angier R B, *Tetrahedran*, 26 (1970) 825.
6 Bunnett J F, Miles J H & Nahabedian K V, *J Am chem Soc*, 83 (1961) 2512.
7 Bernasconi C F & Leonarduzzi G D, *J Am chem Soc*, 102 (1980) 1361.
8 Bernasconi C F & Leonarduzzi G D, *J Am chem Soc*, 104 (1982) 5143.

Indian Journal of Chemistry
Vol. 30A, March 1991, pp. 275-277

Oxidation of methionine by N-chloroacetamide—Catalytic effect of formaldehyde

M S Ramachandran*, D Easwaramoorthy & T S Vivekanandam
School of Chemistry, Madurai Kamaraj University, Madurai 625 021

Received 7 June 1990; revised 27 August 1990; accepted 31 October 1990

Oxidation of DL-methionine (Met) by N-chloroacetamide (NCA) in buffered medium (*p*H ~ 7) in the presence and absence of formaldehyde is first order each in [NCA] and [Met] and first order in [HCHO] when present. The observed rate constant shows a complex dependence on [H^+]. The catalytic behaviour of HCHO could be explained by the fact that the rehybridization of sulphur atom from tetrahedral to trigonal bipyramidal structure is influenced by HCHO. The derived rate laws are consistent with the observed kinetics.

We present in this note the results of the title reaction which does not seem to have been studied earlier. In preliminary experiments we observed that NCA reacts rapidly with methionine at [H^+] $\gg$ 0.05 mol dm^{-3} and does not react at all in 0.1 mol dm^{-3} NaOH. Hence the reactions were studied in buffered medium at *p*H 6-7.

Experimental

L-Methionine (Astra-IDL) was used as supplied. N-Chloroacetamide (NCA) was prepared and purified before use. The reaction was studied under pseudo-first order conditions ([methionine] $\gg$ [NCA]) in a buffered medium (*p*H = 7) (phosphate buffer). The rates of the reactions were followed by monitoring unreacted [NCA] iodometrically at regular time intervals.

Oxidation of methionine by NCA at *p*H 7.0 led to the formation of methionine sulfoxide[1] in 80% yield. The overall stoichiometry corresponds to Eq. (1)

$$\text{Methionine} + \text{NCA} \rightarrow \text{Methionine sulfoxide} + \text{Acetamide} + \text{Cl} \quad \ldots (1)$$

Results and discussion

Under pseudo-first order conditions i.e. [Met] $\gg$ [NCA], plots of log V_t (V_t-volume of thiosulphate consumed) versus time are linear upto 40% conversion of [oxidant] and then the plot shows a positive curvature. Therefore for the calculation of the pseudo-first order rate constants, k_{obs}, only the initial slope of the plot is considered. The values of k_{obs} thus calculated in the presence and absence of HCHO are independent of $[NCA]_0$ showing that the rate of oxidation is first order in [NCA]. Addition of the reaction product, acetamide has no effect on the rate. Therefore the retarding effect in the latter part of the reaction may come from the other reaction product namely the sulfoxide.

Values of k_{obs} increase with increase in [Met]. Plot of k_{obs} versus [Met], is linear passing through the origin, both in the presence and absence of HCHO, indicating a first order dependence in [Met] (Fig. 1).

The rate increases by the addition of HCHO and a plot of k_{obs} versus [HCHO] is linear with a positive intercept (Fig. 1). The effect of *p*H on k_{obs} is a complex one and the plot of k_{obs} versus *p*H is a sigmoidal curve (Fig. 2). Variation of [phosphate] at constant *p*H, ionic strength or [chloride ion] has no effect on the rate.

The reactions were studied at three different temperates (30-45°C) and the activation parameters

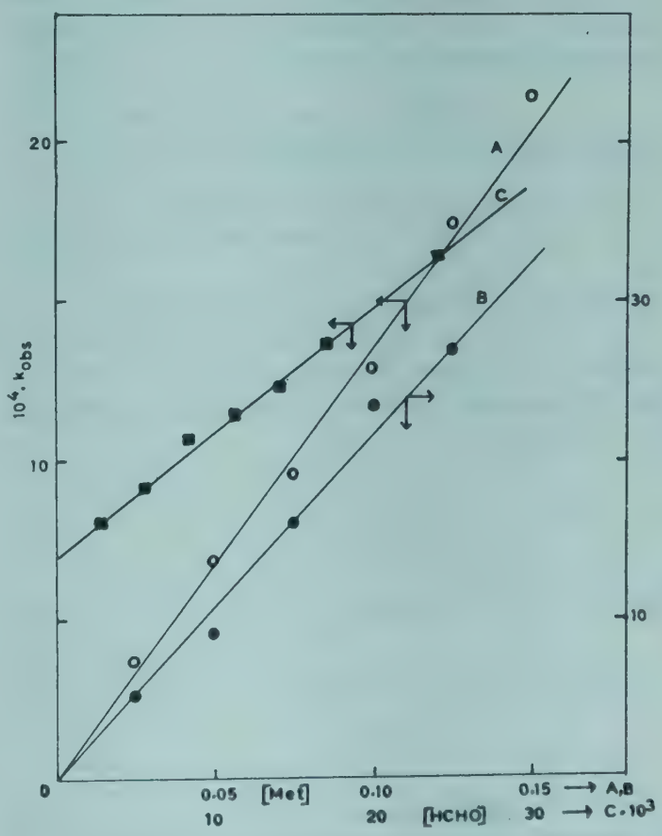

Fig. 1 – Plot of k_{obs} versus [Met] at 32°C. (A) – [HCHO] = 0.0 mol dm^{-3}; (B) – [HCHO] = 5.66×10^{-3} mol dm^{-3}; [NCA] = 3.36×10^{-3} mol dm^{-3}, *p*H = 7.0 and (C) – plot of k_{obs} versus [HCHO] at 32°C, [Met] = 0.05 mol dm^{-3}, [NCA] = 3.26×10^{-3} mol dm^{-3}, *p*H = 7.0

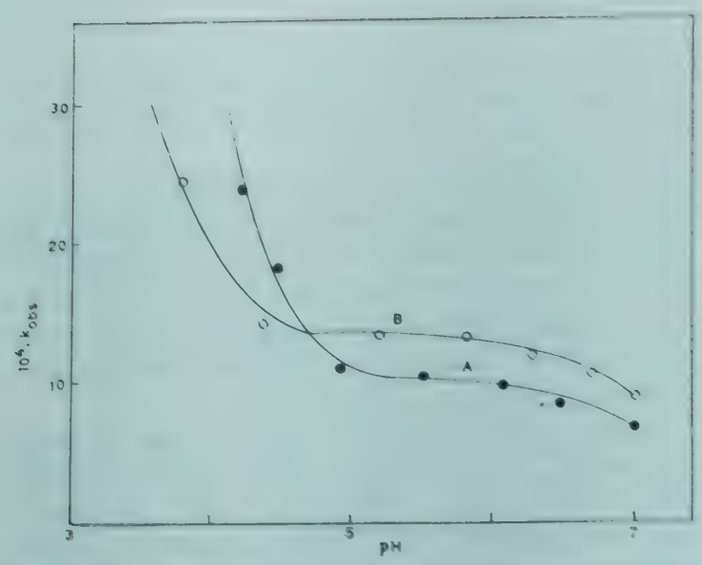

Fig. 2 – Plot of k_{obs} versus *p*H at 32°C (A) – [HCHO] = 0.0 mol dm^{-3}; (B) – [HCHO] = 5.66×10^{-3} mol dm^{-3}; [Met] = 0.05 mol dm^{-3}; [NCA] = 3.24×10^{-3} mol dm^{-3}

were calculated both in the presence of HCHO ($\Delta H^{\ddagger}$ 39.4 kJ/mol) and in its absence ($\Delta H^{\ddagger}$ 49.8 kJ mol).

The reaction may involve either NCA as such or other products derived from it, such as hypochlorite, N,N-dichloroacetamide, as the active oxidising species. The first order dependence of rate on [NCA] and the non-participation of acetamide in the rate shows that the equilibria (2) and (3) are insignificant in the oxidation process.

$$2\,CH_3CONHCl \overset{K_d}{\rightleftharpoons} CH_3CON\begin{matrix}Cl\\Cl\end{matrix} + CH_3CONH_2 \quad \ldots(2)$$

$$CH_3CONHCl \overset{K_h}{\rightleftharpoons} CH_3CONH_2 + HOCl \quad \ldots(3)$$

Based on the experimental observation we propose the mechanism shown in Scheme 1 for the oxidation process.

$$NCA + Met \overset{k_1}{\rightarrow} product \quad \ldots(4)$$

$$Met + HCHO \overset{K_1}{\rightleftharpoons} complex \quad \ldots(5)$$

$$Complex + NCA \overset{k_2}{\rightarrow} product \quad \ldots(6)$$

Scheme 1

Under the experimental conditions (*p*H 6.5-7.0) methionine will be in the form of zwitterion[2] since the pK_s are 2.28 and 9.24. The catalytic effect of formaldehyde clearly shows that some reactive intermediate is formed between methionine and HCHO since HCHO does not react with NCA under the present conditions. α-Amino acids react with formaldehyde in a complex manner[3]. The products have the composition of N-methylene compounds. The complex proposed in Eq. (5) is the schiff's base formed between methionine and HCHO.

The rate law derived from Scheme 1 can be expressed by Eq. (7).

$$-\frac{d[NCA]}{dt} = k_1[Met][NCA] + K_1k_2[Met][HCHO][NCA] \quad \ldots(7)$$

Therefore,

$$k_{obs} = k_1[Met] + K_1k_2[Met][HCHO] \quad \ldots(8)$$

Equation (8) should explain all the experimental observations. According to Eq. (8) the plot of k_{obs} versus [Met] in the absence of HCHO should be linear passing through the origin with k_1 as slope (Fig. 1). The value of k_1 thus obtained is 135×10^{-4} mol^{-1} dm^3 s^{-1}. Plot of k_{obs} versus [HCHO] should give k_1 [Met] as intercept from which k_1 is calculated as 140×10^{-4} mol^{-1} dm^3 s^{-1}. This supports the mechanism given in Scheme 1.

The plot of k_{obs} versus [HCHO] gives K_1k_2 as 80×10^{-2} mol^{-2} dm^6 s^{-1}. Similarly the value of K_1k_2 calculated from the plot of k_{obs} versus [Met] in the presence of formaldehyde is 135×10^{-2} mol^{-2} dm^6 s^{-1}. There is a close agreement between k_1 values calculated from different plots but only the order of magnitude agrees for K_1k_2 probably due to some experimental error.

The study of the Mann-Pope reaction by Ruff and Kucsman[4,5] showed the formation of halogenosulphonium sulphonamide type ion pair intermediate. The detailed mechanism of the oxidation of methionine by N-halogeno oxidants[6] show an initial formation of halogeno sulphonium ion in the rate-determining step which is attacked rapidly by the nucleophillic solvent. However in our work non-participation of acetamide in rate equation (8) clearly shows the formation of methionine-N-chloroacetamide complex as the intermediate which is then hydrolysed in the rate-determining step (Scheme 2) to give the products. This is also supported by the large negative entropy of activation ($\Delta S^{\ddagger} = -136.8$ J K^{-1} mol^{-1}).

The development of a positive charge on sulphur would be expected to be unfavourable for oxidation as this involves the removal of an electron pair from sulphur. Protonation, however, enhances the reactivity of sulphur towards nucleophiles e.g. H_2O. Evi-

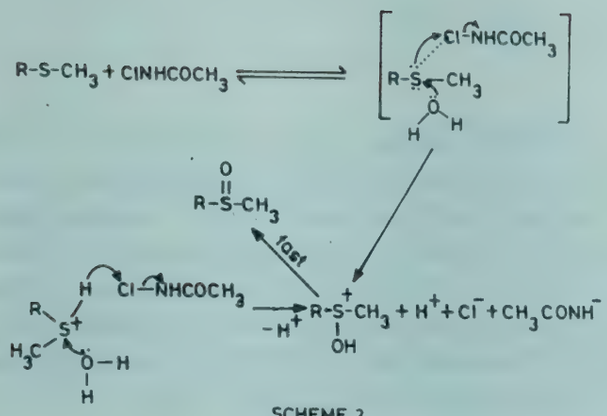

SCHEME 2

dences[7] show that nucleophilic attack on sulphur proceeds through a trigonal bipyramidal transition state as in the hydrolysis of sulphide-halogen adducts to produce sulfoxides. The bonding at sulphur in sulphides and protonated sulphides is qualitatively similar and NMR measurements indicate a tetrahedral structure[8,9]. The mechanistic sequence for the acid catalysis in the reaction of organic sulphides with iodosylbenzene diacetate[10], involves a rehybridization to a trigonal bipyramidal substrate followed by simultaneous nucleophilic attack by water and oxidant. This accounts for the zero-order kinetics in oxidant in the reaction of organic sulphides with iodosylbenzenediacetate. However in the present work the reaction is first order with respect to the oxidant and consequently a trigonal bipyramidal transition state seems more likely than the formation of a trigonal bipyramidal sulphur species.

A comparison of the kinetic parameters in the presence and absence of formaldehyde shows that formaldehyde catalyses the reaction. This suggests that the formation of $-\overset{+}{N}H=CH_2$ group favours the trigonal bipyramidal activated state rather than the $-NH_3^+$ group. Dunn and coworkers[11,12] have shown that the acidity of the amino group of α-amino acids increases considerably in the presence of aqueous formaldehyde. Therefore some type of intramolecular H-bonding of $-\overset{+}{N}H=CH_2$ group with the sulphur atom may be facile than with $-NH_3^+$ and this may be the reason for the observed *p*H effect on the rate constant. In the presence of formaldehyde the protonation of sulphur atom may be difficult as there is already an intramolecular H-bonding between the $-\overset{+}{N}H=CH_2$ with the sulphur. Because of this the observed rate at lower *p*H is slower than that in the absence of HCHO.

Acknowledgement

D.E. acknowledges the UGC, New Delhi for the financial assistance.

References

1 Mitchell J, *Organic analysis*, Vol. 1 (Interscience, New York) 1953, pp. 375.
2 Lange's, *Hand book of chemistry*, edited by J A Dean, (McGraw-Hill, New York) pp. 973.
3 French D & Edsau J T, *Advances in protein chemistry*, 2 (1945) 278.
4 Ruff F & Kucsmann A, *J chem Soc, Perkin Trans*, (1975) 509.
5 Ruff F & Kucsmann A, *J chem Soc, Perkin Trans*, (1982) 1075.
6 Mittal S, Sharma V & Banerji K K, *J chem Research (s)*, (1986) 264.
7 Oae S, *Quart Rep Sulfur chem*, 5 (1970) 33.
8 Olah G A, Brien D H O & Pittman C V, *J Am chem Soc*, 89 (1967) 2996.
9 Coyle T D & Stone F G A, *J Am chem Soc*, 83 (1961) 4138.
10 Humffray A A & Imberger H E, *J chem Soc, Perkin Trans*, (1981) 382.
11 Dunn M S & Loshakoff A, *J Biol Chem*, 113 (1936) 691.
12 Dunn M S & Weiner J G, *J Biol chem*, 117 (1937) 381.

Indian Journal of Chemistry
Vol. 30A, March 1991, pp. 278-280

Synthesis and characterization of ruthenium (II) complexes with monotertiary phosphines and arsines

M M Taqui Khan
Central Salt & Marine Chemicals Research Institute, Bhavnagar 364 002
and
M Satyanarayan Reddy*
Department of Chemistry, Osmania University, Hyderabad 500 007

Received 14 May 1990; revised and accepted 10 September 1990

The reaction of ruthenium (III) perchlorate with some monotertiary phosphines and arsines has been investigated. Ionic complexes of the type $[RuL_5(ClO_4)](ClO_4)$ where L = PPh_3, $AsPh_3$, PMe_2Ph, $AsMe_2Ph$ or $AsEt_2Ph$ have been isolated. Some of these complexes react with nitric oxide to give complexes of the type $[RuL_5(NO)](ClO_4)_2$ where L = PPh_3 or $AsPh_3$. The complexes have been characterized on the basis of their elemental analysis, IR, NMR, conductivity and magnetic moment data.

A number of stable ionic ruthenium complexes containing a wide variety of phosphorus[1,2] or arsine[2] ligands have been reported during the past few years. These compounds are of interest in view of their catalytic role in a variety of homogeneous reactions[3-6].

In the present note preparation of ionic complexes of ruthenium (II) by the interaction of ruthenium (III) perchlorate with some unidentate phosphine and arsine ligands is reported.

Experimental

Ruthenium trichloride was a Johnson Matthey product while silver perchlorate was a BDH reagent. The ligand PPh_3 was obtained from the Ventron Corporation, U.S.A. $AsPh_3$ and PMe_2Ph were obtained from the Maybridge Chem. Co., U.K. $AsMe_2Ph$ and $AsEt_2Ph$ were prepared by reacting $AsMe_2I$ and $AsEt_2I$ respectively with PhMgBr in dry ether. $AsMe_2I$ and $AsEt_2I$ were prepared by standard methods[7].

Nitric oxide was prepared by the reaction of nitric acid with copper turnings and was purified according to the literature method[8].

Microanalyses for carbon, hydrogen and chlorine were carried out by the Australian Mineral Development Laboratories (amdel), Australia (Table 1). The magnetic susceptibilities of the solid samples were measured at room temperature (302K) on a Faraday balance using $Hg[Co(SCN)_4]$ as the external calibrant. ^1H NMR spectra were recorded on a FX 100 MHz spectrometer in $CDCl_3$. Melting points were determined on a Toshniwal hot stage melting point apparatus. Conductivity measurements were done on a Digisun direct reading conductivity bridge (DL-90) using a cell which had been calibrated previously. Infrared spectra were recorded on a Beckman IR-12 spectrophotometer in KBr phase.

Ruthenium (III) perchlorate[2]

Ruthenium trichloride (0.261g, 1 mmol) was stirred with a stoichiometric amount of silver perchlorate (0.622g, 3 mmol) in absolute ethanol for 2-3 h and the precipitated silver chloride removed by centrifugation. The remaining light red-brown ruthenium (III) perchlorate solution was immediately utilised for subsequent preparations.

Preparation of ruthenium (II) complexes

Complexes of the type $[RuL_5(ClO_4)](ClO_4)$; [L = PPh_3 (**1**), $AsPh_3$ (**2**), PMe_2Ph (**3**), $AsMe_2Ph$ (**4**), $AsEt_2Ph$ (**5**)]

An ethanolic solution of ruthenium (III) perchlorate (0.40g, 1.0 mmol) was added to a refluxing ethanolic solution of the ligand (6 mmol) (L = PPh_3, $AsPh_3$, PMe_2Ph, $AsMe_2Ph$ and $AsEt_2Ph$) under nitrogen atmosphere and the contents were refluxed for 6 h. The colour of the solution remained brown in the case of L = PPh_3 and $AsPh_3$. In the case of L = PMe_2Ph, $AsMe_2Ph$ and $AsEt_2Ph$, the initial red-brown colour changed to yellow. The solutions were evaporated to a small volume *in vacuo* and the products precipitated by the addition of dry ether. The products were filtered, washed with ether and dried *in vacuo*. The complexes were recrystallized from dichloromethane and *n*-hexane.

(ii) Complexes of the type $[RuL_5(NO)](ClO_4)_2$; [$L = PPh_3$ (**6**), $AsPh_3$ (**7**)]

Complexes **6** and **7** were obtained by bubbling nitric oxide through dichloromethane solutions of the parent ionic complexes **1** and **2** (0.1 mmol) for 4-5 h. The solutions were evaporated *in vacuo* at room temperature and the compounds precipitated by the addition of petroleum ether (40-60°) and dried *in vacuo*.

Results and discussion

Complexes **1-5** (Table 1) contain one perchlorate group and five phosphine or arsine ligands in the coordination sphere of the metal ion. The metal ion was

Table 1—Physicochemical data for ruthenium (II) complexes

Sl. No.	Complex	Colour (%, yield)	Melting/Dec. point	Found (Calc.), %		
				C	H	Cl
1	$[Ru(PPh_3)_5(ClO_4)](ClO_4)$	Dark brown (80)	182	65.73 (67.08)	4.56 (4.65)	4.81 (4.40)
2	$[Ru(AsPh_3)_5(ClO_4)](ClO_4)$	Grey (65)	154	57.87 (59.00)	4.15 (4.09)	4.23 (3.88)
3	$[Ru(PMe_2Ph)_5(ClO_4)](ClO_4)$	Greenish Yellow (61)	175	46.90 (48.50)	5.37 (5.55)	8.04 (7.17)
4	$[Ru(AsMe_2Ph)_5(ClO_4)](ClO_4)$	Orange (83)	158	38.64 (39.66)	4.50 (4.54)	6.12 (5.87)
5	$[Ru(AsEt_2Ph)_5(ClO_4)](ClO_4)$	Yellow (59)	143	43.11 (44.44)	5.63 (5.55)	5.18 (5.25)
6	$[Ru(PPh_3)_5(NO)](ClO_4)_2$	Brown (50)	210	65.21 (65.77)	4.49 (4.57)	—
7	$[Ru(AsPh_3)_5(NO)](ClO_4)_2$	Grey (50)	182	57.22 (58.06)	4.07 (4.03)	

also reduced to the divalent state during the reaction with the use of one equivlent excess of phosphine or arsine. Such simple ionic complexes are not known in the literature and they present the first examples with a C_4 symmetry. Magnetic susceptibility measurements showed that the complexes were diamagnetic and possessed spin paired $(t_{2g})^6$ configuration. The molar conductivity values of all the complexes in dimethylacetamide corresponded to 1:1 electrolytic behaviour (64-185 $ohm^{-1}cm^2mol^{-1}$).

The infrared spectra of the complexes suggest the presence of a monodentate coordinated perchlorate. Very strong bands observed at 1070 and 1165 cm^{-1} in complex **1**, at 1080 and 1140 cm^{-1} in complex **2**, at 1080 and 1150 cm^{-1} in complex **3**, at 1070 and 1150 cm^{-1} in complex **4** and at 1040 and 1100 cm^{-1} in complex **5** due to the split peaks of ν_3 mode[9] confirm this assignment.

The presence of coordinated phosphine or arsine was indicated[10,11] by a strong band at 520 or 475 cm^{-1}. In the far infrared spectra of all the complexes, the region 250-350 cm^{-1} was devoid of bands that could be assigned to the Ru-Cl stretching mode[12].

The NMR spectra of complexes **1-5** supported the assigned configuration. The phenyl protons were observed at δ 7.47 ppm and δ 7.55 ppm in the case of phosphine and arsine complexes respectively.

The NMR spectrum of complex **4** was very well resolved and supported the suggested configuration. The methyl protons of dimethylphenylarsine ligand were observed as two singlets of 4:1 intensity at δ 1.50 ppm and δ 1.20 ppm respectively. The phenyl protons for all the ligands merged to give a broad multiplet centered at δ 7.25 ppm.

The NMR spectrum of complex **5** showed a triplet centered at δ 1.00 ppm corresponding to methyl protons (CH_3) and a quartet centered at δ 2.00 ppm corresponding to methylene (CH_2) protons of diethylphenylarsine ligand. The phenyl protons were observed as a large multiplet centered at δ 7.37 ppm. The integration values of phenyl protons, methyl protons and methylene protons were in the ratio of 5:6:4.

The nitric oxide derivatives (**6** and **7**) were obtained by passing nitric oxide through the dichloromethane solutions of complexes **1** and **2**. The substitution of perchlorate by NO suggest the lability of the weakly coordinated perchlorate groups. The resulting products were tentatively characterised on the basis of elemental analysis, conductivity and infrared data. The conductivity measurements showed that they were 1:2 electrolytes with the coordinated perchlorate displaced by nitric oxide. These complexes showed a strong band 1890 cm^{-1} due to coordinated NO[13]. A broad and intense absorption band was also observed around 1850 cm^{-1} due to ionic perchlorate. The far infrared spectra of the complexes showed bands at 520 and 460 cm^{-1} that could be assigned to Ru-P and Ru-As stretching modes.

Acknowledgement

One of the authors (MSNR) is thankful to the CSIR, New Delhi for financial assistance.

References

1 Chatt J & Hayter R G, *J chem Soc*, (1961) 896.

2 Taqui Khan M M, Bajaj H C, Siddiqui R H, Khan B T, Satyanarayan Reddy M & Veera Reddy K, *J chem Soc Dalton Trans*, (1985) 2603.

3 Bancroft G M, Mays M J, Prater B F & Stefanini F F, *J chem Soc A*, (1970) 2146.

4 Sandars J R, *J chem Soc Dalton Trans*, (1973) 743.

5 Taqui Khan M M & Martel A E, *Homogeneous catalysis by metal complexes*, Vol 1 (Academic Press, New York) 1974, 11.

6 Cavit B E, Grandy K R & Roper W, *J chem Soc Chem Commun*, (1972) 60.

7 Burrows G J & Turner E E, *J chem Soc*, (1921) 426.

8 (a) James B R, Ochiai E & Rampel G L, *Inorg nucl chem Lett*, 7 (1971) 781.
(b) Evans I P, Spencers A & Wilkinson G, *J chem Soc Dalton Trans*, (1973) 204.

9 Hathaway B J & Underhill A E, *J chem Soc*, (1961) 3091.

10 Shobatako K, Postmus C, Ferraro J R & Nakamoto R, *Appl Spectrosc*, 23 (1969) 12.

11 Dwing J R, McAllister W A & Mercen E E, *J inorg nucl Chem*, 29 (1967) 1441.

12 Deacon G B & Green J H, *Chem Commun*, (1963) 629.

13 Robinson S D & Uttley M F, *J chem Soc Dalton Trans*, (1972) 1.

Indian Journal of Chemistry
Vol. 30A, March 1991, pp. 281-282

Synthesis and vibrational studies of molybdenum dinitrosyl complexes with hydroxamic acids as ligands

T K Banerjee, S K Brahma & S P Bag*
Department of Chemistry, Jadavpur University, Calcutta 700 032

Received 2 May 1990; revised and accepted 24 July 1990

Complexes of the type $Mo(NO)_2(HA)_2$, where H_2A represents benzohydroxamic acid or salicylhydroxamic acid, have been isolated by a single step process for the first time. The complexes have been prepared by reductive nitrosylation of ammonium heptamolybdate by hydroxylamine hydrochloride in presence of H_2A in aqueous aerobic conditions. When the stoichiometric ratio of molybdate: hydroxylamine is 1:4 in slightly basic (DMF) media, the formation of $Mo(NO)_2(HA)_2$, is achieved. The complexes have been characterised on the basis of various physicochemical data of the complexes.

Molybdenum-nitrosyl complexes have been used as homogeneous olefin disproportionation catalyst precursors[1,2]. In acidic, neutral or alkaline medium, molybdate reacts with hydroxylamine to yield an yellow complex ion of the type of $Mo(NO)^{4+}$. However, the formation of dinitrosyl species $Mo(NO)_2^{2+}$ is achieved by heating oxomolybdenum salt and hydroxylamine in the stoichiometric ratio of 1:4 in slightly basic media[3-5]. Some hydroxamic acid derivatives of molybdenum dinitrosyl species have been isolated by a single step process for the first time. The complexes have been prepared by reductive nitrosylation of molybdate (VI) by hydroxylamine in aqueous-aerobic conditions.

Experimental

Ammonium heptamolybdate (AR grade) and hydroxylamine hydrochloride (AR grade) were used as such. Benzohydroxamic acid, $C_6H_5CONHOH$ (BH_2A), and salicylhydroxamic acid, $HOC_6H_4CONHOH$ (SH_2A), were prepared by standard methods[6,7]. The purities of the ligands were checked by their melting points and IR spectra. DMF, used as the solvent, was purified by conventional methods. Molybdenum was estimated gravimetrically by the usual method[8]. Nitrogen and carbon were estimated by micro-analytical methods using a Perking Elmer 240 C Elemental Analyser. The results of the elemental analysis are listed in Table 1.

Preparation of complexes

$Mo(NO)_2(BHA)_2$: Ammonium heptamolybdate (1.0 g) and hydroxylamine hydrochloride (1.7 g) were heated in 10 ml of DMF at 90°C for an hour to get a green solution. It was cooled and a solution of sodium salt of benzohydroxamic acid (150 ml, 0.1 *M*) in water was added with stirring at room temperature. A golden yellow product thus formed was allowed to settle for an hour, filtered off, washed with water and diethyl ether and finally dried over calcium chloride.

$Mo(NO)_2(SHA)_2$: It was prepared similarly as described above using salicylhydroxamic acid (SH_2A) instead of benzohydroxamic acid (BH_2A).

$MoO_2(BHA)_2$ and $MoO_2(SHA)_2$: An aqueous solution of ammonium heptamolybdate (20 ml, 0.1 *M*) was treated with hydroxamic acid (20 ml, 0.2 *M*) in water at room temperature. The *p*H of the mixture was adjusted to 3-4 by adding a few drops of dilute HCl when an orange coloured product was obtained. The product was filtered off, washed with water and ethyl alcohol and finally dried *in vacuo* over calcium chloride.

The conductances of all the complexes were measured in DMF solvent using an Elico conductivity bridge (type C M82 T). The IR spectra of the ligands and their complexes were recorded in KBr on a Perkin Elmer 1800 FTIR spectrophotometer in the region 4000-400 cm^{-1}. Raman spectra of the powder sample were recorded on a SPEX Ramalog spectrometer using 514.5 nm radiation from a Spectra-Physics argon ion laser.

Results and discussion

Analytical data of the complexes (Table 1) show that the stoichiometric ratio of $Mo(NO)_2^{2+}$: hydroxamic acid is 1:2. All the complexes are thermally stable and are diamagnetic. They are sparingly soluble in water and chloroform but are soluble in ethanol and acetone. The conductivities of these molybdenum complexes were measured in DMF. The molar conductance values for the complexes (17-23 $ohm^{-1}cm^2mol^{-1}$) indicate that the complexes are nonelectrolytes.

For BH_2A ligand the most characteristic bands in the IR (Raman) spectra are: 1602 (1601) [$\nu_{C=O}$]; 1575 (1580) [$\nu_{C=C}$]; 905 (900) [ν_{NO}]. For SH_2A the corresponding bands are 1618 (1608), 1576 (1577) and 906 (900) cm^{-1} respectively. The very strong absorption peaks at 945 cm^{-1} for $MoO_2(BHA)_2$

Table 1—Analytical and physical data of complexes

Complex (colour)	Found (Calc.), %			
	C	N	H	Mo
$MoO_2(BHA)_2$	42.55	6.35	3.02	25.21
(Orange)	(42.00)	(7.00)	(3.00)	(24.00)
$MoO_2(SHA)_2$	39.45	5.85	3.25	23.15
(Light green)	(38.88)	(6.48)	(3.70)	(22.22)
$Mo(NO)_2(BHA)_2$	41.17	12.71	3.12	21.18
(Golden yellow)	(39.25)	(13.08)	(2.80)	(22.42)
$Mo(NO)_2(SHA)_2$	36.98	10.89	2.998	20.15
(Light brown)	(36.52)	(12.17)	(2.60)	(20.86)

and 930 cm^{-1} for $MoO_2(SHA)_2$ are assigned to the symmetric stretching mode of the terminal Mo=O bond[9]. However, the corresponding Raman band is observed as a weak absorption at 930 cm^{-1}. It has also been observed that in the IR spectra of $MoO_2(BHA)_2$ and $MoO_2(SHA)_2$, the sharp NO (hydroxamic acid) band which appears in the simple hydroxamic acids is split up due to the appearance of $\nu_{Mo=O}$ and ν_{NO} mode of vibrations in the same region. For the nitrosyl complexes $Mo(NO)_2(BHA)_2$ and $Mo(NO)_2(SHA)_2$, the ν_{N-O} bands appear at 1675 and 1780 cm^{-1}; and 1670 and 1780 cm^{-1} respectively. Though the Raman spectra of the nitrosyl complexes were not very good due to the strong absorption of the complexes by laser (because of their dark colour), the characteristic peak

positions could be clearly identified. The frequencies of the bands (1600-1800 cm^{-1}) in the nitrosyl complexes suggest that the NO^+ formalism is appropriate here[10]. If valence shell electron population of 18 is to be achieved, these compound might occur in either *cis* or *trans* form (Ia, Ib). Since the vibrational spectra of these complexes contain two strong well separated bands near 1700 cm^{-1} in addition to the characteristic bands of other ligands, the two nitrosyl groups are *cis* to one another.

References

1 *Zuech E A, Hughes W B, Kubiceck D M & Kittleman, J Am chem Soc*, 92 (1970) 528.
2 Hughes W B, *Inorg Chem*, 13 (1974) 1531.
3 Cotton F A & Johnson B F G, *Inorg Chem*, 3 (1964) 1609.
4 Enemark J H & Feltham R D, *Coord Chem Rev*, 13 (1974) 339.
5 Connelly N G, *Inorg chim Acta Rev*, 6 (1972) 48.
6 Werner A, *Ber*, 41 (1908) 1062.
7 Mussante C, *Gazz chim ital*, 78 (1948) 536.
8 Vogel A I, *Vogel's text book of quantitative inorganic analysis* (Longmans, London), 1978, 472.
9 Mitchell P C, *J inorg nucl Chem*, 23 (1963) 963.
10 Lewis J, Irving R J & Wilkinsons, *J inorg nucl Chem*, 7 (1958) 32.

Indian Journal of Chemistry
Vol. 30A, March 1991, pp. 283-285

Synthesis and spectral studies of methylsilicon(IV) chloride complexes with biologically active heterocyclic benzothiazolines

(Mrs) Kiran Singh*

Department of Chemistry, Kurukshetra University, Kurukshetra 132 119

and

J P Tandon

Department of Chemistry, University of Rajasthan, Jaipur 302 004

Received 8 March 1990; revised 10 September 1990; accepted 6 November 1990

Some neutral adducts of methylsilicon(IV) chlorides with nitrogen donor ligands, Me_2SiCl_2(HBZt) and Me_3SiCl(HBZt)(HBZt = benzothiazolines), have been synthesised and characterised on the basis of elemental analysis, molecular weight, IR and NMR (^1H and ^{13}C) spectral data. These data suggest that the N-donors function as bidentate ligands.

Organosilicon compounds of sulphur-containing ligands have attracted much attention recently[1,2] due to their biological importance. The sulphur-containing ligands are well known for their anticarcinogenic[3], antibacterial, turberculostatic[4] and antifungal activities. It has been reported that the activity of sulphur-containing ligand increases on complexation[5,6]. In continuation of our earlier work[7,8] on biologically active complexes, we report here some schiff base complexes of organosilicon(IV) chlorides.

The condensation of 2-mercaptoaniline with an aldehyde or ketone does not normally lead to the isolation of the corresponding schiff base, but rather to a thiazoline[9-11] moiety. It has, however, been observed[12] that alcoholic solution of various β-diketones react with β-mercaptoethylamine in the presence of nickel ions to give nickel complexes of the corresponding schiff bases in good yield.

Experimental

Preparations of benzothiazolines

Benzothiazolines of pyridine-2-aldehyde, furfuraldehyde, thiophene-2-aldehyde and indol-3-carbaldehyde were prepared by the condensation of the appropriate aldeyde with 2-mercaptoaniline in a 1:1 molar ratio in benzene. The solution was heated under reflux for 2-3 h after which the solvent was removed *in vacuo*. The crude solid so obtained was recrystallized from benzene[7]. The following compounds were prepared: (i) pyridine-2-aldehyde benzothiazoline (H.Py.BZt) ($C_{12}H_{10}N_2S$), yellow solid, m.p., 81°C; (ii) furfuraldeyde benzothiazoline (H. Furf. BZt) ($C_{11}H_9NSO$), yellow solid, m.p., 72°C; (iii) thiophene-2-aldehyde benzothiazoline (H.Thio. BZt) ($C_{11}H_9NS_2$), yellow solid, m.p., 91°C; and (iv) indol-3-carbaldehyde benzothiazoline (H.Indol. BZt) ($C_{15}H_{12}N_2S$), yellow solid, m.p., 154°C.

Synthesis of methylsilicon(IV) complexes

To a weighed amount of trimethylsilicon chloride or dimethylsilicon dichloride in dry benzene was added to the calculated amount of the ligand (1:1 molar ratio). The product separated immediately as a coloured solid but the reaction mixture was stirred for 1-2 h to complete the reaction. The solvent was removed and the product dried *in vacuo*. It was repeatedly washed with dry cyclohexane and again dried under reduced pressure for 3-4 h (yield 81-87%).

Silicon was estimated gravimetrically as silicon dioxide. Other methods of analysis and physical measurements were the same as reported earlier[13]. The antifungal activities of the ligands and the complexes with organosilicon(IV) were evaluated against the fungi by the agar plate technique[14] at different concentrations.

Results and discussion

The proposed stoichiometry of the complexes was confirmed by the analytical data (Table 1). The complexes were soluble in DMSO, DMF and methanol. The molar conductance values of 10^{-3} *M* solutions of the complexes (10-15 $ohm^{-1}cm^2mol^{-1}$) in DMF showed them to be non-electrolytes. The monomeric nature of these complexes was confirmed by their molecular weight measurements.

In the IR spectra of the ligands, NH stretching and deformation modes were observed at ~3370-3200 and 1670-1705 cm^{-1}, respectively. The absence of ν(SH) (2500-2600 cm^{-1}) and ν(C=N) (1600-1650 cm^{-1}) modes is indicative of benzothiazoline rather than schiff base structure[15]. In the spectra of the complexes, bands due to NH vibrations disappear, indicating the chelation of nitrogen with the silicon atom. Two new bands appearing at ~1600 and ~2500 cm^{-1} are assigned to the ν(C=N) and ν(SH) respectively. These bands suggest that the complexes contain the ligands in the form of schiff base moieties, the benzothiazoline ring rearranging

Table 1—Characterisation of silicon(IV) complexes

Compound	Colour (m.pt.; °C), Yield (%)	Found (Calc.) C %	H %	N %	S %	Cl %	Si %	Mol. wt.
$Me_3SiCl(C_{11}H_9NSO)$	Brown (88),86	53.89 (54.09)	5.29 (5.79)	4.03 (4.52)	10.75 (10.32)	11.20 (11.43)	8.30 (8.71)	291 (310)
$Me_3SiCl(C_{11}H_9NS_2)$	Yellow (135),87	51.12 (51.44)	5.12 (5.51)	4.31 (4.29)	19.22 (19.63)	10.45 (10.87)	8.11 (8.29)	308 (326)
$Me_3SiCl(C_{15}H_{12}N_2S)$	Light yellow (d),81	60.00 (60.06)	5.34 (5.84)	7.55 (7.79)	8.50 (8.91)	9.55 (9.87)	7.32 (7.53)	340 (359)
$Me_3SiCl(C_{12}H_{10}N_2S)$	Yellow (180),85	55.55 (55.97)	8.21 (8.71)	8.31 (8.72)	9.55 (9.97)	10.85 (11.04)	8.10 (8.42)	301 (321)
$Me_2SiCl_2(C_{11}H_9NSO)$	Brown (81),82	46.92 (47.12)	4.23 (4.53)	4.00 (4.23)	9.95 (9.67)	21.14 (21.44)	8.00 (8.18)	311 (331)
$Me_2SiCl_2(C_{11}H_9NS_2)$	Yellow (137),87	44.74 (44.95)	4.11 (4.32)	4.35 (4.03)	18.00 (18.44)	20.15 (20.46)	7.30 (7.80)	329 (347)
$Me_2SiCl_2(C_{15}H_{12}N_2S)$	Yellow (d),82	53.35 (53.67)	4.43 (4.74)	7.11 (7.37)	8.12 (8.42)	18.25 (18.68)	7.00 (7.13)	361 (380)
$Me_2SiCl_2(C_{12}H_{10}N_2S)$	Yellow (207),85	49.00 (49.11)	4.35 (4.68)	8.45 (8.19)	9.77 (9.36)	20.26 (20.76)	7.51 (7.92)	323 (342)

to give the schiff base derivative in the presence of silicon atom[16].

New bands oberved in the complexes at ~580, 540 and 510 cm^{-1} are due to the $\nu(Si-N)$[17], $\nu(Si-S)$[18] and $\nu(Si-Cl)$[19] modes respectively. Thus, the IR spectral studies suggest that the azomethine nitrogen and the sulphur of the thiol group participate in the complexation reaction.

The PMR spectra of the benzothiazolines $C_4H_3OCH.NHC_6H_4S$ and $C_4H_3SCH.NHC_6H_4S$ show the N−H proton signals at δ4.20 and 4.36 ppm respectively, which disappear in the spectra of the corresponding complexes. The appearance of new signals at δ5.44, 5.28, 5.58 and 5.47 ppm in the spectra of $Me_3SiCl(C_4H_3OCH{:}NC_6H_4SH)$, $Me_2SiCl_2(C_4H_3OCH{:}NC_6H_4SH)$, $Me_3SiCl(C_4H_3SCH{:}NC_6H_4SH)$ and $Me_2SiCl_2(C_4H_3SCH{:}NC_6H_4SH)$ respectively due to SH proton indicates that the benzothiazoline ring rearranges in the presence of silicon to give the schiff base derivative. The azomethine proton signal shifts downfield in the spectra of the complexes. Methyl protons are also observed in the region δ0.16-0.36 ppm in the spectra of the complexes.

The involvement of thiolic sulphur and azomethine nitrogen in complexation is further confirmed by the ^{13}C NMR spectral data.

The ^{13}C NMR spectral data of two representative complexes $(CH_3)_3SiCl(C_5H_4NCHNC_6H_4SH)$ and $(CH_3)_2SiCl_2(C_5H_4NCHNC_6H_4SH)$ and the ligand $C_5H_4NCHNHC_6H_4S$ have been recorded.

In the spectrum of the ligand, the signals for the azomethine carbon and thiolic carbon appear at δ149.57 and 126.92 respectively, whereas in the corresponding trimethylsilicon and dimethylsilicon complexes the signals appear at δ170.74, 168.00 and 150.09, 153.72 respectively. Such a large shift indicates the involvement of azomethine nitrogen and thiolic sulphur in complexation.

On the basis of the foregoing discussion an octahedral geometry has been proposed for all the complexes.

Evaluation of antifungal activity

Helminthosporium gramineum and *Rhizopus oryzae* were employed to check the antifungal activity of the benzothiazolines and their complexes. The fungitoxicity of the benzothiazolines and their complexes decreases on lowering the concentration. It is clear from the fungicidal screen data that the metal chelates are more fungitoxic than the corresponding ligands.

Acknowledgement

One of us (K.S.) is grateful to the CSIR, New Delhi for financial assistance.

References

1 Biradar N S, Roddobasanagoudor V L & Aminabhavi T M, *Indian J Chem*, 24A (1985) 793.
2 Biradar N S, Aminabhavi T M & Rudzinski W E, *Inorg chim Acta*, 82 (1984) 211.
3 Fudlander B L & Fraust A, *J Am chem Soc*, 81 (1952) 638.
4 Ionvick R, Pansy F, Stryker G & Bornstein J, *J Bact*, 59 (1930) 667.
5 Skade Y, *Jpn Patent* (1970) 7017189; *Chem Abstr*, 73 (1970) 77252Y.

6 Srivastava R S, *J inorg nucl Chem*, 42 (1980) 1526.
7 Singh K, Singh R V & Tandon J P, *Inorg chim Acta*, 151 (1988) 179.
8 Singh K, Dixit P, Singh R V & Tandon J P, *Main Group Met Chem*, 12 (1989) 155.
9 Ratnu S & Clarke H T, *J Am chem Soc*, 59 (1937) 200.
10 Krepia F J, Mafure V, Finn J J, McCloman J G & Hombordo F, *J Am chem Soc*, 73 (1951) 1155.
11 Thompson M C & Busch D M, *J Am chem Soc*, 84 (1962) 1162.
12 Thompson M C & Busch D M, *J Am chem Soc*, 86 (1964) 213.
13 Singh K, Singh R V & Tandon J P, *Bull chem Soc Japan*, 61 (1988) 4494.
14 Horsfall J G, *Bot Rev*, 11 (1945) 357.
15 Pfeiffer P, Offerman W & Werner A, *J prakt Chem*, 313 (1942) 159.
16 Varshney A & Tandon J P, *Polyhedron*, 4 (1982) 1311.
17 Ebsworth E A V & Mays M J, *J chem Soc*, (1964) 3450.
18 Dashora R, Singh R V & Tandon J P, *Synth React inorg met-org Chem*, 13 (1983) 209.
19 Aminabhavi T M, Biradar N S & Patil S B, *Indian J Chem*, 25A (1986) 285.

Indian Journal of Chemistry
Vol. 30A, March 1991, pp. 286-289

Synthesis and characterization of metal complexes with a schiff base formed by condensation of S-benzyl dithiocarbazate with isatin (H_2IBD)

G M Abu El-Reash*, Fim Taha, A M Shallaby & O A El-Gamal

Chemistry Department, Faculty of Science,
Mansoura University, Mansoura, Egypt

Received 12 February 1990; revised and accepted
30 October 1990

Synthesis and characterization of Mn(II), Co(II), Ni(II), Zn(II), Cd(II), Hg(II) and UO_2^{2+} complexes of isatin-hydrazone-S-benzyldithiocarbazate (H_2IBD) are reported. Elemental analysis, molar conductance, magnetic moment and spectral (IR, visible, NMR) data have been used to characterize the complexes. IR spectral data show that the ligand behaves in a bidentate, tridentate or tetradentate manner in different complexes. An octahedral structure is proposed for the Mn(II), Co(II) and Ni(II) complexes while a square-planar structure is proposed for Cu(II) complexes on the basis of magnetic and spectral measurements.

Studies on metal complexes of thio-schiff bases containing S-benzyldithiocarbazate have been reported[1-7]. These ligands as well as their metal complexes are frequently used as anticancer[8], antibacterial[9] and antifungal[10] agents. In continuation of our interest in the ligational behaviour of nitrogen, oxygen and sulphur donor schiff bases, we describe here new metal complexes of isatin hydrazine-S-benzyldithiocarbazate. The existing literature on the coordination chemistry of this ligand is obscure.

All the chemicals used were of AR grade. The hydrazine-S-benzyldithiocarbazate was synthesized according to the general literature method[11]. The schiff base was prepared by heating equimolar amounts of the isatin (14.7 g, 0.1 mol) and the S-benzyldithiocarbazate (20 g, 0.1 mol) in 100 ml ethanol under reflux for 1 hr. The yellow crystals which separated were recrystallized from benzene; m.p. 231°C; yield 28.6 g, 82% [Found; C, 58.5; H, 3.8. Reqd. for H_2IBD: C, 58.7; H, 4.0%].

Preparation of the complexes

The complexes were prepared by refluxing equimolar amounts of H_2IBD (3.27 g, 0.01 mol) in 50 ml absolute ethanol and hydrated metal chloride or uranyl acetate (0.01 mol) in 20 ml absolute ethanol, but the other acetate salts of Cu(II), Zn(II) and Cd(II) (0.01 mol) were dissolved in 30 ml doubly distilled water for 1-2 hr. The product was filtered off, washed with hot ethanol, then with diethyl ether and dried *in vacuo*. The solid complexes were heated in an electric oven for 3 hr at 120°C.

All the measurements were carried out as reported earlier[12].

Results and discussion

The analytical and physical data for the metal complexes are listed in Table 1. The complexes are quite stable in air and insoluble in common organic solvents but soluble in DMF and DMSO. The molar conductivities in DMF solution (6-30 ohm^{-1} cm^2 mol^{-1}) indicate a nonelectrolytic nature for all of the complexes[13].

The IR spectrum of H_2IBD in KBr shows two bands at 1700 and 1580 cm^{-1} which can be assigned to ν(CO) and ν(C=N), respectively. The bands at 1480, 1255, 1020 and 680 cm^{-1} are due to thioamide-I, -II, -III and -IV bands[14], respectively. The bands assigned to thioamide vibrations are not pure and have substantial contributions from ν(C−N), δ(C−H), δ(N−H) and ν(C−S) vibrations[15]. The doublets at 2900 and 2960 cm^{-1} are attributed to the symmetric and asymmetric stretching vibrations of the $-S-CH_2-Ph$ grouping, which are reduced to a weak doublet in the IR spectra of the complexes. In addition, two bands at 3180 and 3140 cm^{-1} are assigned to the ν(NH) of isatin and S-benzyl moiety, respectively. The broad but weak bands in the regions 1960-1900 and 2360-2280 cm^{-1}, mainly due to O···H——N stretching vibrations[16,17], indicate intramolecular hydrogen bonding between oxygen of isatin moiety and the NH group as shown in structure (I). No bands due to SH and OH stretching modes are observed near 2570 and 3400, respectively. The absence of these bands indicates the presence of H_2IBD in the thione and keto form.

The NMR spectrum of H_2IBD in DMSO-d_6 shows four signals at δ = 4.6, 6.9-7.14, 7.3-7.6 and 11.4 ppm relative to TMS which may be assigned to the methylene protons of the S-benzyl moiety

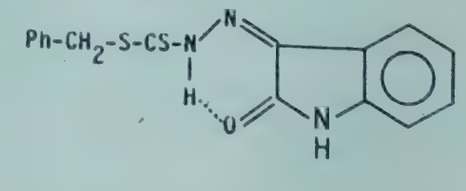

(I)

Table 1—Analytical and physical data of H_2IBD and its metal complexes

Compound (Yield, %)	Colour (mp., °C)	Found (Calc.), %				μ_{eff} (BM)
		C	H	M	Cl	
$[Mn(HIBD)Cl(H_2O)_3]$	Deep violet	41.2	3.34	10.8	7.6	5.76
(56)	(>300)	(40.8)	(3.85)	(11.7)	(7.5)	
$[Co(HIBD)_2]$	Brown	54.2	3.8	8.0	—	4.73
(64)	(200d)	(54.0)	(3.4)	(8.3)		
$[Ni(HIBD)_2]$	Brown	53.7	3.6	8.1	—	3.20
(82)	(198d)	(54.0)	(3.4)	(8.3)		
[Cu(HIBD)Cl]	Brown	44.9	3.1	14.3	8.8	1.85
(78)	(>300)	(45.2)	(2.8)	(14.9)	(8.3)	
[Cu(IBD)]	Brown	50.6	3.1	15.8	—	1.50
(86)	(215d)	(49.4)	(2.9)	(16.3)		
$[Cd(HIBD)_2]$	Orange	50.4	3.6	13.9	—	—
(60)	(>300)	(50.2)	(3.2)	(14.6)		
[Cd(HIBD)Ac]	Orange	43.1	3.6	22.4	—	—
(68)		(43.4)	(3.0)	(21.6)		
$[Zn(HIBD)_2]$	Orange	53.7	2.3	8.8	—	—
(48)	(234)	(53.5)	(1.96)	(9.1)		
[Zn(HIBD)Ac]	Orange	48.2	3.7	14.8	—	—
(66)	(>300)	(48.0)	(3.4)	(14.5)		
$[Hg(HIBD)_2]$	Reddish-orange	—	—	24.3	—	—
(54)	(289)	(45.0)	(2.8)	(23.5)		
$[UO_2(H_2IBD)Ac_2]$	Red	33.9	3.1	36.9		
(73)	(>300)	(33.6)	(2.7)	(37.8)		

(−S−CH_2−Ph), the aromatic protons of both isatin and phenyl rings overlapped with the imino proton (−NH−C−) and the NH proton of isatin residue, respectively.

The IR spectrum of Cu(IBD) complex, which was prepared from the acetate salt, shows that H_2IBD behaves as binegative tetradentate ligand, coordinating through the enolic oxygen and the nitrogen of the NH group from one end, and the thiol sulphur atom and the nitrogen atom of the C=N group on the other, with loss of two protons. Steric factors prevent the coordination of all the donors in a ligand molecule to a single metal ion; therefore, the ligand must act as a bridging unit between two metal centres, giving a polymeric structure as shown in structure (II). This mode of complexation is confirmed by the following evidences: (i) the disappearance of the ν(C=O), the ν(NH) and the clear change in thioamide bands; and (ii) the appearance of new bands at 1625, 1590, 1320 and 655 cm^{-1} due to ν(S−C=N), ν(O−C=N) cyclic, ν(C−O) and ν(C−S) modes.

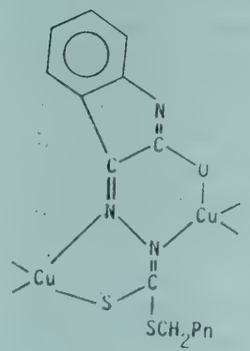

(II)

In the [Cu(HIBD)Cl], $[Ni(HIBD)_2]$ and $Co(HIBD)_2$ complexes, the ligand (H_2IBD) behaves as a mononegative tridentate ligand coordinating via the CO, the C=N and the CS in the thiol form after its deprotonation as shown in structure (III). This mode of complexation is suggested by the shift of both ν(CO) and ν(C=N) to lower wavenumbers (~20 cm^{-1}), the disappearance of ν(CS) and the appearance of new bands at 1620 and 660 cm^{-1} due to ν(S−C=N) and ν(C−S).

In addition, H_2IBD behaves as a mononegative bidentate ligand coordinating via the C=N and the

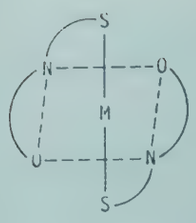

M = Ni(II) and Co(II)

(III)

CS in the thiol form. This behaviour, which is found in the $[Mn(HIBD)Cl.(H_2O)_3]$, $[Zn(HIBD)_2]$, [Zn(HIBD)Ac], $[Cd(HIBD)_2]$ and $[Hg(HIBD)_2]$ complexes, is revealed by (i) the disappearance of ν(CS) and appearnace of new bands at 1620 and 665 cm^{-1} due to $\nu(S-C=N)$ and $\nu(C-S)$, and (ii) the shift of ν(CN) to lower wavenumber (10 cm^{-1}); the shift of ν(CO) to higher wavenumber shows that CO group does not participate in the complexation. The bands observed at 3440, 1610, 890 and 770 cm^{-1} in the IR spectrum of the complex $[Mn(HIBD)Cl.(H_2O)_3]$ complex are assigned to ν(OH), $\nu(H_2O)$, $\rho_r(H_2O)$ and $\rho_w(H_2O)$ vibrations[18] respectively of the coordinated water molecules. On drying this complex by heating in an oven up to 120°C no water molecule is removed which indicates the presence of water molecules in the coordination sphere.

In the $UO_2(H_2IBD)Ac_2$ complex, H_2IBD behaves as a neutral bidentate ligand coordinating via the CO and CN groups since both νCO and νCN modes shift to lower wavenumbers. The NMR spectrum shows new signals at 2.3-2.7 ppm due to CH_3-protons of the acetate group and the signal due to NH proton of isatin residue is shifted to 10.4 ppm as a result of the participation of CO in coordination. The uranyl complex exhibits three bands at 930, 840 and 265 cm^{-1} assigned to ν_3, ν_1 and ν_4 modes, respectively, of the dioxouranium ion[19]. The force constant (F) for bonding sites of the U = O vibration was calculated by the method of McGlynn *et al.*[20], as 7.14 mdynes $Å^{-1}$.

New bands observed in the complexes at 580-520, 485-450, 315-310 and 310-270 cm^{-1} are tentatively assigned to the ν(M-O)[21], ν(M-N)[22], ν(M-S)[21] and ν(M-Cl)[23] modes.

The magnetic moments of the complexes are listed in Table 1. The electronic spectrum (DMF) of $[Mn(HIBD)Cl.(H_2O)_3]$ complex, shows two bands at 22220 and 27780 cm^{-1} assignable to $^6A_{1g} \rightarrow {}^4T_{2g}(G)$ and $^6A_{1g} \rightarrow {}^4T_{2g}(D)$ transitions[24], respectively. The *Dq*, *B* and β values are 1018.4, 925.8 and 0.96 cm^{-1}, respectively suggesting the octahedral geometry[25,26]. In addition the magnetic moment (5.76 BM) can be taken as additional evidence for the octahedral structure. On increasing delocalization, β decreases and becomes less than unity in the complex.

The magnetic moment value (4.73 BM) for the $[Co(HIBD)_2]$ complex is near the value expected for high spin octahedral Co(II) complexes. The electronic spectrum (DMF) shows strong band at 22220 cm^{-1} ($\varepsilon = 30.9$) and shoulder around 20000 cm^{-1} assigned to the $^4T_{1g}(F) \rightarrow {}^4T_{1g}(P)$ (ν_3) transition[27]. The lowest bands ν_2 and ν_1 could not be observed in our instrument and thereby the ligand field parameters could not be calculated. The broad band at 26315 cm^{-1} ($\varepsilon = 101$) is assigned to charge-transfer probably of the type $H_2BID \rightarrow Co$.

The electronic spectrum (DMF) of $[Ni(HIBD)_2]$ shows a broad band centered at 19880 cm^{-1} due to the $^3A_{2g}(F) \rightarrow {}^3T_{1g}(F)$ (ν_2) ($\varepsilon = 17$) transition. Also, a broad band at 26315 cm^{-1} is observed which may be due to ν_3 transition $[^3A_{2g} \rightarrow {}^3T_{1g}(P)]$ ($\varepsilon = 850$) or a charge transfer transition[28]. The value of its magnetic moment (3.2 BM) is an evidence for an octahedral structure.

The magnetic moments of [Cu(HIBD)Cl] and [Cu(IBD)] are 1.85 and 1.5 BM respectively at room temperature. The value observed for Cu(HIBD)Cl is in the range for high spin Cu(II) complexes having monomeric structures[29]. The lowering of μ_{eff} value in the case of Cu(IBD) may be attributed to the polymeric structure. The electronic spectra of these complexes show bands at 14490, 23260 and 27027 cm^{-1} for the former and at 15150, 16666, 17450, 22730 and 25970 cm^{-1} for the latter. The positions of the bands indicate that these complexes have a square-planar stereochemistry[28]. The appearance of a high energy band at 22000-27000 cm^{-1} may be due to polymeric structure or charge transfer phenomenon.

Finally, the U.V. spectrum of the $UO_2(H_2IBD)Ac_2$ shows a band at 21270, 22222 cm^{-1} assigned to $^1E_g^+ \rightarrow \pi_u^3$. This band is similar to the OUO symmetric stretching frequency for the first excited state[30].

References

1 Ali M A & Livingstone S E, *Coord Chem Rev*, 13 (1974) 101.
2 Cleare M J, *Coord Chem Rev*, 12 (1974) 349.
3 Williams D R, *Chem Rev*, 72 (1972) 203.
4 Das M & Livingstone S E, *Inorg chim acta*, 9 (1976) 5.
5 Ali M A & Bose R N, *Polyhedron*, 3 (1984) 517.
6 Ali M A & Bose R N, *J inorg nucl Chem*, 39 (1977) 265.
7 Ali M A & Tarafdar M T H, *J inorg nucl Chem*, 39 (1977) 1785.
8 Feedlander B L & Fraust A, *J Am chem Soc*, 81 (1952) 638.

9 Buu-Hoi N P, Voc T B & Xuong N D, *Bull Soc chim France*, (1955) 694.
10 Benns B G, Gingras B A & Bayley C H, *App Microbiol*, 8 (1960) 353.
11 Ali M A & Teoh S G, *J inorg nucl Chem*, 41 (1979) 809.
12 Bekheit M M, Ibrahim K M & Abu El-Reash G M, *Indian J Chem*, 28A (1989) 261.
13 Geary W J, *Coord Chem Rev*, 7 (1971) 81.
14 Rao C N R, *Chemical applications of infrared spectroscopy* (Academic Press) 1963, 300.
15 Sahni S K & Rana V B, *Indian J Chem*, 15A (1977) 890.
16 Senti F & Harker D, *J Am chem Soc*, 62 (1940) 2008.
17 Hall D, *Acta Crystallogr*, 18 (1965) 955.
18 Nakamoto K, *Infrared spectra of inorganic and coordination compounds* (Wiley, New York) 1970.
19 Hsieh A T T, Sheahan R M & Water B O, *Aust J Chem*, 28 (1975) 885.
20 McGlynn S P, Smith J K & Neely W C, *J chem Phys*, 35 (1961)105.
21 Ferraro J R, *Low frequency vibrations of inorganic and coordination compounds* (Plenum Press, New York) 1971.
22 Ferraro J R & Walkers W R, *Inorg Chem*, 4 (1965) 1382.
23 Clark R J H, *J chem Soc*, (1963) 1377.
24 Figgis B N, *Introduction to ligand fields* (Wiley-Interscience, New York) 1966.
25 Olavi S & Harry B G, *Inorg Chem*, 13 (1974) 1185.
26 Preti C & Tosi G, *Aust J Chem*, 29 (1976) 543.
27 Ferraro J R & Walkers W R, *Inorg Chem*, 4 (1965) 1382.
28 Lever A B P, *Inorganic electronic spectroscopy* (Elsevier, Amsterdam), 1968.
29 Kato M, Fanning J C & Jonassen H B, *Chem Rev*, 64 (1969) 99.
30 McGlynn S P, Smith J K & Neely W C, *J molec Spectroc*, 6 (1961) 164.

Indian Journal of Chemistry
Vol. 30A, March 1991, pp. 290-292

Synthesis and characterization of Co(II), Ni(II), Cu(II), Zn(II), Cd(II), Hg(II), dioxouranium(VI) and Th(IV) complexes with a schiff base

A C Hiremath*, Z S Qureshi, K M Reddy & M B Halli
Department of P G Studies and Research in Chemistry,
Gulbarga University, Gulbarga 585 106

Received 11 December 1989; revised 4 April 1990;
rerevised and accepted 3 September 1990

Complexes of the type ML_2Cl_2[M = Co(II), Ni(II), Cu(II) and Cd(II)] and ML_2Cl_2[M = Zn(II), Hg(II), dioxouranium(VI) and Th(IV)] and L = schiff base derived from 4-hydrazinobenzofuro[3,2-*d*]pyrimidine and 4-hydroxy-3-aldehydodiphenyl have been reported and characterized on the basis of analytical, magnetic moment, conductance, electronic and infrared spectral data. The ligand field parameters have been evaluated for Co(II), Ni(II) and Cu(II) complexes which suggest an octahedral geometry for each of them. The infrared spectral data reveal the bidentate nature of the ligand.

4-Hydrazinobenzofuro[3,2-d]pyrimidine has been reported to form complexes with the metal ions[1]. A literature survey revealed that metal complexes of the schiff base derived from the condensation of 4-hydrazinobenzofuro[3,2-d]pyrimidine with 4-hydroxy-3-aldehydodiphenyl were not reported. We report here the preparation and characterization of Co(II), Ni(II), Cu(II), Zn(II), Cd(II), Hg(II), dioxouranium(VI) and Th(IV) complexes with the above mentioned schiff base (I).

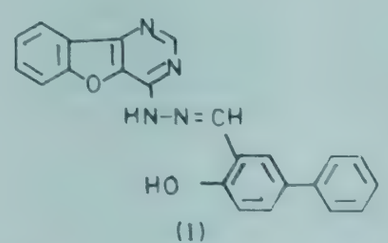

(I)

Experimental

All the chemicals used were of AR or CP grade. Infrared spectra were recorded in nujol on a Hitachi 270-50 IR spectrophotometer in the range 4000-250 cm^{-1}. The electronic spectra of $10^{-3}M$ solutions were recorded on a Hitachi spectrophotometer in DMF. The mass spectrum of the ligand was taken on a Finnigan Mat 8230 mass spectrometer. The conductivities of the complexes were measured at 25°C in DMF ($10^{-3}M$) using an Elico CM-82 conductometer. Magnetic susceptibilities were measured on a Gouy balance using $Hg[Co(SCN)_4]$ as the calibrant. The metal, nitrogen and halogen were estimated by standard methods[2].

Preparation of schiff base

The schiff base was prepared by reacting ethanolic solutions of 4-hydrazinobenzofuro[3,2-d]pyrimidine (0.50 g, 2.5 mmol) and 4-hydroxy-3-aldehydodiphenyl[3] (0.5 g, 2.5 mmol). The mixture was refluxed on a water-bath for about 4-5 hr. The excess of solvent was partially evaporated and the separated yellowish mass was filtered out, washed with ethanol and crystallised from ethanol. The compound was dried *in vacuo* at room temperature (yield 85%, m.p. 298°C).

General method for the preparation of complexes

4-Hydroxy-3-aldehydodiphenyl (2.5 mmol) and 4-hydrazinobenzofuro[3,2-d]pyrimidine (2.5 mmol) were dissolved in 50 ml of ethanol and the contents were refluxed on a waterbath for about 4 hr. To this was added an ethanolic solution of the appropriate metal salt (2.5 mmol) with stirring. The resulting coloured mixture was further refluxed on a water bath for about 0.5 hr. The separated complex was filtered. In the case of dioxouranium(VI) and Th(IV) complexes, the reactants were refluxed for about 8-10 hr, the separated complexes were filtered and washed with ethanol and dried *in vacuo*.

Results and discussion

All the complexes (Table 1) were found to be quite stable at room temperature. The complexes were non-electrolytic in nature (Λ_M = 5-18 $ohm^{-1}cm^2mol^{-1}$) suggesting that the anions were covalently bonded in all the cases.

The $\mu_{eff.}$ value for Co(II) complex was found to be 4.47 BM which falls within the expected range for the high-spin octahedral Co(II) complexes[4]. The $\mu_{eff.}$ value for Ni(II) complex (2.87 BM) was also within the expected range for octahedral Ni(II) complexes. The $\mu_{eff.}$ value for Cu(II) complex (1.81 BM) is consistent with the presence of one unpaired electron.

In the mass spectrum of the schiff base the molecular ion peak was noticed at *m/z* 380 (36%). The other fragments were observed at 363 (25%), 197 (22%), 185 (100%), 169 (8%), 211 (8%) and 115 (16%) which are consistent with the structure of the schiff base.

Table 1—Analytical and magnetic susceptibility data of the complexes

Complex	Found (Calc), %			$\mu_{eff.}$ (B.M.)
	M	N	Cl	
$CoLCl_2$	11.35 (11.56)	10.20 (10.98)	12.90 (13.93)	4.47
$NiLCl_2$	11.73 (11.55)	10.22 (10.98)	12.80 (13.92)	2.87
$CuLCl_2$	11.99 (12.35)	10.55 (10.88)	13.55 (13.79)	1.81
ZnL_2Cl_2	6.67 (7.29)	12.00 (12.49)	6.90 (7.92)	—
$CdLCl_2$	19.50 (19.95)	9.58 (9.94)	12.86 (12.60)	—
HgL_2Cl_2	19.03 (19.44)	10.70 (10.85)	6.33 (6.88)	—
$UO_2L_2(NO_3)_2$	31.00 (30.75)	6.90 (7.28)	—	—
$ThL_2(NO_3)_4$	18.13 (18.70)	13.30 (13.55)	—	—

In the IR spectrum of the schiff base, a strong band present at ~3180 cm^{-1} may be attributed to secondary NH stretching vibration. This band in complexes remains almost unaltered and in some cases it becomes broad and weak; this indicates the noninvolvement of NH group in bonding with the metal ions.

Two groups of strong bands observed at 1635, 1625 cm^{-1}, and 1600, 1580 cm^{-1} can be assigned to stretches of C=N groups belonging to azomethine and pyrimidine ring respectively[5,6]. The bands appearing at 1635 and 1625 cm^{-1} are shifted to higher frequency side by about 10-30 cm^{-1} in the complexes suggesting the involvement in coordination of azomethine group[7-9]. The pyrimidine ring C=N stretching vibrations remain unchanged indicating non-participation of pyrimidine ring nitrogen in coordination. The high intensity band observed for the ligand around 1295 cm^{-1} is assigned to phenolic C−O stretching vibrations[10]. The νOH band observed at 3060 cm^{-1} in the ligand appears at approximately the same position in the complexes. This suggests that OH group may be coordinated to the metal ion; otherwise, the cleavage of H-bonding in the ligand on complexation would have resulted in upward shift of the band. The C−O band shifts towards higher frequency region (1320-1380 cm^{-1}) in the complexes suggesting the involvement of OH group in bond formation with the metal ions[11,12].

In the far IR spectra of the complexes, the bands in the region 550-450 cm^{-1} can be assigned to ν(M−O) (phenolic) vibrations[13,14] and the bands at 450-300 cm^{-1} can be assigned to ν(M−N) vibrations in all the complexes.

In the case of polymeric complexes, ν(M−Cl) for terminal halogens is observed at higher frequencies compared to that for the bridging halogens[15]. In view of this fact, we have assigned $\nu(M-Cl)_t$ around 360 and $\nu(M-Cl)_b$ in the region 285-260 cm^{-1} for Cd(II), Co(II), Cu(II) and Ni(II) complexes[16]. In the case of HgL_2Cl_2 and ZnL_2Cl_2 complexes ν(M−Cl) is assigned in the region 310-260 cm^{-1}.

In the electronic spectrum of Co(II) complex in DMF solution ($10^{-3}M$), two bands observed at 16670 cm^{-1} and 21740 cm^{-1} are assigned to $^4T_{1g}(F) \rightarrow {}^4A_{2g}(F)$ (ν_2) and $^4T_{1g}(F) \rightarrow {}^4T_{1g}(P)$($\nu_3$) transitions respectively in a distorted octahedral geometry[17]. The highest energy band observed around 30000 cm^{-1} is assigned to CT transition. The spectral parameters like Dq, B', β, β% and LFSE have been computed[18] and their values are 829 cm^{-1}, 884 cm^{-1}, 0.91, 24.41% and 14.21 kcal/mol respectively. The reduction in Racah parameter value from the free ion value of 971 cm^{-1} and β% value of 24.4% testify the presence of strong M−L covalent bonding in the complexes. The ν_2/ν_1 ratio of 1.94 supports the distorted octahedral geometry for Co(II) complex.

In the electronic spectrum of Ni(II) complex two bands observed at 13330 cm^{-1} and 23810 cm^{-1} correspond to $^3A_{2g} \rightarrow {}^3T_{1g}(F)(\nu_2)$ and $^3A_{2g} \rightarrow {}^3T_{1g}(P)(\nu_3)$ transitions respectively, which support distorted octahedral geometry. The ν_1 band could not be observed due to instrumental limitations and it was computed using Underhill and Billing equation (8300)[18]. The value of Racah parameter (960 cm^{-1}) is less than the freee ion value (1040 cm^{-1}) indicating covalent character of the complex. The ν_2/ν_1 ratio of 1.60 further supports octahedral geometry[19]. The calculated values of spectral parameters Dq, B', β, β% and LFSE are 830 cm^{-1}, 960 cm^{-1}, 0.94, 7.69% and 28.50 kcal/mol respectively. These values are suggestive of distorted octahedral geometry for Ni(II) complex.

The light green coloured Cu(II) complex shows a broad asymmetric band in the region 16670-15380 cm^{-1} with a maximum around 14900 cm^{-1} which is assignable to $^2E_g \rightarrow {}^2T_{2g}$ transition in a distorted octahedral geometry[20]. The $\mu_{eff.}$ value calculated using Figgis equation[21] is very close to the observed value. The Dq value and LFSE are 1490 cm^{-1} and 25.55 kcal mol^{-1} respectively. These facts led us to propose distorted octahedral structure for the Cu(II) complex.

Based on the above spectral data and magnetic moments, we assign halogen bridged octahedral po-

lymeric structures for Cd(II), Cu(II), Co(II) and Ni(II) complexes, and ligand bridged polymeric octahedral structures for Zn(II) and Hg(II) complexes. Thorium(IV) and dioxouranium(VI) complexes are assigned six and eight coordination numbers respectively.

Acknowledgement

The authors are thankful to Prof. S P Hiremath, Chairman, Department of Chemistry for providing facilities. One of the authors (ZSQ) is thankful to Shri S S Inamdar, Principal, Anjuman Degree College, Bijapur for encouragement and the UGC New Delhi for financial assistance.

References

1 Hiremath A C, Halli M B & Huggi N V, *Indian J Chem*, 23A (1984) 1969.
2 Vogel A I, *A text book of quantitative inorganic analysis* (Longman, London) 1961.
3 Duff C J, *J chem Soc*, (1941) 547.
4 Figgis B M & Lewis J, *Progr inorg Chem*, 6 (1969) 37.
5 Nityananda Saha & Susant K Kar, *J inorg nucl Chem*, 39 (1977) 195.
6 John R Dyer, *Application of absorption spectroscopy of organic compounds* (Prentice-Hall of India, New Delhi) 1984.
7 Busch D H & Bailar J C, *J Am chem Soc*, 78 (1956) 1137.
8 Rizvi S F H & Nazzera, *Indian J Chem*, 13 (1975) 1084.
9 Shukla P R & Takru Renu, *J Indian chem Soc*, 57 (1980) 252.
10 Kovacic J E, *Spectrochim Acta*, 23A (1967) 183.
11 Zaidi S A A & Siddiqi Z A, *J inorg nucl Chem*, 38 (1976) 1405.
12 Marvel C S, Asepey S A & Dudley A, *J Am chem Soc*, 78 (1956) 4909.
13 Prabhu P S & Dodwad S S, *J Indian chem Soc*, 63 (1986) 475.
14 Anjaneyulu Y, Kameswara Rao N & Prabhakar Rao R, *Indian J Chem*, 27A (1988) 555.
15 Adams D M & Chander P, *Chem Commun*, 10 (1971) 798.
16 Flint C D & Goodgame M, *J chem Soc*, A (1966) 744.
17 Rama Rao N, Shrya Rao D & Ganorkar M C, *Indian J Chem*, 21A (1982) 839.
18 Underhill A E & Billing D E, *Nature*, 210 (1966) 834.
19 Ballhausen C J, *Introduction to ligand field theory* (McGraw-Hill, New York) 1962, 256.
20 Mostaffa M M, Hassan S M & Ibrahim G M, *J inorg nucl Chem*, 42 (1980) 285.
21 Figgis B N, *Introduction to ligand fields* (Interscience, New York) 1966.

Indian Journal of Chemistry
Vol. 30A, March 1991, pp. 293-295

Kinetics of extraction of cobalt(II) by quinolinol and its back extraction using ^{58}Co tracer

(Late) Arvind T Rane & Deepawati R Nepali*
Tata Institute of Fundamental Research,
Homi Bhabha Road, Bombay 400 005, India

Received 6 April 1990; revised 16 July 1990;
accepted 3 September 1990

The kinetics of extraction of cobalt(II) by 8-quinolinol has been studied using ^{58}Co tracer in the *p*H range 5-6.2 at 29°C and in the temperature range 26.8-44°C for *p*H 5.2 and 5.4 at an ionic strength 0.1 *M*. The rate of cobalt(II) extraction by oxine is pseudo-first-order with respect to [oxine]. The kinetics of back extraction of bis(8-quinolinato)cobalt(II) from chloroform to aqueous phase by mineral acids has been also studied. The activation energy, enthalpy and entropy of the extraction reaction have been evaluated.

8-Quinolinol has been used for the determination[1] as well as solvent extraction[2] of a number of metal ions. Ritcey and Lucas[3] have shown that in the extraction of Cu-Fe mixture by Kelex 100, a derivative of 8-quinolinol, some iron is rapidly extracted initially (in less than 1 min), then no further extraction occurs for about 30 min, after which extraction increases with time. The iron initially extracted could be quantitatively accounted for by the oxine in Kelex 100. These results pointed to a significant kinetic role of the oxine impurity in Kelex 100 and led to a study of the kinetics of extraction of Cu and Fe by oxine as a prelude to a study of the Kelex 100 reactions[4].

Guesnet *et al.*[5] observed that Co(II) undergoes oxidation by atmospheric oxygen to Co(III), irreversibly, during the course of extraction with 8-quinolinol and Kelex 100. They also reported that the cobalt(II) chelates were poorly strippable from organic phase, but their oxidation could be delayed by the addition of versatic 10 acid and TOPO.

Similar oxidation of Co(II) was observed during the extraction of Co(II) adducts of 2-methyl-8-quinolinol and 4-methyl-8-quinolinol with 2,4-lutidine and 2,4,6-collidine; the adducts were extracted as Co(III) species[6]. A kinetic study of the extraction of the Co(II) chelates in presence of 2,4-lutidine and 2,4,6-collidine revealed that the extraction was first order and the rate of oxidation decreased with the increase in [pyridine][7]. Kinetics of the adduct formation in the Co(II) chelates of 8-quinolinol and its analogues were also studied spectrophotometrically, in a single phase system[8]. The present work on the kinetics of the extraction of Co(II) was undertaken as a part of our research programme dealing with certain metal adducts of 8-quinolinol in two phase system.

Experimental

Carrier-free $^{58}Co_{(t_{1/2}=71d)}$ was supplied by BRIT, Trombay as $CoCl_2$ in dilute HCl. It was mixed with a few drops of saturated solution of hydroxylamine hydrochloride to prevent the oxidation of Co(II) and was sufficiently diluted with distilled water. Aliquots of ^{58}Co (0.2 ml) were taken every time for the equilibration study so as to give 2×10^5 cts/min.

ExcelaR grade 8-quinolinol and chloroform, supplied by Glaxo India, were used for the kinetic study.

A set of Clarke and Lubs buffer solutions was prepared for the *p*H range 5.0-6.2. Ionic strength was maintained at 0.1 *M* by adding requisite amount of sodium perchlorate in buffers.

Radioactivity was counted on $2'' \times 2''$ well type Na(Tl) detector system connected to a scintillation spectrometer supplied by ECIL (Hyderabad).

A Kahn type shaking machine was used for the equilibration study. A shaking rate of 250 strokes/min was employed at ambient temperature.

Individual samples were equilibrated in stoppered centrifuge tubes in reciprocated manner for varying time intervals. For the kinetic study at different temperatures, the samples were shaken in 50 ml stoppered conical flasks fitted in a thermostated water bath.

For the kinetic study of stripping, a pre-extracted cobalt(II)-8-quinolinate solution in chloroform was used and equilibrated with hydrochloric acid of different concentrations with varying time interval.

In the extraction kinetics, samples of the aqueous phase were taken at different time intervals and ^{58}Co activity was counted; whereas, in the stripping study, samples of the organic phase were taken for counting of the activity.

Results and discussion

In the classical reaction scheme, the rate controlling step is often the stepwise addition reaction of the chelating agent, i.e.,

$M^{n+} + R \rightarrow$ Products

When the back reaction is negligible, the rate of metal removed from the aqueous phase is,

$$\frac{d(M^{n+})}{dt} = k_f (M^{n+})(R^-) \quad \ldots (1)$$

where k_f is the forward reaction rate constant.

The extraction of cobalt from the start and upto approaching equilibrium can be represented as,

a_0 ---------- a_t ---------- a_e

where a_0 and a_e are the initial and equilibrium cobalt concentrations, respectively. and a_t is the cobalt concentration, at time t in the aqueous phase.

Then the rate constant for the forward extraction reaction of the first order is given as[9],

$$k_f t = \frac{a_0 - a_e}{a_0} \ln \frac{a_0 - a_e}{a_t - a_e} \quad \ldots (2)$$

The rate constant for the back extraction of cobalt is given as,

$$k_b t = \ln \frac{C_0}{C_t} \quad \ldots (3)$$

where C_0 and C_t are the cobalt concentrations at the start and at time t, in the organic phase.

The kinetic data obtained for the extraction of cobalt(II) with 8-quinolinol were plotted in accordance with Eq. (2) for different [8-HQ] for respective *p*H when straight line plots were obtained with varying slopes. Fig. 1 shows typical plots obtained from Eq. 2. These straight line plots confirm that the rate of extraction is pseudo-first order with respect to cobalt(II). The slopes of these plots give directly the value of observed rate constants for the extraction of cobalt(II). The observed rate constants were obtained for various *p*H values between 5.0 and 6.2. These are given in Table 1. The data show that the observed extraction rate increases with increasing *p*H and [8-HQ].

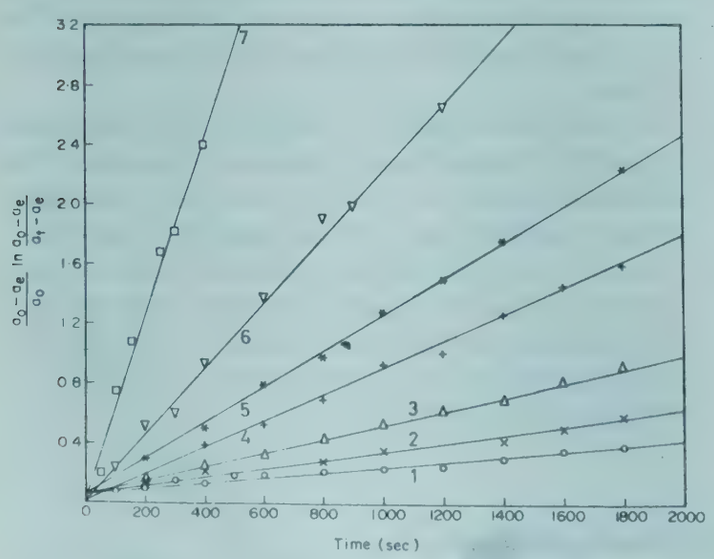

Fig. 1—The first order expression as a function of time for different *p*H {[8-HQ] = 10^{-2} *M*; curve 1: *p*H = 5.0; curve 2: *p*H = 5.2; curve 3: *p*H = 5.4; curve 4: *p*H = 5.6; curve 5: *p*H = 5.8; curve 6: *p*H = 6.0; curve 7: *p*H = 6.2}

The variations of the observed rate constants at various [8-HQ] and *p*H values were plotted. These plots showed good linear relationships between the log of observed rate constant, [oxine] and *p*H respectively. The slopes of these plots were found to be 1.48 and 1.

Stripping of Co(II)

The formation of CoQ_3 chelate due to oxidation of Co(II) to Co(III) by oxygenation was confirmed by the bathochromic shift observed in the absorption spectrum of CoQ_2 when the λ_{max} got shifted from 403 nm to 410 nm[10]. The stripping ratio at equilibrium decreased when the time-lapse between the extraction and beginning of stripping increased. Addition of acidic compounds, such as versatic 10 acid or dichloroacetic acid, to the organic phase after extraction with 8-quinolinol decreased the oxidation rate[5].

Back extraction of Co-8-quinolinate into aqueous phase was tried with mineral acids like HCl, H_2SO_4 as well as with EDTA. Surprisingly, no stripping was observed with EDTA. Results of the back extraction of Co(II)with HCl and H_2SO_4 at various concentrations are given in Table 2 along with the observed rate constants obtained with HCl. From the data obtained it can be seen that HCl is a better stripping agent than H_2SO_4 and it is possible to back-extract cobalt from chloroform in contradiction to an earlier report[5]. From the present data, it can be seen that the rate constant of stripping increases very rapidly with the increase in [HCl].

This study elaborates the possibility of the ex-

Table 1—Observed extraction rate constants of Co(II) by 8-quinolinol at various *p*H values and at 28°C

[8-HQ] × 10^3 (mol.l^{-1})	$k \times 10^4$ (s^{-1}) at *p*H						
	5.0	5.2	5.4	5.6	5.8	6.0	6.2
6				4.75	6.9	7.7	26
8		2.68	4.8	6.77	9.87	16	48.75
10	1.53	2.9	5.6	9.01	12.1	22.46	67
12.5	2.88	5.8	6.65	14.2	19	34.9	
15	3.37	6.7	11.15	17.49	24.67	43.7	98.4
20	5.5	9.5	13.6	22.02	43.6	41.9	
25	13.65	11.76	14.4	32.8	46.7		
30.2	11.15						
40.7	15.4						

Table 2—Back extraction of Co(II) from $CHCl_3$ with HCl and H_2SO_4 and observed back-extraction rate constants with HCL at 28°C

[Acid] ($mol.l^{-1}$)	% Back extn. with H_2SO_4	% Back extn. with HCl	Rate constants $\times 10^4$ (s^{-1}) with HCl
1	26.18	7.98	
2	27.15	8.41	
3	29.1	10.34	
4	29.86	14.56	
5	33.36	47.61	3
5.5	35	71.5	6.2
6	36.9	90	11
6.6		100	17.4
7		100	19
7.5		100	55
8		100	35

traction of Co(II) with oxine, without Co(II) undergoing oxidation reversibly, using carrier-free ^{58}Co in presence of strong reducing agent, hydroxylamine hydrochloride which could be back-extracted into aqueous phase. The only difference between the present study and the earlier investigation[5,3], where cobalt could not be stripped from the organic phase, is that earlier extraction of Co(II) was studied in macro quantity (1.5×10^{-3} M) compared to the traces (carrier-free) used presently. Cobalt(II) undergoes oxidation during the course of extraction even when it is present in traces[7]. Therefore, the quantity of the metal taken for extraction is unimportant/immaterial and the medium used for the extraction of Co(II), i.e., reducing medium, is important.

Activation energy:

During this study, it was observed that the extraction of Co(II) increased markedly with the increase in temperature. The log D value increased from 0.05 at ambient temperature to 0.8 at 43°C. The thermodynamic constants of the extraction reaction could be determined from the experimental data taken at different temperatures. By plotting the log k values obtained against $1/T$, the reciprocal of the absolute temperature, Arrhenius plots were obtained. The activation energy E_a, and the pre-exponential factor A were calculated from the slope and the vertical intercept, respectively, of the linear plots by means of the least squares method. From these values, the activation enthalpy $H\ddagger$ and the activation entropy $S^{\neq}$ were calculated by the following equations,

$$H^{\neq} = E_a - RT \quad \ldots (4)$$

$$S^{\neq} = R[\ln(Ah/kT) - 1] \quad \ldots (5)$$

where h is the planck constant; k, the Boltzmann constant and R, the gas constant. These values obtained are as follows: $E_a = 19.56$ kJ mol^{-1}, $\Delta H^{\neq} = 17.06$ kJ mol^{-1}, $\Delta S^{\neq} = -200.5$ jK^{-1} mol^{-1}.

Acknowledgement

The authors are grateful to (Miss) Vandana Nanal for calculating least squares fittings on computer.

References

1 Philips J P, *Chem Rev*, 56 (1956) 271.
2 Morrison G H & Freiser H, *Solvent extraction in analytical chemistry* (Willey, New York) 1957.
3 Ritcey G M & Lucas B M, *Paper presented at the Ann Conf Metallurgists*, CIMM, Quebec city (1973).
4 Fleming C A & Nicol M J, *J inorg nucl Chem*, 42 (1980) 1335.
5 Guesnet P, Sabot J L & Bauer D, *J inorg nucl Chem*, 42 (1980) 1459.
6 Bhatki K S & Rane A T, *Transition Metal Chem*, 3 (1978) 181.
7 Rane A T, *Indian J Chem*, 21A (1982) 144.
8 Rane A T, *Indian J Chem*, 21A (1982) 718.
9 Flett D S, Okuhara D N & Spink D R, *J inorg nucl Chem*, 35 (1976) 2471.
10 Rane A T, *Proc Indian Natl Sci Acad*, 51A (1985) 550.

Indian Journal of Chemistry
Vol. 30A, March 1991, pp. 296-298

A spectrophotometric method for the determination of traces of silicon in copper and aluminium alloys

Deepa Bhatnagar, R Ramchandran & D C Parashar*
Chemistry Division, National Physical Laboratory, New Delhi 110 012, India

Received 15 May 1990; revised 30 July 1990; accepted 5 September 1990

A rapid and accurate spectrophotometric method has been developed for the determination of silicon in the range 0.02-1 ppm in copper and aluminium alloys based on the formation of reduced silicomolybdate in the presence of bismuth as catalyst. The possibility of extraction of the silicomolybdate complex formed, with an organic solvent like isoamyl alcohol has been explored. It is found that the method is more sensitive compared to existing methods and it gives a molar absorptivity of 30,000 at 800 nm. The standard deviation calculated at the 0.45 μg Si/ml level is found to be 0.008 ppm for a set of four weighings. Interference studies for some of the important ions which are relevant to silicon determination have also been carried out.

Determination of trace impurities like silica in high purity materials and non-ferrous alloys of different types is of great importance. Very few colorimetric methods are available for the determination of silica in copper and aluminium based alloys. The well known molybdosilicic acid method has been described by Boltz[1] for the determination of silica in copper alloys. A spectrophotometric method for the determination of silica in high phosphorus-copper alloys has been reported by Shkaravskii *et al.*[2] Pakalns and Flynn[3,4] have developed an extraction method in which unreduced yellow silicomolybdate is extracted into an organic solvent and subsequently reduced to silicomolybdate blue. Hargis[6] has reported the formation of ternary complex of bismuth phosphomolybdate by interaction of bismuth ions with phosphate and molybdate ions in acid solution. It has been observed by us that bismuth does not form a similar complex with silicomolybdate but only helps in the quick reduction of silicomolybdate at room temperature and also enhances the colour intensity[5]. This effect of bismuth has been made use of in the determination of silica in copper and aluminium alloys, both in aqueous as well as in organic medium.

Effect of different reductant systems, i.e., ascorbic acid alone, ascorbic acid with the addition of antimony, and ascorbic acid with the addition of bismuth was studied. For 0.45 ppm of silicon, Bi/ascorbic acid, Sb/ascorbic acid and ascorbic acid alone showed absorbance values of 0.470, 0.467 and 0.422 respectively. This shows the efficiency of Bi/ascorbic acid reductant system.

Experimental

A Perkin-Elmer Lambda-3 spectrophotometer with digital read-out system was used for recording absorbance values. An Elico digital *p*H meter was used for recording the *p*H values.

Doubly distilled water was used for preparing the solutions. All the reagents used were of AR grade.

Standard silica solution

It was prepared by fusing 0.2141 g of pure anhydrous silica (SiO_2) with 2g of sodium carbonate in a platinum crucible and dissolving the melt in warm water, cooling and making up the volume to one litre. The solution was stored in a polythene bottle.

Acid ammonium molybdate solution was prepared by adding 4.3 ml of 9*N* H_2SO_4 to 100 ml of 2.5% ammonium molybdate solution.

Tartaric acid solution was prepared by dissolving 20 g of tartaric acid in 100 ml of doubly distilled water.

Reducing solution

Bismuth nitrate $Bi(NO_3)_3.5H_2O$ (A R) (0.232 g) was dissolved in 100 ml of 0.5 *N* nitric acid to obtain a solution containing 1 mg Bi/ml. Ascorbic acid (2 g) was dissolved in doubly distilled water and volume made up to 100 ml. Fresh solution of this was prepared daily.

Analytical procedure

Copper and copper alloys

A sample of pure copper or copper containing alloy (0.2-0.5 g) was weighed and transferred to a polythene beaker. The contents were dissolved in a mixture of nitric acid (4.5 ml), hydrochloric acid (1.5 ml), hydrofluoric acid (0.4 ml) and doubly distilled water (20 ml). After the vigorous reaction had subsided, the contents were heated gently to near boiling point on a water bath for complete dissolution. The solution was transferred into a 100 ml volumetric flask containing 30 ml of saturated boric with the aid of a long stemmed plastic funnel. The beaker was rinsed with water and the contents transferred to the flask. The flask was shaken well to mix the solutions thoroughly and volume made upto 100 ml.

Aluminium and aluminium alloys

A sample (0.2-0.5 g) was taken in a polythene beaker and 20 ml of 4% sodium hydroxide was added to it; the solution was heated around 80°C to allow complete dissolution of the sample. The solution was acidified with 1:2 sulphuric acid, and hydrofluoric acid (0.25 ml) was added. The solution was warmed for 30 min at a temperature of 80°C. The solution was transferred to a 100 ml volumetric flask containing 30 ml of saturated boric acid with the aid of a plastic funnel and volume was made up.

For analysis of the sample, a 5 ml or 10 ml aliquot was transferred into polythene beaker (50 ml). To this was added 6 ml of saturated boric acid and volume made up to 25 ml approximately, the *p*H was adjusted to 1.1-1.2. Hydroxylamine hydrochoride (0.2 ml) and acid ammonium molybdate (20 ml) were added and the solution stirred gently with a plastic rod. After 15 min, 5 ml of tartaric acid was added and just after 1 min, 17 ml of 9 *N* sulphuric acid was added. The solution was transferred to a 100 ml volumetric flask. To this was added 0.5 ml of 1 mg Bi/ml, followed by 2.5 ml of 2% ascorbic acid. The solutions were mixed well after making up the volume. The absorbance was measured at 800 nm against a blank containing the same concentration of copper as in the sample, 10 min after the colour development. Standard addition of silica was preferred in the case of alloys of copper and aluminium containing $<0.1\%$ silicon.

For analysis of the sample in the organic medium, the solutions were treated in a similar manner until the formation of the unreduced silicomolybdate occurred. Tartaric acid (5 ml) was added and after an interval of 1 minute, 6.5 ml of 9*N* H_2SO_4 was added stirring the solution well after each addition. The solution was transferred to a separating funnel and extraction with isoamyl alcohol was carried out in two lots by maintaining the ratio, aqueous solution: acid at approximately 10:1. The extracted lots were allowed to stand for 5 min in a dry separating funnel and any droplets of water collecting at the bottom were run off carefully. The reducing solution containing 2.5 ml of 2% ascorbic acid, 0.5 ml of 1 mg Bi/ml and 1 ml water was added to the extract, it was shaken for 30s and allowed to stand for 5 min. The contents were run into a dry 25 ml flask and volume made up with methanol to homogenise the solution. The absorbance of the solution was measured at 800 nm against blank containing the same concentration of copper as in the sample but without any silica and treated in the same say as the sample, 15 min after the development of colour.

Calibration procedure

The control solution for construction of calibration curve was prepared by taking electrolytic grade copper (0.2-0.5 g) and following the same procedure as described for sample alloy as far as decomposition, solution preparation and making up of volume to 100 ml. Five ml portions of the control solution were transferred into polythene beakers. Standard additions of silica were made in varying concentrations in steps of 4.5 µg, i.e., 2 ml, 4 ml, 6 ml of solution having 2.25 µg/ml. Saturated boric acid (6 ml) was added and volume made up to 25 ml approximately; the *p*H was adjusted to 1.1-1.2. Next, hydroxylamine hydrochloride (0.2 ml) was added followed by 20 ml of acid ammonium molybdate; the solution was stirred well with a polyethylene rod. Fifteen minutes were allowed for quantitative formation of silicomolybdate. Tartaric acid (5 ml) was added followed by the addition, after an interval of 1 min, of 17 ml of 9*N* sulphuric acid. Then the solutions were transferred to 100 ml volumetric flasks. Next 0.5 ml of 1 mg Bi/ml was added followed by the addition of 2.5 ml of 2% ascorbic acid and the solutions were mixed well after making up the volume. The solutions were allowed to stand for 10 min and the absorbance measured at 800 nm against the solution containing no silica.

Results and discussion

Under the recommended conditions, 0.02-1 ppm silicon could be determined reproducibly with close adherence to Beer's Law. The molar absorptivity, was found to be 30,000 l $mol^{-1}cm^{-1}$. A set of four readings for four different weighings of Cu was taken. For the silicon concentrations of 0.45 and 0.9 ppm, the estimated values were 0.448 and 0.880, relative % errors were 0.4 and 2.2, and standard deviations were 0.008 and 0.040 respectively. It was found that for complete formation of yellow silicomolybdate in the presence of hydrofluoric acid and boric acid, the optimum *p*H was 1.1-1.2 especially when sample contains large amount of nitrates. Use of acidified ammonium molybdate was helpful in getting reproducible results in the presence of large concentrations of copper and aluminium. The presence of hydrofluoric acid helped in the formation of stable complexes with tin and iron, preventing the precipitation of metastannic acid and the formation of the iron molybdate complex. The effects of acidity and other reagent concentrations were found to be same as reported for antimony[5]. There was no evidence for the formation of a mixed bismuth molybdosilicic acid, as the absorption spectra of unreduced molybdosilicic acid in the presence and

Table 1—Silicon determination in various materials

Sample	% Silicon certified	% Silicon found
NBS 124	0.075	0.074
BCS 179	0.024	0.024
E.L. grade Cu	0.011	0.011 (with standard addition)
Aluminium (high purity)	0.0012	0.0011 (with standard addition)

absence of bismuth were found to follow the same pattern. Further, bismuth addition did not enhance the yellow colour of unreduced molybdosilicic acid. Hence, the effect of bismuth during reduction is only catalytic. A small amount of hydroxylamine hydrochloride was added to remove any traces of oxidants from solution as oxidising acids were used for sample dissolution. The presence of hydroxylamine hydrochloride or copper or aluminium in the concentration range used does not affect the stability of the complex. The complex was found to be more stable in the organic medium than in the aqueous medium though the sensitivity in the two media is about the same. The complex was stable for more than 6 hr at 25 ± 5°C in aqueous medium and for about 24 hr in organic medium. The data of various samples analysed are given in Table 1.

Interference studies

The possibility of interference by copper in the determination of silica in the aqueous medium was studied. It was found that in the working range used for silica, there was no interference from copper upto 250 ppm. Phosphate, arsenate, germanate and vanadate interfered in the determination of silica. Arsenate and germanate could be removed by volatilisation with HCl and HBr. Vanadium is not encountered in copper and aluminium alloys. Phosphate interference was overcome by addition of 20% tartaric acid. It was found that phosphorus present upto 1% in the sample did not interfere. Arsenic (III) interfered when present in excess of 50 ppm.

Acknowledgement

The authors thank Dr. P.K. Gupta, Scientist, Materials Characterization Division for useful discussions. The authors are grateful to Dr. Krishan Lal, Deputy Director, National Physical Laboratory for his keen interest and Dr. S.K. Joshi, Director, National Physical Laboratory for encouragement throughout this work.

References

1 Boltz D F & Howell J A, in *Colorimetric determination of nonmetals*, edited by P T Elving & J D Winefordner (John Wiley, New York) 1977.
2 Shkaravskii Yu E, Lynchak K A & Chemogrenko V B, *Zavod Lab*, 51 (1985) 5.
3 Pakalns P & Flynn W W, *Anal chim Acta*, 38 (1967) 403.
4 Pakalns P, *Anal chim Acta*, 40 (1968) 328.
5 Ramchandran R & Gupta P K, *Anal chim Acta*, 172 (1985) 307.
6 Hargis L G, *Anal Lett*, 1 (1968) 799.

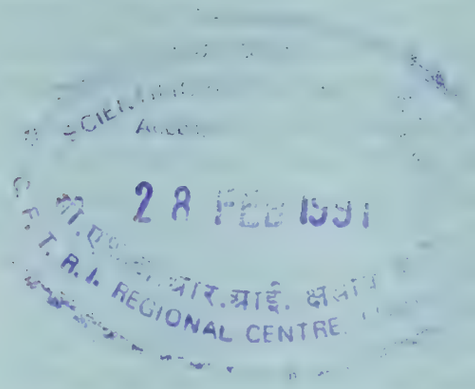

Indian Journal of Chemistry
Vol. 30A, March 1991, pp. 299-300

Extraction and spectrophotometric determination of microgram amounts of niobium(V)

B Keshavan* & K P Krishnaprasad
Department of Post-graduate Studies and Research in Chemistry, University of Mysore, Mysore 570 006

Received 14 May 1990; revised and accepted 13 August 1990

Niobium forms a mixed ligand yellow complex with promethazine hydrochloride (PH) in the presence of thiocyanate at room temperature in hydrochloric acid medium. The ternary complex exhibits maximum absorbance at 400 nm. Its molar absorptivity is 2.72×10^4 l $mol^{-1}cm^{-1}$. Beer's law is valid over the concentration range 0.2-3.0 ppm. The composition of the complex is 1:1:2 (metal:ligand:thiocyanate). The reagent has been used successfully for the spectrophotometric determination of niobium in ores.

Promethazine hydrochloride has been proposed as a spectrophotometric reagent for palladium (II)[1], ruthenium (III)[2] and osmium (VIII)[3]. In the present investigation we have studied the reaction between niobium (V) and promethazine hydrochloride (PH). PH has been found to be a sensitive reagent for the spectrophotometric determination of niobium (V) in the presence of thiocyanates.

Experimental

Standard niobium (V) solution was prepared by melting a known quantity of niobium pentoxide with potassium pyrosulphate in a silica crucible. The cooled melt was dissolved in 10% tartaric acid and the solution was made upto 250 ml in 2% tartaric acid solution. The stock solution was further diluted with 2% tartaric acid solution to get a solution containing 5 μg/ml.

A 0.5% aqueous solution of PH (Bayer, Leverkusen, West Germany) was prepared and stored in a refrigerator.

Solutions of hydrochloric acid, 20% ammonium thiocyanate and diverse ions of suitable concentrations were prepared using analytical reagent grade reagents. Analytical reagent grade benzene was used as the solvent.

Procedure

An aliquot of the stock solution containing 2-30 μg of niobium(V) was transferred into a 100 ml separating funnel. To this were added 4 ml of 10 *M* hydrochloric acid, 2 ml of 20% ammonium thiocyanate, 4 ml of 0.5% PH and 6 ml of benzene. The funnel was shaken vigorously for 2 min and the layers were allowed to separate for five min. The benzene phase was transferred into a dry beaker. The aqueous phase was shaken again with 2 ml of benzene. The benzene phases were mixed and dried with anhydrous sodium sulphate, transferred into a 10 ml standard flask and volume was made up with benzene. The absorbance was measured at 400 nm against a reagent blank prepared in the same way. The amount of niobium was determined using a standard calibration curve.

Results and discussion

Niobium (V) formed a yellow coloured mixed ligand complex with PH(I) and thiocyanate at room

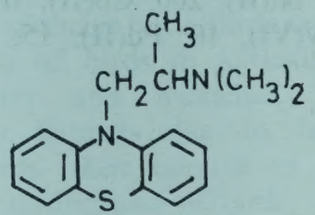

(I)

temperature in hydrochloric acid medium which could be completely extracted into benzene. A number of organic solvents such as benzene, chloroform, toluene, chlorobenzene and xylene extracted the ternary complex into organic phase. Benzene was found to be the most suitable solvent as the complex exhibited maximum sensitivity and stability in this solvent. The stability of the colour depended on the strength of the acid. The complex exhibited maximum absorbance at 398-402 nm in which region the reagent blank absorbed negligibly. Maximum absorbance was achieved in 2-5 *M* hydrochloric acid. Below 2 *M* HCl, the colour development was slow and above 5 *M* the reagent was slowly oxidized. An acid strength of 4 *M* was chosen for all the subsequent work.

Constant absorbance values were obtained immediately after making up the solution to 10 ml with benzene. The absorbance values remained constant for 24 hr. For full colour development 3 to 5 ml of 0.5% PH reagent was required. For all subsequent work 4 ml of 0.5% PH solution was used.

Beer's law was valid over the concentration range

Table 1—Determination of niobium in ores

Sample used	Nb content (%)*	Nb found (%)†
IGS-33	47.93	48.02
IGS-34	18.83	18.96

* Certified value

† Average value of five replicate determinations

of 0.2 to 3 μg ml^{-1}. The Sandell's sensitivity as calculated from Beer's law data was 0.0034 $\mu g/cm^2$ and the molar absorptivity was 2.72×10^4 l $mol^{-1}cm^{-1}$. A sample containing 20 μg of Nb(V), prepared by the standard procedure, gave a mean absorbance of 0.585 with a standard deviation of 0.012, and a relative error of ± 0.8%. Job's method of continuous variation[4] and equilibrium shift method[5] indicated the formation of a 1:1:2 (metal:ligand: thiocyanate) complex.

The following amounts (μg ml^{-1}) of foreign ions were found to cause an error of <2% in the determination of 2 μg of Nb(V) per ml: Ta(V), 50; Mn(II), 2000; Ni(II), 200; Co(II), 100; V(V), 10; Cu(II), 30; W(VI), 10; Pd(II), 15; Ru(III), 10; Os(VIII), 20; F^-, 50; Cl^-, 1000; Br^-, 20; I^-, 10; NO_3^-, 100; PO_4^{3-}, 100; SO_4^{2-}, 1000; CH_3COO^-, 100; $C_2O_4^{2-}$, 50; and EDTA, 2000. The tolerance limit of Fe(III) was 250 μg/ml in the presence of 4 ml of 20% ascorbic acid as masking agent.

The proposed method was applied to the determination of niobium in standard ores. The results of these investigations are shown in Table 1.

Acknowledgement

The authors are grateful to Bayer A G, Liverkusen, FRG for the supply of pure PH and Dr B K Balaji, Atomic Minerals Division, Bangalore, for the supply of ore samples.

References

1 Keshavan B & Sanke Gowda H, *Indian J Chem*, 14A (1976) 293.

2 Keshavan B & Sanke Gowda H, *Indian J Chem*, 14A (1976) 630.

3 Keshavan B & Sanke Gowda H, *J Indian chem Soc*, 54 (1977) 688.

4 Job P, *Ann Chim*, 9 (1928) 113.

5 Tarasiewicz H P, Grudmiewska A & Tarasiewicz M, *Anal chim Acta*, 94 (1977) 435.

NOW AVAILABLE

BIRDS

The Indian subcontinent is home to a breath-takingly vast range of Bird species besides being host to a large number of migratory birds. Between the hot, dry open plains in the west and the tropical rainforests of the east, between the snowclad alpine peaks of the Himalayas in the north and the ocean washed Land's end in the south are to be found bird species which are distinctly different from one another. Each region has its own species which may or may not be found in other regions. Of the World's estimated total of 8600 species of Birds, India has at least 1200 species, apart from seasonal visitors. Indian bird species range from the largest sized Sarus Crane and the Himalayan Bearded Vulture to the smallest thumb-sized flower-pecker, from the colourful pheasants to the dull coloured house sparrows; from the sweet-voiced golden oriole and koel to the raucous house crows and peacocks, from the rarest Mountain Quail to the common myna and sparrow.

Aptly described as "feathered bipeds", the importance of birds in literature, art, sport, communication, religion as well as an article of food cannot be over-emphasized.

Such a vast wealth of avifauna has naturally given rise to a large number of publications dealing with different aspects of India's Birds such as distribution, taxonomy and classification. However, a single compilation highlighting all their economically important aspects is perhaps non-existent.

The present publication lays emphasis on the economic aspects of Indian Birds. The volume covers all aspects of the life of Birds and their interaction with man. The different chapters deal with game, song and plumage birds, birds as pets and for game, role of birds in agriculture, horticulture, forestry and medicine, bird migration, aviation hazards due to birds, management of birds, their control as also conservation. The classification of birds, their inter-relationships and their description are given in great detail. The different indexes—Latin, English and Vernacular names—should be of help to users of the volume.

The volume is well illustrated with colour plates and priced moderately so as to be within the reach of students as well as others.

ISBN 81-85038-90-2

PP 157+xii; Price: Rs 125.00; $ 45.00; £ 30.00

To order copy please send Rs 125.00 (+Rs 10.00 as postage charges) by Demand Draft or cheque drawn in favour of Publications & Information Directorate, New Delhi-110 012 (INDIA) to:-

Senior Sales & Distribution Officer
Publications & Information Directorate (CSIR)
Hillside Road, NEW DELHI-110012 (INDIA)

RECENT ADVANCES IN MAN-MADE FIBRES

Special Issue of

Indian Journal of Fibre & Textile Research

The March 1991 issue of the ***Indian Journal of Fibre & Textile Research*** is being brought out as a special issue on "*RECENT ADVANCES IN MAN-MADE FIBRES*".

Guest edited by Prof.V B Gupta of IIT-Delhi, the special issue will contain invited papers from internationally known experts. Among the authors are Prof. J W S Hearle, Dr.R Huisman, Dr. H M Heuvel, Dr T Manabe, Dr.A S Abhiraman, Dr. Satish Kumar, Prof. V B Gupta, Dr. K V Datye, Prof. A K Sengupta, Prof. Pushpa Bajaj, Prof. N V Bhat, Dr. B N Bandyopadhyay, Prof. A K Mukherjee, Prof. V K Kothari & Prof. B L Deopura.

The topics covered include: Unsolved problems in the science of nylon & polyester fibres; Advances in high performance and other man-made fibres; Fibres from polymer blends; Crystals: their nature & influence on fibre properties; Ceramic fibre precursors; Science & technology of man-made fibres: the Indian R & D scenario; Utilization of polyester waste; Recycling processes and products in nylon-6 fibre industry; Melt flow behaviour of poly(ethylene terephthalate); High-speed spinning of PET yarns; Nylon-6 tyre yarns; and Air-jet texturing.

The contents of this special issue are bound to be of immense use to researchers, technologists, managers and industrialists and would serve as a valuable reference.

Price	Rs 60.00	£ 16.00	$ 30.00

Orders accompanied by Bank Drafts/Cheques drawn in favour of PUBLICATIONS & INFORMATION DIRECTORATE, NEW DELHI 110 012 may be sent to the Senior Sales & Distribution Officer, Publications & Information Directorate (CSIR), Hillside Road, New Delhi-110 012 .

Printed & Published by Dr. G. P. Phondke, Director, Publications & Information Directorate (PID)
Hillside Road, New Delhi 110 012, at PID Photocomposition Unit

D(W) 103

RN 7090/63